

Mechanisms of exercise pressor reflex dysfunction in heart failure

by

Alec Lloyd Edward Butenas

B.S., Kansas State University, 2018

AN ABSTRACT OF A DISSERTATION

submitted in partial fulfillment of the requirements for the degree

DOCTOR OF PHILOSOPHY

Department of Kinesiology  
College of Health and Human Sciences

KANSAS STATE UNIVERSITY  
Manhattan, Kansas

2023

## Abstract

Heart failure patients with reduced ejection fraction (HF-rEF) have augmented sympathetic nervous system activity (SNA) at rest, and during exercise which is linked to decreased exercise tolerance and increased mortality. A reflex arising from within contracting skeletal muscles, termed the exercise pressor reflex, contributes importantly to that exaggerated SNA in HF-rEF. This reflex is activated when the sensory endings of thin fiber muscle afferents are stimulated by mechanical and/or metabolic signals associated with skeletal muscle contraction. Activation of this reflex in healthy subjects acts to increase and redistribute cardiac output and increase blood flow to the contracting skeletal muscles. Conversely, activation of this reflex in HF-rEF patients contributes to an exaggerated increase in SNA and augmented peripheral and coronary vasoconstriction and increases a heart failure patient's risk of myocardial ischemia and fibrillation. Thus, in health the exercise pressor reflex functions to support the metabolic demands of exercise, whereas in HF-rEF the reflex becomes dysfunctional and impairs exercise tolerance. In this sequence of experiments presented in my dissertation, we used a rat model of myocardial infarction-induced HF-rEF (produced by coronary artery ligation). To isolate the exercise pressor reflex, we electrically stimulated the sciatic nerve to elicit hindlimb skeletal muscle contractions in decerebrated, unanesthetized rats. We also passively stretched the hindlimb skeletal muscle to isolate the activation of muscle afferents that are mechanically sensitive which allows us to study the mechanoreflex component of the exercise pressor reflex isolated from the metaboreflex component of the exercise pressor reflex. The contraction and stretch maneuvers produced an exaggerated increase in renal SNA (RSNA) and mean arterial pressure (MAP) in rats with HF-rEF compared to sham-operated control rats (SHAM rats). In the first study (chapter 2), we found that hindlimb arterial injection of a thromboxane A<sub>2</sub> receptor (TxA<sub>2</sub>-R) antagonist reduced the RSNA and MAP response to muscle stretch in rats with HF-rEF, but not SHAM rats. In the second study (chapter 3), we found that hindlimb arterial injection of a TxA<sub>2</sub>-R antagonist reduced the RSNA and MAP response to muscle contraction in rats with HF-rEF, but not SHAM rats. In the third study (chapter 4), we found that preventing translocation of protein kinase C subtype epsilon (PKC $\epsilon$ ), an important second messenger which is translocated to the cell membrane when G<sub>q</sub> proteins, such as TxA<sub>2</sub>-Rs, are activated, reduced the RSNA and MAP response to muscle contraction and muscle stretch in rats with HF-rEF, but not SHAM rats. In the final study, we found that hindlimb

arterial injection of an acid-sensing ion channel subtype 1a (ASIC1a) antagonist reduced the RSNA and MAP response to muscle contraction and RSNA response to muscle stretch in rats with HF-rEF, but not SHAM rats. The culmination of these studies indicates that TxA<sub>2</sub>-R and ASIC1a on the sensory endings of thin fiber muscle afferents as well as second messenger signaling involving PKC $\epsilon$  within the sensory ending of these afferents, contributes importantly to evoking an exaggerated increase in SNA during exercise in HF-rEF consequent to mechanoreflex and exercise pressor reflex activation.

Mechanisms of exercise pressor reflex dysfunction in heart failure

by

Alec Lloyd Edward Butenas

B.S., Kansas State University, 2018

A DISSERTATION

submitted in partial fulfillment of the requirements for the degree

DOCTOR OF PHILOSOPHY

Department of Kinesiology  
College of Health and Human Sciences

KANSAS STATE UNIVERSITY  
Manhattan, Kansas

2023

Approved by:  
Major Professor  
Dr. Steven W. Copp

# Copyright

© Alec Butenas 2023.

## Abstract

Heart failure patients with reduced ejection fraction (HF-rEF) have augmented sympathetic nervous system activity (SNA) at rest, and during exercise which is linked to decreased exercise tolerance and increased mortality. A reflex arising from within contracting skeletal muscles, termed the exercise pressor reflex, contributes importantly to that exaggerated SNA in HF-rEF. This reflex is activated when the sensory endings of thin fiber muscle afferents are stimulated by mechanical and/or metabolic signals associated with skeletal muscle contraction. Activation of this reflex in healthy subjects acts to increase and redistribute cardiac output and increase blood flow to the contracting skeletal muscles. Conversely, activation of this reflex in HF-rEF patients contributes to an exaggerated increase in SNA and augmented peripheral and coronary vasoconstriction and increases a heart failure patient's risk of myocardial ischemia and fibrillation. Thus, in health the exercise pressor reflex functions to support the metabolic demands of exercise, whereas in HF-rEF the reflex becomes dysfunctional and impairs exercise tolerance. In this sequence of experiments presented in my dissertation, we used a rat model of myocardial infarction-induced HF-rEF (produced by coronary artery ligation). To isolate the exercise pressor reflex, we electrically stimulated the sciatic nerve to elicit hindlimb skeletal muscle contractions in decerebrated, unanesthetized rats. We also passively stretched the hindlimb skeletal muscle to isolate the activation of muscle afferents that are mechanically sensitive which allows us to study the mechanoreflex component of the exercise pressor reflex isolated from the metaboreflex component of the exercise pressor reflex. The contraction and stretch maneuvers produced an exaggerated increase in renal SNA (RSNA) and mean arterial pressure (MAP) in rats with HF-rEF compared to sham-operated control rats (SHAM rats). In the first study (chapter 2), we found that hindlimb arterial injection of a thromboxane A<sub>2</sub> receptor (TxA<sub>2</sub>-R) antagonist reduced the RSNA and MAP response to muscle stretch in rats with HF-rEF, but not SHAM rats. In the second study (chapter 3), we found that hindlimb arterial injection of a TxA<sub>2</sub>-R antagonist reduced the RSNA and MAP response to muscle contraction in rats with HF-rEF, but not SHAM rats. In the third study (chapter 4), we found that preventing translocation of protein kinase C subtype epsilon (PKC $\epsilon$ ), an important second messenger which is translocated to the cell membrane when G<sub>q</sub> proteins, such as TxA<sub>2</sub>-Rs, are activated, reduced the RSNA and MAP response to muscle contraction and muscle stretch in rats with HF-rEF, but not SHAM rats. In the final study, we found that hindlimb arterial injection of an acid-sensing ion channel subtype 1a (ASIC1a)

antagonist reduced the RSNA and MAP response to muscle contraction and RSNA response to muscle stretch in rats with HF-rEF, but not SHAM rats. The culmination of these studies indicates that TxA<sub>2</sub>-R and ASIC1a on the sensory endings of thin fiber muscle afferents as well as second messenger signaling involving PKC $\epsilon$  within the sensory ending of these afferents, contributes importantly to evoking an exaggerated increase in SNA during exercise in HF-rEF consequent to mechanoreflex and exercise pressor reflex activation.

## Table of Contents

|  |      |
|--|------|
| List of Figures .....  | x    |
| List of Tables .....   | xii  |
| Acknowledgements.....  | xiii |
| Dedication .....   | xiv  |
| Preface.....   | xv   |
| Chapter 1 - Introduction.....  | 1    |
| References.....  | 5    |
| Chapter 2 - Exaggerated sympathetic and cardiovascular responses to dynamic mechanoreflex<br>activation in rats with heart failure: Role of endoperoxide 4 and thromboxane A <sub>2</sub> receptors. | 8    |
| 2.1 Abstract.....  | 8    |
| 2.2 Introduction.....  | 9    |
| 2.3 Methods .....  | 11   |
| 2.4 Results.....   | 16   |
| 2.5 Discussion.....  | 18   |
| 2.6 Conclusion .....   | 23   |
| 2.7 References.....  | 24   |
| Chapter 3 - Thromboxane A <sub>2</sub> receptors contribute to the exaggerated exercise pressor reflex in<br>male rats with heart failure .....  | 40   |
| 3.1 Abstract.....  | 40   |
| 3.2 Introduction.....  | 40   |
| 3.3 Methods .....  | 42   |
| 3.4 Results.....   | 49   |
| 3.5 Discussion.....  | 50   |
| 3.6 Conclusion .....   | 55   |
| 3.7 References.....  | 56   |
| Chapter 4 - Protein Kinase C Epsilon Contributes to the Chronic Mechanoreflex Sensitization in<br>rats with Heart Failure .....  | 72   |
| 4.1 Abstract.....  | 72   |
| 4.2 Introduction.....  | 73   |
| 4.3 Methods .....  | 75   |



|  |     |
|--|-----|
| 4.4 Results.....   | 81  |
| 4.5 Discussion.....  | 84  |
| 4.6 Conclusion .....   | 86  |
| 4.6 References.....  | 88  |
| Chapter 5 - Novel mechanosensory role for acid sensing ion channel subtype 1a in evoking the<br>exercise pressor reflex in rats with heart failure ..... | 107 |
| 5.1 Abstract.....  | 107 |
| 5.2 Introduction.....  | 107 |
| 5.3 Methods .....  | 109 |
| 5.4 Results.....   | 117 |
| 5.5 Discussion.....  | 119 |
| 5.6 Conclusion .....   | 125 |
| 5.7 References.....  | 126 |
| Chapter 6 - Conclusion .....   | 147 |
| Appendix A - Curriculum Vitae .....  | 150 |

## List of Figures

|   |    |
|---|----|
| Figure 2.1 Effect of HF-rEF on the sympathetic and cardiovascular responses to dynamic mechanoreflex activation. ....   | 33 |
| Figure 2.2 Effect of HF-rEF on the time course of the reflex sympathetic and cardiovascular responses to dynamic mechanoreflex activation.....                            | 34 |
| Figure 2.3 Original tracing of the RSNA, BP, and HR response to dynamic hindlimb muscle stretch in a SHAM rat and HF-rEF rat.....   | 35 |
| Figure 2.4 Effect of EP4-R blockade on the sympathetic and cardiovascular responses to dynamic mechanoreflex activation. ....   | 36 |
| Figure 2.5 Effect of EP4-R blockade on the time courses of the sympathetic and cardiovascular responses to dynamic mechanoreflex activation.....                          | 37 |
| Figure 2.6 Effect of TxA2-R blockade on the sympathetic and cardiovascular responses to dynamic mechanoreflex activation. ....  | 38 |
| Figure 2.7 Effect of TxA2-R blockade on the time courses of the sympathetic and cardiovascular responses to dynamic mechanoreflex activation.....                         | 39 |
| Figure 3.1 Effect of HF-rEF on dynamic exercise pressor reflex activation. ....   | 65 |
| Figure 3.2 Effect of HF-rEF on the time course of dynamic exercise pressor reflex activation. .   | 66 |
| Figure 3.3 Original tracing of the RSNA, BP, and HR response to dynamic contraction in a SHAM rat and HF-rEF rat .....  | 67 |
| Figure 3.4 Effect of TxA <sub>2</sub> -R blockade on dynamic exercise pressor reflex activation. ....   | 68 |
| Figure 3.5 Effect of TxA <sub>2</sub> -R blockade on the time course of dynamic exercise pressor reflex activation.....   | 69 |
| Figure 3.6 Original tracing of first five seconds on the RSNA response to contraction before and after Daltroban in two HF-rEF rats .....                                 | 70 |
| Figure 3.7 Effect of HF-rEF on interstitial PGE <sub>2</sub> and TxB <sub>2</sub> concentrations and COX-2 activity in the white portion of the gastrocnemius muscle..... | 71 |
| Figure 4.1 :Effect of inositol 1,4,5-trisphosphate (IP <sub>3</sub> ) receptor blockade with Xestospongin C on the time course of isolated mechanoreflex activation.....  | 97 |
| Figure 4.2 : Effect of inositol 1,4,5-trisphosphate (IP <sub>3</sub> ) receptor blockade with Xestospongin C on isolated mechanoreflex activation.....                    | 98 |

|  |     |
|--|-----|
| Figure 4.3 Effect of protein kinase C epsilon (PKC $\epsilon$ ) receptor blockade with PKC $\epsilon$ 141 on the time course of isolated mechanoreflex activation.....                             | 99  |
| Figure 4.4 Effect of protein kinase C epsilon (PKC $\epsilon$ ) inhibition with PKC $\epsilon$ 141 on isolated mechanoreflex activation .....  | 100 |
| Figure 4.5 Original tracings showing the RSNA and pressor response to dynamic stretch before and after Xestospongin C and PKC $\epsilon$ 141.....  | 101 |
| Figure 4.6 Systemic and vehicle controls for the protein kinase C epsilon (PKC $\epsilon$ ) inhibitor PKC $\epsilon$ 141 on isolated mechanoreflex activation .....                                | 102 |
| Figure 4.7 : Effect of protein kinase C epsilon (PKC $\epsilon$ ) inhibition with PKC $\epsilon$ 141 on isolated metaboreflex activation in HF-rEF rats .....                                      | 103 |
| Figure 4.8 Effect of protein kinase C epsilon (PKC $\epsilon$ ) receptor blockade with PKC $\epsilon$ 141 on the time course of exercise pressor reflex activation .....                           | 104 |
| Figure 4.9 : Effect of protein kinase C epsilon (PKC $\epsilon$ ) inhibition with PKC $\epsilon$ 141 on exercise pressor reflex activation .....   | 105 |
| Figure 4.10 Effect of HF-rEF on PKC $\epsilon$ expression in DRG tissue .....  | 106 |
| Figure 5.1 Effect of ASIC1a blockade on renal sympathetic and pressor response to lactic acid injection.....   | 139 |
| Figure 5.2 Effect of ASIC1a blockade on the time course of exercise pressor reflex activation  | 140 |
| Figure 5.3 Effect of ASIC1a blockade on exercise pressor reflex activation .....   | 141 |
| Figure 5.4 Examples of original tracings of RSNA and blood pressure evoked during 30 seconds of static hindlimb muscle contraction before and after ASIC1a blockade in a SHAM and HF-rEF rat. .... | 142 |
| Figure 5.5 Effect of ASIC1a blockade on the time course of mechanoreflex activation .....  | 143 |
| Figure 5.6 Effect of ASIC1a blockade on mechanoreflex activation .....   | 144 |
| Figure 5.7 Effect of $\mu$ - and $\delta$ -opioid receptor blockade and ASIC1a blockade on mechanoreflex activation in HF-rEF rats.....  | 145 |
| Figure 5.8 Effect of HF-rEF on ASIC1a expression.....  | 146 |
| Figure 6.1 Summary of results.....   | 149 |

## List of Tables

|   |     |
|---|-----|
| Table 2.1 Body and tissue weights and heart morphometrics in SHAM and HF-rEF rats.....  | 30  |
| Table 2.2 Baseline MAP and HR in SHAM and HF-rEF rats.....  | 32  |
| Table 3.1 Body and tissue masses and heart morphometrics in SHAM and HF-rEF rats.....   | 63  |
| Table 3.2 Baseline MAP and HR in SHAM and HF-rEF rats.....  | 64  |
| Table 4.1 Body and tissue weights and heart morphometrics in SHAM and HF-rEF rats.....  | 94  |
| Table 4.2 Baseline MAP, baseline HR, and Peak $\Delta$ HR in SHAM and HF-rEF rats.....  | 95  |
| Table 4.3 Tension-time index in SHAM and HF-rEF rats.....   | 96  |
| Table 5.1 Body and tissue masses and heart morphometrics in SHAM and HF-rEF rats.....   | 135 |
| Table 5.2 Baseline MAP in SHAM and HF-rEF rats.....   | 136 |
| Table 5.3 Baseline HR and cardioaccelerator responses in SHAM and HF-rEF rats.....  | 137 |
| Table 5.4 Pressor, cardioaccelerator, and peak renal sympathetic response to static hindlimb muscle stretch before (control), after $\mu$ , $\delta$ opioid receptor blockade (Naloxone), and after ASIC1a blockade in HF-rEF rats ( $n=5$ )..... | 138 |

## Acknowledgements

I would like to start by thanking my mentor, Dr. Steven Copp, for all he has done for me these past seven years. He has taught me so much. The amount of time he has invested in my training is unparalleled. He has truly given me the tools I need to launch me into the next stage of my career. Additionally, I would like to thank my mentoring team consisting of Dr. Tim Musch, Dr. David Poole, and Dr. Stephanie Hall. These scientists are some of the most talented, well-spoken, and generous individuals I have ever met.

I would also like to thank each of the members of the Copp lab who have shared their lab space with me throughout the years. Namely, Dr. Korynne Rollins, Evan Kempf, Tyler Hopkins, Bailey Sanderson, Kennedy Felice, Auni Williams, Raimi Carroll, and Ashley Baranczuk. I have made a lot of memories with these individuals. Additionally, I would like to thank Sue Hageman for not just her technical expertise, but our friendship. Lastly, all the graduate students past (Dr. Joshua Smith, Dr. Shane Hammer, Dr. Andrew Alexander, Dr. Jacob Caldwell, Dr. Dryden Baumfalk, Dr. Trenton Colburn, Dr. Stephen Hammond, Taylor Rand, and Garrett Lovoy) and present (Andrew Horn, Olivia Kunkle, Kiana Schulze, Ramona Weber, Shannon Parr, Vanessa Turpin, and Britton Scheuermann) for the help they have provided me and the friendships we have developed over the years.

My family has been so patient with me attending school for this long. My parents, Ann and Ed Butenas, my brothers, Zach and Noah, my grandmothers, Susan Hollinger and the late Donna Butenas, my aunts, my uncles, and my cousins. My friends from home (Colton Donahue, Collin Mardis, Colin Gregory, Nicholas Patterson, and Nate Provost. Also, my St. Isidore's family (Fr. Gale Hammerschmidt, Fr. Matt Davied, Michael Melgares, Andy Brandt, Suan Sonna, Justin and Kylee Jennings, Ozzy and Abby Baez, Robbie Jennings, Anna Biggins, Alissa Towsley, Nick and Lindsay Hodges, Ridge Pinkston and many others) for the friendships we have formed in my time at Kansas State. Finally, I would like to thank my fiancée, Ali, for all she has done this past year in choosing to love me in difficult times and helping me become the man I am today. I love you dearly! Thank you everyone for helping me along the way!

## **Dedication**

I would like to dedicate my work to my grandfathers who passed away before I was born. Namely, Dr. Lloyd Alvin Hollinger and Sgt. Maj. Edward E. Butenas, USMC. Although I never met either of you, you still had a lasting impact on my life via those you left behind.

## Preface

Chapters 2, 3, and 5 of my dissertation represent original research articles that have been published following the peer-review process.

### Chapter 2:

**Butenas ALE, Rollins KS, Williams AC, Parr SK, Hammond ST, Ade CJ, Hageman KS, Musch TI, and Copp SW.** Exaggerated sympathetic and cardiovascular responses to dynamic mechanoreflex activation in rats with heart failure: Role of endoperoxide 4 and thromboxane A2 receptors. *Auton Neurosci* 232: 102784, 2021.

### Chapter 3:

**Butenas ALE, Rollins KS, Williams AC, Parr SK, Hammond ST, Ade CJ, Hageman KS, Musch TI, and Copp SW.** Thromboxane A2 receptors contribute to the exaggerated exercise pressor reflex in male rats with heart failure. *Physiological reports* 9: e15052, 2021.

### Chapter 5:

**Butenas ALE, Rollins KS, Parr SK, Hammond ST, Ade CJ, Hageman KS, Musch TI, and Copp SW.** Novel mechanosensory role for acid sensing ion channel subtype 1a in evoking the exercise pressor reflex in rats with heart failure. *J Physiol* 600: 2105-2125, 2022.

## Chapter 1 - Introduction

The ability to perform even moderate exercise, such as activities of daily living, is dependent upon appropriate autonomic adjustments to the cardiovascular system. Afferent feedback originating from within contracting skeletal muscle contributes importantly to these adjustments during exercise (1). Specifically, sensory endings of thin fiber muscle afferents are activated during exercise by both mechanical stimuli (*e.g.*, increases in muscle tension and intramuscular pressure) and metabolic stimuli (*e.g.*, increases in lactic acid, bradykinin, prostaglandins, and decreases in pH) associated with skeletal muscle contraction which, when activated, contribute to a withdrawal of parasympathetic outflow and an increase in sympathetic outflow. This reflex, termed the exercise pressor reflex, facilitates the increases in blood pressure, heart rate, myocardial contractility, and venous return to the heart (2), as well as the increases and redistribution of cardiac output, and increase blood flow to the contracting skeletal muscle (3). Thus, in health, the exercise pressor reflex supports exercise performance (4).

In patients with heart failure with reduced ejection fraction (HF-rEF), the exercise pressor reflex is exaggerated compared to that found in healthy subjects which contributes to the elevated increases in sympathetic nerve activity (SNA) and altered cardiovascular responses to exercise (5, 6). For example, Smith et al. (7) showed that attenuating the exercise pressor reflex in HF-rEF patients with intrathecal fentanyl increased stroke volume, cardiac output and leg blood flow during cycling exercise compared to those increases found in the placebo condition. Similarly, attenuating the exercise pressor reflex in HF-rEF improves oxygen uptake kinetics during cycling exercise, whereas no effect was observed in healthy controls (8). Thus, in HF-rEF, activation of the exercise pressor reflex leads to exaggerated peripheral vasoconstriction which impairs increases in blood to the muscle which carries oxygen and crucial nutrients (9) and, thus, exacerbates fatigue.

The mechanically sensitive portion of the exercise pressor reflex has been termed the mechanoreflex, whereas the metabolically sensitive portion of the reflex has been termed the metaboreflex. The mechanoreflex contributes importantly to the overall exaggerated reflex in HF-rEF patients (10-13). For example, Middlekauff et al. (14) found that passive limb movement (a model of mechanoreflex activation isolated from metaboreflex activation) resulted in a greater increase in muscle SNA (MSNA) in patients with HF-rEF than those increases found in healthy



counterparts. Furthermore, these authors found that administration of the cyclooxygenase (COX) inhibitor, indomethacin, attenuated the increases in MSNA in patients with HF-rEF (15). Those findings are further supported by findings using the decerebrate, unanesthetized rat model of mechanoreflex activation. Specifically, in rats with myocardial infarction-induced HF-rEF Morales et al., (13) found that hindlimb arterial injection of the COX-2 inhibitor, but not COX-1 inhibitor, attenuated the renal SNA (RSNA) response to static hindlimb muscle stretch (a model of mechanoreflex activation isolated from metaboreflex activation), whereas no effect of COX-1 or COX-2 inhibition was found in healthy control rats. These findings collectively suggest that COX-2 products of arachidonic acid metabolism sensitize muscle afferents that underly mechanoreflex activation.

In chapters 2, 3, and 4, we investigated the mechanism behind this COX-2 mediated mechanoreflex sensitization. Specifically, in both sham-operated control rats (*i.e.*, SHAM rats) and myocardial infarction-induced HF-rEF rats, we investigated the effects on isolated mechanoreflex activation following inhibition of two of the main receptors on the sensory endings of thin fiber muscle afferents for COX-2 products, namely endoperoxide 4 receptor (EP4-R) and thromboxane A<sub>2</sub> (TxA<sub>2</sub>-R) (*i.e.*, chapter 2). We found that TxA<sub>2</sub>-R, but not EP4-R, inhibition attenuated the RSNA and pressor response to dynamic hindlimb muscle stretch in HF-rEF rats, but not SHAM rats. Next, we sought to determine whether the effects of TxA<sub>2</sub>-R blockade persisted when the metaboreflex was also engaged (*i.e.*, during muscle contraction). In this study (chapter 3) we found that TxA<sub>2</sub>-R blockade attenuated the RSNA and pressor response to dynamic hindlimb muscle contraction in HF-rEF rats. In chapter 4, we sought to determine the intracellular mechanisms within the sensory ending of thin fiber muscle afferents which mediate this mechanoreflex/exercise pressor reflex sensitization produced by TxA<sub>2</sub>-Rs. Specifically, we sought to determine the roles played by inositol triphosphate (IP3) receptors and protein kinase C epsilon (PKC $\epsilon$ ) (*i.e.*, two major components of second-messenger signaling associated with TxA<sub>2</sub>-Rs activation) in the mechanoreflex/exercise pressor reflex sensitization in HF-rEF rats. We found that PKC $\epsilon$  inhibition, but not IP3 receptor blockade, attenuated the RSNA and pressor response to dynamic hindlimb muscle stretch in HF-rEF rats, but not SHAM rats. Additionally, we found that PKC $\epsilon$  inhibition attenuated the RSNA and pressor response to muscle contraction in HF-rEF rats. Thus, these findings suggest that TxA<sub>2</sub>-R signaling (likely through PKC $\epsilon$ ) contributes importantly to the COX-2 mediated mechanoreflex sensitization in HF-rEF.

Chapter 5 focuses on the metaboreflex component of the exercise pressor reflex, which in contrast to the mechanoreflex, has had considerable debate surrounding its role in the overall exercise pressor reflex exaggeration in HF-rEF. There are reports that show that the metaboreflex-induced increase in blood pressure is increased (16, 17) as well as decreased (18-20) in HF-rEF patients compared to healthy controls. However, the general notion surrounding exercise pressor reflex dysfunction in HF-rEF for the past three decades has been that the metaboreflex is reduced and the mechanoreflex is exaggerated and contributes to the entirety of the exaggerated exercise pressor reflex. Over the course of the experiments contained within chapters 2-4, I collected preliminary data surrounding the role played by acid-sensing ion channels (ASICs) in the exaggerated exercise pressor reflex in rats with HF-rEF. Specifically, at the end of those experiments I injected lactic acid (24mMol; pH=2.00) into the arterial supply of the hindlimb of SHAM and HF-rEF rats. This injection of lactic acid stimulates ASICs on the sensory endings of thin fiber muscle afferents, isolated from mechanical stimulation of thin fiber muscle afferents. During the COVID pandemic lockdown, I compared the reflex increases in RSNA and MAP in response to lactic acid injection in SHAM and HF-rEF rats. I was surprised to find that, compared to SHAM rats ( $n=34$ ), HF-rEF rats ( $n=33$ ) had a greater percent change from baseline in RSNA (Peak  $\Delta$ RSNA, SHAM:  $61\pm 11$ ; HF-rEF:  $106\pm 14\%$ ;  $P<0.01$ ) and peak change from baseline in mean arterial pressure (Peak  $\Delta$ MAP, SHAM,  $19\pm 2$ ; HF-rEF:  $27\pm 3$ mmHg;  $P<0.01$ ) in response to lactic acid injection, despite previous findings suggesting that the metaboreflex component of the exercise pressor reflex was attenuated in HF-EF compared to age-matched controls (18, 21). I used this data as preliminary data for my application for the Foundation Doctoral Student Research Grant to the American College of Sports Medicine which was funded in 2021. The experiments reported in chapter 5 were funded in part from that research grant and were published in the Journal of Physiology in March of 2022. We found that ASIC subtype 1a (ASIC1a), a channel known to activate the metaboreflex in healthy rats (22), contributes importantly to the RSNA and pressor response to muscle contraction in HF-rEF rats. Interestingly, the role played by ASIC1a in evoking the exercise pressor reflex also includes a novel role for ASIC1a in evoking the mechanoreflex. Specifically, we found that ASIC1a blockade attenuated the RSNA, but not pressor, response to static hindlimb muscle stretch in HF-rEF rats. Thus, in HF-rEF, ASIC1a plays a role in activating the mechanoreflex and the metaboreflex components of the exercise pressor reflex.

Chapters 2-5 of this dissertation are self-contained and presented in standard journal article format with introduction, methods, results, discussion, and reference sections. The last chapter of this dissertation (Chapter 6) provides an overall summary and conclusion which synthesizes and integrates the primary findings from the individual studies.

## References

1. **Rotto DM, Stebbins CL, and Kaufman MP.** Reflex cardiovascular and ventilatory responses to increasing H<sup>+</sup> activity in cat hindlimb muscle. *JApplPhysiol* 67: 256-263, 1989.
2. **Kaufman MP, and Forster HV.** Reflexes controlling circulatory, ventilatory and airway responses to exercise. In: *Handbook of Physiology, Section 12: Exercise: Regulation and Integration of Multiple Systems II Control of Respiratory and Cardiovascular Systems*, edited by Rowell LB, and Shepherd JT. New York, NY: Oxford University Press, 1996, p. 381-447.
3. **Amann M, Runnels S, Morgan DE, Trinity JD, Fjeldstad AS, Wray DW, Reese VR, and Richardson RS.** On the contribution of group III and IV muscle afferents to the circulatory response to rhythmic exercise in humans. *JPhysiol* 589: 3855-3866, 2011.
4. **Amann M, Blain GM, Proctor LT, Sebranek JJ, Pegelow DF, and Dempsey JA.** Implications of group III and IV muscle afferents for high-intensity endurance exercise performance in humans. *J Physiol* 589: 5299-5309, 2011.
5. **Murphy MN, Mizuno M, Mitchell JH, and Smith SA.** Cardiovascular regulation by skeletal muscle reflexes in health and disease. *Am J Physiol Heart Circ Physiol* 301: H1191-1204, 2011.
6. **Smith SA, Mitchell JH, and Garry MG.** The mammalian exercise pressor reflex in health and disease. *ExpPhysiol* 91: 89-102, 2006.
7. **Smith JR, Joyner MJ, Curry TB, Borlaug BA, Keller-Ross ML, Van Iterson EH, and Olson TP.** Locomotor muscle group III/IV afferents constrain stroke volume and contribute to exercise intolerance in human heart failure. *J Physiol* 598: 5379-5390, 2020.
8. **Van Iterson EH, Johnson BD, Joyner MJ, Curry TB, and Olson TP.** Vo<sub>2</sub> kinetics associated with moderate-intensity exercise in heart failure: impact of intrathecal fentanyl inhibition of group III/IV locomotor muscle afferents. *Am J Physiol Heart Circ Physiol* 313: H114-H124, 2017.
9. **Amann M, Venturelli M, Ives SJ, Morgan DE, Gmelch B, Witman MA, Jonathan Groot H, Walter Wray D, Stehlik J, and Richardson RS.** Group III/IV muscle afferents impair limb blood in patients with chronic heart failure. *Int J Cardiol* 174: 368-375, 2014.
10. **Middlekauff HR, Niztsche EU, Hoh CK, Hamilton MA, Fonarow GC, Hage A, and Moriguchi JD.** Exaggerated muscle mechanoreflex control of reflex renal vasoconstriction in heart failure. *JApplPhysiol* 90: 1714-1719, 2001.

11. **Smith SA, Mitchell JH, Naseem RH, and Garry MG.** Mechanoreflex mediates the exaggerated exercise pressor reflex in heart failure. *Circulation* 112: 2293-2300, 2005.
12. **Koba S, Xing J, Sinoway LI, and Li J.** Sympathetic nerve responses to muscle contraction and stretch in ischemic heart failure. *Am J Physiol Heart Circ Physiol* 294: H311-321, 2008.
13. **Morales A, Gao W, Lu J, Xing J, and Li J.** Muscle cyclo-oxygenase-2 pathway contributes to the exaggerated muscle mechanoreflex in rats with congestive heart failure. *Exp Physiol* 97: 943-954, 2012.
14. **Middlekauff HR, Chiu J, Hamilton MA, Fonarow GC, Maclellan WR, Hage A, Moriguchi J, and Patel J.** Muscle mechanoreceptor sensitivity in heart failure. *Am J Physiol Heart Circ Physiol* 287: H1937-H1943, 2004.
15. **Middlekauff HR, Chiu J, Hamilton MA, Fonarow GC, Maclellan WR, Hage A, Moriguchi J, and Patel J.** Cyclooxygenase products sensitize muscle mechanoreceptors in humans with heart failure. *Am J Physiol Heart Circ Physiol* 294: H1956-1962, 2008.
16. **Keller-Ross ML, Johnson BD, Joyner MJ, and Olson TP.** Influence of the metaboreflex on arterial blood pressure in heart failure patients. *Am Heart J* 167: 521-528, 2014.
17. **Shoemaker JK, Kunselman AR, Silber DH, and Sinoway LI.** Maintained exercise pressor response in heart failure. *J Appl Physiol* 85: 1793-1799, 1998.
18. **Sterns DA, Ettinger SM, Gray KS, Whisler SK, Mosher TJ, Smith MB, and Sinoway LI.** Skeletal muscle metaboreceptor exercise responses are attenuated in heart failure. *Circulation* 84: 2034-2039, 1991.
19. **Li J, Sinoway AN, Gao Z, Maile MD, Pu M, and Sinoway LI.** Muscle mechanoreflex and metaboreflex responses after myocardial infarction in rats. *Circulation* 110: 3049-3054, 2004.
20. **Smith SA, Williams MA, Mitchell JH, Mammen PP, and Garry MG.** The capsaicin-sensitive afferent neuron in skeletal muscle is abnormal in heart failure. *Circulation* 111: 2056-2065, 2005.
21. **Xing J, Lu J, and Li J.** ASIC3 contributes to the blunted muscle metaboreflex in heart failure. *Med Sci Sports Exerc* 47: 257-263, 2015.

22. **Ducrocq GP, Kim JS, Estrada JA, and Kaufman MP.** ASIC1a plays a key role in evoking the metabolic component of the exercise pressor reflex in rats. *Am J Physiol Heart Circ Physiol* 318: H78-H89, 2020.

## **Chapter 2 - Exaggerated sympathetic and cardiovascular responses to dynamic mechanoreflex activation in rats with heart failure: Role of endoperoxide 4 and thromboxane A<sub>2</sub> receptors.**

### **2.1 Abstract**

The primary purpose of this investigation was to determine the role played by endoperoxide 4 receptors (EP4-R) and thromboxane A<sub>2</sub> receptors (TxA<sub>2</sub>-R) during isolated dynamic muscle mechanoreflex activation in rats with heart failure with reduced ejection fraction (HF-rEF) and sham-operated healthy controls. We found that injection of the EP4-R antagonist L-161,982 (1µg) into the arterial supply of the hindlimb had no effect on the peak pressor response to dynamic hindlimb muscle stretch in HF-rEF ( $n=6$ , peak  $\Delta$ MAP pre:  $27\pm 7$ ; post:  $27\pm 4$  mmHg;  $P=0.99$ ) or sham ( $n=6$ , peak  $\Delta$ MAP pre:  $15\pm 3$ ; post:  $13\pm 3$  mmHg;  $P=0.67$ ) rats. In contrast, injection of the TxA<sub>2</sub>-R antagonist daltroban (80µg) into the arterial supply of the hindlimb reduced the pressor response to dynamic hindlimb muscle stretch in HF-rEF ( $n=11$ , peak  $\Delta$ MAP pre:  $28\pm 4$ ; post:  $16\pm 2$  mmHg;  $P=0.02$ ) but not sham ( $n=8$ , peak  $\Delta$ MAP pre:  $17\pm 3$ ; post:  $16\pm 3$ ;  $P=0.84$ ) rats. Our data suggest that TxA<sub>2</sub>-Rs on thin fibre muscle afferents contribute to the exaggerated mechanoreflex in HF-rEF.

## 2.2 Introduction

Sympathetic nervous system activity (SNA) is augmented at rest (1), and during exercise (2, 3) in patients with heart failure with reduced ejection fraction (HF-rEF) compared to healthy control subjects. Exaggerated SNA in HF-rEF patients is linked to decreased exercise tolerance (4, 5) and increased mortality (6). The lack of tolerance for exercise and activities of daily living reduces functional independence and quality of life, and is a significant driver of the escalated cost of care for heart failure patients (7). Thus, advancing our understanding of the exaggerated SNA in the over 26 million people worldwide with HF-rEF (8) is fundamentally important towards improving quality of life for this patient population.

The exercise pressor reflex is one mechanism that contributes to the heightened SNA during exercise in HF-rEF patients (9). This reflex is activated when the sensory endings of group III and IV thin fibre muscle afferents are stimulated by mechanical and/or metabolic signals associated with skeletal muscle contraction (10-13). A substantial body of evidence suggests that this reflex is exaggerated in patients with HF-rEF compared to the reflex found in healthy control subjects (14, 15). The exaggerated exercise pressor reflex in HF-rEF contributes to an impairment in oxygen delivery to contracting skeletal muscles (16-20), which contributes to reductions in exercise capacity in this patient population (20). Thus, there is pressing need to investigate the mechanisms of exaggerated exercise pressor reflex activation in HF-rEF patients.

The mechanically sensitive portion of the exercise pressor reflex (*i.e.*, the mechanoreflex) contributes importantly to the overall reflex exaggeration in HF-rEF patients (21, 22) and in animals with HF-rEF (23-26). Importantly, in rats with HF-rEF compared to healthy counterparts, Wang et al. (27) found greater activation of primarily mechanically sensitive group III muscle afferents in response to static hindlimb muscle contraction and static hindlimb muscle stretch (a model of static mechanoreflex activation isolated from contraction-induced metabolic stimuli; 28). The augmented thin fibre muscle afferent responsiveness to the contraction and stretch protocols were likely attributable, at least in part, to a chronic sensitization of mechanically activated channels on the sensory endings of those afferents produced by cyclooxygenase (COX) products of arachidonic metabolism (22, 25, 29, 30). For example, Morales, Gao, Lu, Xing and Li (25) showed that inhibition of the COX-2 isoform, but not the COX-1 isoform, within hindlimb skeletal muscles of rats with HF-rEF reduced the increase in renal SNA (RSNA) and blood pressure evoked during static hindlimb skeletal muscle stretch. Conversely, no effect of COX-1 or COX-2



inhibition on the increase in RSNA and blood pressure in response to static stretch was found in healthy control rats (25). We recently attempted to build on those findings by investigating in HF-rEF rats the role played by two major receptors for products of COX metabolism present on sensory neurons, namely endoperoxide 4 receptors (EP4-Rs) and thromboxane A<sub>2</sub> receptors (TxA<sub>2</sub>-Rs), in the mechanoreflex sensitization (31). However, we found that neither injection of an EP4-R antagonist nor a TxA<sub>2</sub>-R antagonist into the arterial supply of the hindlimb of HF-rEF rats had an effect on the reflex increase in RSNA and blood pressure evoked during static hindlimb skeletal muscle stretch (31).

Static stretch of rat hindlimb skeletal muscles serves as a valuable model of mechanoreflex activation isolated from the metabolic stimuli present during static contractions. However, static stretch does not reproduce the pattern of rhythmic mechanical stimuli present during dynamic contractions such as those that produce locomotion (*e.g.*, walking, climbing stairs, etc.). Moreover, static versus dynamic mechanoreflex activation may stimulate substantially different classes of mechanically activated channels (32, 33) which may exhibit different inactivation or adaptation kinetics (34-36) and which may be governed by different intracellular signaling pathways. To address these issues, our laboratory has used a 1 Hz dynamic rat hindlimb skeletal muscle stretch model of isolated mechanoreflex activation which closely replicates the rhythmic nature of skeletal muscle contraction during locomotory exercise (32, 37-40). Whether this dynamic hindlimb skeletal muscle stretch model of mechanoreflex activation results in greater reflex sympathetic and/or cardiovascular responses in rats with HF-rEF compared to healthy control rats is unknown. Additionally, whether the reflex sympathetic and cardiovascular responses to isolated dynamic mechanoreflex activation in HF-rEF rats are governed by the intracellular pathways linked to EP4-Rs and/or TxA<sub>2</sub>-Rs, is unknown.

Based on the information above, the purpose of this investigation was twofold. First, we sought to determine whether dynamic hindlimb skeletal muscle stretch results in greater reflex sympathetic and cardiovascular responses in HF-rEF rats compared to healthy (SHAM operated) control rats. Second, we sought to determine if the dynamic stretch modality would unmask an important role for EP4-Rs and TxA<sub>2</sub>-Rs on thin fibre muscle afferents in the regulation of mechanoreflex activation in HF-rEF. Specifically, we tested the hypotheses that: 1) 30 seconds of 1 Hz dynamic hindlimb skeletal muscle stretch would result in greater reflex increases in RSNA, mean arterial pressure (MAP), and heart rate (HR) in HF-rEF rats compared to SHAM rats, and 2)

the injection of the EP4-R antagonist L-161,982 (1  $\mu$ g) or the TxA<sub>2</sub>-R antagonist daltroban (80  $\mu$ g) into the arterial supply of the hindlimb would reduce the reflex increases in RSNA, MAP, and HR evoked in response to dynamic hindlimb skeletal muscle stretch in HF-rEF rats, but not SHAM rats.

## **2.3 Methods**

### *Ethical Approval*

All experimental procedures were approved by the Institutional Animal Care and Use Committee of Kansas State University (Protocol #4076) and conducted in accordance with the National Institutes of Health Guide for the Care and Use of Laboratory Animals (41).

### *Animals*

Experiments were performed on ~14-19 week old male Sprague-Dawley rats ( $n=37$ ; Charles River Laboratories). Rats were housed two per cage in temperature (maintained at ~22°C) and light (12-12 hour light-dark cycle running from 7 AM to 7 PM)-controlled accredited facilities with standard rat chow and water provided ad libitum. Data from 25 of the 37 rats in this manuscript were collected as part of a set of experiments in which we investigated the role played by EP4-Rs and TxA<sub>2</sub>-Rs during both static and dynamic mechanoreflex activation in HF-rEF rats. The data related to static mechanoreflex activation in those 25 rats have been reported previously (31) whereas data related to dynamic mechanoreflex activation has not been reported previously. The additional 12 experiments in which only dynamic mechanoreflex activation was performed were necessary to increase statistical power of the primary study end points ( $n=7$ ) or because control experiments were required ( $n=5$ ).

### *Surgical Procedure*

Myocardial infarction (MI) was induced in 23 of the 37 rats by surgically ligating the left main coronary artery (42). Briefly, rats were anesthetized initially with a 5% isoflurane-O<sub>2</sub> mixture (Butler Animal Health Supply, Elk Grove Village, IL, and Linweld, Dallas, TX) and maintained subsequently on 2.5% isoflurane-O<sub>2</sub> and then intubated and mechanically ventilated with a rodent respirator (Harvard model 680, Harvard Instruments, Holliston, MA) for the duration of the surgical procedure. A left thoracotomy was performed to expose the heart through the fifth intercostal space, and the left main coronary artery was ligated 1–2 mm distal to the edge of the left atrium with a 6-0 braided polyester suture. The thorax was then closed with 2-0 gut, and the skin was closed with 2-0 silk. Prior to termination of anesthesia, bupivacaine (1.5 mg/kg sc) and

buprenorphine (~0.03 mg/kg im) were administered to reduce pain associated with the surgery, along with ampicillin (50 mg/kg im) to reduce the risk of infection. After rats were removed from mechanical ventilation and anesthesia, they were monitored closely for ~6 h post-surgery. In the remaining 14 of 37 rats, a sham ligation of the coronary artery was performed in which 6-0 braided polyester suture was passed under the left main coronary artery, but not tied. These rats are referred to as “SHAM” rats from this point forward. Following completion of either MI or SHAM procedures, rats were housed one per cage for ten days to minimize risk of infection of the surgical site. During these ten days, the antibiotic baytril (100 mg/mL) was administered in the drinking water. Following completion of the baytril treatment, rats were housed two per cage as described above. All animals were monitored daily for 14 days following MI or SHAM procedure for changes in behavior, gait/posture, breathing, appetite and body weight.

#### *Echocardiograph Measurements*

Transthoracic echocardiograph measurements were performed with a commercially available system (Logiq S8; GE Health Care, Milwaukee, WI) ~24-96 hours before the final experimental protocol. Briefly, the rats were anaesthetized as described above. Once the rat was fully anesthetized, the isoflurane mixture was reduced to 2% isoflurane-O<sub>2</sub>. Following 5 minutes at 2% isoflurane, echocardiograph measurements began. The transducer was positioned on the left anterior chest, and left ventricular dimensions were measured. The left ventricular fractional shortening (FS), ejection fraction (EF), end diastolic (LVEDV), end systolic volume (LVESV), and stroke volume (SV) were determined by echocardiographic measurements as previously described (43).

#### *Surgical Procedures for Experimental Protocols*

*In vivo* experiments were performed between four and six weeks following the MI or SHAM procedure and experiments incorporating the dynamic stretch maneuver were successfully performed on 37 rats (SHAM n=14, HF-rEF n=23). On the day of the experiment, rats were anesthetized as described above. Adequate depth of anesthesia was confirmed by the absence of toe-pinch and blink reflexes. The trachea was cannulated, and the lungs were mechanically ventilated (Harvard Apparatus, Holliston, MA) with a 2% isoflurane-balance O<sub>2</sub> gaseous mixture until the decerebration was completed (see below). The right jugular vein and both carotid arteries were cannulated with PE-50 catheters which were used for the injection of fluids, measurement of arterial blood pressure (physiological pressure transducer, AD Instruments), and sampling of

arterial blood gasses (Radiometer). HR was measured by electrocardiogram (AD Instruments). The left superficial epigastric artery was cannulated with a PE-8 catheter whose tip was placed near the junction of the superficial epigastric and femoral arteries and a reversible snare (2-0 silk suture) was placed around the left iliac artery and vein as described previously (40). The left calcaneal bone was severed and linked by string to a force transducer (Grass FT03), which, in turn, was attached to a rack and pinion. A retroperitoneal approach was used to expose bundles of the left renal sympathetic nerve, which were then glued (Kwik-Sil, World Precision Instruments) onto a pair of thin stainless-steel recording electrodes connected to a high impedance probe (Grass Model HZP) and amplifier (Grass P511). Multiunit signals from the renal sympathetic nerve fibers were filtered at high and low frequencies (1 KHz and 100 Hz, respectively) for the measurement of RSNA. Successful RSNA recordings were made in 11 SHAM rats and 14 HF-rEF rats.

Upon completion of the initial surgical procedures, rats were placed in a Kopf stereotaxic frame. After administering dexamethasone (0.2 mg i.v.) to minimize swelling of the brainstem, a pre-collicular decerebration was performed in which all brain tissue rostral to the superior colliculi was removed (44). Following decerebration, anesthesia was terminated, and the rats' lungs were ventilated with room air. Rats were allowed a minimum of 60 minutes to recover from anesthesia before initiation of any experimental protocol. Experiments were performed on decerebrate, unanesthetized rats because anesthesia has been shown to markedly blunt the mechanoreflex and exercise pressor reflex in the rat (44). Body core temperature was measured via a rectal probe and maintained at  $\sim 37\text{--}38^\circ\text{C}$  by an automated heating system (Harvard Apparatus) and heat lamp. Arterial pH and blood gases were analyzed periodically throughout the experiment from arterial blood samples ( $\sim 75\ \mu\text{L}$ ) and maintained within physiological ranges (pH: 7.35–7.45,  $\text{PCO}_2$ :  $\sim 38\text{--}40\ \text{mmHg}$ ,  $\text{PO}_2$ :  $\sim 100\ \text{mmHg}$ ) by administration of sodium bicarbonate and/or adjusting ventilation as necessary.

#### *Primary Experimental Protocols*

We compared the RSNA, pressor, and cardioaccelerator responses evoked in response to 30 seconds of 1 Hz dynamic stretch of the triceps surae muscle before and after the injection of either the EP4-R antagonist L-161,982 (SHAM  $n=6$ , HF-rEF  $n=6$ ) or the  $\text{TxA}_2$ -R antagonist daltroban (SHAM  $n=10$ , HF-rEF  $n=12$ ) into the arterial supply of the left hindlimb. In detail, at least 60 minutes following the decerebration procedure and termination of anesthesia and  $\sim 5$  minutes following a 30 second static hindlimb muscle stretch in the 25 rats for which static

mechanoreflex responses were reported recently (31), baseline muscle tension was set at ~80-100 g by manually turning the rack and pinion. Baseline blood pressure and heart rate were measured for ~30 seconds. An experienced investigator then initiated the stretch protocol in which the rack and pinion was turned back and forth manually at a 1 Hz frequency with the aid of a metronome for 30 seconds. The investigator aimed for a developed tension of ~0.6-0.8 kg on each stretch which is the tension generation typically developed during 1 Hz intermittent contraction protocols in decerebrate rats (38, 45). This dynamic stretch protocol was adapted from protocols described originally by Stebbins, Brown, Levin and Longhurst (28) and Daniels et al. (46) in the cat. Approximately five minutes following the completion of the control dynamic stretch protocol, and after ensuring that blood pressure had returned to its pre-stretch baseline value, the iliac snare was tightened and either the EP4-R antagonist L-161,982 (Tocris Bioscience; 1  $\mu$ g dissolved in 0.2 ml of 0.15% DMSO in saline solution; 47) or the TxA<sub>2</sub>-R antagonist daltroban (Santa Cruz Biotechnology, Inc.; 80  $\mu$ g dissolved in 0.4 mL of 1% DMSO in saline solution; 48) was injected into the arterial supply of the hindlimb through the superficial epigastric artery catheter. The receptor antagonist remained snared in the hindlimb circulation for 5 minutes, at which time the iliac snare was released. In EP4-R blockade experiments, the hindlimb was reperfused for 25 min. This dose of L-161,982 and timing of the injection protocol have been shown to reduce the pressor response to static hindlimb muscle contraction in rats with simulated peripheral artery disease (39, 47). In TxA<sub>2</sub>-R blockade experiments, the hindlimb was reperfused for 10 minutes. This dose of daltroban and the timing of the injection protocol have been shown to reduce the pressor response to hindlimb muscle stretch and contraction in rats with simulated peripheral artery disease (39, 48). Following the 25 or 10 min hindlimb reperfusion period and ~5 minutes following a 30 second static hindlimb muscle stretch in the 25 rats for which static mechanoreflex responses were reported recently (31), the isolated dynamic stretch protocol was repeated exactly as described above. The tension generated during the post antagonist maneuvers was matched as closely as possible to that produced during the control stretch. Evans blue dye was then injected into the arterial supply of the hindlimb in the same manner as the receptor antagonists to ensure that the antagonists had access to the triceps surae muscle circulation. The triceps surae muscles were observed to stain blue in all but one experiment. Specifically, in one HF-rEF rat in which daltroban was injected into the hindlimb, the triceps surae muscles were not observed to stain blue and,

therefore, only the data from the control stretch maneuver were used (for the SHAM vs. HF-rEF comparison).

At the end of all experiments in which RSNA was measured, postganglionic sympathetic nerve activity was abolished with administration of hexamethonium bromide (20 mg/kg iv) to allow for the quantification of background noise as described previously (38). The decerebrate rats were then euthanized with an injection of saturated (>3 mg/kg) potassium chloride. The lungs were then excised and weighed. The heart was excised and the atria and right ventricle (RV) were separated from the left ventricle (LV) and septum, and the RV, LV, and atria were weighed. In rats with HF-rEF, the LV infarction surface area was measured using planimetry and expressed as percent of LV endocardial surface area as described previously (49).

#### *Control experiments*

A total of five HF-rEF rats were used to investigate the potential effects of either 1% DMSO (*i.e.*, the vehicle for daltroban) and/or whether systemic circulation of daltroban may have accounted for the attenuating effects in the main experimental group in which daltroban was injected into the hindlimb arterial circulation. In one rat, the DMSO protocol described below was the only protocol performed. In a different rat, the intravenous injection protocol described below was the only protocol performed. In three rats, the DMSO and the intravenous injection protocols were performed in series with ~5 minutes recovery time between protocols. The 1% DMSO ( $n=4$  total) protocols were performed exactly as described above for the daltroban experiments except 0.4 ml of 1% DMSO alone was injected into the arterial supply of the hindlimb via the left superficial epigastric artery catheter. The systemic circulation control protocols ( $n=4$  total) were performed as described above except 80  $\mu$ g of daltroban was injected into the catheter placed in the jugular vein. The dynamic hindlimb muscle stretch maneuver was then performed 15 minutes after injection to match the timing of the daltroban injection into the arterial supply of the hindlimb described above.

#### *Data analysis*

Muscle tension, blood pressure, HR and RSNA were measured and recorded in real time with a PowerLab and LabChart data acquisition system (AD Instruments). The original RSNA data were rectified and corrected for the background noise determined after the administration of hexamethonium bromide. Baseline mean arterial pressure (MAP), RSNA and HR were determined from the 30-second baseline periods that preceded each maneuver. The peak increase in MAP

(peak  $\Delta$ MAP), RSNA (peak  $\Delta$ RSNA), and HR (peak  $\Delta$ HR) during dynamic stretch were calculated as the difference between the peak values wherever they occurred during the maneuvers and their corresponding baseline value. The tension-time indexes (TTIs), integrated RSNA for the first 5 sec of the stretch maneuver ( $\int\Delta$ RSNA<sub>5 sec</sub>) and blood pressure indexes (BPIs) were calculated by integration of the area under curve during the stretch maneuver and subtracting the integrated area under the curve during the baseline period. We calculated the peak  $\Delta$ RSNA and the  $\int\Delta$ RSNA<sub>5sec</sub> because the renal sympathetic nerve response to dynamic stretch is often characterized by large bursts early (*i.e.*, the first ~5 secs) that may occur in sync with tension development which then subside over the duration of the stretch maneuver. Time courses of the increase in RSNA, MAP and HR were plotted as their change from baseline. Data were first assessed for the presence of a normal distribution, equal variance, and/or effectiveness of pairing as appropriate. Baseline MAP, baseline HR, Peak  $\Delta$ MAP, Peak  $\Delta$ HR, Peak  $\Delta$ RSNA, BPI,  $\int\Delta$ RSNA<sub>5 sec</sub>, and TTIs were compared with Sidak multiple comparisons tests. Time course data were analyzed with two-way ANOVAs and Sidak multiple comparisons tests. Data for echocardiograph measurements, body, heart, and lung weights were analyzed with unpaired Student's *t*-tests or Mann-Whitney U tests as appropriate. Data are expressed as mean $\pm$ SEM. Statistical significance was defined as  $P \leq 0.05$ .

## 2.4 Results

### *Body weight and heart morphometrics*

Body weight was not different between SHAM and HF-rEF rats (Table 1). The ratios of the lung weight to body weight and atria weight to body weight were significantly higher in HF-rEF rats compared to SHAM rats. There was no difference in the ratios of either the LV or RV weight to body weight between groups. Additionally, LVEDV and LVESV were significantly higher, while ejection fraction and fractional shortening were significantly lower, in HF-rEF rats compared to SHAM rats. Stroke volume was not different between groups.

### *Effect of HF-rEF on responses to dynamic mechanoreflex activation*

Pooled data from control conditions across all experiments in the present investigation (*i.e.*, 14 SHAM and 23 HF-rEF rats) indicate that, compared to SHAM rats, HF-rEF rats had significantly larger peak  $\Delta$ MAP, BPI, and peak  $\Delta$ HR (Fig. 1) responses to 30 seconds of dynamic hindlimb muscle stretch. In experiments in which RSNA was successfully recorded (11 SHAM and 15 HF-rEF rats), the  $\int\Delta$ RSNA for the first 5 sec (*i.e.*,  $\int\Delta$ RSNA<sub>5sec</sub>) of the stretch maneuver was significantly larger ( $P=0.04$ ) in HF-rEF compared to SHAM rats, with a trend ( $P=0.07$ , Cohen's

D=0.77, see Fig. 1D) towards a larger peak  $\Delta$ RSNA in HF-rEF rats compared to SHAM rats. Furthermore, analysis of the time course of the responses to dynamic stretch revealed significant differences between SHAM and HF-rEF rats at one time point for the  $\Delta$ RSNA, and multiple time points for both the  $\Delta$ MAP and  $\Delta$ HR (Fig. 2). The TTIs of the stretch maneuver were not different between groups (Fig. 1F). Examples of original tracings of the increase in RSNA, blood pressure and HR in response to 30 seconds of 1 Hz dynamic hindlimb skeletal muscle stretch from one SHAM rat and one HF-rEF rat are shown in Figure 3.

#### *Effect of an EP4-R antagonist on the mechanoreflex*

In SHAM ( $n=6$ ) and HF-rEF ( $n=6$ ) rats, we found that injection of the EP4-R antagonist L-161,982 into the arterial supply of the hindlimb had no effect on peak  $\Delta$ MAP, BPI, peak  $\Delta$ HR, peak  $\Delta$ RSNA, or  $\int\Delta$ RSNA<sub>5sec</sub> response to dynamic stretch (Fig. 4). Likewise, analysis of the time course of the responses to dynamic stretch revealed no effect of the EP4-R antagonist on the increase in RSNA, MAP, or HR in SHAM and HF-rEF rats (Fig. 5). The TTIs of the stretch maneuvers were not different between control and EP4-R blockade conditions in SHAM or HF-rEF rats (Fig. 4F). Baseline MAP and HR were not different between conditions in SHAM or HF-rEF rats (Table 2;  $P > 0.23$  for all).

#### *Effect of a TxA<sub>2</sub>-R antagonist on the mechanoreflex*

In SHAM rats ( $n=8$ ), we found that the injection of the TxA<sub>2</sub>-R antagonist daltroban into the arterial supply of the hindlimb had no effect on the peak  $\Delta$ MAP, BPI, peak  $\Delta$ HR, peak  $\Delta$ RSNA, or  $\int\Delta$ RSNA<sub>5sec</sub> response to dynamic stretch (Fig 6). Conversely, in HF-rEF rats ( $n=11$ ), we found that the injection of the TxA<sub>2</sub>-R antagonist into the arterial supply of the hindlimb significantly reduced the peak  $\Delta$ MAP, BPI,  $\int\Delta$ RSNA<sub>5sec</sub>, and peak  $\Delta$ HR response to dynamic stretch. There was no effect of TxA<sub>2</sub>-R blockade on the peak  $\Delta$ RSNA response to stretch in HF-rEF rats (Fig. 6). Analysis of the time course of the responses to stretch revealed that TxA<sub>2</sub>-R blockade had no effect in SHAM rats, but significantly reduced the increase in RSNA, MAP, and HR at various time points throughout the maneuver in HF-rEF rats (Fig. 7). The TTIs of the stretch maneuvers were not different between control and TxA<sub>2</sub>-R blockade conditions in either SHAM rats or HF-rEF rats (Fig. 6F). Baseline MAP and HR were not different between conditions in SHAM or HF-rEF rats (Table 2;  $P > 0.59$  for all).

#### *Control experiments*



In four HF-rEF rats, we investigated the effect of injection of 1% DMSO in 0.4 mL saline (*i.e.*, the vehicle for daltroban) into the arterial supply of the hindlimb on the pressor and cardioaccelerator response to dynamic stretch. We found that 1% DMSO had no effect on the peak  $\Delta$ MAP (control:  $22 \pm 6$ , 1% DMSO:  $28 \pm 9$  mmHg;  $P=0.16$ ), BPI (control:  $390 \pm 129$ , 1% DMSO:  $536 \pm 186$  mmHg·s;  $P=0.22$ ), or peak  $\Delta$ HR (control:  $13 \pm 5$ , 1% DMSO:  $18 \pm 6$  bpm;  $P=0.16$ ) response to dynamic stretch. The TTIs of the stretch maneuvers were not different between control ( $17 \pm 2$  kg·s) and 1% DMSO ( $18 \pm 2$  kg·s;  $P=0.25$ ) conditions. Baseline MAP (Control:  $90 \pm 6$ ; 1% DMSO:  $91 \pm 9$  mmHg,  $P=0.96$ ) and HR (Control:  $447 \pm 17$ ; 1% DMSO:  $446 \pm 17$  bpm,  $P=0.81$ ) were not different between conditions. These findings suggest that the attenuating effect of daltroban produced when it was injected into the arterial supply of the hindlimb of HF-rEF rats was not attributable to effects produced by its vehicle 1% DMSO.

In four HF-rEF rats, we investigated the effect of intravenous (*i.v.*) injection of daltroban on the pressor and cardioaccelerator response to dynamic stretch. We found that *i.v.* injection of daltroban had no effect on the peak  $\Delta$ MAP (control:  $30 \pm 8$ , daltroban *i.v.*:  $34 \pm 10$  mmHg;  $P=0.36$ ), BPI (control:  $597 \pm 154$ , daltroban *i.v.*:  $617 \pm 128$  mmHg·s;  $P=0.81$ ), or peak  $\Delta$ HR (control:  $19 \pm 5$ , daltroban *i.v.*:  $19 \pm 3$  bpm;  $P=0.77$ ) response to dynamic stretch. The TTIs of the stretch maneuvers were not different between control ( $16 \pm 2$  kg·s) and daltroban *i.v.* ( $16 \pm 2$  kg·s;  $P=0.65$ ) conditions. Baseline MAP (control:  $96 \pm 10$ ; daltroban *i.v.*:  $92 \pm 7$  mmHg,  $P=0.77$ ) and HR (control:  $447 \pm 18$ ; daltroban *i.v.*:  $458 \pm 16$  bpm,  $P=0.31$ ) were not different between conditions. These findings suggest that the attenuating effect of daltroban produced when it was injected into the arterial supply of the hindlimb of HF-rEF rats is most likely attributable to blockade of  $\text{TxA}_2\text{-R}$  on the sensory endings of thin fiber muscle afferents and not systemic effects elsewhere in the mechanoreflex arc such as the brainstem and/or the spinal cord.

## **2.5 Discussion**

We investigated the effect of HF-rEF on the reflex sympathetic and cardiovascular responses to dynamic mechanoreflex activation isolated from acute contraction-induced metabolite production, and the possible roles played by EP-4s and  $\text{TxA}_2\text{-Rs}$  in producing those responses. Consistent with our hypothesis, we found that, in HF-rEF rats, the increase in RSNA, blood pressure, and HR in response to 1 Hz dynamic hindlimb skeletal muscle stretch was greater than the increases observed in healthy SHAM rats. Moreover, we found that hindlimb arterial injection of an antagonist for  $\text{TxA}_2\text{-Rs}$ , but not EP4-Rs, reduced the exaggerated responses to

dynamic hindlimb muscle stretch in HF-rEF rats, whereas there was no effect of either antagonist in SHAM rats. The present findings suggest that, in HF-rEF rats,  $\text{TxA}_2$ -Rs on the sensory endings of thin fibre muscle afferents contribute to a chronic sensitization of the mechanically activated channels that underlie dynamic mechanoreflex activation. The findings enhance our understanding of the altered reflex control of the sympathetic nervous system and cardiovascular system during exercise in HF-rEF patients.

The isolated mechanoreflex protocol used in the present investigation produces a rhythmic mechanical stimulus similar in pattern and magnitude to the mechanical stimulus present during electrically-induced dynamic skeletal muscle contractions with this same decerebrate rat model (38). The protocol resulted in substantial reflex increases in RSNA and MAP. The reflex increases in HR were relatively modest when considered in relation to the high resting HR in the rat. Our present finding that the sympathetic and cardiovascular responses to 1 Hz repetitive/dynamic skeletal muscle stretch were exaggerated in HF-rEF rats compared to SHAM rats builds upon several previous findings in which various models of isolated intermittent/dynamic mechanoreflex activation have been used in HF-rEF subjects. Koba, Xing, Sinoway and Li (24) found that the increase in RSNA and lumbar SNA averaged across 12 individual, one-second duration hindlimb muscle stretches was larger in HF-rEF rats compared to healthy rats. Middlekauff et al. (50) found that three minutes of passive wrist flexion (30 times/min) produced larger increases in muscle SNA (MSNA) in HF-rEF patients than in aged-matched healthy counterparts, an effect later attributed to a sensitization of mechanoreceptors by COX products of arachidonic metabolism (30). More recently, Antunes-Correa, Nobre, Groehs, Alves, Fernandes, Couto, Rondon, Oliveira, Lima, Mathias, Brum, Mady, Almeida, Rossoni, Oliveira, Middlekauff and Negrao (22) found that passive knee joint flexion/extension (30 times/min) produced a larger increase in MSNA in HF-rEF patients before exercise training compared to after exercise training. Those prior studies provided valuable information regarding the augmented mechanoreflex control of SNA in HF-rEF. However, the various isolated intermittent/dynamic mechanoreflex models produced little to no change in cardiovascular variables. In contrast, Witman et al. (51) found that continuous 1 Hz passive knee joint flexion/extension produced larger increases in HR in healthy control subjects than in HF-rEF patients, whereas the increase in MAP was not different between groups. The reason for the differences between the present investigation and that of Witman, Ives, Trinity,

Groot, Stehlik and Richardson (51) is unclear but may include the pharmacological therapies of the HF-rEF patients.

The present investigation employed established and validated experimental protocols (see Methods) to examine the role played by EP4-Rs and TxA<sub>2</sub>-Rs on the sensory endings of thin fibre muscle afferents during isolated dynamic mechanoreflex reflex activation in SHAM and HF-rEF rats. In SHAM rats, we found that hindlimb arterial injection of the EP4-R antagonist had no effect on the sympathetic, pressor, or cardioaccelerator response to dynamic stretch, which is consistent with our recent findings (39). Those findings are similar to previous findings in SHAM/healthy rats in which EP4-R blockade had no effect on the sympathetic and/or pressor responses to static hindlimb muscle stretch (31, 47), or static hindlimb muscle contraction (47, 52). Moreover, our present finding in SHAM rats that the hindlimb arterial injection of the TxA<sub>2</sub>-R antagonist had no effect on the pressor response to dynamic hindlimb muscle stretch is consistent with our recent investigations in which dynamic (39) and static (31) hindlimb stretch was performed. Collectively, the present results, and the bulk of the available literature (31, 37, 39, 40, 47), suggest that EP4-Rs and TxA<sub>2</sub>-Rs on the sensory endings of thin fibre muscle afferents in SHAM/healthy rats do not produce a chronic sensitization of the mechanically activated channels that underlie isolated static or dynamic mechanoreflex activation.

The present investigation of the role played by EP4-Rs and TxA<sub>2</sub>-Rs during dynamic mechanoreflex activation in HF-rEF rats was undertaken to shed further mechanistic light on previous findings suggesting a role for COX metabolism in the exaggerated sympathetic responses to dynamic mechanoreflex/exercise pressor reflex activation in HF-rEF subjects (22, 29, 30). Our finding in HF-rEF rats that the EP4-R antagonist had no effect on the sympathetic, pressor, or cardioaccelerator response to dynamic hindlimb muscle stretch extends our recent findings in HF-rEF rats that the same EP4-R blockade protocol had no effect on the reflex responses to static hindlimb muscle stretch (31). Moreover, the present findings are consistent with our recent investigation in which EP4-R blockade had no effect on the pressor response to dynamic stretch in a rats with simulated peripheral artery disease (PAD, 39). The possibility that redundancy among various receptors on the sensory endings of thin fibre muscle afferents may have masked a role for EP4-Rs in the exaggerated mechanoreflex in HF-rEF rats should also be considered (53). Furthermore, a role for EP4-Rs in the exaggerated exercise pressor reflex in HF-rEF may yet exist, wherein contraction-induced increases in metabolite production (*e.g.*, PGE<sub>2</sub>) results in EP4-R

stimulation. In support of this notion, Scott et al. (54) showed that, compared with age-matched control subjects, HF-rEF patients had a greater concentration of PGE<sub>2</sub> and PGF<sub>1α</sub> within venous effluent from rhythmically contracting forearm muscles, a maneuver that resulted in larger increases in HR and ventilation in HF-rEF patients compared to age-matched healthy control subject. Moreover, the PGE<sub>2</sub> and PGF<sub>1α</sub> concentrations correlated positively with the contraction-induced increase in ventilation in HF-rEF patients (54).

Our present finding in HF-rEF rats that hindlimb arterial injection of the TxA<sub>2</sub>-R antagonist daltroban reduced the sympathetic, pressor, and cardioaccelerator response to dynamic stretch is consistent with our recent report that daltroban reduced the pressor and cardioaccelerator response to dynamic stretch in rats with simulated PAD (39). Our present finding stands in contrast, however, to our recent finding that daltroban had no effect on the reflex responses to static hindlimb muscle stretch in HF-rEF rats (31). The contrasting findings related to the role played by TxA<sub>2</sub>-Rs during different mechanoreflex modalities may be best explained by the fact that the different modalities may activate substantially different classes of mechanically activated channels, and that, in HF-rEF, TxA<sub>2</sub>-R signaling may modulate the function of the channels that are stimulated to a greater extent during dynamic compared to static mechanoreflex activation. There is at least indirect support for this explanation in the literature. For example, Nakamoto and Matsukawa (33) suggested that some mechanically activated channels associated with the mechanoreflex are located within the belly of skeletal muscles and respond primarily to changes in muscle length whereas others are located near myotendinous junctions and respond primarily to muscle tension generation. More recently, Copp et al. (55) found that, in healthy rats, the tarantula peptide GsMTx4 (a modulator of mechanically gated channel function that is partially selective for specific classes of channels including piezo channels, 56) reduced the pressor response only during the very early phase of static hindlimb muscle stretch when muscle length changed rapidly. In a follow-up study, Sanderson, Rollins, Hopkins, Butenas, Felice, Ade and Copp (32) found that GsMTx4 reduced the pressor response throughout the duration of dynamic rat hindlimb muscle stretch wherein muscle length changed repetitively. Based on the findings above, it is reasonable to speculate that, in HF-rEF rats, TxA<sub>2</sub>-Rs on the sensory endings of thin fibre muscle afferents mediate a chronic sensitization of the mechanically activated channels that respond primarily to changes in muscle length; the identity of which may include piezo channels. It is also possible that

TxA<sub>2</sub>-Rs are expressed differently on sensory neurons innervating different regions of the muscle (*i.e.*, muscle belly vs. myotendinous junction). These possibilities remain to be investigated.

The specific mechanism that results in the TxA<sub>2</sub>-R mediated mechanoreflex sensitization in HF-rEF rats is unknown. An increase in the expression of TxA<sub>2</sub>-Rs on sensory endings of muscle afferents does not appear to contribute, however, as we previously reported no difference between SHAM and HF-rEF rats in TxA<sub>2</sub>-R protein or mRNA expression in lumbar dorsal root ganglia tissue (31). We should note, however, that in heart failure patients, exercise training reduced mechanoreflex control of MSNA and TxA<sub>2</sub>-R gene expression in skeletal muscle homogenates (22). A possible explanation for the effect of daltroban in HF-rEF rats in this study is that the development of HF-rEF resulted in increased basal levels of COX products of arachidonic metabolism. There is at least indirect evidence supporting this notion. For example, we (31) and others (25, 29) have reported greater COX-2 protein expression within skeletal muscle homogenates of HF-rEF patients/animals compared to healthy controls. Another possible explanation is that an amplification of inositol trisphosphate (IP<sub>3</sub>) and diacylglycerol signaling (the G protein-coupled signaling pathways associated with TxA<sub>2</sub>-Rs) within sensory neuron endings may exist in HF-rEF rats compared to SHAM rats. Possible HF-rEF-induced alterations in IP<sub>3</sub> signaling within the sensory ending of thin fibre muscle afferents, for example, may result in an increased cytosolic calcium concentration which, in turn, may sensitize mechanically activated channels (57). Whether the effect of TxA<sub>2</sub>-R inhibition in HF-rEF rats presented herein reflects an alteration in IP<sub>3</sub> second messaging remains unclear.

A few experimental considerations should be noted. First, the rat hindlimb stretch model of isolated mechanoreflex activation is that it divorces mechanical stimuli from the influence of acute contraction-induced metabolite production. Thus, hindlimb muscle stretch allows for investigation of the presence and mechanisms of chronic sensitization of mechanically activated channels. A limitation of the model is that it stimulates mechanically activated channels differently than they are stimulated when skeletal muscles contract and intramuscular pressure increases (58). Importantly, however, Stone et al. (53) found that the vast majority (*i.e.*, >86%) of the muscle afferents that respond to rat hindlimb muscle stretch also respond to hindlimb muscle contraction. Moreover, investigations that have identified a mechanism that modulates the reflex responses to rat hindlimb muscle stretch have consistently found that mechanism also modulates the reflex responses to hindlimb muscle contraction (23, 45, 48, 55, 59-67). Second, RSNA was not

measured in the vehicle and systemic control experiments. We elected to perform the vehicle and systemic control protocols in experiments in which technical factors precluded successful RSNA recording in order to maximize the statistical power of the RSNA comparisons in the main experimental protocols. Finally, HF-rEF patients constitute roughly half of all patients with heart failure (68). Whether our present findings extend to patients with heart failure with preserved ejection fraction and/or non-ischemic heart failure remains unknown.

## **2.6 Conclusion**

In the present investigation, we found that the sympathetic, pressor, and cardioaccelerator responses to 1 Hz dynamic hindlimb muscle stretch were larger in rats with HF-rEF compared to the responses in SHAM operated healthy control rats. Furthermore, we found that the hindlimb arterial injection of a TxA<sub>2</sub>-R antagonist, but not an EP<sub>4</sub>-R antagonist, reduced the exaggerated responses to dynamic hindlimb muscle stretch in HF-rEF rats. The data suggest that TxA<sub>2</sub>-Rs on the sensory endings of thin fiber muscle afferents contribute to a chronic sensitization of the mechanically activated channels that underlie dynamic/rhythmic mechanoreflex activation. The data enhance our understanding of the reflex control of the sympathetic nervous system during dynamic exercise and the mechanistic underpinnings of exercise intolerance and cardiovascular risk for the over 26 million people worldwide with HF-rEF (8).

**Funding:** This work was supported by National Institutes of Health grant R01 HL-142877 (to SWC) and a Kansas Academy of Sciences grant (to ALEB).

## 2.7 References

1. **Leimbach WN, Jr., Wallin BG, Victor RG, Aylward PE, Sundlof G, and Mark AL.** Direct evidence from intraneural recordings for increased central sympathetic outflow in patients with heart failure. *Circulation* 73: 913-919, 1986.
2. **Notarius CF, Ando S, Rongen GA, and Floras JS.** Resting muscle sympathetic nerve activity and peak oxygen uptake in heart failure and normal subjects. *Eur Heart J* 20: 880-887, 1999.
3. **Murai H, Takamura M, Maruyama M, Nakano M, Ikeda T, Kobayashi D, Otowa K, Ootsuji H, Okajima M, Furusho H, Takata S, and Kaneko S.** Altered firing pattern of single-unit muscle sympathetic nerve activity during handgrip exercise in chronic heart failure. *J Physiol* 587: 2613-2622, 2009.
4. **Notarius CF, Millar PJ, Keir DA, Murai H, Haruki N, O'Donnell E, Marzolini S, Oh P, and Floras JS.** Training heart failure patients with reduced ejection fraction attenuates muscle sympathetic nerve activation during mild dynamic exercise. *Am J Physiol Regul Integr Comp Physiol* 317: R503-R512, 2019.
5. **Piepoli M, Clark AL, Volterrani M, Adamopoulos S, Sleight P, and Coats AJ.** Contribution of muscle afferents to the hemodynamic, autonomic, and ventilatory responses to exercise in patients with chronic heart failure: effects of physical training. *Circulation* 93: 940-952, 1996.
6. **Barretto AC, Santos AC, Munhoz R, Rondon MU, Franco FG, Trombetta IC, Roveda F, de Matos LN, Braga AM, Middlekauff HR, and Negrao CE.** Increased muscle sympathetic nerve activity predicts mortality in heart failure patients. *Int J Cardiol* 135: 302-307, 2009.
7. **Borlaug BA.** The pathophysiology of heart failure with preserved ejection fraction. *Nat Rev Cardiol* 11: 507-515, 2014.
8. **Ponikowski P, Anker SD, AlHabib KF, Cowie MR, Force TL, Hu S, Jaarsma T, Krum H, Rastogi V, Rohde LE, Samal UC, Shimokawa H, Budi Siswanto B, Sliwa K, and Filippatos G.** Heart failure: preventing disease and death worldwide. *ESC Heart Fail* 1: 4-25, 2014.
9. **Sinoway LI, and Li J.** A perspective on the muscle reflex: implications for congestive heart failure. *J Appl Physiol (1985)* 99: 5-22, 2005.
10. **McCloskey DI, and Mitchell JH.** Reflex cardiovascular and respiratory responses originating in exercising muscle. *J Physiol* 224: 173-186, 1972.

11. **Kaufman MP, Longhurst JC, Rybicki KJ, Wallach JH, and Mitchell JH.** Effects of static muscular contraction on impulse activity of groups III and IV afferents in cats. *JApplPhysiol* 55: 105-112, 1983.
12. **Kaufman MP, Iwamoto GA, Longhurst JC, and Mitchell JH.** Effects of capsaicin and bradykinin on afferent fibers with endings in skeletal muscle. *CircRes* 50: 133-139, 1982.
13. **Kaufman MP, Rybicki KJ, Waldrop TG, and Ordway GA.** Effect of ischemia on responses of group III and IV afferents to contraction. *JApplPhysiol* 57: 644-650, 1984.
14. **Piepoli MF, and Crisafulli A.** Pathophysiology of human heart failure: importance of skeletal muscle myopathy and reflexes. *Exp Physiol* 99: 609-615, 2014.
15. **Murphy MN, Mizuno M, Mitchell JH, and Smith SA.** Cardiovascular regulation by skeletal muscle reflexes in health and disease. *Am J Physiol Heart Circ Physiol* 301: H1191-1204, 2011.
16. **Amann M, Venturelli M, Ives SJ, Morgan DE, Gmelch B, Witman MA, Jonathan Groot H, Walter Wray D, Stehlik J, and Richardson RS.** Group III/IV muscle afferents impair limb blood in patients with chronic heart failure. *Int J Cardiol* 174: 368-375, 2014.
17. **Ives SJ, Amann M, Venturelli M, Witman MA, Groot HJ, Wray DW, Morgan DE, Stehlik J, and Richardson RS.** The Mechanoreflex and Hemodynamic Response to Passive Leg Movement in Heart Failure. *Med Sci Sports Exerc* 48: 368-376, 2016.
18. **Kaur J, Senador D, Krishnan AC, Hanna HW, Alvarez A, Machado TM, and O'Leary DS.** Muscle metaboreflex-induced vasoconstriction in the ischemic active muscle is exaggerated in heart failure. *Am J Physiol Heart Circ Physiol* 314: H11-H18, 2018.
19. **O'Leary DS, Sala-Mercado JA, Augustyniak RA, Hammond RL, Rossi NF, and Ansoorge EJ.** Impaired muscle metaboreflex-induced increases in ventricular function in heart failure. *AmJPhysiol Heart CircPhysiol* 287: H2612-H2618, 2004.
20. **Smith JR, Joyner MJ, Curry TB, Borlaug BA, Keller-Ross ML, Van Iterson EH, and Olson TP.** Locomotor muscle group III/IV afferents constrain stroke volume and contribute to exercise intolerance in human heart failure. *J Physiol* 2020.
21. **Middlekauff HR, Nitzsche EU, Hoh CK, Hamilton MA, Fonarow GC, Hage A, and Moriguchi JD.** Exaggerated muscle mechanoreflex control of reflex renal vasoconstriction in heart failure. *JApplPhysiol* 90: 1714-1719, 2001.



22. **Antunes-Correa LM, Nobre TS, Groehs RV, Alves MJ, Fernandes T, Couto GK, Rondon MU, Oliveira P, Lima M, Mathias W, Brum PC, Mady C, Almeida DR, Rossoni LV, Oliveira EM, Middlekauff HR, and Negrao CE.** Molecular basis for the improvement in muscle metaboreflex and mechanoreflex control in exercise-trained humans with chronic heart failure. *Am J Physiol Heart Circ Physiol* 307: H1655-1666, 2014.
23. **Smith SA, Mitchell JH, Naseem RH, and Garry MG.** Mechanoreflex mediates the exaggerated exercise pressor reflex in heart failure. *Circulation* 112: 2293-2300, 2005.
24. **Koba S, Xing J, Sinoway LI, and Li J.** Sympathetic nerve responses to muscle contraction and stretch in ischemic heart failure. *Am J Physiol Heart Circ Physiol* 294: H311-321, 2008.
25. **Morales A, Gao W, Lu J, Xing J, and Li J.** Muscle cyclo-oxygenase-2 pathway contributes to the exaggerated muscle mechanoreflex in rats with congestive heart failure. *Exp Physiol* 97: 943-954, 2012.
26. **Li J, Sinoway AN, Gao Z, Maile MD, Pu M, and Sinoway LI.** Muscle mechanoreflex and metaboreflex responses after myocardial infarction in rats. *Circulation* 110: 3049-3054, 2004.
27. **Wang HJ, Li YL, Gao L, Zucker IH, and Wang W.** Alteration in skeletal muscle afferents in rats with chronic heart failure. *J Physiol* 588: 5033-5047, 2010.
28. **Stebbins CL, Brown B, Levin D, and Longhurst JC.** Reflex effect of skeletal muscle mechanoreceptor stimulation on the cardiovascular system. *J Appl Physiol* 65: 1539-1547, 1988.
29. **Smith JR, Hart CR, Ramos PA, Akinsanya JG, Lanza IR, Joyner MJ, Curry TB, and Olson TP.** Metabo- and mechanoreceptor expression in human heart failure: Relationships with the locomotor muscle afferent influence on exercise responses. *Exp Physiol* 2020.
30. **Middlekauff HR, Chiu J, Hamilton MA, Fonarow GC, Maclellan WR, Hage A, Moriguchi J, and Patel J.** Cyclooxygenase products sensitize muscle mechanoreceptors in humans with heart failure. *Am J Physiol Heart Circ Physiol* 294: H1956-1962, 2008.
31. **Butenas ALE, Rollins KS, Matney JE, Williams AC, Kleweno TE, Parr SK, Hammond ST, Ade CJ, Hageman KS, Musch TI, and Copp SW.** No effect of endoperoxide 4 or thromboxane A2 receptor blockade on static mechanoreflex activation in rats with heart failure. *Exp Physiol* 2020.

32. **Sanderson BC, Rollins KS, Hopkins TD, Butenas AL, Felice KP, Ade CJ, and Copp SW.** GsMTx4 reduces the reflex pressor response during dynamic hindlimb skeletal muscle stretch in decerebrate rats. *Physiol Rep* 7: e13974, 2019.
33. **Nakamoto T, and Matsukawa K.** Muscle mechanosensitive receptors close to the myotendinous junction of the Achilles tendon elicit a pressor reflex. *J Appl Physiol* (1985) 102: 2112-2120, 2007.
34. **Drew L, Wood JN, and Cesare P.** Distinct mechanosensitive properties of capsaicin-sensitive and -insensitive sensory neurons. *The Journal of neuroscience : the official journal of the Society for Neuroscience* 22: RC228-RC232, 2002.
35. **Lewin GR, and Moshourab R.** Mechanosensation and pain. *J Neurobiol* 61: 30-44, 2004.
36. **Wood JN, and Eijkelkamp N.** Noxious mechanosensation - molecules and circuits. *Curr Opin Pharmacol* 12: 4-8, 2012.
37. **Butenas ALE, Hopkins TD, Rollins KS, Felice KP, and Copp SW.** Investigation of the mechanisms of cyclooxygenase-mediated mechanoreflex sensitization in a rat model of simulated peripheral artery disease. *Am J Physiol Heart Circ Physiol* 317: H1050-H1061, 2019.
38. **Kempf EA, Rollins KS, Hopkins TD, Butenas AL, Santin JM, Smith JR, and Copp SW.** Chronic femoral artery ligation exaggerates the pressor and sympathetic nerve responses during dynamic skeletal muscle stretch in decerebrate rats. *Am J Physiol Heart Circ Physiol* 314: H246-H254, 2018.
39. **Rollins KS, Butenas ALE, Felice KP, Matney JEM, Williams AC, Kleweno TE, and Copp SW.** Thromboxane A2 Receptors Mediate Chronic Mechanoreflex Sensitization in a Rat Model of Simulated Peripheral Artery Disease. *Am J Physiol Heart Circ Physiol* 2020.
40. **Rollins KS, Hopkins TD, Butenas AL, Felice KP, Ade CJ, and Copp SW.** Cyclooxygenase inhibition does not impact the pressor response during static or dynamic mechanoreflex activation in healthy decerebrate rats. *Am J Physiol Regul Integr Comp Physiol* 317: R369-R378, 2019.
41. **National Research Council (U.S.). Committee for the Update of the Guide for the Care and Use of Laboratory Animals., Institute for Laboratory Animal Research (U.S.), and National Academies Press (U.S.).** Guide for the care and use of laboratory animals. Washington, D.C.: National Academies Press., 2011, p. xxv, 220 p.

42. **Musch TI, and Terrell JA.** Skeletal muscle blood flow abnormalities in rats with a chronic myocardial infarction: rest and exercise. *AmJPhysiol* 262: H411-H419, 1992.
43. **Craig JC, Colburn TD, Caldwell JT, Hirai DM, Tabuchi A, Baumfalk DR, Behnke BJ, Ade CJ, Musch TI, and Poole DC.** Central and peripheral factors mechanistically linked to exercise intolerance in heart failure with reduced ejection fraction. *Am J Physiol Heart Circ Physiol* 317: H434-H444, 2019.
44. **Smith SA, Mitchell JH, and Garry MG.** Electrically induced static exercise elicits a pressor response in the decerebrate rat. *JPhysiol* 537: 961-970, 2001.
45. **Copp SW, Kim JS, Ruiz-Velasco V, and Kaufman MP.** The mechano-gated channel inhibitor GsMTx4 reduces the exercise pressor reflex in rats with ligated femoral arteries. *Am J Physiol Heart Circ Physiol* 310: H1233-1241, 2016.
46. **Daniels JW, Stebbins CL, and Longhurst JC.** Hemodynamic responses to static and dynamic muscle contractions at equivalent workloads. *AmJPhysiol* 279 (5): R1849-R1855, 2000.
47. **Yamauchi K, Kim JS, Stone AJ, Ruiz-Velasco V, and Kaufman MP.** Endoperoxide 4 receptors play a role in evoking the exercise pressor reflex in rats with simulated peripheral artery disease. *J Physiol* 591: 2949-2962, 2013.
48. **Leal AK, McCord JL, Tsuchimochi H, and Kaufman MP.** Blockade of the TP receptor attenuates the exercise pressor reflex in decerebrated rats with chronic femoral artery occlusion. *AmJPhysiol Heart CircPhysiol* 301: H2140-H2146, 2011.
49. **Craig JC, Colburn TD, Hirai DM, Musch TI, and Poole DC.** Sexual dimorphism in the control of skeletal muscle interstitial Po<sub>2</sub> of heart failure rats: effects of dietary nitrate supplementation. *J Appl Physiol (1985)* 126: 1184-1192, 2019.
50. **Middlekauff HR, Chiu J, Hamilton MA, Fonarow GC, Maclellan WR, Hage A, Moriguchi J, and Patel J.** Muscle mechanoreceptor sensitivity in heart failure. *AmJPhysiol Heart CircPhysiol* 287: H1937-H1943, 2004.
51. **Witman MA, Ives SJ, Trinity JD, Groot HJ, Stehlik J, and Richardson RS.** Heart failure and movement-induced hemodynamics: partitioning the impact of central and peripheral dysfunction. *Int J Cardiol* 178: 232-238, 2015.
52. **Stone AJ, Copp SW, Kim JS, and Kaufman MP.** Combined, but not individual, blockade of ASIC3, P2X, and EP4 receptors attenuates the exercise pressor reflex in rats with freely perfused hindlimb muscles. *J Appl Physiol (1985)* 119: 1330-1336, 2015.

53. **Stone AJ, Copp SW, McCord JL, and Kaufman MP.** Femoral artery ligation increases the responses of thin-fiber muscle afferents to contraction. *J Neurophysiol* 113: 3961-3966, 2015.
54. **Scott AC, Wensel R, Davos CH, Kemp M, Kaczmarek A, Hooper J, Coats AJ, and Piepoli MF.** Chemical mediators of the muscle ergoreflex in chronic heart failure: a putative role for prostaglandins in reflex ventilatory control. *Circulation* 106: 214-220, 2002.
55. **Copp SW, Kim JS, Ruiz-Velasco V, and Kaufman MP.** The mechano-gated channel inhibitor GsMTx4 reduces the exercise pressor reflex in decerebrate rats. *J Physiol* 594: 641-655, 2016.
56. **Bae C, Sachs F, and Gottlieb PA.** The mechanosensitive ion channel Piezo1 is inhibited by the peptide GsMTx4. *Biochemistry* 50: 6295-6300, 2011.
57. **Zhuang GZ, Keeler B, Grant J, Bianchi L, Fu ES, Zhang YP, Erasso DM, Cui JG, Wiltshire T, Li Q, Hao S, Sarantopoulos KD, Candiotti K, Wishnek SM, Smith SB, Maixner W, Diatchenko L, Martin ER, and Levitt RC.** Carbonic anhydrase-8 regulates inflammatory pain by inhibiting the ITPR1-cytosolic free calcium pathway. *PLoS one* 10: e0118273, 2015.
58. **Gallagher KM, Fadel PJ, Smith SA, Norton KH, Query RG, Olivencia-Yurvati A, and Raven PB.** Increases in intramuscular pressure raise arterial blood pressure during dynamic exercise. *J Appl Physiol (1985)* 91: 2351-2358, 2001.
59. **McCord JL, Tsuchimochi H, Yamauchi K, Leal A, and Kaufman MP.** Tempol attenuates the exercise pressor reflex independently of neutralizing reactive oxygen species in femoral artery ligated rats. *J Appl Physiol (1985)* 111: 971-979, 2011.
60. **Tsuchimochi H, Yamauchi K, McCord JL, and Kaufman MP.** Blockade of acid sensing ion channels attenuates the augmented exercise pressor reflex in rats with chronic femoral artery occlusion. *J Physiol* 589: 6173-6189, 2011.
61. **Yamauchi K, Stone AJ, Stocker SD, and Kaufman MP.** Blockade of ATP-sensitive potassium channels prevents the attenuation of the exercise pressor reflex by tempol in rats with ligated femoral arteries. *Am J Physiol Heart Circ Physiol* 303: H332-340, 2012.
62. **Smith SA, Mammen PP, Mitchell JH, and Garry MG.** Role of the exercise pressor reflex in rats with dilated cardiomyopathy. *Circulation* 108: 1126-1132, 2003.
63. **Downey RM, Mizuno M, Mitchell JH, Vongpatanasin W, and Smith SA.** Mineralocorticoid receptor antagonists attenuate exaggerated exercise pressor reflex responses in hypertensive rats. *Am J Physiol Heart Circ Physiol* 313: H788-H794, 2017.

64. **Nakamoto T, and Matsukawa K.** Muscle receptors close to the myotendinous junction play a role in eliciting exercise pressor reflex during contraction. *Auton Neurosci* 138: 99-107, 2008.
65. **Schiller AM, Hong J, Xia Z, and Wang HJ.** Increased Brain-Derived Neurotrophic Factor in Lumbar Dorsal Root Ganglia Contributes to the Enhanced Exercise Pressor Reflex in Heart Failure. *Int J Mol Sci* 20: 2019.
66. **Wang HJ, Wang W, Patel KP, Rozanski GJ, and Zucker IH.** Spinal cord GABA receptors modulate the exercise pressor reflex in decerebrate rats. *Am J Physiol Regul Integr Comp Physiol* 305: R42-49, 2013.
67. **Kim JS, and Kaufman MP.** Stimulation of spinal delta-opioid receptors attenuates the exercise pressor reflex in decerebrate rats. *Am J Physiol Regul Integr Comp Physiol* 316: R727-R734, 2019.
68. **Owan TE, Hodge DO, Herges RM, Jacobsen SJ, Roger VL, and Redfield MM.** Trends in prevalence and outcome of heart failure with preserved ejection fraction. *N Engl J Med* 355: 251-259, 2006.

### Table 2.1

Table 2.1. Body and tissue weights and heart morphometrics in SHAM and HF-rEF rats

|                           | SHAM (n=14) | HF-rEF (n=23) | P-Value |
|---------------------------|-------------|---------------|---------|
| Body weight (g)           | 502 ± 16    | 503 ± 8       | 0.39    |
| Lung/body weight (mg/g)   | 3.19 ± 0.12 | 3.51 ± 0.13   | 0.05*   |
| RV/body weight (mg/g)     | 0.55 ± 0.02 | 0.59 ± 0.02   | 0.07    |
| LV/body weight (mg/g)     | 1.92 ± 0.10 | 1.90 ± 0.03   | 0.41    |
| Atria/body weight (mg/g)  | 0.20 ± 0.01 | 0.26 ± 0.02   | 0.03*   |
| LV EDV (mL)               | 1.28 ± 0.08 | 2.12 ± 0.14   | <0.01*  |
| LV ESV (mL)               | 0.23 ± 0.04 | 1.13 ± 0.11   | <0.01*  |
| Stroke volume (mL)        | 1.05 ± 0.05 | 0.96 ± 0.05   | 0.12    |
| Fractional shortening (%) | 48 ± 2      | 22 ± 1        | <0.01*  |
| Ejection fraction (%)     | 83 ± 2      | 49 ± 2        | <0.01*  |
| Infarct size (%)          | -           | 28 ± 2        | -       |

---

Values are means  $\pm$  SEM. LV, left ventricle; RV, right ventricle; EDV, end diastolic volume; ESV, end systolic volume. Data were compared using student's t-test or Mann-Whitney tests as appropriate. Asterisks indicate a statistically significant difference between groups.

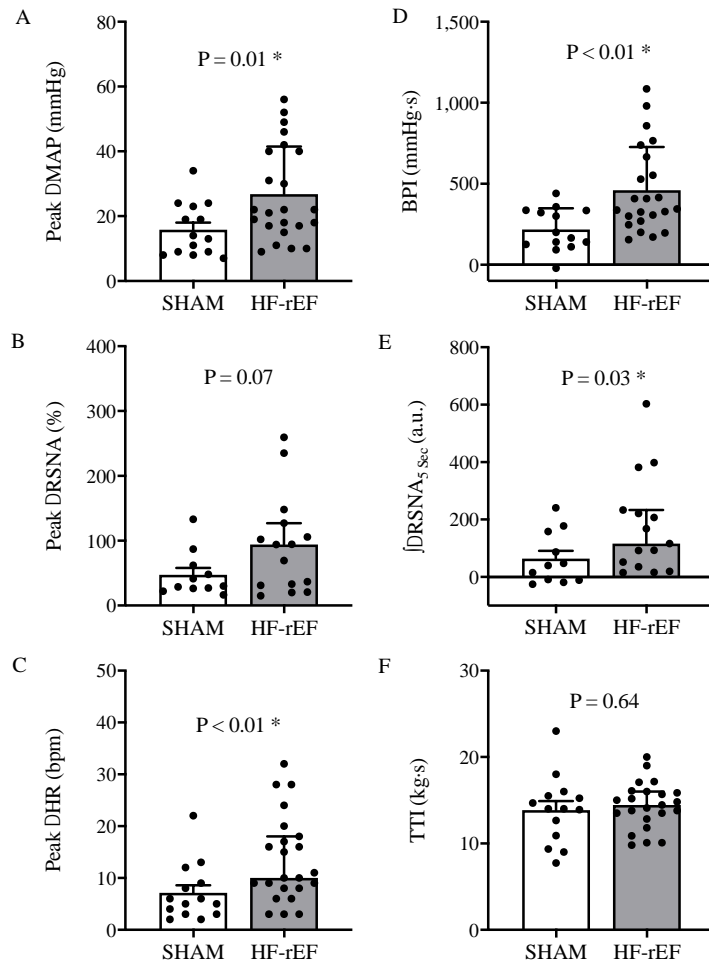
**Table 2.2**

Table 2.2. Baseline MAP and HR in SHAM and HF-rEF rats.

|                      | MAP (mmHg) | HR (bpm) |
|----------------------|------------|----------|
| <u>SHAM (n=6)</u>    |            |          |
| Control              | 103 ± 4    | 492 ± 12 |
| Post L-161,982       | 92 ± 3     | 477 ± 9  |
| <u>HF-rEF (n=6)</u>  |            |          |
| Control              | 90 ± 7     | 495 ± 11 |
| Post L-161,982       | 94 ± 6     | 495 ± 15 |
| <u>SHAM (n=9)</u>    |            |          |
| Control              | 89 ± 5     | 493 ± 17 |
| Post daltroban       | 87 ± 4     | 496 ± 19 |
| <u>HF-rEF (n=11)</u> |            |          |
| Control              | 92 ± 5     | 486 ± 9  |
| Post daltroban       | 90 ± 5     | 490 ± 9  |

Values are means ± SEM. MAP, mean arterial pressure; HR, heart rate. Data were compared with Sidak multiple comparisons tests. There was no significant difference for any comparison.

**Figure 2.1**



*Figure 1: Effect of HF-rEF on the sympathetic and cardiovascular responses to dynamic mechanoreflex activation. The peak  $\Delta$  mean arterial pressure (MAP; A), peak  $\Delta$  renal sympathetic nerve activity (RSNA; B), peak  $\Delta$  heart rate (HR; C), blood pressure index (BPI, D), and the first 5 seconds of the integrated change in RSNA ( $\int \Delta$ RSNA<sub>5sec</sub>, E) in response to 30 seconds of dynamic hindlimb muscle stretch in SHAM ( $n=14$ ) and HF-rEF ( $n=23$ ) rats. TTI, tension-time index. Data were analyzed with Student's *t*-tests or Mann-Whitney tests as appropriate and are expressed as mean $\pm$ SEM with individual data points. Asterisks indicates statistically significant differences between groups.*



**Figure 2.2**

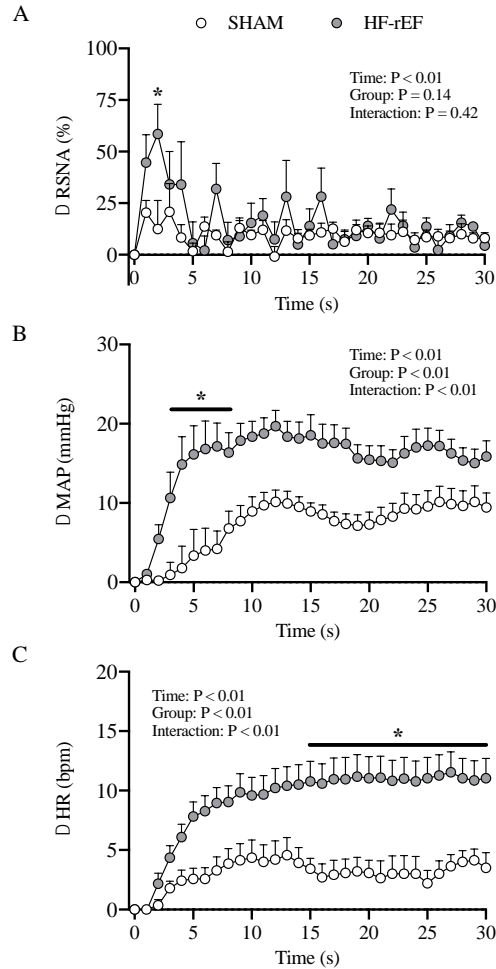


*Figure 2: Effect of HF-rEF on the time course of the reflex sympathetic and cardiovascular responses to dynamic mechanoreflex activation. The  $\Delta$  renal sympathetic nerve activity (RSNA; A),  $\Delta$  mean arterial pressure (MAP; B), and  $\Delta$  heart rate (HR; C) response to 30 seconds of dynamic hindlimb muscle stretch in SHAM (n=14) and HF-rEF (n=23) rats. Data were analyzed with two-way ANOVAs with Sidak multiple comparisons tests and are expressed as mean $\pm$ SEM. Asterisks and/or black lines indicate time points where comparisons were statistically significant ( $P < 0.05$ ).*

**Figure 2.3**

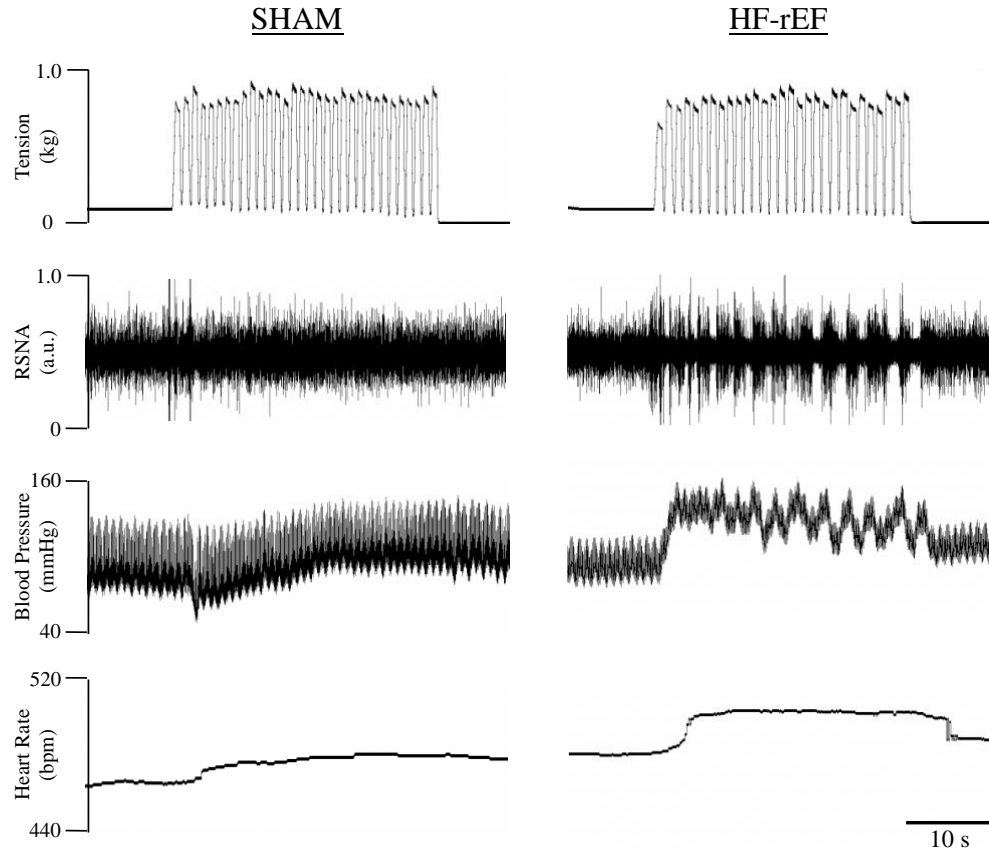


*Figure 3: Examples of original tracings of the renal sympathetic nerve activity (RSNA), blood pressure (BP) and heart rate (HR) response to 30 seconds of dynamic hindlimb muscle stretch in a SHAM rat (left) and HF-rEF rat (right).*

**Figure 2.4**

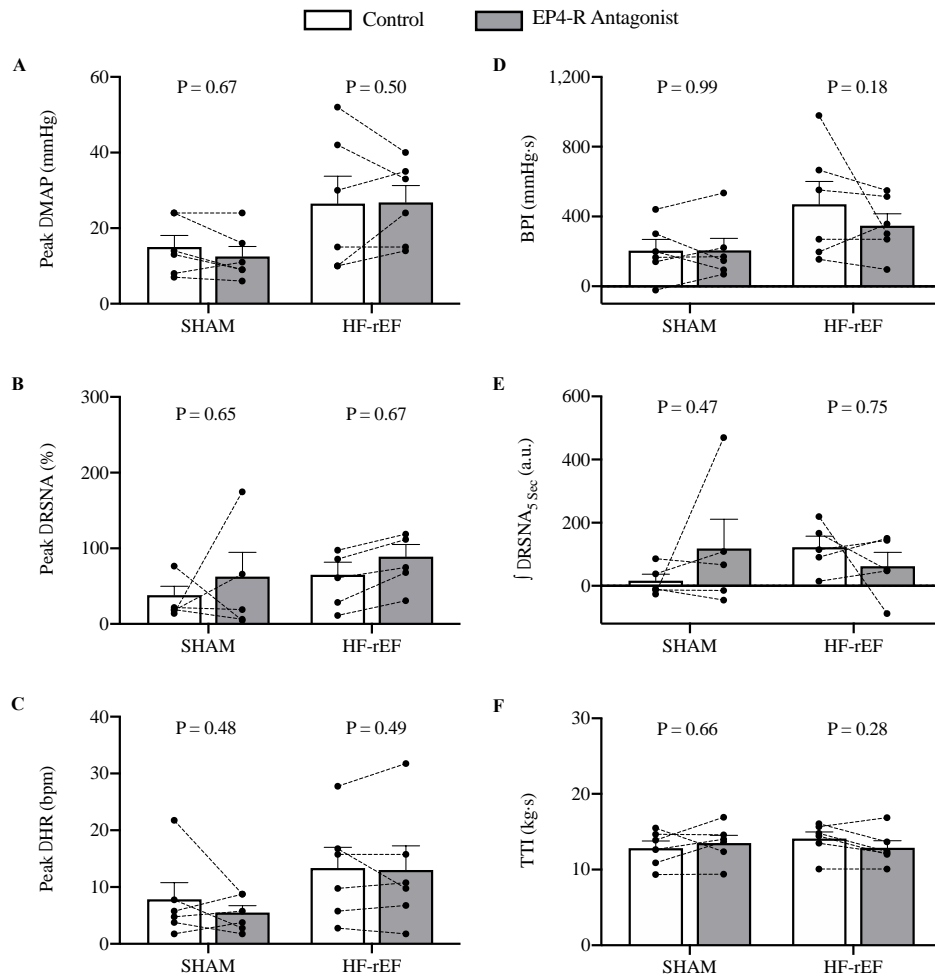


*Figure 4: Effect of EP4-R blockade on the sympathetic and cardiovascular responses to dynamic mechanoreflex activation. The peak  $\Delta$  mean arterial pressure (MAP; A), peak  $\Delta$  renal sympathetic nerve activity (RSNA; B), peak  $\Delta$  heart rate (HR; C), blood pressure index (BPI, D), and the first 5 seconds of the integrated change in RSNA ( $\int \Delta$ RSNA<sub>5sec</sub>, E) in response to 30 seconds of dynamic hindlimb muscle stretch before (Control) and after injection of the EP4-R antagonist L-161,982 (1  $\mu$ g) into the arterial supply of the hindlimb in SHAM (n=6) and HF-rEF (n=6) rats. TTI, tension-time index. Data were analyzed with Sidak multiple comparisons tests and are expressed as mean $\pm$ SEM overlaid with individual responses.*

**Figure 2.5**

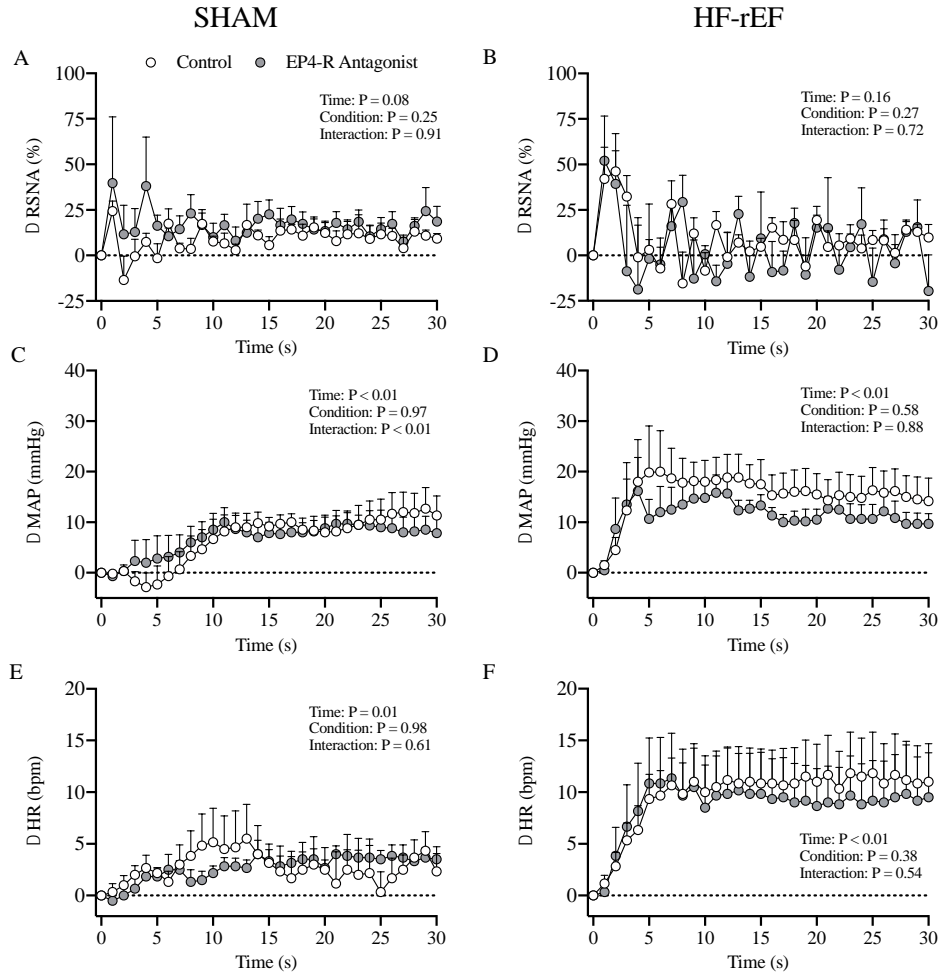
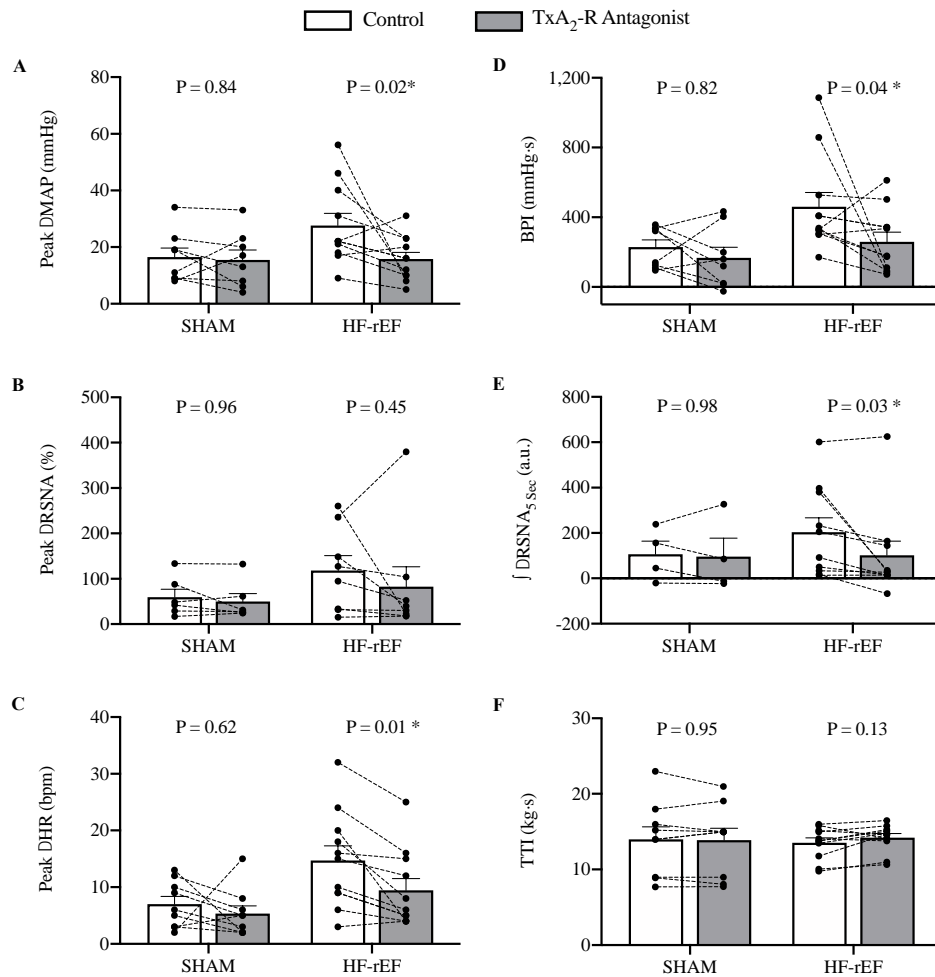


Figure 5: *Effect of EP4-R blockade on the time courses of the sympathetic and cardiovascular responses to dynamic mechanoreflex activation.* The  $\Delta$  renal sympathetic nerve activity (RSNA; A & B),  $\Delta$  mean arterial pressure (MAP; C & D), and  $\Delta$  heart rate (HR; E & F) response to 30 seconds of dynamic hindlimb muscle stretch before (Control) and after injection of 1  $\mu$ g of the EP4-R antagonist L-161,982 into the arterial supply of the hindlimb in SHAM (n=6) and HF-rEF (n=6) rats. Data were analyzed with two-way ANOVAs and Sidak multiple comparisons tests and are expressed as mean $\pm$ SEM.

**Figure 2.6**



*Figure 6: Effect of TxA<sub>2</sub>-R blockade on the sympathetic and cardiovascular responses to dynamic mechanoreflex activation. The peak  $\Delta$  mean arterial pressure (MAP; A), peak  $\Delta$  renal sympathetic nerve activity (RSNA; B), peak  $\Delta$  heart rate (HR; C), blood pressure index (BPI, D), and the first 5 seconds of the integrated change in RSNA ( $\int\Delta$ RSNA<sub>5sec</sub>, E) in response to 30 seconds of dynamic hindlimb muscle stretch before (Control) and after injection of the TxA<sub>2</sub>-R antagonist daltroban (80  $\mu$ g) into the arterial supply of the hindlimb in SHAM (n=8) and HF-rEF (n=11) rats. TTI, tension-time index. Data were analyzed with Sidak multiple comparisons tests and are expressed as mean $\pm$ SEM overlaid with individual responses. Asterisks indicate statistically significant differences between groups.*

**Figure 2.7**

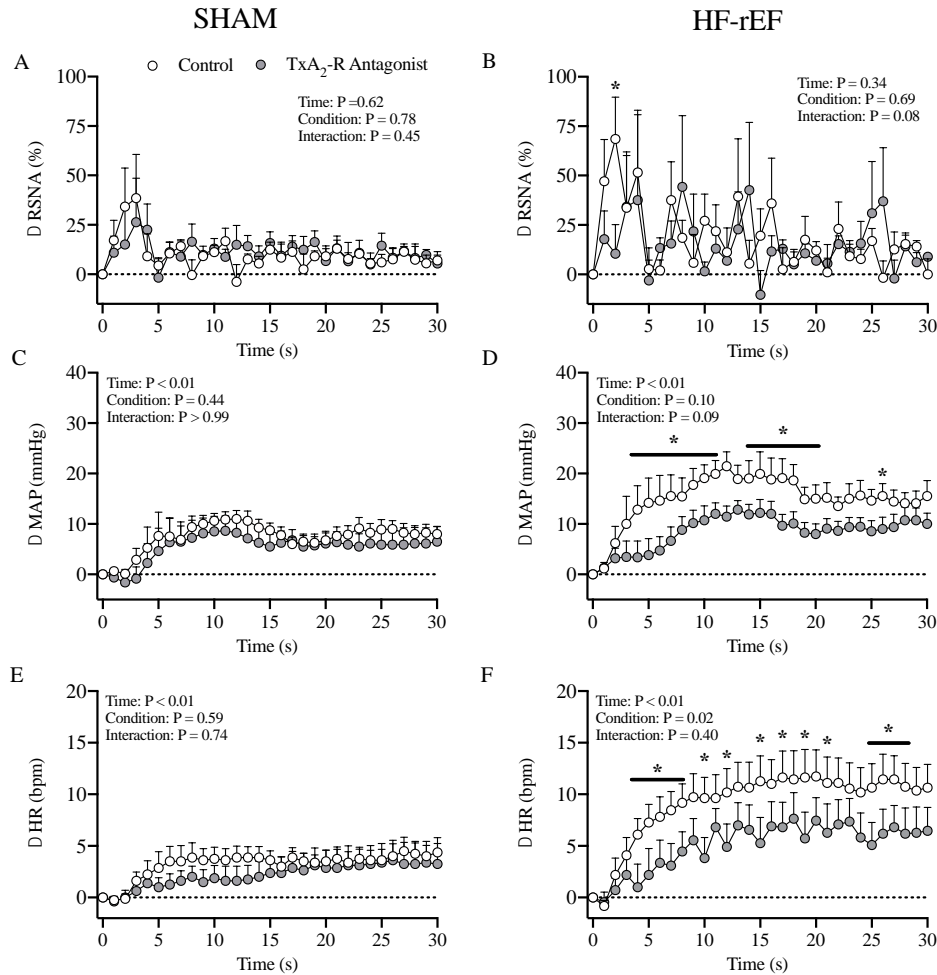


*Figure 7: Effect of TxA<sub>2</sub>-R blockade on the time courses of the sympathetic and cardiovascular responses to dynamic mechanoreflex activation.  $\Delta$  renal sympathetic nerve activity (RSNA; A & B),  $\Delta$  mean arterial pressure (MAP; C & D), and  $\Delta$  heart rate (HR; E & F) during 30 seconds of dynamic hindlimb muscle stretch before (Control) and after injection of 80  $\mu$ g of the TxA<sub>2</sub>-R antagonist (daltroban) into the arterial supply of the hindlimb in SHAM (n=8) and HF-rEF (n=11) rats. Data were analyzed with two-way ANOVAs and Sidak multiple comparisons tests and are expressed as mean $\pm$ SEM. Asterisks and/or black lines indicate time points where comparisons were statistically significant (P < 0.05).*

## **Chapter 3 - Thromboxane A<sub>2</sub> receptors contribute to the exaggerated exercise pressor reflex in male rats with heart failure**

### **3.1 Abstract**

Mechanical and metabolic signals associated with skeletal muscle contraction stimulate the sensory endings of thin fiber muscle afferents and produce reflex increases in sympathetic nerve activity and blood pressure during exercise (*i.e.*, the exercise pressor reflex; EPR). The EPR is exaggerated in patients and animals with heart failure with reduced ejection fraction (HF-rEF) and its activation contributes to reduced exercise capacity within this patient population. Accumulating evidence suggests that the exaggerated EPR in HF-rEF is partially attributable to a sensitization of mechanically activated channels produced by thromboxane A<sub>2</sub> receptors (TxA<sub>2</sub>-Rs) on those sensory endings, however this has not been investigated. Accordingly, the purpose of this investigation was to determine the role played by TxA<sub>2</sub>-Rs on the sensory endings of thin fiber muscle afferents in the exaggerated EPR in rats with HF-rEF induced by coronary artery ligation. In decerebrate, unanesthetized rats, we found that injection of the TxA<sub>2</sub>-R antagonist daltroban (80µg) into the arterial supply of the hindlimb reduced the pressor response to 30 seconds of electrically-induced 1 Hz dynamic hindlimb muscle contraction in HF-rEF ( $n=8$ , peak  $\Delta$ MAP pre:  $22\pm 3$ ; post:  $14\pm 2$  mmHg;  $P=0.01$ ) but not sham ( $n=10$ , peak  $\Delta$ MAP pre:  $13\pm 3$ ; post:  $11\pm 2$  mmHg;  $P=0.68$ ) rats. In a separate group of HF-rEF rats ( $n=4$ ), we found that the systemic (intravenous) injection of daltroban had no effect on the EPR (peak  $\Delta$ MAP pre:  $26\pm 7$ ; post:  $25\pm 7$  mmHg;  $P=0.50$ ). Our data suggest that TxA<sub>2</sub>-Rs on thin fiber muscle afferents contribute to the exaggerated EPR evoked in response to dynamic muscle contraction in HF-rEF.

### **3.2 Introduction**

Heart failure with reduced ejection fraction (HF-rEF) may develop following myocardial damage and result in systemic manifestations that include increased sympathetic nervous system activity (SNA) at rest (1, 2) and during exercise (3, 4), as well as reduced exercise capacity (5). The elevated SNA during exercise in heart failure contributes importantly to the exercise intolerance within this patient population (6). While the mechanisms underlying the exaggerated sympathetic responses to exercise in HF-rEF patients are complex and multifaceted, a significant body of literature indicates a key role for the exercise pressor reflex (7). The exercise pressor reflex is activated when the sensory endings of group III and IV thin fiber muscle afferents are stimulated

by mechanical and/or metabolic signals associated with skeletal muscle contraction (8-11), and in healthy populations, contributes importantly to appropriate increases in SNA, heart rate (HR) and blood pressure (8, 9, 12-18). In contrast to healthy populations, the exercise pressor reflex is exaggerated in HF-rEF, and its activation impairs oxygen delivery to contracting skeletal muscles (6, 17, 19-21), thereby reducing exercise capacity in this patient population (17). Thus, there is pressing need to investigate the mechanisms of exaggerated exercise pressor reflex activation in HF-rEF patients.

The mechanically sensitive portion of the exercise pressor reflex (i.e., the mechanoreflex) contributes importantly to the overall exercise pressor reflex exaggeration in HF-rEF (22-26). Our laboratory has used a dynamic rat hindlimb skeletal muscle stretch experimental model, adapted from Stebbins and colleagues (27, 28), to study the mechanisms of mechanoreflex activation isolated from contraction-induced metabolic influence (29-33). This dynamic mechanoreflex activation model in which hindlimb skeletal muscles are stretched at a 1 Hz frequency for 30 seconds replicates the rhythmic nature of the mechanical stimulus present during locomotory skeletal muscle contractions. Using this model, we found recently that the reflex increases in renal sympathetic nerve activity (RSNA), blood pressure, and heart rate (HR) in response to muscle stretch were greater in rats with HF-rEF compared with sham-operated healthy control rats (34). Moreover, we found that blockade of thromboxane A<sub>2</sub> receptors (TxA<sub>2</sub>-Rs), a key receptor for cyclooxygenase (COX) metabolites, on sensory endings of thin fiber muscle afferents reduced the sympathetic and cardiovascular responses to hindlimb skeletal muscle stretch in rats with HF-rEF but not in healthy rats (34). We also reported recently that skeletal muscle COX-2 isoform protein expression, but not skeletal muscle COX-1 isoform or dorsal root ganglia TxA<sub>2</sub>-R protein expression, was greater in HF-rEF rats than in healthy control rats. Those findings collectively suggest that TxA<sub>2</sub>-R signaling contributes importantly to a chronic or persistent sensitization of the mechanically activated channels that underlie dynamic/rhythmic mechanoreflex activation; an effect that is most likely attributable to HF-rEF-induced elevations in COX-2 metabolites within skeletal muscles. That conclusion built upon a significant body of prior work establishing a role for COX signaling in the exaggerated exercise pressor reflex and mechanoreflex in HF-rEF patients (25, 35-37) and animals (25).

Several critical extensions of our recent work summarized above (34) remains to be investigated. First, although the hindlimb muscle stretch model of mechanoreflex activation may



provide valuable information regarding the presence of chronic mechanoreflex sensitization in rats with HF-rEF, the model activates mechanically activated channels in a non-physiological manner. As such, we sought to determine whether the exaggerated sympathetic and cardiovascular responses to 1 Hz hindlimb muscle stretch in rats with HF-rEF translated to exaggerated responses to dynamic muscle contraction which produces physiological mechanoreflex activation consequent to muscle shortening and concurrent increases in intramuscular pressure (38). Second, whether the role for TxA<sub>2</sub>-Rs in producing the exaggerated responses to 1 Hz muscle stretch extends to experiments evoking 1 Hz muscle contraction is unknown. Lastly, whether HF-rEF-induced elevations in skeletal muscle COX-2 protein expression translate into elevated basal levels of COX metabolites within the skeletal muscle interstitial space remains unknown. Accordingly, we tested the following hypotheses in decerebrate, unanesthetized rats: 1) 30 s of 1 Hz dynamic hindlimb skeletal muscle contraction would result in greater reflex increases in RSNA, mean arterial pressure (MAP), and HR in HF-rEF rats compared to sham-operated (SHAM) healthy control rats, 2) injection of the TxA<sub>2</sub>-R antagonist daltroban (80 µg) into the arterial supply of the hindlimb would reduce the contraction-induced reflex increases in RSNA, MAP, and HR in HF-rEF rats but not SHAM rats, and 3) basal skeletal muscle interstitial concentrations of the COX metabolites prostaglandin E<sub>2</sub> (PGE<sub>2</sub>) and TxB<sub>2</sub> (a stable derivative of TxA<sub>2</sub>) would be greater in HF-rEF rats compared with SHAM rats.

### **3.3 Methods**

#### *Ethical Approval.*

All experimental procedures were approved by the Institutional Animal Care and Use Committee of Kansas State University and conducted in accordance with the National Institutes of Health Guide for the Care and Use of Laboratory Animals (39). Experiments were performed on ~14-19-week-old male Sprague-Dawley rats (n=60; Charles River Laboratories). Rats were housed two per cage in temperature (maintained at ~22°C) and light (12-12 hour light-dark cycle running from 7 AM to 7 PM)-controlled accredited facilities with standard rat chow and water provided ad libitum.

#### *Surgical Procedure.*

Myocardial infarction (MI) was induced in 29 of the 60 rats by surgically ligating the left main coronary artery (40). Briefly, rats were anesthetized initially with a 5% isoflurane-O<sub>2</sub> mixture (Butler Animal Health Supply, Elk Grove Village, IL, and Linweld, Dallas, TX) and maintained

subsequently on 2.5% isoflurane-O<sub>2</sub> and then intubated and mechanically ventilated with a rodent respirator (Harvard model 680, Harvard Instruments, Holliston, MA) for the duration of the surgical procedure. After a single injection of amiodarone (100 mg/kg ip), a left thoracotomy was performed to expose the heart through the fifth intercostal space, and the left main coronary artery was ligated 1–2 mm distal to the edge of the left atrium with a 6-0 braided polyester suture. The thorax was then closed with 2-0 gut, and the skin was closed with 2-0 silk. Prior to termination of anesthesia, bupivacaine (1.5 mg/kg sc) and buprenorphine (~0.03 mg/kg im) were administered to reduce pain associated with the surgery, along with ampicillin (50 mg/kg im) to reduce the risk of infection. After rats were removed from mechanical ventilation and anesthesia, they were monitored closely for ~6 h post-surgery. In the remaining 31 of 60 rats, a sham ligation of the coronary artery was performed in which 6-0 braided polyester suture was passed under the left main coronary artery, but not tied. These rats are referred to as “SHAM” rats from this point forward. Following completion of either MI or SHAM procedures, rats were housed one per cage for ten days to minimize risk of infection of the surgical site. During these ten days, the antibiotic baytril (100 mg/mL) was administered in the drinking water. Following completion of the baytril treatment, rats were housed two per cage as described above. All animals were monitored daily for 14 days following MI or SHAM procedure for changes in behavior, gait/posture, breathing, appetite and body weight.

#### *Echocardiograph Measurements.*

Transthoracic echocardiograph measurements were performed with a commercially available system (Logiq S8; GE Health Care, Milwaukee, WI) no more than one week before the final experimental protocol. Briefly, the rats were anaesthetized as described above. Once the rat was fully anesthetized, the isoflurane mixture was reduced to 2.5% isoflurane-O<sub>2</sub>. Following 5 minutes at 2.5% isoflurane, echocardiograph measurements began. The transducer was positioned on the left anterior chest, and left ventricular dimensions were measured. The left ventricular fractional shortening (FS), ejection fraction (EF), end diastolic (LVEDV), end systolic volume (LVESV), and stroke volume (SV) were determined by echocardiographic measurements as previously described (41). Rats with HF-rEF were required to meet an inclusion criterion of either an FS  $\leq$  30% and/or a left ventricular infarct size of  $\geq$  15%, which is consistent with values previously reported from our laboratory (26, 34, 42). We have previously shown that, compared

with SHAM operated healthy control rats, HF-rEF rats that meet similar criterion have a reduced maximal oxygen uptake and time to exhaustion to treadmill running (42).

#### *Surgical Procedures for Experimental Protocols.*

In vivo experiments were performed on 34 rats (15 SHAM, 19 HF-rEF) between six and eight weeks following the MI or SHAM procedure. On the day of the experiment, rats were anesthetized as described above. Adequate depth of anesthesia was confirmed by the absence of toe-pinch and blink reflexes. The trachea was cannulated, and the lungs were mechanically ventilated (Harvard Apparatus, Holliston, MA) with a 2% isoflurane-balance O<sub>2</sub> gaseous mixture until the decerebration was completed (see below). The right jugular vein and both carotid arteries were cannulated with PE-50 catheters which were used for the injection of fluids, measurement of arterial blood pressure (physiological pressure transducer, AD Instruments), and sampling of arterial blood gasses (Radiometer). HR was calculated from the R-R interval measured by electrocardiogram (AD Instruments). The left superficial epigastric artery was cannulated with a PE-8 catheter whose tip was placed near the junction of the superficial epigastric and femoral arteries. A reversible snare was placed around the left iliac artery and vein (i.e., proximal to the location of the catheter placed in the superficial epigastric artery). The left calcaneal bone was severed and linked by string to a force transducer (Grass FT03), which, in turn, was attached to a rack and pinion. An ~1-2 cm section of the left sciatic nerve was exposed by reflecting back the overlying skeletal muscles.

Upon completion of the initial surgical procedures, rats were placed in a Kopf stereotaxic frame. After administering dexamethasone (0.2 mg i.v.) to minimize swelling of the brainstem, a pre-collicular decerebration was performed in which all brain tissue rostral to the superior colliculi was removed (43). Following decerebration, anesthesia was reduced to 0.5%. A retroperitoneal approach was used to expose bundles of the left renal sympathetic nerve, which were then glued (Kwik-Sil, World Precision Instruments) onto a pair of thin stainless-steel recording electrodes connected to a high impedance probe (Grass Model HZP) and amplifier (Grass P511). Multiunit signals from the renal sympathetic nerve fibers were filtered at high and low frequencies (1 KHz and 100 Hz, respectively) for the measurement of RSNA. Successful RSNA recordings were made in 13 SHAM rats and 13 HF-rEF rats.

Upon completion of all surgical procedures, anesthesia was terminated, and the rats' lungs were ventilated with room air. Experimental protocols commenced at least one hour after reduction

of isoflurane from 2% to 0.5%, and at least 30 minutes after reduction of isoflurane from 0.5% to 0%. Experiments were performed on decerebrate, unanesthetized rats because anesthesia has been shown to markedly blunt the exercise pressor reflex in the rat (43). Body core temperature was measured via a rectal probe and maintained at ~37–38°C by an automated heating system (Harvard Apparatus) and heat lamp. Arterial pH and blood gases were analyzed periodically throughout the experiment from arterial blood samples (~75  $\mu$ L) and maintained within physiological ranges (pH: 7.35–7.45, PCO<sub>2</sub>: ~38–40 mmHg, PO<sub>2</sub>: ~100 mmHg) by administration of sodium bicarbonate and/or adjusting ventilation as necessary. At the end of all experiments in which RSNA was measured, postganglionic sympathetic nerve activity was abolished with administration of hexamethonium bromide (20 mg/kg iv) to allow for the quantification of background noise as described previously (30). Rats were then anaesthetized with 5% isoflurane and humanely euthanized with an injection of potassium chloride (>3 mg/kg ia). A pneumothorax was then performed, and the heart was excised. The atria and right ventricle (RV) were separated from the left ventricle (LV) and septum, and the RV, LV, and atria were weighed. In rats with HF-rEF, the LV infarction surface area was measured using planimetry and expressed as percent of LV endocardial surface area as described previously (44).

#### *Exercise pressor reflex protocols.*

In 34 rats (15 SHAM, 19 HF-rEF), we studied the exercise pressor reflex evoked in response to 1 Hz dynamic hindlimb muscle contraction. Following recovery of isoflurane anesthesia, baseline muscle tension was set to ~100 g and baseline RSNA, blood pressure, and HR were measured for ~30 seconds. The sciatic nerve was then electrically stimulated using stainless steel electrodes for 30 seconds at a voltage of ~1.5x motor threshold (0.01 ms pulse duration, 500 ms train duration, 40 Hz frequency) which produced 1 Hz repetitive/dynamic contractions of the triceps surae muscles. In 18 of these 35 rats (10 SHAM, 8 HF-rEF) we investigated the effect of TxA<sub>2</sub>-R blockade on the exercise pressor reflex. In these 18 rats, ~10 minutes following the control contraction maneuver, the snare on the left iliac artery and vein was tightened and the TxA<sub>2</sub>-R antagonist daltroban (Santa Cruz Biotechnology, Inc.; 80  $\mu$ g dissolved in 0.4 mL of 1% DMSO/saline solution; 45) was injected into the arterial supply of the hindlimb through the superficial epigastric artery catheter. Daltroban remained snared in the hindlimb circulation for 5 minutes, at which time the iliac snare was released. The hindlimb was reperfused for 10 minutes and the dynamic contraction maneuver was then repeated exactly as described above. At the end

of all experiments, we injected the paralytic pancuronium bromide (1 mg/kg i.v.) and the sciatic nerve was stimulated for 30 seconds with the same parameters as those used to elicit contraction to ensure that the increase in RSNA, blood pressure, and HR during contraction was not due to the electrical activation of the axons of the thin fiber muscle afferents in the sciatic nerve. No increase in RSNA, blood pressure or HR, were observed during the stimulation period following the administration of pancuronium bromide. Additionally, at the end of each experiment Evans blue dye was injected in the same manner as the experimental solution to confirm that the injectate had access to the triceps surae muscle circulation. The triceps surae muscles were observed to stain blue in all experiments.

#### *Control experiments.*

In four of the 19 HF-rEF rats in which the exercise pressor reflex was evoked, we investigated whether 1% DMSO (i.e., the vehicle for daltroban) or a systemic circulation of daltroban may have accounted for the attenuating effects in the main experimental group in which daltroban was injected into the hindlimb arterial circulation. In these four rats, the DMSO and the intravenous injection protocols were performed in series with ~10 min recovery time between protocols. The 1% DMSO protocols were performed exactly as described above for the daltroban experiments except 0.4 mL of 1% DMSO alone was injected into the arterial supply of the hindlimb via the left superficial epigastric artery catheter. The systemic circulation control protocols were performed as described above except 80 µg of daltroban was injected into the catheter placed in the jugular vein. The dynamic hindlimb muscle contraction maneuver was then performed 15 min after injection to match the timing of the daltroban injection into the arterial supply of the hindlimb described above.

#### *Muscle microdialysis to measure PGE<sub>2</sub>.*

Microdialysis experiments were performed on a total of 22 rats (SHAM n=11, HF-rEF n=9). Briefly, microdialysis probes (LM-10, BASi Research Products) were connected to a PE-50 tubing which was attached to an adaptor tip and syringe filled with sterile physiological saline. Immediately following the decerebration and termination of anesthesia, one microdialysis probe was inserted into the white portion of the gastrocnemius muscle with a 20-gauge hollow needle. At least one hour of recovery was allowed following probe placement before beginning the microdialysis protocol. Following the one-hour recovery period, sterile saline was perfused through the probes at a constant rate of 5 µl/min. Baseline dialysate fluid was collected for 25

minutes in order to measure baseline concentrations for PGE2 and TxB2 (i.e., the stable derivative of TxA2). Microdialysate fluid was stored immediately after collection at -80°C freezer until further analysis using the commercially available ELISA kits for PGE2 (Cayman Chemical; Item no. 514010) and TxB2 (Cayman Chemical; Item no. 501020).

#### *Cyclooxygenase (COX)-2 activity analysis*

Enzyme activity experiments were performed on a sample of nine rats (4 SHAM, 5 HF-rEF). A tissue sample (~180 mg) from the white portion of the gastrocnemius muscle was collected from the right hindlimb. Samples were rinsed with 0.1 M TRIS-Buffer (pH 7.4), and homogenized in 1 ml of 0.1 M TRIS-HCl, pH 7.8, containing 1 mM EDTA for 1 min at 5 m/s using 2 ml tubes containing ~0.5 g of 1.4 mm ceramic beads using Bead Mill 4 (Fisherbrand™). Samples were then centrifuged at 10,000 x g for 15 min at 4° C. The supernatant was removed and analyzed for COX-2 activity (Cayman Chemical; Item no. 760151) according to manufacturer's instructions. Absorbance was read at 590 nm using accuSkan™ FC Filter-Based Microplate Photometer (Fisherbrand™).

#### *Western blot experiments quantitative reverse transcriptase polymerase chain reaction experiments for TxA2-R expression.*

In nine rats (4 SHAM, 4 HF-rEF) the left and right L4 and L5 DRG were harvested. Samples were isolated into 2 mL bead mill tubes containing ~0.5g of 1.4 mm ceramic beads and 300 µL of ML lysis buffer (Macherey-Nagel) and homogenized for 1 min at 5 m/s using Bead Mill 4 (Fisherbrand™). Total protein and mRNA from tissues were prepared with the Nucleospin miRNA/Protein Kit (Macherey-Nagel, Düren, Germany; Ref. no. 740971.50) according to the manufacturer's instructions. Total Protein and RNA concentrations were determined using the Qubit 2.0 Fluorometer (Life Technologies, Grand Island, NY, USA). Protein samples (40 µg) were separated on 4-12% Bis-Tris Protein Gels (Invitrogen™) by gel electrophoresis in MES running buffer (Invitrogen™) employing 220 V for 22 min. Gels were then transferred to mini-PVDF membranes using the iBlot 2 Dry Transfer Device (Invitrogen™). The membrane was incubated for ~3 hours with the iBind device with iBind solution (Invitrogen™) with the primary antibodies: anti TxA2R diluted 1:100 (Santa Cruz Biotechnology, Dallas, TX, USA; cat. no. SC-515033; RRID: AB\_2847878) and loading control antibody anti-GAPDH diluted 1:1,000 (Thermofisher Scientific; Rockford, IL, USA; cat. no. MA5-15738; RRID: AB\_10977387) as well as the secondary antibody conjugated with Horse Radish Peroxidase diluted 1:1,500 (Thermofisher

Scientific; Rockford, IL, USA; cat. no. 31430; RRID: AB\_228307). Membranes were then incubated for 5 min with SuperSignal™ West Pico PLUS Chemiluminescent Substrate (ThermoFisher) and imaged with C-DiGit® Blot Scanner (Li-Cor). The protein bands were quantified and analyzed using the Image Studio software (Li-Cor). Complementary DNA (cDNA) was synthesized from RNA isolates (see above) using the High Capacity RNA-cDNA™ kit (ThermoFisher) according to the manufacturer's instructions as described previously (46). Quantitative reverse transcriptase polymerase chain reaction experiments were then performed on the cDNA samples using TaqMan gene expression assays specific for: TxA2-R (Sequence proprietary; Assay ID: Rn00690601\_m1), and GAPDH with forward primer: 5'-ACCGCCTGTTGCGTGTTA-3' and reverse primer: 5'-CAATCGCCAACGCCTCAA-3'. All samples were run in duplicate for the gene of interest, and the endogenous control (GAPDH). The results were analyzed with the comparative threshold ( $\Delta\Delta C_t$ ) method.

#### *Data analysis.*

Muscle tension, blood pressure, HR and RSNA were measured and recorded in real time with a PowerLab and LabChart data acquisition system (AD Instruments). The original RSNA data were rectified and corrected for the background noise determined after the administration of hexamethonium bromide. Baselines for mean arterial pressure (MAP), RSNA and HR were determined from the 30-second baseline periods that preceded each maneuver. The peak increase in MAP (peak  $\Delta$ MAP), RSNA (peak  $\Delta$ RSNA), and HR (peak  $\Delta$ HR) during dynamic contraction were calculated as the difference between the peak values wherever they occurred during the maneuvers and their corresponding baseline value. The integrated RSNA for the first 5 seconds ( $\int\Delta$ RSNA 5 Sec) was calculated by integrating the  $\Delta$ RSNA ( $>0$ ) during the first 5 seconds of the contraction maneuver. The change in tension-time indexes ( $\Delta$ TTIs) and blood pressure indexes (BPIs) were calculated by integration of the area under curve during the contraction maneuver and subtracting the integrated area under the curve during the baseline period. Time courses of the increase in RSNA, MAP and HR were plotted as their change from baseline. Student's t-tests or Mann-Whitney tests were performed to compare baseline MAP, baseline HR, Peak  $\Delta$ MAP, Peak  $\Delta$ HR, Peak  $\Delta$ RSNA, BPI,  $\int\Delta$ RSNA, and  $\Delta$ TTI across groups. Šidák multiple comparisons tests were performed for within animal comparisons of those same variables. Data for echocardiograph measurements, body and organ masses, heart morphometrics, protein and mRNA expression were

analyzed with unpaired Student's t-tests or Mann-Whitney U tests as appropriate. All data are expressed as mean±SEM. Statistical significance was defined as  $P \leq 0.05$ .

### 3.4 Results

#### *Body mass and heart morphometrics.*

Body mass as well as the ratio of LV to body mass were not different between SHAM and HF-rEF rats (Table 1). The ratios of the RV and atria mass to body mass were higher in HF-rEF rats compared to SHAM rats. Additionally, LVEDV, LVESV, and SV were significantly higher, while ejection fraction and fractional shortening were significantly lower, in HF-rEF rats compared to SHAM rats.

#### *Effect of HF-rEF on the exercise pressor reflex.*

Dynamic hindlimb muscle contraction evoked larger sympathetic and cardiovascular responses in HF-rEF rats (n=19) compared with SHAM rats (n=15, Fig. 1 and 2). The TTI of the contraction maneuver was not different between groups (Fig. 1F). Examples of original tracings of the increase in blood pressure (BP) and integrated RSNA in response to 30 seconds of 1 Hz dynamic hindlimb skeletal muscle contraction from one SHAM rat and one HF-rEF rat are shown in Figure 3.

#### *Effect of TxA2-R blockade on the exercise pressor reflex.*

In SHAM rats (n=10), we found that injection of the TxA2-R antagonist daltroban into the arterial supply of the hindlimb had no effect on the sympathetic and cardiovascular responses to dynamic contraction (Fig. 4 and 5). Conversely, in HF-rEF rats (n=11), injection of daltroban into the arterial supply of the hindlimb significantly reduced the sympathetic and cardiovascular responses to dynamic contraction (Fig. 4 and 5). Figure 6 shows original tracings from two HF-rEF rats of the first five seconds of contraction demonstrating that the RSNA bursts were synchronized with muscle tension development and that the bursts were reduced following TxA2-R blockade. The TTI of the contraction maneuver was not different between control and TxA2-R blockade conditions in either SHAM or HF-rEF rats (Fig. 4F). Baseline MAP and HR were not different between conditions in SHAM or HF-rEF rats (Table 2;  $P > 0.15$  for both).

#### *Control experiments.*

In four HF-rEF rats, we found that 1% DMSO had no effect on the peak  $\Delta$ MAP (control:  $23 \pm 8$ , 1% DMSO:  $20 \pm 6$  mmHg;  $P=0.40$ ), BPI (control:  $463 \pm 224$ , 1% DMSO:  $335 \pm 133$  mmHg·s;  $P=0.26$ ), or peak  $\Delta$ HR (control:  $27 \pm 8$ , 1% DMSO:  $24 \pm 6$  bpm;  $P=0.75$ ) response to dynamic



contraction. The TTI of the contraction maneuver was not different between control ( $11 \pm 1$  kg·s) and 1% DMSO ( $11 \pm 2$  kg·s;  $P=0.57$ ) conditions. Baseline MAP and HR were not different between conditions (Table 2). These findings suggest that the attenuating effect of daltroban produced when it was injected into the arterial supply of the hindlimb of HF-rEF rats was not attributable to effects produced by its vehicle 1% DMSO.

In the same four HF-rEF rats used in 1% DMSO experiments, we found that i.v. injection of daltroban had no effect on the peak  $\Delta$ MAP (control:  $26 \pm 7$ , daltroban i.v.:  $25 \pm 7$  mmHg;  $P=0.50$ ), BPI (control:  $362 \pm 132$ , daltroban i.v.:  $490 \pm 213$  mmHg·s;  $P=0.22$ ), or peak  $\Delta$ HR (control:  $20 \pm 4$ , daltroban i.v.:  $28 \pm 8$  bpm;  $P=0.28$ ) response to dynamic contraction. The TTI of the contraction maneuver was not different between control ( $11 \pm 2$  kg·s) and daltroban i.v. ( $12 \pm 1$  kg·s;  $P=0.65$ ) conditions. Baseline MAP and HR were not different between conditions (Table 2). These findings suggest that the attenuating effect of daltroban produced when it was injected into the arterial supply of the hindlimb of HF-rEF rats is most likely attributable to blockade of TxA2-R on the sensory endings of thin fiber muscle afferents and not systemic effects elsewhere in the exercise pressor reflex arc such as the brainstem and/or the spinal cord.

*Basal skeletal muscle interstitial PGE2 and TxB2 concentrations and COX-2 activity.*

In 11 SHAM rats and 9 HF-rEF rats, we found that baseline microdialysate fluid concentrations from the white portion of the gastrocnemius muscle for PGE2 as well as TxB2 were not different (Fig. 7A). Further, in different rats not used in microdialysis experiments (4 SHAM and 5 HF-rEF) we found no difference in COX-2 enzymatic activity within skeletal muscle homogenates taken from the white portion of the gastrocnemius muscle (Fig. 7B).

*DRG TxA2-R protein and mRNA expression.*

We found no difference between SHAM ( $n=4$ ) and HF-rEF ( $n=4$ ) rats in TxA2-R protein (SHAM:  $1.00 \pm 0.49$ ; HF-rEF:  $0.72 \pm 0.44$  a.u.;  $P=0.60$ ) or mRNA expression (SHAM:  $1.00 \pm 0.07$ ; HF-rEF:  $0.93 \pm 0.09$  a.u.;  $P=0.51$ ) within L4 and L5 DRG tissue. This was an important reproduction and confirmation of the same findings reported in our recent investigation (26).

### **3.5 Discussion**

The present investigation is an important extension of our previous findings which showed that TxA2-Rs contribute to the exaggerated sympathetic and cardiovascular responses to 1 Hz dynamic hindlimb muscle stretch in rats with HF-rEF (34). Specifically, we have now extended those previous findings from the muscle stretch model of isolated mechanoreflex activation to a 1

Hz dynamic muscle contraction protocol which produces physiological mechanoreflex activation consequent to muscle shortening and intramuscular pressure development. We found that the increases in RSNA, blood pressure, and HR evoked in response to 1 Hz dynamic hindlimb skeletal muscle contraction were greater in HF-rEF rats than the increases observed in healthy SHAM rats. We also found that hindlimb arterial injection of an antagonist for TxA<sub>2</sub>-Rs reduced the exaggerated responses to hindlimb muscle contraction in HF-rEF rats, whereas there was no effect of TxA<sub>2</sub>-R antagonism in SHAM rats. In contrast to our hypothesis, we found no difference between SHAM and HF-rEF rats in resting hindlimb skeletal muscle (white portion of the gastrocnemius) interstitial concentrations for two primary agonists for TxA<sub>2</sub>-Rs (i.e., PGE<sub>2</sub> and TxB<sub>2</sub>) as well as no difference between SHAM and HF-rEF rats in basal COX-2 enzymatic activity from skeletal muscle homogenates of the same muscle region. Collectively, our findings suggest that TxA<sub>2</sub>-Rs on the sensory endings of thin fiber muscle afferents contribute to the exaggerated exercise pressor reflex in rats with HF-rEF, but that the effect does not appear attributable to augmented basal concentrations of COX metabolites within hindlimb skeletal muscles.

We used a 1 Hz dynamic hindlimb muscle contraction maneuver designed to closely replicate the frequency of muscle contractions during locomotion. This contraction maneuver presents the sensory endings of thin fiber muscle afferents with a robust mechanical stimulus as evidenced by the synchronization of RSNA bursting with skeletal muscle tension development (Fig. 3 and 6, as well as refs: 30, 46, 47), as well as by the similar increases in RSNA and blood pressure during 1 Hz dynamic stretch compared to contraction (30). A metabolic stimulus to the sensory endings of thin fiber muscle afferents during the maneuver is also possible but presumably significantly less important than the mechanical stimulus. Indeed, dynamic hindlimb muscle contraction as evoked in the present investigation markedly increases hindlimb skeletal muscle blood flow (48) which likely minimizes metabolite accumulation within the hindlimb, especially when compared to a static hindlimb muscle contraction maneuver during which blood flow is reduced compared to rest and metabolites likely accumulate to a substantial degree (49, 50). Thus, we believe the dynamic hindlimb muscle contraction maneuver is an excellent experimental model that can be used to study the exercise pressor reflex with substantial contribution from the mechanoreflex. In this regard, our present finding that the sympathetic and cardiovascular responses to dynamic muscle contraction were exaggerated in HF-rEF rats compared to SHAM rats builds upon our previous findings which showed that the sympathetic and cardiovascular

responses to 1 Hz dynamic skeletal muscle stretch were exaggerated in HF-rEF rats compared to SHAM rats (34). Our findings are also consistent with reports of greater sympathetic responses to single, one second hindlimb muscle contractions in HF-rEF rats compared to sham rats (24). Most importantly, our present findings confirm that the 1 Hz dynamic rat hindlimb muscle stretch and contraction models are valuable experimental tools that may be used to study exaggerated sympathetic/cardiovascular responses to isolated dynamic mechanoreflex activation and exercise pressor reflex activation in human HF-rEF patients (6, 51-53).

In healthy humans (54, 55) and animals (56), inhibition of the COX enzyme reduces the sympathetic and cardiovascular responses to exercise/skeletal muscle contraction. The effect of COX inhibition is attributable to, at least in part, an attenuation of the responsiveness of thin fiber muscle afferents to skeletal muscle contraction (57). Several studies have investigated the identity of the receptor(s) on sensory endings of thin fiber muscle afferents for COX metabolites that account for the attenuation of the exercise pressor reflex following COX inhibition. Specifically, inhibition of TxA<sub>2</sub>-Rs (45), but not EP<sub>3</sub>-Rs or EP<sub>4</sub>-Rs (58, 59), has been shown to reduce the exercise pressor reflex responses to static hindlimb muscle contraction in healthy rats. In contrast to the findings of Leal, McCord, Tsuchimochi and Kaufman (45), in the present investigation we found that inhibition TxA<sub>2</sub>-R had no effect on the sympathetic or cardiovascular responses to 1 Hz dynamic skeletal muscle contraction. This discrepancy may be attributed to the different modalities employed to elicit hindlimb skeletal muscle contraction (i.e., static vs. dynamic). The possibility of redundancy among the receptors evoking the exercise pressor reflex in health during dynamic contractions must also be considered (59).

Previously, we demonstrated in HF-rEF rats that hindlimb arterial injection of the TxA<sub>2</sub>-R antagonist daltraban reduced the sympathetic and cardiovascular responses to 1 Hz dynamic skeletal muscle stretch (34), but not static hindlimb skeletal muscle stretch (26). We speculated that those contrasting findings in HF-rEF rats pertaining to the role played by TxA<sub>2</sub>-Rs during different mechanoreflex modalities (i.e., static stretch vs. dynamic stretch) were best explained by the fact that these different modalities may activate substantially different classes of mechanically activated channels (for discussion, see: 34). We therefore concluded that TxA<sub>2</sub>-Rs on the sensory endings of thin fiber muscle afferents contribute to a chronic sensitization of the mechanically activated channels that underlie dynamic/rhythmic mechanoreflex activation. We now believe our present finding that TxA<sub>2</sub>-R blockade with daltraban reduced the sympathetic and cardiovascular

responses to 1 Hz dynamic skeletal muscle contraction in HF-rEF rats likely reflected that chronic sensitization of mechanically activated channels produced by TxA<sub>2</sub>-Rs. That conclusion is supported by the marked reduction of the RSNA bursts that were synchronized to muscle tension development in HF-rEF rats following TxA<sub>2</sub>-R blockade, especially within the first five seconds (see Figure 6). An acute sensitization of mechanically activated channels produced by contraction-induced elevations in COX metabolites (57, 60), as well as a small role for TxA<sub>2</sub>-R in the metaboreflex component of the exercise pressor reflex in HF-rEF rats is also possible (45). If present, those actions may have occurred additively with the chronic sensitization to produce the overall TxA<sub>2</sub>-R mediated effects in our experiments.

The precise mechanism behind the chronic mechanoreflex sensitization produced by TxA<sub>2</sub>-Rs in HF-rEF remains unclear. In the present investigation we found no difference between SHAM and HF-rEF rats in TxA<sub>2</sub>-R protein or mRNA expression in lumbar DRG which is an important reproduction of our recent findings (26). Thus, it does not appear that an increased expression of TxA<sub>2</sub>-Rs on the sensory endings of thin fiber muscle afferents accounts for the TxA<sub>2</sub>-R mediated chronic mechanoreflex sensitization in HF-rEF. An increased basal concentration of COX products of arachidonic metabolism in HF-rEF may have offered an alternative explanation for the TxA<sub>2</sub>-R mediated chronic mechanoreflex sensitization. We hypothesized as much based on previous findings showing elevated COX-2 protein expression within skeletal muscle homogenates of HF-rEF patients/animals compared with controls (25, 26, 35). Specifically, we hypothesized that HF-rEF would result in higher levels of basal COX-2 metabolites within the white portion of the gastrocnemius muscle compared to SHAM counterparts. We selected this region of the triceps surae muscle as this muscle region has been shown specifically to have elevated COX-2 protein expression in HF-rEF rats compared with healthy controls (25, 26). In contrast to our hypothesis, we found that basal microdialysate fluid concentrations for PGE<sub>2</sub> and TxB<sub>2</sub> from the white portion of the gastrocnemius muscle were not different between SHAM and HF-rEF rats. This is generally consistent with the findings of Scott et al. (61) who reported no difference in venous effluent concentrations from the resting forearm for PGE<sub>2</sub> and PGF<sub>1</sub>α between HF-rEF patients and age-matched controls. Those findings of similar COX metabolite concentrations are further supported by our present finding that COX-2 enzymatic activity within skeletal muscle homogenates from the white portion of the gastrocnemius muscle was not different between SHAM and HF-rEF rats. Collectively, our

findings suggest that the TxA<sub>2</sub>-R mediated chronic mechanoreflex sensitization in HF-rEF is not attributed to an increased presence of COX metabolites within the skeletal muscle interstitial space. It remains possible, however, that skeletal muscle contraction results in a greater accumulation of COX metabolites within the skeletal muscle interstitial space in HF-rEF compared to SHAM rats which acts in addition to the chronic mechanoreflex sensitization.

Given we found no difference in TxA<sub>2</sub>-R expression within lumbar DRG or basal COX metabolites within the skeletal muscle interstitial space between SHAM and HF-rEF rats, how may we explain the effect of TxA<sub>2</sub>-R blockade on the sympathetic and cardiovascular responses to hindlimb muscle contraction (present study) and hindlimb muscle stretch (34)? It is possible that the site of amplification of the TxA<sub>2</sub>-R signaling in HF-rEF resides within the intracellular pathways within the sensory neuron endings. Although speculative, there is at least some indirect evidence for such a phenomenon. Specifically, it may be that in HF-rEF there is an amplification of inositol trisphosphate (IP<sub>3</sub>) and/or diacylglycerol signaling (the G protein-coupled signaling pathways associated with TxA<sub>2</sub>-Rs) within sensory neuron endings. Such an amplification may result in an increased cytosolic calcium concentration within the sensory neuron ending which, in turn, may sensitize mechanically activated channels (62). Investigation into these intracellular signaling pathways and their possible contribution to the mechanoreflex and exercise pressor reflex in HF-rEF is warranted.

Several experimental considerations should be noted. First, the exercise pressor reflex is one of several autonomic control signals that likely contributes to the aberrant sympathetic and cardiovascular adjustments to exercise in HF-rEF. For example, central command (63), the carotid chemoreflex (64-66), and the arterial baroreflex (67, 68) have all been reported to contribute to aberrant sympathetic and cardiovascular responses during exercise in HF-rEF. Whether TxA<sub>2</sub>-Rs contribute to exaggerated increases in SNA during exercise in HF-rEF patients when all these autonomic control mechanisms are working in concert with one another (i.e., during whole body exercise) remains unknown. Second, RSNA was not measured in the vehicle and systemic control experiments. We elected to perform the vehicle and systemic control protocols in experiments in which technical factors precluded successful RSNA recording in order to maximize the statistical power of the RSNA comparisons in the main experimental protocols. Third, only male rats were used in the present investigation. Future studies are needed to determine the role of TxA<sub>2</sub>-R signaling in the exercise pressor reflex in female rats with and without HF-rEF. Lastly, we cannot

rule out the possibility that an increase in hindlimb muscle blood flow and consequent washout of metabolites produced during muscle contraction may also have contributed to the attenuated exercise pressor reflex following TxA<sub>2</sub>-R blockade in rats with HF-rEF. Although this seems unlikely given that TxA<sub>2</sub>-R blockade had no effect in SHAM rats.

### **3.6 Conclusion**

In summary, we found that the sympathetic and cardiovascular responses to 1 Hz dynamic hindlimb muscle contraction were larger in rats with HF-rEF compared to the responses in SHAM operated healthy control rats. We also found that the hindlimb arterial injection of a TxA<sub>2</sub>-R antagonist reduced these exaggerated responses to dynamic hindlimb muscle contraction in HF-rEF rats. Although the precise mechanism underlying the TxA<sub>2</sub>-R signaling amplification remains unknown, these data suggest that TxA<sub>2</sub>-R signaling within the sensory endings of thin fiber muscle afferents contribute to the exaggerated exercise pressor reflex evoked during dynamic muscle contractions in HF-rEF. Future studies should seek to determine the precise mechanism underlying the TxA<sub>2</sub>-R signaling amplification. Our findings may have important implications for our understanding of the reflex control of the sympathetic nervous system during exercise in the over 26 million people worldwide with HF-rEF (69).

### 3.7 References

1. **Leimbach WN, Jr., Wallin BG, Victor RG, Aylward PE, Sundlof G, and Mark AL.** Direct evidence from intraneural recordings for increased central sympathetic outflow in patients with heart failure. *Circulation* 73: 913-919, 1986.
2. **Roveda F, Middlekauff HR, Rondon MU, Reis SF, Souza M, Nastari L, Barretto AC, Krieger EM, and Negrao CE.** The effects of exercise training on sympathetic neural activation in advanced heart failure: a randomized controlled trial. *J Am CollCardiol* 42: 854-860, 2003.
3. **Notarius CF, Ando S, Rongen GA, and Floras JS.** Resting muscle sympathetic nerve activity and peak oxygen uptake in heart failure and normal subjects. *Eur Heart J* 20: 880-887, 1999.
4. **Murai H, Takamura M, Maruyama M, Nakano M, Ikeda T, Kobayashi D, Otowa K, Ootsuji H, Okajima M, Furusho H, Takata S, and Kaneko S.** Altered firing pattern of single-unit muscle sympathetic nerve activity during handgrip exercise in chronic heart failure. *J Physiol* 587: 2613-2622, 2009.
5. **Poole DC, Hirai DM, Copp SW, and Musch TI.** Muscle oxygen transport and utilization in heart failure: implications for exercise (in)tolerance. *Am J Physiol Heart Circ Physiol* 302: H1050-1063, 2012.
6. **Amann M, Venturelli M, Ives SJ, Morgan DE, Gmelch B, Witman MA, Jonathan Groot H, Walter Wray D, Stehlik J, and Richardson RS.** Group III/IV muscle afferents impair limb blood in patients with chronic heart failure. *Int J Cardiol* 174: 368-375, 2014.
7. **Sinoway LI, and Li J.** A perspective on the muscle reflex: implications for congestive heart failure. *J Appl Physiol (1985)* 99: 5-22, 2005.
8. **McCloskey DI, and Mitchell JH.** Reflex cardiovascular and respiratory responses originating in exercising muscle. *J Physiol* 224: 173-186, 1972.
9. **Kaufman MP, Longhurst JC, Rybicki KJ, Wallach JH, and Mitchell JH.** Effects of static muscular contraction on impulse activity of groups III and IV afferents in cats. *J Appl Physiol* 55: 105-112, 1983.
10. **Kaufman MP, Iwamoto GA, Longhurst JC, and Mitchell JH.** Effects of capsaicin and bradykinin on afferent fibers with endings in skeletal muscle. *Circ Res* 50: 133-139, 1982.
11. **Kaufman MP, Rybicki KJ, Waldrop TG, and Ordway GA.** Effect of ischemia on responses of group III and IV afferents to contraction. *J Appl Physiol* 57: 644-650, 1984.

12. **Kaufman MP, and Forster HV.** Reflexes controlling circulatory, ventilatory and airway responses to exercise. In: *Handbook of Physiology, Section 12: Exercise: Regulation and Integration of Multiple Systems II Control of Respiratory and Cardiovascular Systems*, edited by Rowell LB, and Shepherd JT. New York, NY: Oxford University Press, 1996, p. 381-447.
13. **Mitchell JH, Kaufman MP, and Iwamoto GA.** The exercise pressor reflex: Its cardiovascular effects, afferent mechanisms, and central pathways. *AnnRevPhysiol* 45: 229-242, 1983.
14. **Strange S, Secher NH, Pawelczyk JA, Karpakka J, Christensen NJ, Mitchell JH, and Saltin B.** Neural control of cardiovascular responses and of ventilation during dynamic exercise in man. *JPhysiol* 470: 693-704, 1993.
15. **Amann M, Blain GM, Proctor LT, Sebranek JJ, Pegelow DF, and Dempsey JA.** Group III and IV muscle afferents contribute to ventilatory and cardiovascular response to rhythmic exercise in humans. *JApplPhysiol* 109: 966-976, 2010.
16. **Amann M, Runnels S, Morgan DE, Trinity JD, Fjeldstad AS, Wray DW, Reese VR, and Richardson RS.** On the contribution of group III and IV muscle afferents to the circulatory response to rhythmic exercise in humans. *JPhysiol* 589: 3855-3866, 2011.
17. **Smith JR, Joyner MJ, Curry TB, Borlaug BA, Keller-Ross ML, Van Iterson EH, and Olson TP.** Locomotor muscle group III/IV afferents constrain stroke volume and contribute to exercise intolerance in human heart failure. *J Physiol* 598: 5379-5390, 2020.
18. **Grotle AK, Macefield VG, Farquhar WB, O'Leary DS, and Stone AJ.** Recent advances in exercise pressor reflex function in health and disease. *Auton Neurosci* 228: 102698, 2020.
19. **Ives SJ, Amann M, Venturelli M, Witman MA, Groot HJ, Wray DW, Morgan DE, Stehlik J, and Richardson RS.** The Mechanoreflex and Hemodynamic Response to Passive Leg Movement in Heart Failure. *Med Sci Sports Exerc* 48: 368-376, 2016.
20. **Kaur J, Senador D, Krishnan AC, Hanna HW, Alvarez A, Machado TM, and O'Leary DS.** Muscle metaboreflex-induced vasoconstriction in the ischemic active muscle is exaggerated in heart failure. *Am J Physiol Heart Circ Physiol* 314: H11-H18, 2018.
21. **O'Leary DS, Sala-Mercado JA, Augustyniak RA, Hammond RL, Rossi NF, and Ansoorge EJ.** Impaired muscle metaboreflex-induced increases in ventricular function in heart failure. *AmJPhysiol Heart CircPhysiol* 287: H2612-H2618, 2004.



22. **Middlekauff HR, Nitzsche EU, Hoh CK, Hamilton MA, Fonarow GC, Hage A, and Moriguchi JD.** Exaggerated muscle mechanoreflex control of reflex renal vasoconstriction in heart failure. *JApplPhysiol* 90: 1714-1719, 2001.
23. **Smith SA, Mitchell JH, Naseem RH, and Garry MG.** Mechanoreflex mediates the exaggerated exercise pressor reflex in heart failure. *Circulation* 112: 2293-2300, 2005.
24. **Koba S, Xing J, Sinoway LI, and Li J.** Sympathetic nerve responses to muscle contraction and stretch in ischemic heart failure. *Am J Physiol Heart Circ Physiol* 294: H311-321, 2008.
25. **Morales A, Gao W, Lu J, Xing J, and Li J.** Muscle cyclo-oxygenase-2 pathway contributes to the exaggerated muscle mechanoreflex in rats with congestive heart failure. *Exp Physiol* 97: 943-954, 2012.
26. **Butenas ALE, Rollins KS, Matney JE, Williams AC, Kleweno TE, Parr SK, Hammond ST, Ade CJ, Hageman KS, Musch TI, and Copp SW.** No effect of endoperoxide 4 or thromboxane A2 receptor blockade on static mechanoreflex activation in rats with heart failure. *Exp Physiol* 105: 1840-1854, 2020.
27. **Stebbins CL, Brown B, Levin D, and Longhurst JC.** Reflex effect of skeletal muscle mechanoreceptor stimulation on the cardiovascular system. *JApplPhysiol* 65: 1539-1547, 1988.
28. **Daniels JW, Stebbins CL, and Longhurst JC.** Hemodynamic responses to static and dynamic muscle contractions at equivalent workloads. *AmJPhysiol* 279 (5): R1849-R1855, 2000.
29. **Butenas ALE, Hopkins TD, Rollins KS, Felice KP, and Copp SW.** Investigation of the mechanisms of cyclooxygenase-mediated mechanoreflex sensitization in a rat model of simulated peripheral artery disease. *Am J Physiol Heart Circ Physiol* 317: H1050-H1061, 2019.
30. **Kempf EA, Rollins KS, Hopkins TD, Butenas AL, Santin JM, Smith JR, and Copp SW.** Chronic femoral artery ligation exaggerates the pressor and sympathetic nerve responses during dynamic skeletal muscle stretch in decerebrate rats. *Am J Physiol Heart Circ Physiol* 314: H246-H254, 2018.
31. **Rollins KS, Hopkins TD, Butenas AL, Felice KP, Ade CJ, and Copp SW.** Cyclooxygenase inhibition does not impact the pressor response during static or dynamic mechanoreflex activation in healthy decerebrate rats. *Am J Physiol Regul Integr Comp Physiol* 317: R369-R378, 2019.

32. **Sanderson BC, Rollins KS, Hopkins TD, Butenas AL, Felice KP, Ade CJ, and Copp SW.** GsMTx4 reduces the reflex pressor response during dynamic hindlimb skeletal muscle stretch in decerebrate rats. *Physiological reports* 7: e13974, 2019.
33. **Rollins KS, Butenas ALE, Felice KP, Matney JE, Williams AC, Kleweno TE, and Copp SW.** Thromboxane A2 receptors mediate chronic mechanoreflex sensitization in a rat model of simulated peripheral artery disease. *Am J Physiol Heart Circ Physiol* 319: H320-H330, 2020.
34. **Butenas ALE, Rollins KS, Williams AC, Parr SK, Hammond ST, Ade CJ, Hageman KS, Musch TI, and Copp SW.** Exaggerated sympathetic and cardiovascular responses to dynamic mechanoreflex activation in rats with heart failure: Role of endoperoxide 4 and thromboxane A2 receptors. *Auton Neurosci* 232: 102784, 2021.
35. **Smith JR, Hart CR, Ramos PA, Akinsanya JG, Lanza IR, Joyner MJ, Curry TB, and Olson TP.** Metabo- and mechanoreceptor expression in human heart failure: Relationships with the locomotor muscle afferent influence on exercise responses. *Exp Physiol* 105: 809-818, 2020.
36. **Antunes-Correa LM, Nobre TS, Groehs RV, Alves MJ, Fernandes T, Couto GK, Rondon MU, Oliveira P, Lima M, Mathias W, Brum PC, Mady C, Almeida DR, Rossoni LV, Oliveira EM, Middlekauff HR, and Negrao CE.** Molecular basis for the improvement in muscle metaboreflex and mechanoreflex control in exercise-trained humans with chronic heart failure. *Am J Physiol Heart Circ Physiol* 307: H1655-1666, 2014.
37. **Middlekauff HR, Chiu J, Hamilton MA, Fonarow GC, Maclellan WR, Hage A, Moriguchi J, and Patel J.** Cyclooxygenase products sensitize muscle mechanoreceptors in humans with heart failure. *Am J Physiol Heart Circ Physiol* 294: H1956-1962, 2008.
38. **Gallagher KM, Fadel PJ, Smith SA, Norton KH, Querry RG, Olivencia-Yurvati A, and Raven PB.** Increases in intramuscular pressure raise arterial blood pressure during dynamic exercise. *J Appl Physiol (1985)* 91: 2351-2358, 2001.
39. **National Research Council (U.S.). Committee for the Update of the Guide for the Care and Use of Laboratory Animals., Institute for Laboratory Animal Research (U.S.), and National Academies Press (U.S.).** Guide for the care and use of laboratory animals. Washington, D.C.: National Academies Press., 2011, p. xxv, 220 p.
40. **Musch TI, and Terrell JA.** Skeletal muscle blood flow abnormalities in rats with a chronic myocardial infarction: rest and exercise. *AmJPhysiol* 262: H411-H419, 1992.

41. **Baumfalk DR, Opoku-Acheampong AB, Caldwell JT, Butenas ALE, Horn AG, Kunkel ON, Copp SW, Ade CJ, Musch TI, and Behnke BJ.** Effects of high-intensity training on prostate cancer-induced cardiac atrophy. *Am J Transl Res* 13: 197-209, 2021.
42. **Butenas ALE, Colburn TD, Baumfalk DR, Ade CJ, Hageman KS, Copp SW, Poole DC, and Musch TI.** Angiotensin converting enzyme inhibition improves cerebrovascular control during exercise in male rats with heart failure. *Respir Physiol Neurobiol* 103613, 2021.
43. **Smith SA, Mitchell JH, and Garry MG.** Electrically induced static exercise elicits a pressor response in the decerebrate rat. *JPhysiol* 537: 961-970, 2001.
44. **Craig JC, Colburn TD, Hirai DM, Musch TI, and Poole DC.** Sexual dimorphism in the control of skeletal muscle interstitial Po<sub>2</sub> of heart failure rats: effects of dietary nitrate supplementation. *J Appl Physiol (1985)* 126: 1184-1192, 2019.
45. **Leal AK, McCord JL, Tsuchimochi H, and Kaufman MP.** Blockade of the TP receptor attenuates the exercise pressor reflex in decerebrated rats with chronic femoral artery occlusion. *AmJPhysiol Heart CircPhysiol* 301: H2140-H2146, 2011.
46. **Copp SW, Kim JS, Ruiz-Velasco V, and Kaufman MP.** The mechano-gated channel inhibitor GsMTx4 reduces the exercise pressor reflex in decerebrate rats. *J Physiol* 594: 641-655, 2016.
47. **Victor RG, Bertocci LA, Pryor SL, and Nunnally RL.** Sympathetic nerve discharge is coupled to muscle cell pH during exercise in humans. *JClinInvest* 82: 1301-1305, 1988.
48. **Copp SW, Stone AJ, Li J, and Kaufman MP.** Role played by interleukin-6 in evoking the exercise pressor reflex in decerebrate rats: effect of femoral artery ligation. *Am J Physiol Heart Circ Physiol* 309: H166-173, 2015.
49. **Ducrocq GP, Kim JS, Estrada JA, and Kaufman MP.** ASIC1a plays a key role in evoking the metabolic component of the exercise pressor reflex in rats. *Am J Physiol Heart Circ Physiol* 318: H78-H89, 2020.
50. **Grotle AK, Crawford CK, Huo Y, Ybarbo KM, Harrison ML, Graham J, Stanhope KL, Havel PJ, Fadel PJ, and Stone AJ.** Exaggerated cardiovascular responses to muscle contraction and tendon stretch in UCD type-2 diabetes mellitus rats. *Am J Physiol Heart Circ Physiol* 317: H479-H486, 2019.

51. **Middlekauff HR, Chiu J, Hamilton MA, Fonarow GC, Maclellan WR, Hage A, Moriguchi J, and Patel J.** Muscle mechanoreceptor sensitivity in heart failure. *AmJPhysiol Heart CircPhysiol* 287: H1937-H1943, 2004.
52. **Cui J, Blaha C, Moradkhan R, Gray KS, and Sinoway LI.** Muscle sympathetic nerve activity responses to dynamic passive muscle stretch in humans. *J Physiol* 576: 625-634, 2006.
53. **Cui J, Leuenberger UA, Blaha C, King NC, and Sinoway LI.** Effect of P2 receptor blockade with pyridoxine on sympathetic response to exercise pressor reflex in humans. *JPhysiol* 589: 685-695, 2011.
54. **Middlekauff HR, and Chiu J.** Cyclooxygenase products sensitize muscle mechanoreceptors in healthy humans. *AmJPhysiol Heart CircPhysiol* 287: H1944-H1949, 2004.
55. **Cui J, McQuillan P, Momen A, Blaha C, Moradkhan R, Mascarenhas V, Hogeman C, Krishnan A, and Sinoway LI.** The role of the cyclooxygenase products in evoking sympathetic activation in exercise. *Am J Physiol Heart Circ Physiol* 293: H1861-H1868, 2007.
56. **Stebbins CL, Maruoka Y, and Longhurst JC.** Prostaglandins contribute to cardiovascular reflexes evoked by static muscular contraction. *Circ Res* 59: 645-654, 1986.
57. **Hayes SG, Kindig AE, and Kaufman MP.** Cyclooxygenase blockade attenuates responses of group III and IV muscle afferents to dynamic exercise in cats. *AmJPhysiol Heart CircPhysiol* 290: H2239-H2246, 2006.
58. **Yamauchi K, Kim JS, Stone AJ, Ruiz-Velasco V, and Kaufman MP.** Endoperoxide 4 receptors play a role in evoking the exercise pressor reflex in rats with simulated peripheral artery disease. *J Physiol* 591: 2949-2962, 2013.
59. **Stone AJ, Copp SW, Kim JS, and Kaufman MP.** Combined, but not individual, blockade of ASIC3, P2X, and EP4 receptors attenuates the exercise pressor reflex in rats with freely perfused hindlimb muscles. *J Appl Physiol (1985)* 119: 1330-1336, 2015.
60. **McCord JL, Hayes SG, and Kaufman MP.** PPADS does not block contraction-induced prostaglandin E2 synthesis in cat skeletal muscle. *Am J Physiol Heart Circ Physiol* 295: H2043-H2045, 2008.
61. **Scott AC, Wensel R, Davos CH, Kemp M, Kaczmarek A, Hooper J, Coats AJ, and Piepoli MF.** Chemical mediators of the muscle ergoreflex in chronic heart failure: a putative role for prostaglandins in reflex ventilatory control. *Circulation* 106: 214-220, 2002.

62. **Zhuang GZ, Keeler B, Grant J, Bianchi L, Fu ES, Zhang YP, Erasso DM, Cui JG, Wiltshire T, Li Q, Hao S, Sarantopoulos KD, Candiotti K, Wishnek SM, Smith SB, Maixner W, Diatchenko L, Martin ER, and Levitt RC.** Carbonic anhydrase-8 regulates inflammatory pain by inhibiting the ITPR1-cytosolic free calcium pathway. *PloS one* 10: e0118273, 2015.
63. **Koba S, Gao Z, Xing J, Sinoway LI, and Li J.** Sympathetic responses to exercise in myocardial infarction rats: a role of central command. *AmJPhysiol Heart CircPhysiol* 291: H2735-H2742, 2006.
64. **Li YL, Xia XH, Zheng H, Gao L, Li YF, Liu D, Patel KP, Wang W, and Schultz HD.** Angiotensin II enhances carotid body chemoreflex control of sympathetic outflow in chronic heart failure rabbits. *Cardiovasc Res* 71: 129-138, 2006.
65. **Machado AC, Vianna LC, Gomes EAC, Teixeira JAC, Ribeiro ML, Villacorta H, Nobrega ACL, and Silva BM.** Carotid chemoreflex and muscle metaboreflex interact to the regulation of ventilation in patients with heart failure with reduced ejection fraction. *Physiological reports* 8: e14361, 2020.
66. **Stickland MK, Miller JD, Smith CA, and Dempsey JA.** Carotid chemoreceptor modulation of regional blood flow distribution during exercise in health and chronic heart failure. *Circ Res* 100: 1371-1378, 2007.
67. **Mancia G, Seravalle G, Giannattasio C, Bossi M, Preti L, Cattaneo BM, and Grassi G.** Reflex cardiovascular control in congestive heart failure. *The American journal of cardiology* 69: 17G-22G; discussion 22G-23G, 1992.
68. **Grassi G, Seravalle G, Cattaneo BM, Lanfranchi A, Vailati S, Giannattasio C, Del Bo A, Sala C, Bolla GB, and Pozzi M.** Sympathetic activation and loss of reflex sympathetic control in mild congestive heart failure. *Circulation* 92: 3206-3211, 1995.
69. **Ponikowski P, Anker SD, AlHabib KF, Cowie MR, Force TL, Hu S, Jaarsma T, Krum H, Rastogi V, Rohde LE, Samal UC, Shimokawa H, Budi Siswanto B, Sliwa K, and Filippatos G.** Heart failure: preventing disease and death worldwide. *ESC Heart Fail* 1: 4-25, 2014.

**Table 3.1**

Table 3.1. Body and tissue masses and heart morphometrics in SHAM and HF-rEF rats

|                           | SHAM ( <i>n</i> =31) | HF-rEF ( <i>n</i> =29) | P-value |
|---------------------------|----------------------|------------------------|---------|
| Body mass                 | 526 ± 7              | 521 ± 7                | 0.67    |
| LV/body mass (mg/g)       | 2.02 ± 0.04          | 2.08 ± 0.04            | 0.25    |
| RV/body mass (mg/g)       | 0.51 ± 0.01          | 0.58 ± 0.02            | <0.01*  |
| Atria/body mass (mg/g)    | 0.16 ± 0.01          | 0.20 ± 0.01            | <0.01*  |
| LV EDV (mL)               | 1.07 ± 0.06          | 2.30 ± 0.12            | <0.01*  |
| LV ESV (mL)               | 0.17 ± 0.02          | 1.23 ± 0.08            | <0.01*  |
| Stroke volume (mL)        | 0.90 ± 0.05          | 1.08 ± 0.06            | 0.03*   |
| Ejection fraction (%)     | 84 ± 1               | 46 ± 2                 | <0.01*  |
| Fractional shortening (%) | 49 ± 1               | 21 ± 1                 | <0.01*  |
| Infarct size (%)          | -                    | 28 ± 1                 | -       |

Values are means ± SEM. LV, left ventricle; RV, right ventricle; EDV, end diastolic volume; ESV, end systolic volume. Data were compared using student's t-tests or Mann-Whitney tests as appropriate. Asterisks indicate a statistically significant difference between groups ( $P < 0.05$ ).

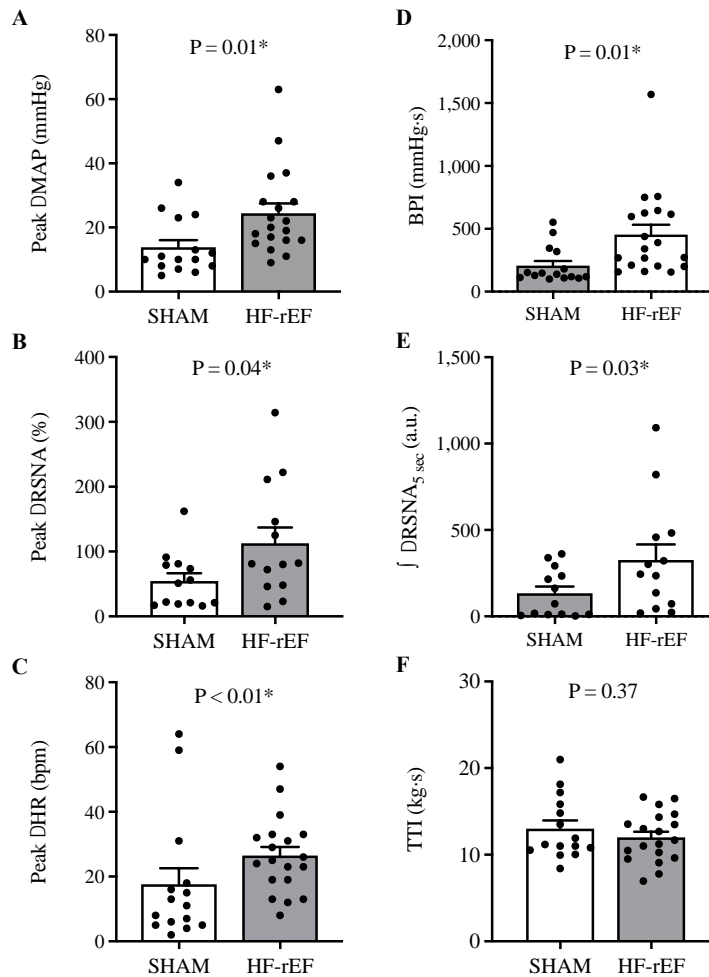
**Table 3.2**

Table 3.2. Baseline MAP and HR in SHAM and HF-rEF rats

|                    | SHAM    |                | HF-rEF  |                |
|--------------------|---------|----------------|---------|----------------|
|                    | Control | Post condition | Control | Post condition |
| Baseline MAP, mmHg |         |                |         |                |
| Daltroban i.a.     | 85±5    | 81±5           | 81±4    | 84±6           |
| Daltroban i.v.     | -       | -              | 87±9    | 83±10          |
| 1% DMSO i.a.       | -       | -              | 83±10   | 86±8           |
| Baseline HR, bpm   |         |                |         |                |
| Daltroban i.a.     | 429±9   | 438±11         | 448±18  | 452±20         |
| Daltroban i.v.     | -       | -              | 454±15  | 462±18         |
| 1% DMSO i.a.       | -       | -              | 462±18  | 475±4          |

Values are means±SEM. MAP, mean arterial pressure; HR, heart rate. Data were compared between conditions (Control vs. Post condition) with paired Student's t-tests. There was no significant difference for any comparison.

**Figure 3.1**



*Figure 1: Effect of HF-rEF on dynamic exercise pressor reflex activation. The peak  $\Delta$  mean arterial pressure (MAP; A), peak  $\Delta$  renal sympathetic nerve activity (RSNA; B), peak  $\Delta$  heart rate (HR; C), blood pressure index (BPI, D), and the first 5 s of the integrated change in RSNA ( $\int \Delta$ RSNA<sub>5 sec</sub>, E) in response to 30 seconds of dynamic hindlimb muscle contraction in SHAM ( $n=15$ ) and HF-rEF ( $n=19$ ) rats. TTI, tension-time index. Data were analyzed with Student's  $t$ -tests or Mann-Whitney tests as appropriate and are expressed as mean $\pm$ SEM with individual data points. Asterisks indicates statistically significant differences between groups ( $P < 0.05$ ).*



**Figure 3.2**

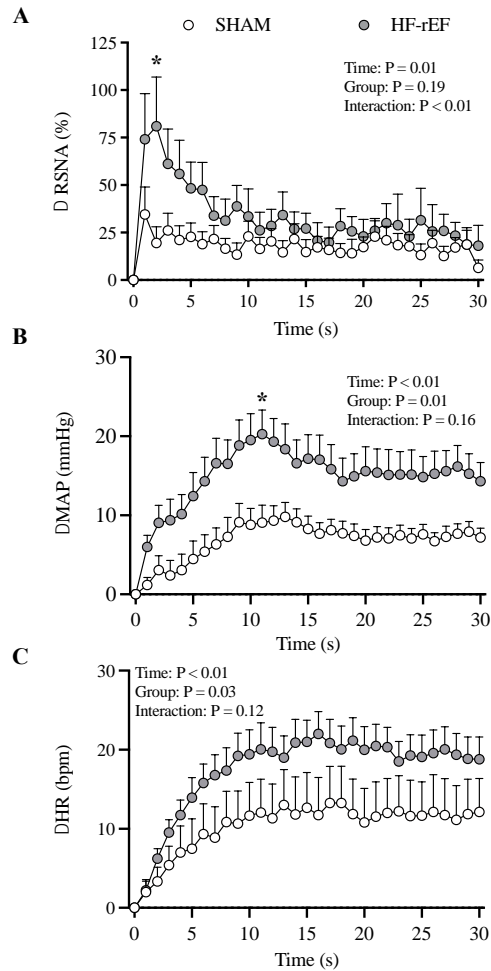


*Figure 2: Effect of HF-rEF on the time course of dynamic exercise pressor reflex activation. The  $\Delta$  renal sympathetic nerve activity (RSNA; A),  $\Delta$  mean arterial pressure (MAP; B), and  $\Delta$  heart rate (HR; C) response to 30 seconds of dynamic hindlimb muscle contraction in SHAM ( $n=15$ ) and HF-rEF ( $n=19$ ) rats. Data were analyzed with two-way ANOVAs with Šidák multiple comparisons tests and are expressed as mean $\pm$ SEM. Asterisks indicate time points where comparisons were statistically significant ( $P < 0.05$ ).*

**Figure 3.3**

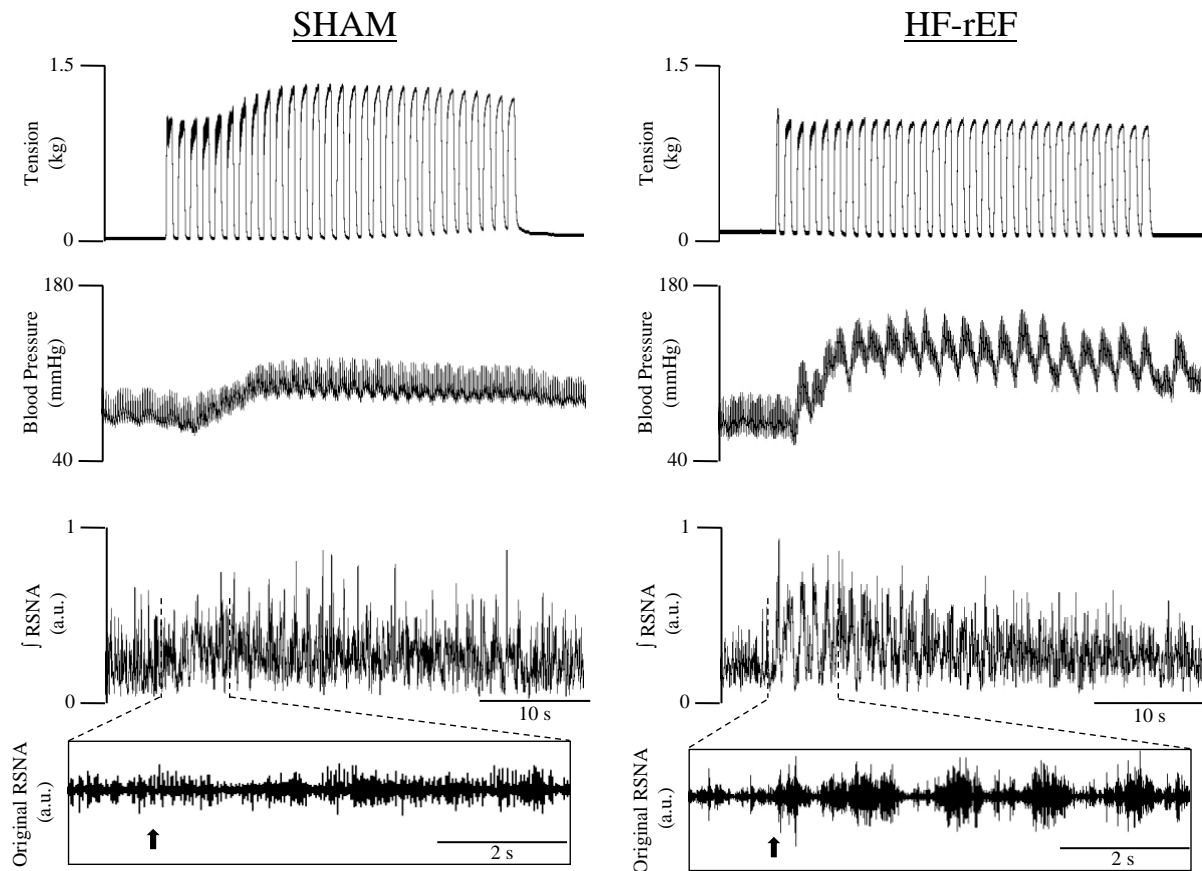


*Figure 3:* Examples of original tracings of the blood pressure, and integrated renal sympathetic nerve activity [jRSNA, in arbitrary units (a.u.)] response to 30 seconds of dynamic hindlimb muscle contraction in a SHAM rat (left) and HF-rEF rat (right). *Insets:* original renal sympathetic nerve recording. Arrows indicate onset of contraction.

**Figure 3.4**

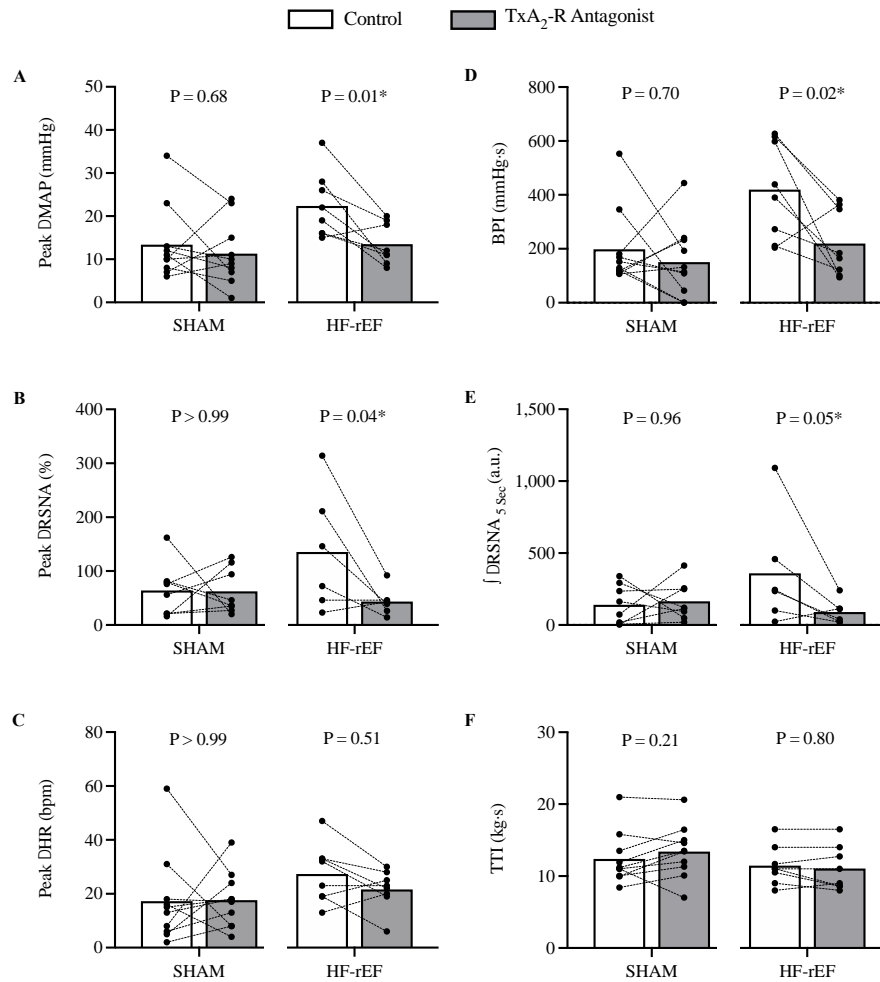


*Figure 4: Effect of TxA<sub>2</sub>-R blockade on dynamic exercise pressor reflex activation. The peak  $\Delta$  mean arterial pressure (MAP; A), peak  $\Delta$  renal sympathetic nerve activity (RSNA; B), peak  $\Delta$  heart rate (HR; C), blood pressure index (BPI, D), and the first 5 s of the integrated change in RSNA ( $\int\Delta$ RSNA<sub>5 sec</sub>, E) in response to 30 seconds of dynamic hindlimb muscle contraction before (Control) and after injection of the TxA<sub>2</sub>-R antagonist daltroban (80  $\mu$ g) into the arterial supply of the hindlimb in SHAM ( $n=10$ ) and HF-rEF ( $n=8$ ) rats. TTI, tension-time index. Data were analyzed with Šidák multiple comparisons tests and are expressed as mean $\pm$ SEM overlaid with individual responses. Asterisks indicate statistically significant differences between groups ( $P < 0.05$ ).*

**Figure 3.5**

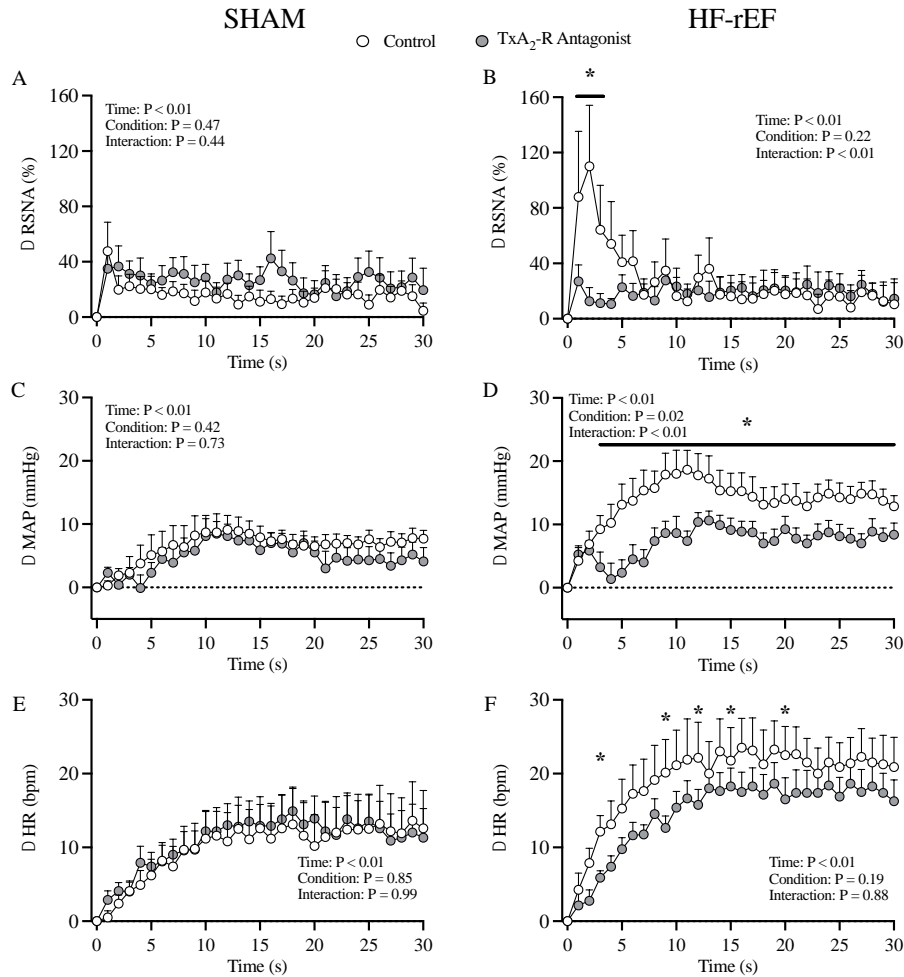


*Figure 5: Effect of TxA<sub>2</sub>-R blockade on the time course of dynamic exercise pressor reflex activation. Δ renal sympathetic nerve activity (RSNA; A & B), Δ mean arterial pressure (MAP; C & D), and Δ heart rate (HR; E & F) during 30 seconds of dynamic hindlimb muscle contraction before (Control) and after injection of 80 μg of the TxA<sub>2</sub>-R antagonist into the arterial supply of the hindlimb in SHAM (n=10) and HF-rEF (n=8) rats. Data were analyzed with two-way ANOVAs and Šidák multiple comparisons tests and are expressed as mean±SEM. Asterisks and/or black lines indicate time points where comparisons were statistically significant (P < 0.05).*

**Figure 3.6**

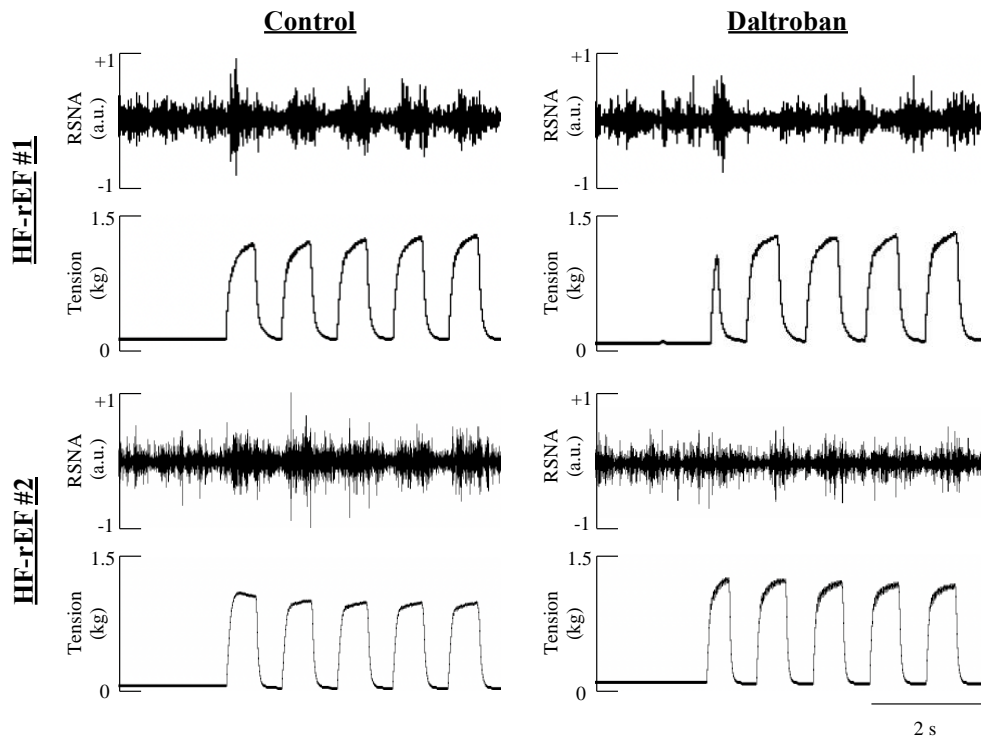


*Figure 6: Examples of the distinct renal sympathetic nerve activity (RSNA) bursts that occur with each tension development during 1-Hz dynamic contraction in two HF-rEF rats before (Control) and after injection of 80 µg of the TxA<sub>2</sub>-R antagonist into the arterial supply of the hindlimb. The synchronization between RSNA and the tension development in the control condition suggests that dynamic hindlimb muscle contractions primarily provide a mechanical stimulus, which was effectively attenuated following TxA<sub>2</sub>-R antagonism.*

**Figure 3.7**

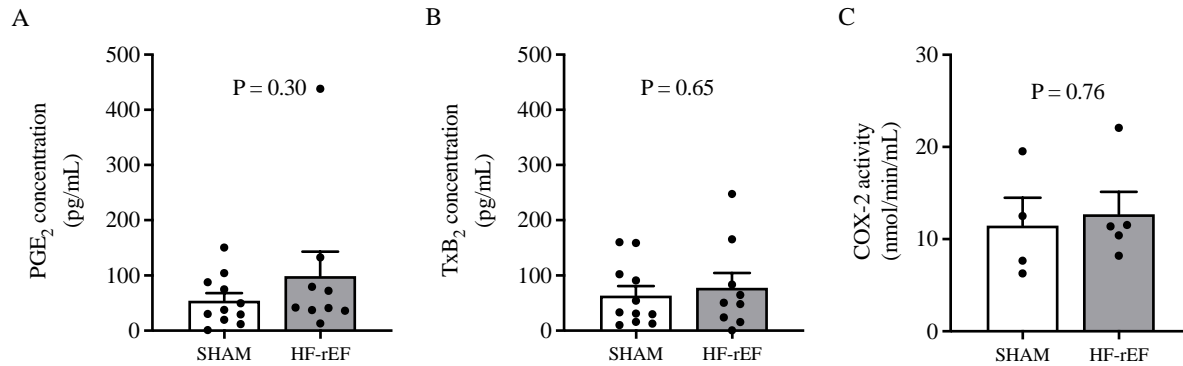


*Figure 7: Effect of HF-rEF on interstitial PGE<sub>2</sub> and TxB<sub>2</sub> concentrations and COX-2 activity in the white portion of the gastrocnemius muscle. Basal concentrations of PGE<sub>2</sub> (A) and TxB<sub>2</sub> (B) within microdialysate fluid collected from the white portion of the gastrocnemius muscle in SHAM ( $n=11$ ) and HF-rEF ( $n=9$ ) rats. Confirmation of COX-2 enzymatic activity from muscle homogenates taken from the white portion of the gastrocnemius muscle (C) of a distinct group of SHAM ( $n=4$ ) and HF-rEF ( $n=5$ ) rats. Data were analyzed with Student's  $t$ -tests and are expressed as mean $\pm$ SEM with individual data points.*

## Chapter 4 - Protein Kinase C Epsilon Contributes to the Chronic Mechanoreflex Sensitization in rats with Heart Failure

### 4.1 Abstract

We investigated the role of second-messenger signaling associated with the stimulation of G<sub>q</sub> protein-coupled receptors (*e.g.*, thromboxane A<sub>2</sub>, and bradykinin 2 receptors) on the sensory endings of thin fiber muscle afferents in the chronic mechanoreflex sensitization in rats with myocardial infarction-induced heart failure with reduced ejection fraction (HF-rEF). We hypothesized that injection of either the inositol 1,4,5-trisphosphate (IP<sub>3</sub>) receptor antagonist Xestospongine C (5 µg) or the protein kinase C epsilon (PKCε) translocation inhibitor PKCε141 (45 µg) into the arterial supply of the hindlimb would reduce the increase in renal sympathetic nerve activity (RSNA) evoked in response to 30 s of 1 Hz dynamic hindlimb muscle stretch in decerebrate, unanesthetized HF-rEF rats but not sham-operated control rats (SHAM). Ejection fraction was significantly reduced in HF-rEF (45±3%) compared to SHAM (80±2%; P < 0.001) rats. In SHAM and HF-rEF rats we found that the IP<sub>3</sub> receptor antagonist had no effect on the RSNA response to stretch (peak ΔRSNA SHAM, n=5M/3F, pre: 59±21, post: 102±37, P = 0.061; HF-rEF n=3M/2F, pre: 99±33, post: 133±35%, P = 0.974). Conversely, the PKCε translocation inhibitor reduced the RSNA response to stretch in HF-rEF rats (n=4M/3F, pre: 110±29, post: 62±22%, P = 0.029) but not SHAM rats (n=3M/3F, pre: 87±38, post: 94±44%, P = 0.639). These data suggest that PKCε mediated, but not IP<sub>3</sub> receptor-mediated, signaling associated with the stimulation of G<sub>q</sub> protein-coupled receptors contributes to a chronic sensitization of the mechanically activated channels that underly mechanoreflex and the exercise pressor reflex activation in rats with HF-rEF.

## 4.2 Introduction

The autonomic adjustments to exercise are essential for cardiovascular function during exercise. These autonomic adjustments to exercise include a reflex increase in sympathetic nerve activity (SNA) and simultaneous withdrawal of parasympathetic nerve activity (PSNA). Feedforward mechanisms (*e.g.*, central command) and feedback mechanisms (*e.g.*, the exercise pressor reflex and the carotid chemoreflex) underly these adjustments to the autonomic nervous system (1-3). Moreover, the activation of each of these mechanisms contribute to exaggerated increases in SNA during even mild exercise in patients with heart failure with reduced ejection fraction (HF-rEF) compared with healthy counterparts (3-5). The exaggerated increase in SNA in HF-rEF patients contributes to an increased mortality in this patient population (6). Recent findings in humans with HF-rEF have highlighted that activation of the exercise pressor reflex not only contributes to exaggerated increases in SNA, but also contributes to a constraint of exercising cardiac output and peak oxygen uptake (7). Thus, understanding the mechanisms behind the exaggerated exercise pressor reflex in HF-rEF is fundamentally important toward improving quality of life for the over 26 million people with HF-rEF worldwide (8).

The exercise pressor reflex is activated when the sensory endings of group III and IV skeletal muscle afferents (collectively termed thin fiber muscle afferents) are stimulated by mechanical and/or metabolic stimuli associated with skeletal muscle contraction (9-15). The mechanically sensitive portion of the exercise pressor reflex (*i.e.*, the mechanoreflex) contributes importantly to the overall reflex exaggeration in HF-rEF patients (16, 17) and in rats with myocardial infarction-induced HF-rEF (18-23). For example, hindlimb muscle stretch (a model of mechanoreflex activation) evokes a greater response from primarily mechanically sensitive group III muscle afferents in rats with HF-rEF compared to those responses in healthy controls (24). Moreover, we recently found that G<sub>q</sub> protein coupled thromboxane A<sub>2</sub> (TxA<sub>2</sub>) receptors on the sensory endings of thin fiber muscle afferents contribute importantly to the exaggerated mechanoreflex (19) and exercise pressor reflex (18) control of renal SNA (RSNA) in rats with HF-rEF. Similarly, Koba et al. (25) found that the G<sub>q</sub> protein coupled bradykinin B<sub>2</sub> receptors on the sensory endings of thin fiber muscle afferents also contributed to the exaggerated mechanoreflex control of RSNA. However, neither TxA<sub>2</sub> or B<sub>2</sub> receptors contribute to the mechanoreflex or exercise pressor reflex control of RSNA in healthy rats (18, 19, 25). Collectively, these data suggest that the development of HF-rEF results in a chronic sensitization of the thin fiber muscle



afferents that underly mechanoreflex activation which is produced, at least in part, by  $G_q$  protein coupled  $TxA_2$  and B2 receptors on the sensory endings of these afferents.

The mechanisms behind this  $G_q$  protein-mediated chronic mechanoreflex sensitization in HF-rEF has not been investigated, but likely involves second messenger signaling associated with their stimulation. Stimulation of these  $G_q$  proteins results in an activation of phospholipase C which induces an increase in diacylglycerol (DAG) and inositol 1,4,5-trisphosphate ( $IP_3$ ) formation (26-28), both of which have been linked to sensory neuron sensitization (29). There is indirect experimental support for the possibility that these two branches of  $G_q$  coupled second-messenger systems are involved in sensitizing the mechanoreflex in HF-rEF. For example, when  $IP_3$  is formed, it binds to its receptor on the endoplasmic reticulum, which when activated, increases intracellular calcium concentrations (29). Importantly, elevated intracellular calcium has been shown to sensitize mechanically activated PIEZO channel-mediated currents in HEK293 cells (30). Furthermore, we recently found that  $IP_3$  receptor signaling, contributed importantly to sensitizing the mechanoreflex in rats with simulated peripheral artery disease (31). The second branch of  $G_q$  coupled second-messenger systems likely involves a DAG-induced translocation of protein kinase C (PKC) from the cytosol to the sensory ending. For example, PKC translocation has been shown to contribute to a B2 receptor-mediated sensitization of mechanically activated PIEZO 2 channels in HEK cells (32). It is likely that the  $PKC\epsilon$  isoform is particularly important for the sensitization of mechanically activated channels as  $PKC\epsilon$  translocation produced mechanical hyperalgesia in mice (33). Together, these findings suggest that second-messenger signaling resulting from  $G_q$  stimulation on sensory endings of thin fiber muscle afferents, especially through  $IP_3$  receptors and  $PKC\epsilon$  translocation, contribute to the exaggerated mechanoreflex in HF-rEF.

Based off the information above, the purpose of the present investigation was to determine the role of  $IP_3$  receptor and  $PKC\epsilon$  signaling in evoking the exaggerated mechanoreflex in rats with HF-rEF. We tested the following hypotheses: *a*) hindlimb arterial injection of the  $IP_3$  receptor antagonist Xestospongine C (5  $\mu$ g) would reduce the reflex increase RSNA and mean arterial pressure (MAP) evoked during 30 seconds of 1 Hz dynamic hindlimb muscle stretch in HF-rEF rats, but not in healthy control rats, and *b*) hindlimb arterial injection of the selective  $PKC\epsilon$  translocation inhibitor  $PKC\epsilon 141$  (45  $\mu$ g) would reduce the reflex increase RSNA and MAP evoked

during 30 seconds of 1 Hz dynamic hindlimb muscle stretch in HF-rEF rats, but not in healthy control rats.

### 4.3 Methods

*Ethical Approval.* All experimental procedures were approved by the Institutional Animal Care and Use Committee of Kansas State University (Protocol #4552) and conducted in accordance with the National Institutes of Health Guide for the Care and Use of Laboratory Animals (34). Experiments were performed on ~14-19-week-old male and female Sprague-Dawley rats ( $n=68$ ; Charles River Laboratories). Rats were housed two per cage in temperature (maintained at  $\sim 22^{\circ}\text{C}$ ) and light (12-12 hour light-dark cycle running from 7 AM to 7 PM)-controlled accredited facilities with standard rat chow and water provided ad libitum.

*Myocardial infarction procedure.* Myocardial infarction (MI) was induced in 45 of the 68 rats by surgically ligating the left main coronary artery (35). Briefly, rats were anesthetized initially with a 5% isoflurane- $\text{O}_2$  mixture (Butler Animal Health Supply, Elk Grove Village, IL, and Linweld, Dallas, TX) and maintained subsequently on 2.5% isoflurane- $\text{O}_2$  and then intubated and mechanically ventilated with a rodent respirator (Harvard model 680, Harvard Instruments, Holliston, MA) for the duration of the surgical procedure. After a single injection of the antiarrhythmic drug amiodarone (100 mg/kg ip), which was administered to improve survival rate following the ensuing coronary artery ligation surgery (36), a left thoracotomy was performed to expose the heart through the fifth intercostal space, and the left main coronary artery was ligated 1–2 mm distal to the edge of the left atrium with a 6-0 braided polyester suture. The thorax was then closed with 2-0 gut, and the skin was closed with 2-0 silk. Prior to termination of anesthesia, bupivacaine (1.5 mg/kg sc) and buprenorphine ( $\sim 0.03$  mg/kg im) were administered to reduce pain associated with the surgery, along with ampicillin (50 mg/kg im) to reduce the risk of infection. After rats were removed from mechanical ventilation and anesthesia, they were monitored closely for  $\sim 6$  h post-surgery. In the remaining 19 of 59 rats, a sham ligation of the coronary artery was performed in which 6-0 braided polyester suture was passed under the left main coronary artery, but not tied. These rats are referred to as “SHAM” rats from this point forward. Following completion of either MI or SHAM procedures, rats were housed one per cage for ten days to minimize risk of infection of the surgical site. During these ten days, the antibiotic Baytril (100 mg/mL) was administered in the drinking water. Following completion of the Baytril treatment, rats were housed two per cage as described above. All animals were monitored daily for 14 days

following the MI or SHAM procedure for changes in behavior, gait/posture, breathing, appetite and body weight.

*Echocardiograph Measurements.* Transthoracic echocardiograph measurements were performed with a commercially available system (Logiq S8; GE Health Care, Milwaukee, WI) one week before the final experimental protocol. Briefly, the rats were anaesthetized as described above. Once the rat was fully anesthetized, the isoflurane mixture was reduced to 2.5% isoflurane-O<sub>2</sub>. Following 5 minutes at 2.5% isoflurane, echocardiograph measurements began. The transducer was positioned on the left anterior chest, and left ventricular dimensions were measured. The left ventricular fractional shortening (FS), ejection fraction (EF), end diastolic (LVEDV), end systolic volume (LVESV), and stroke volume (SV) were determined by echocardiographic measurements as previously described (37).

*Surgical Procedures for Experimental Protocols.* *In vivo* experiments were performed between six and eight weeks following the MI or SHAM procedure. On the day of the experiment, rats were anesthetized as described above. Adequate depth of anesthesia was confirmed by the absence of toe-pinch and blink reflexes. The trachea was cannulated, and the lungs were mechanically ventilated (Harvard Apparatus, Holliston, MA) with a 2% isoflurane-balance O<sub>2</sub> gaseous mixture until the decerebration was completed (see below). The right jugular vein and both carotid arteries were cannulated with PE-50 catheters which were used for the injection of fluids, measurement of arterial blood pressure (physiological pressure transducer, AD Instruments), and sampling of arterial blood gasses (Radiometer). HR was calculated from the R-R interval measured by electrocardiogram (AD Instruments). The left superficial epigastric artery was cannulated with a PE-8 catheter whose tip was placed near the junction of the superficial epigastric and femoral arteries. A reversible snare was placed around the left iliac artery and vein (i.e., proximal to the location of the catheter placed in the superficial epigastric artery). The left calcaneal bone was severed and linked by string to a force transducer (Grass FT03), which, in turn, was attached to a rack and pinion.

Upon completion of the initial surgical procedures, rats were placed in a Kopf stereotaxic frame. After administering dexamethasone (0.2 mg i.v.) to minimize swelling of the brainstem, a pre-collicular decerebration was performed in which all brain tissue rostral to the superior colliculi was removed (38). The cranial cavity was filled with cotton balls and covered with glue (Kwik-

Sil, World Precision Instruments). Following decerebration, anesthesia was reduced to 0.5%. A retroperitoneal approach was used to expose bundles of the left renal sympathetic nerve, which were then glued with Kwik-Sil onto a pair of thin stainless-steel recording electrodes connected to a high impedance probe (Grass Model HZP) and amplifier (Grass P511). Multiunit signals from the renal sympathetic nerve fibres were filtered at high and low frequencies (1 KHz and 100 Hz, respectively) for the measurement of RSNA.

Upon completion of all surgical procedures, anesthesia was terminated, and the rats' lungs were ventilated with room air. Experimental protocols commenced at least one hour after reduction of isoflurane from 2% to 0.5%, and at least 30 minutes after reduction of isoflurane from 0.5% to 0%. Experiments were performed on decerebrate, unanesthetized rats because anesthesia has been shown to markedly blunt the exercise pressor reflex in the rat (38). Body core temperature was measured via a rectal probe and maintained at ~37–38°C by an automated heating system (Harvard Apparatus) and heat lamp. Arterial pH and blood gases were analyzed periodically throughout the experiment from arterial blood samples (~75 µL) and maintained within physiological ranges (pH: 7.35–7.45, PCO<sub>2</sub>: ~38–40 mmHg, PO<sub>2</sub>: ~100 mmHg) by administration of sodium bicarbonate and/or adjusting ventilation as necessary. At the end of all experiments in which RSNA was measured, postganglionic sympathetic nerve activity was abolished with administration of hexamethonium bromide (20 mg/kg iv) to allow for the quantification of background noise as described previously (39). A pneumothorax was then performed, and the lungs were then excised and weighed. The heart was excised, and the atria and right ventricle (RV) were separated from the left ventricle (LV) and septum, and the RV, LV, and atria were weighed. In rats with HF-rEF, the LV infarction surface area was measured using planimetry and expressed as percent of LV endocardial surface area as described previously (40).

*Isolated mechanoreflex protocols.* We first compared the RSNA, pressor, and cardioaccelerator responses evoked in response to 30 seconds of 1 Hz dynamic stretch of the triceps surae muscle before and after the injection of either the IP<sub>3</sub> receptor antagonist Xestospongine C (SHAM  $n=5M/3F$ , HF-rEF  $n=3M/2F$ ) or the PKC $\epsilon$  inhibitor PKC $\epsilon$ 141 (SHAM  $n=3M/3F$ , HF-rEF  $n=4M/3F$ ) into the arterial supply of the left hindlimb. Before initiating the protocol, we paralyzed the rats with pancuronium bromide (1 mg/kg iv). In detail, at least 60 minutes following the decerebration procedure and termination of anesthesia, baseline muscle tension was set at ~80-100 g by manually turning the rack and pinion. Baseline blood pressure and

heart rate were measured for ~30 seconds. An experienced investigator then initiated the stretch protocol in which the rack and pinion was turned back and forth manually at a 1 Hz frequency with the aid of a metronome for 30 seconds. The investigator aimed for a developed tension of ~0.6-0.8 kg on each stretch which is the tension generation typically developed during 1 Hz intermittent contraction protocols in decerebrate rats (39, 41). This dynamic stretch protocol was adapted from protocols described originally by Stebbins et al. (42) and Daniels et al. (43) in the cat. Approximately five minutes following the completion of the control dynamic stretch protocol, and after ensuring that blood pressure had returned to its pre-stretch baseline value, the appropriate solution (see below) was injected into the arterial supply of the left hindlimb via the left superficial epigastric artery catheter. After the appropriate time had passed the dynamic stretch protocol was repeated as aforementioned. At the end of each experiment, Evans blue dye was injected in the same manner as the experimental solution to confirm that the injectate had access to the triceps surae muscle circulation.

The following isolated mechanoreflex protocols were performed. The injectate, whether an iliac artery and vein snare was pulled tight, the time the hindlimb was allowed to reperfuse if a snare was pulled tight, and the sample sizes are indicated. *Protocol 1:* Xestospongine C (IP3 receptor antagonist, 5 µg dissolved in 0.2 mL of 0.02% ethanol; established by ref. 31), snare tight for 10 min, reperfuse for 30 min,  $n=5M/3F$  SHAM rats and  $n=3M/2F$  HF-rEF rats. *Protocol 2:* PKCε141 (PKCε translocation inhibitor, 45 µg dissolved in 0.2mL of 2.25% DMSO), no snare and infused with the aid of a constant infusion pump (Harvard Apparatus) at a flow rate of 20 µL/min for 10 min,  $n=3M/3F$  SHAM rats and  $n=4M/3F$  HF-rEF rats. *Protocol 3:* 0.2mL of 2.25% DMSO (vehicle for PKCε141), no snare and infused with the aid of a constant infusion pump (Kent Scientific) at a flow rate of 20 µL/min for 10 min,  $n=1M/3F$  HF-rEF rats. In an additional group of HF-rEF rats dynamic hindlimb skeletal muscle stretch maneuvers were performed before and after PKCε141 (45 µg dissolved in 0.2mL of 2.25% DMSO) was injected into the right jugular vein with the aid of a constant infusion pump (Kent Scientific) at a flow rate of 20 µL/min for 10 min and therefore allowed to circulate systemically. Ten minutes elapsed between the intravenous injection of PKCε141 and the subsequent stretch maneuver exactly as aforementioned in *Protocol 2* when PKCε141 was injected into the arterial supply of the hindlimb.

*Isolated metaboreflex protocols.* In three groups of HF-rEF rats, we compared the renal sympathetic, pressor, and cardioaccelerator response to injection of either lactic acid (24mMol in

0.2mL saline;  $n=1M/4F$ ),  $\alpha,\beta$ -methylene ATP (20  $\mu\text{g}$  in 0.2mL saline;  $n=2M/2F$ ), or bradykinin (5  $\mu\text{g}$  in 0.2mL saline;  $n=2M/2F$ ) before and after the injection of the PKC $\epsilon$  inhibitor PKC $\epsilon$ 141 (45  $\mu\text{g}$  dissolved in 0.2mL of 2.25% DMSO) into the arterial supply of the left hindlimb. Before initiating the protocol, we paralyzed the rats with pancuronium bromide (1 mg/kg iv). Lactic acid,  $\alpha,\beta$ -methylene ATP, and bradykinin were all injected as a bolus over  $\sim 2$  seconds into the arterial supply of the left hindlimb. For  $\alpha,\beta$ -methylene ATP and bradykinin injections, an iliac artery and vein snare was pulled tight 30 seconds prior to injection and remained snared for 30 seconds after the injection was completed. Approximately five minutes following the completion of the control injection protocol, and after ensuring that blood pressure had returned to its pre-injection baseline value PKC $\epsilon$ 141 was infused as described above. After infusion of PKC $\epsilon$ 141, a second injection of either lactic acid,  $\alpha,\beta$ -methylene ATP, or bradykinin was performed exactly as performed in the control injection. At the end of each experiment, Evans blue dye was injected in the same manner as the experimental solution to confirm that the injectate had access to the triceps surae muscle circulation.

*Exercise pressor reflex protocols.* In a group of SHAM ( $n=3M/2F$ ) and HF-rEF rats ( $n=5M/1F$ ), we compared the renal sympathetic, pressor, and cardioaccelerator responses evoked in response to 30 seconds of 1 Hz dynamic hindlimb muscle contraction before and after the injection of PKC $\epsilon$ 141 (45  $\mu\text{g}$  in 0.2mL saline containing 2.25% DMSO) into the arterial supply of the left hindlimb. Following recovery of isoflurane anesthesia, baseline muscle tension was set to  $\sim 100$  g and baseline RSNA, blood pressure, and HR were measured for  $\sim 30$  seconds. The sciatic nerve was then electrically stimulated using stainless steel electrodes for 30 seconds at a voltage of  $\sim 1.5$ x motor threshold (0.01 ms pulse duration, 500 ms train duration, 40 Hz frequency) which produced 1 Hz repetitive/dynamic contractions of the triceps surae muscles. Approximately 10 min following the control contraction maneuver, PKC $\epsilon$ 141 was infused as described above. At the end of each experiment, the rats were paralyzed with pancuronium bromide (1 mg/kg iv) and the sciatic nerve was stimulated for 30 s with the same parameters as those used to elicit contraction to ensure that the increase in RSNA, blood pressure and HR during contraction was not due to the electrical activation of the axons of the thin fiber muscle afferents in the sciatic nerve. No increase in RSNA, blood pressure or HR was observed during the stimulation period following the administration of pancuronium bromide. Evans blue dye was injected in the same manner as the

experimental solution to confirm that the injectate had access to the triceps surae muscle circulation.

#### *Tissue collection*

In four SHAM and five HF-rEF rats, the left and right L<sub>4</sub>/L<sub>5</sub> DRG were harvested. Rats were first deeply anesthetized (5% isoflurane) and killed with an overdose of saturated KCL. Samples were isolated into 2 mL bead mill tubes containing ~0.5g of 1.4 mm diameter ceramic beads, 300 µL of RP1 lysis buffer (Macherey-Nagel), and homogenized for 1 min at 5 m/s using Bead Mill 4 (Fisherbrand™). Total protein and mRNA from tissues were prepared with the Nucleospin miRNA/Protein Kit (Macherey-Nagel, Düren, Germany) according to the manufacturer's instructions. Total Protein and RNA concentrations were determined using the Qubit 2.0 Fluorometer (Life Technologies, Grand Island, NY, USA) and stored in a -80°C freezer until further analysis.

#### *Western blot experiments*

Protein samples (20 µg) were separated on 4-12% Bis-Tris Protein Gels (Invitrogen™) by gel electrophoresis in MES running buffer (Invitrogen™) employing 200 V for 22 min. Gels were then transferred to mini-PVDF membranes using the iBlot 2 Dry Transfer Device (Invitrogen™). Membranes were incubated for ~3 hours with the iBind device with iBind solution (Invitrogen™) with a primary antibody for PKCε receptor diluted 1:100 (ThermoFisher, Rockford, IL, USA; cat. no. MA5-14908) and a Goat anti-Rabbit IgG (H+L) secondary antibody conjugated with Horse Radish Peroxidase diluted 1:1,500 (Abcam; Cambridge, England; cat. no. ab205718). The membrane was then incubated for 5 min with 6mL of SuperSignal™ West Pico PLUS Chemiluminescent Substrate (Thermo Fisher) and imaged with C-DiGit® Blot Scanner (Li-Cor). The protein bands were quantified and analyzed using the Image Studio software (Li-Cor). The membrane was then re-incubated with a primary antibody for GAPDH diluted 1:1,000 (Thermo Fisher Scientific; Rockford, IL, USA; cat. no. MA5-15738), along with a Goat anti-Mouse IgG (H+L), secondary antibody conjugated with Horse Radish Peroxidase diluted 1:1,000 (Thermo Fisher Scientific; Rockford, IL, USA; cat. no. 31430). Membranes were then re-incubated and re-imaged as just described.

#### *Quantitative Reverse Transcriptase Polymerase Chain Reaction experiments*

Complementary DNA (cDNA) was synthesized from RNA isolates (see above) using the High Capacity RNA-cDNA™ kit (Thermo Fisher) according to the manufacturer's instructions. Quantitative reverse transcriptase polymerase chain reaction experiments were then performed on the cDNA samples using TaqMan gene expression assays specific for: PKCε (Sequence proprietary; assay ID: Rn01785893\_m1), along with GAPDH with (forward primer: 5'-ACCGCCTGTTGCGTGTTA-3' and reverse primer: 5'-CAATCGCCAACGCCTCAA-3'; assay ID: Rn01775763\_g1). All samples were run in duplicate for the gene of interest and the endogenous control (GAPDH). The results were analyzed with the comparative threshold ( $\Delta\Delta Ct$ ) method.

*Data analysis.* Muscle tension, blood pressure, HR and RSNA were measured and recorded in real time with a PowerLab and LabChart data acquisition system (AD Instruments). The original RSNA data were rectified and corrected for the background noise determined after the administration of pancuronium bromide. Baselines for mean arterial pressure (MAP), RSNA and HR were determined from the 30-second baseline periods that preceded each maneuver. The peak increase in MAP (peak  $\Delta MAP$ ), RSNA (peak  $\Delta RSNA$ ), and HR (peak  $\Delta HR$ ) during dynamic contraction were calculated as the difference between the peak values wherever they occurred during the maneuvers and their corresponding baseline value. The integrated RSNA for the first 5 seconds ( $\int \Delta RSNA_{5 \text{ Sec}}$ ) was calculated by integrating the  $\Delta RSNA$  ( $>0$ ) during the first 5 seconds of the contraction maneuver. The change in tension-time indexes ( $\Delta TTI$ s) and blood pressure indexes (BPIs) were calculated by integration of the area under curve during the stretch or contraction maneuver and subtracting the integrated area under the curve during the baseline period. Time courses of the increase in RSNA and MAP were plotted as their change from baseline. Baseline MAP, baseline HR, Peak  $\Delta MAP$ , Peak  $\Delta HR$ , Peak  $\Delta RSNA$ , BPI,  $\int \Delta RSNA$ , and  $\Delta TTI$ s were compared with multiple paired *t*-tests. Data for echocardiograph measurements, body and organ masses, heart morphometrics, protein and mRNA expression were analyzed with unpaired Student's *t*-tests or Mann-Whitney U tests as appropriate. All data are expressed as mean $\pm$ SEM. Statistical significance was defined as  $P \leq 0.05$ .

## 4.4 Results

*Body mass, heart morphometrics*



Body masses were not different between SHAM and HF-rEF rats (Table 1). The ratios of the RV, LV, and atria mass to body mass were greater in HF-rEF rats compared to SHAM rats. Additionally, LVEDV and LVESV were significantly greater, and ejection fraction and fractional shortening were significantly lower, in HF-rEF rats compared to SHAM rats. There was no difference in SV between groups.

#### *Effect of 1,4,5-trisphosphate (IP<sub>3</sub>) receptor blockade on isolated mechanoreflex activation*

Injection of the IP<sub>3</sub> receptor antagonist Xestospongine C into the arterial supply of the hindlimb had no effect on the time course of the RSNA or pressor response to 1 Hz dynamic hindlimb skeletal muscle stretch in SHAM ( $n=5M/3F$ ) or HF-rEF rats ( $n=3M/2F$ ; Fig. 1). The  $\int\Delta\text{RSNA}$  of the stretch maneuver was not different after Xestospongine C injection in either SHAM or HF-rEF rats (Fig. 2A). The  $\int\Delta\text{RSNA}_{5\text{ sec}}$  was significantly greater after in SHAM rats, but not HF-rEF rats after Xestospongine C injection (Fig. 2B). Finally, the Peak  $\Delta\text{MAP}$ , BPI, and Peak  $\Delta\text{HR}$  response to the stretch maneuver was not different after Xestospongine C injection (Fig. 2C & D, Table 2). The tension developed during the stretch maneuver was not different before or after injection of Xestospongine C (Table 3). An example of original recordings showing the RSNA and pressor response to stretch before and after Xestospongine C in a HF-rEF rat is shown in Fig. 5A. Baseline MAP, baseline HR, and Peak  $\Delta\text{HR}$  before and after PKC $\epsilon$ 141 injection in SHAM and HF-rEF rats are shown in Table 2.

#### *Effect of protein kinase C epsilon (PKC $\epsilon$ ) inhibition on isolated mechanoreflex activation*

Injection of the PKC $\epsilon$  inhibitor PKC $\epsilon$ 141 into the arterial supply of the hindlimb significantly reduced the time course of the RSNA and pressor response to 1 Hz dynamic hindlimb skeletal muscle stretch in HF-rEF rats ( $n=4M/3F$ ), but not SHAM rats ( $n=3M/3F$ ; Fig. 3). The  $\int\Delta\text{RSNA}$  and the  $\int\Delta\text{RSNA}_{5\text{ sec}}$  of the stretch maneuver was significantly reduced after PKC $\epsilon$ 141 injection in HF-rEF rats but not SHAM rats (Fig. 4A & B). Finally, the Peak  $\Delta\text{MAP}$ , BPI, and Peak  $\Delta\text{HR}$  response to the stretch maneuver was not different after injection of PKC $\epsilon$ 141 in SHAM rats. Conversely, the Peak  $\Delta\text{MAP}$ , but not BPI or Peak  $\Delta\text{HR}$ , response was reduced following injection of PKC $\epsilon$ 141 in HF-rEF rats (Fig. 4C & D, Table 2). The tension developed during the stretch maneuver was not different before or after injection of PKC $\epsilon$ 141 (Table 3). An example of original recordings showing the RSNA and pressor response to stretch before and after PKC $\epsilon$ 141

in a HF-rEF rat is shown in Fig. 5A. Baseline MAP, baseline HR, and Peak  $\Delta$ HR before and after PKC $\epsilon$ 141 injection in SHAM and HF-rEF rats are shown in Table 2.

In systemic control experiments, we found that injection of PKC $\epsilon$ 141 into the jugular vein to allow it to circulate systemically had no effect on the time course of the RSNA or pressor response to 1 Hz dynamic hindlimb skeletal muscle stretch of HF-rEF rats ( $n=3M/1F$ ; Fig. 6A & C). In vehicle control experiments we found that injection of 0.2mL saline containing 2.25% DMSO into the arterial supply of the hindlimb had no effect on the time course of the RSNA or pressor response to 1 Hz dynamic hindlimb skeletal muscle stretch ( $n=1M/3F$ ; Fig. 6B & D). The tension developed during the stretch maneuver was not different before or after injection of PKC $\epsilon$ 141 (Table 3). Baseline MAP, baseline HR, and Peak  $\Delta$ HR before and after PKC $\epsilon$ 141 injection in SHAM and HF-rEF rats are shown in Table 2.

#### *Effect of PKC $\epsilon$ inhibition on isolated metaboreflex activation*

Injection of the PKC $\epsilon$  inhibitor PKC $\epsilon$ 141 into the arterial supply of the hindlimb had no effect on the Peak  $\Delta$ RSNA or Peak  $\Delta$ MAP response to hindlimb arterial injection of 24 mMol lactic acid ( $n=1M/4F$ ), 20 $\mu$ g of  $\alpha,\beta$ -methylene ATP ( $n=2M/2F$ ), or 5 $\mu$ g of bradykinin ( $n=2M/2F$ ; Fig. 7). Baseline MAP, baseline HR, and Peak  $\Delta$ HR before and after PKC $\epsilon$ 141 injection in SHAM and HF-rEF rats are shown in Table 2. Finally, we found that the Peak  $\Delta$ RSNA response to the control injection of  $\alpha,\beta$ -methylene ATP was significantly lower than the Peak  $\Delta$ RSNA to the control injection of lactic acid ( $P=0.001$ ) and control injection of bradykinin ( $P=0.017$ ), despite a similar Peak  $\Delta$ MAP response between  $\alpha,\beta$ -methylene ATP and lactic acid ( $P=0.309$ ) and  $\alpha,\beta$ -methylene ATP and bradykinin ( $P=0.166$ ).

#### *Effect of PKC $\epsilon$ inhibition on exercise pressor reflex activation*

Injection of the PKC $\epsilon$  inhibitor PKC $\epsilon$ 141 into the arterial supply of the hindlimb significantly reduced the time course of the RSNA and pressor response to 1 Hz dynamic hindlimb skeletal muscle contraction in HF-rEF rats ( $n=5M/1F$ ), but not SHAM rats ( $n=3M/2F$ ; Fig. 8). The  $\int\Delta$ RSNA and the  $\int\Delta$ RSNA<sub>5 Sec</sub> as well as the Peak  $\Delta$ MAP and BPI of the contraction maneuvers before and after PKC $\epsilon$ 141 injection in SHAM and HF-rEF rats are shown in Fig. 9. The tension developed during the contraction maneuvers was not different before or after injection of PKC $\epsilon$ 141 (Table 3). Baseline MAP, baseline HR, and Peak  $\Delta$ HR before and after PKC $\epsilon$ 141 injection in SHAM and HF-rEF rats are shown in Table 2.

### *DRG PKC $\epsilon$ protein and mRNA expression*

We found no difference between SHAM ( $n=4M$ ) and HF-rEF ( $n=5M$ ) rats in PKC $\epsilon$  protein or mRNA expression within L<sub>4</sub>/L<sub>5</sub> DRG tissue (Fig. 10).

## **4.5 Discussion**

The present investigation was intended to extend previous findings which showed that TxA<sub>2</sub> (18, 19) and B2 receptors (25) on the sensory endings of thin fiber muscle afferents contribute to the exaggerated mechanoreflex and exercise pressor reflex in rats with HF-rEF. Specifically, we sought to determine whether IP<sub>3</sub> receptors and PKC $\epsilon$ , components of second-messenger signaling associated with G<sub>q</sub> protein coupled receptors such as TxA<sub>2</sub> and B2 receptors, contribute to the chronic sensitization of mechanically activated channels/afferents that underly mechanoreflex activation in HF-rEF rats. In HF-rEF rats, we found that hindlimb arterial injection of the IP<sub>3</sub> receptor antagonist Xec had no effect on the sympathetic and pressor response to dynamic hindlimb muscle stretch in HF-rEF rats. However, hindlimb arterial injection of the PKC $\epsilon$  translocation inhibitor PKC $\epsilon$ 141 attenuated the sympathetic and pressor response to dynamic hindlimb muscle stretch and dynamic hindlimb muscle contraction in HF-rEF rats. In SHAM rats, we found no effect of hindlimb arterial injection of either Xec or PKC $\epsilon$ 141 on the sympathetic and pressor response to dynamic hindlimb muscle stretch. These results suggest that PKC $\epsilon$  translocation to the cell membrane contributes importantly to the chronic sensitization of mechanically activated channels/afferents that underly mechanoreflex activation in HF-rEF.

We recently found that hindlimb arterial injection of Xec (5  $\mu$ g) attenuated the exaggerated pressor response to dynamic hindlimb muscle stretch and contraction in rats with simulated peripheral artery disease but had no effect on the pressor response to stretch in healthy rats (31). Xec is a cell membrane permeable molecule isolated from a marine sponge species (*Xestospongia*) (44) that, in a variety of species, has been shown to inhibit IP<sub>3</sub> receptors and prevent the release of intracellular calcium stores into the cytosol (45-48). Consistent with our previous findings in healthy rats, in the SHAM cohort contained within the present investigation, we found that hindlimb arterial injection of Xec (5  $\mu$ g) had no effect on the sympathetic or pressor response to dynamic hindlimb muscle stretch. However, in contrast to our previous findings in rats with simulated peripheral artery disease (31), hindlimb arterial injection of Xec (5  $\mu$ g) had no effect on the exaggerated sympathetic or pressor response to dynamic hindlimb muscle stretch in rats with

HF-rEF. Thus, it appears that the second-messenger signaling pathway(s) associated with G<sub>q</sub> protein coupled receptors which contribute to the chronic mechanoreflex sensitization differ between rats with HF-rEF and rats with simulated peripheral artery disease such that IP<sub>3</sub> receptors contribute to the chronic mechanoreflex sensitization in rats with simulated peripheral artery disease, but not in rats with HF-rEF.

PKC $\epsilon$  is an important second-messenger in G<sub>q</sub> protein coupled receptors and its translocation to the cell membrane has been shown to be necessary for the development of mechanical hyperalgesia in the mouse (33). Thus, our finding in HF-rEF rats that hindlimb arterial injection of the PKC $\epsilon$  translocation inhibitor PKC $\epsilon$ 141, but not the vehicle for PKC $\epsilon$ 141, attenuated the sympathetic and pressor response to dynamic hindlimb muscle stretch identifies a second-messenger signaling pathway that may contribute to the G<sub>q</sub> protein coupled receptors which mediate the chronic mechanoreflex sensitization previously identified in this model (i.e., TxA<sub>2</sub> and B<sub>2</sub> receptors 19, 25). Moreover, we also found in HF-rEF rats that PKC $\epsilon$  translocation inhibition attenuated the sympathetic and pressor response to dynamic hindlimb muscle contraction. However, PKC $\epsilon$ 141 injection had no effect on the sympathetic or pressor response to stretch or contraction in SHAM rats. These findings suggest that PKC $\epsilon$  contributes to the chronic sensitization of mechanically activated channels/afferents that underly mechanoreflex activation during rhythmic contraction in HF-rEF. An acute sensitization of mechanically activated channels/afferents produced by contraction-induced elevations in either COX metabolites (49, 50) or bradykinin (51), as well as a small role for G<sub>q</sub> protein coupled receptors in the metaboreflex component of the exercise pressor reflex in HF-rEF rats is also possible (52). If present, those actions may have occurred additively with the chronic sensitization to produce the overall PKC $\epsilon$  mediated effects in our experiments. The fact that injection of PKC $\epsilon$ 141 into the jugular vein had no effect on the sympathetic and pressor response to stretch suggests that the effect of PKC $\epsilon$ 141 when injected into the arterial supply of the hindlimb on the sympathetic and pressor response to stretch in HF-rEF rats is attributable to effects within the sensory endings of thin fiber muscle afferents and not effects elsewhere in the mechanoreflex arc such as the brainstem and/or the spinal cord. Moreover, our finding that PKC $\epsilon$ 141 had no effect on the sympathetic and pressor response to injection of either lactic acid,  $\alpha$ , $\beta$ -methylene ATP, or bradykinin into the arterial supply of the hindlimb suggests that the effect of PKC $\epsilon$ 141 on the sympathetic and pressor response to stretch and contraction in HF-rEF rats is most likely attributable to an interruption of the cellular signaling

between PKC $\epsilon$ 141 and mechanically activated channels and is not attributable to any “off-target” effects which may have produced a generalized reduction in muscle afferent responsiveness.

Our finding that there was no difference in PKC $\epsilon$  protein or mRNA expression within L<sub>4</sub>/L<sub>5</sub> DRG tissue between SHAM and HF-rEF rats suggests that an increased expression of PKC $\epsilon$  does not account for the PKC $\epsilon$ -mediated chronic mechanoreflex sensitization. However, it is possible that the increased expression of the proinflammatory enzyme COX-2 within skeletal muscle homogenates of HF-rEF patients (53) and HF-rEF rats (22, 54) increases the phosphorylation of PKC $\epsilon$  within the sensory endings of muscle afferents. There is even some indirect evidence supporting this possibility. For example, Zhou et al. (55) showed that phosphorylation of PKC $\epsilon$  in L<sub>5</sub> DRG neurons was significantly up-regulated after carrageen- and Complete Freund’s Adjuvant-induced inflammation. Although not investigated herein, this possibility may serve as a potential explanation for the mechanism(s) which may account for the PKC $\epsilon$ -mediated chronic mechanoreflex sensitization in HF-rEF.

A few experimental considerations warrant discussion. First, although both male and female rats were included in each group, we did not control for any potential influences of estrous cycle in the female rats. Second, the hindlimb muscle stretch model of isolated mechanoreflex activation stimulates mechanically activated channels by passively lengthening the muscle. During the muscle contractions associated with most common forms of exercise, mechanically-sensitive channels on the sensory endings of thin fiber muscle afferents are stimulated when muscle length shortens and intramuscular pressure increases (56). Although the nature of the stimulus is different, hindlimb muscle stretch in the rat has been shown to stimulate 87% of the same group III muscle afferents as does hindlimb muscle contraction in the healthy rat (57). Finally, analysis of PKC $\epsilon$  mRNA and protein expression in whole DRG tissue may have masked effects of HF-rEF on receptor expression that were limited to subpopulations of group III/IV muscle afferents.

## **4.6 Conclusion**

In summary, we investigated the second-messenger signaling pathways associated with G<sub>q</sub> protein coupled receptors which underly the chronic mechanoreflex sensitization in male and female rats with HF-rEF. Our findings described above suggest that intracellular signaling within the sensory ending of thin fiber muscle afferents involving PKC $\epsilon$ , but not IP<sub>3</sub> receptors, contribute importantly to the chronic mechanoreflex sensitization and overall exaggerated exercise pressor

reflex in male and female rats with HF-rEF. Importantly, excessive activation of thin fiber muscle afferents during exercise in HF-rEF patients (*i.e.*, exaggerated exercise pressor reflex) constrains limb blood flow (58), stroke volume, and cardiac output (7). Thus, our findings reveal important mechanisms within the sensory endings of these thin fiber muscle afferents that may contribute to the excessive afferent activation within this patient population.

## 4.6 References

1. **Rowell L, and O'Leary D.** Reflex control of the circulation during exercise: Chemoreflexes and mechanoreflexes. *JApplPhysiol* 69: 407-418, 1990.
2. **Goodwin GM, McCloskey DI, and Mitchell JH.** Cardiovascular and respiratory responses to changes in central command during isometric exercise at constant muscle tension. *JPhysiol(Lond)* 226: 173-190, 1972.
3. **Stickland MK, Miller JD, Smith CA, and Dempsey JA.** Carotid chemoreceptor modulation of regional blood flow distribution during exercise in health and chronic heart failure. *Circ Res* 100: 1371-1378, 2007.
4. **Sinoway LI, and Li J.** A perspective on the muscle reflex: implications for congestive heart failure. *J Appl Physiol (1985)* 99: 5-22, 2005.
5. **Koba S, Gao Z, Xing J, Sinoway LI, and Li J.** Sympathetic responses to exercise in myocardial infarction rats: a role of central command. *AmJPhysiol Heart CircPhysiol* 291: H2735-H2742, 2006.
6. **Barretto AC, Santos AC, Munhoz R, Rondon MU, Franco FG, Trombetta IC, Roveda F, de Matos LN, Braga AM, Middlekauff HR, and Negrao CE.** Increased muscle sympathetic nerve activity predicts mortality in heart failure patients. *Int J Cardiol* 135: 302-307, 2009.
7. **Smith JR, Joyner MJ, Curry TB, Borlaug BA, Keller-Ross ML, Van Iterson EH, and Olson TP.** Locomotor muscle group III/IV afferents constrain stroke volume and contribute to exercise intolerance in human heart failure. *J Physiol* 598: 5379-5390, 2020.
8. **Ponikowski P, Anker SD, AlHabib KF, Cowie MR, Force TL, Hu S, Jaarsma T, Krum H, Rastogi V, Rohde LE, Samal UC, Shimokawa H, Budi Siswanto B, Sliwa K, and Filippatos G.** Heart failure: preventing disease and death worldwide. *ESC Heart Fail* 1: 4-25, 2014.
9. **Kaufman MP, Longhurst JC, Rybicki KJ, Wallach JH, and Mitchell JH.** Effects of static muscular contraction on impulse activity of groups III and IV afferents in cats. *JApplPhysiol* 55: 105-112, 1983.
10. **McCloskey DI, and Mitchell JH.** Reflex cardiovascular and respiratory responses originating in exercising muscle. *JPhysiol* 224: 173-186, 1972.

11. **Kaufman MP, Iwamoto GA, Longhurst JC, and Mitchell JH.** Effects of capsaicin and bradykinin on afferent fibers with endings in skeletal muscle. *CircRes* 50: 133-139, 1982.
12. **Kaufman MP, Rybicki KJ, Waldrop TG, and Ordway GA.** Effect of ischemia on responses of group III and IV afferents to contraction. *JApplPhysiol* 57: 644-650, 1984.
13. **Mense S, and Meyer H.** Bradykinin-induced modulation of the response behaviour of different types of feline group III and IV muscle receptors. *JPhysiol* 398: 49-63, 1988.
14. **Mense S, and Stahnke M.** Responses in muscle afferent fibers of slow conduction velocity to contractions and ischemia in the cat. *JPhysiol* 342: 383-397, 1983.
15. **Rotto DM, and Kaufman MP.** Effects of metabolic products of muscular contraction on the discharge of group III and IV afferents. *JApplPhysiol* 64: 2306-2313, 1988.
16. **Antunes-Correa LM, Nobre TS, Groehs RV, Alves MJ, Fernandes T, Couto GK, Rondon MU, Oliveira P, Lima M, Mathias W, Brum PC, Mady C, Almeida DR, Rossoni LV, Oliveira EM, Middlekauff HR, and Negrao CE.** Molecular basis for the improvement in muscle metaboreflex and mechanoreflex control in exercise-trained humans with chronic heart failure. *Am J Physiol Heart Circ Physiol* 307: H1655-1666, 2014.
17. **Middlekauff HR, Chiu J, Hamilton MA, Fonarow GC, Maclellan WR, Hage A, Moriguchi J, and Patel J.** Muscle mechanoreceptor sensitivity in heart failure. *AmJPhysiol Heart CircPhysiol* 287: H1937-H1943, 2004.
18. **Butenas ALE, Rollins KS, Williams AC, Parr SK, Hammond ST, Ade CJ, Hageman KS, Musch TI, and Copp SW.** Thromboxane A2 receptors contribute to the exaggerated exercise pressor reflex in male rats with heart failure. *Physiological reports* 9: e15052, 2021.
19. **Butenas ALE, Rollins KS, Williams AC, Parr SK, Hammond ST, Ade CJ, Hageman KS, Musch TI, and Copp SW.** Exaggerated sympathetic and cardiovascular responses to dynamic mechanoreflex activation in rats with heart failure: Role of endoperoxide 4 and thromboxane A2 receptors. *Auton Neurosci* 232: 102784, 2021.
20. **Butenas ALE, Rollins KS, Parr SK, Hammond ST, Ade CJ, Hageman KS, Musch TI, and Copp SW.** Novel mechanosensory role for acid sensing ion channel subtype 1a in evoking the exercise pressor reflex in rats with heart failure. *J Physiol* 600: 2105-2125, 2022.
21. **Koba S, Xing J, Sinoway LI, and Li J.** Sympathetic nerve responses to muscle contraction and stretch in ischemic heart failure. *Am J Physiol Heart Circ Physiol* 294: H311-321, 2008.



22. **Morales A, Gao W, Lu J, Xing J, and Li J.** Muscle cyclo-oxygenase-2 pathway contributes to the exaggerated muscle mechanoreflex in rats with congestive heart failure. *Exp Physiol* 97: 943-954, 2012.
23. **Smith SA, Mammen PP, Mitchell JH, and Garry MG.** Role of the exercise pressor reflex in rats with dilated cardiomyopathy. *Circulation* 108: 1126-1132, 2003.
24. **Wang HJ, Li YL, Gao L, Zucker IH, and Wang W.** Alteration in skeletal muscle afferents in rats with chronic heart failure. *JPhysiol* 588: 5033-5047, 2010.
25. **Koba S, Xing J, Sinoway LI, and Li J.** Bradykinin receptor blockade reduces sympathetic nerve response to muscle contraction in rats with ischemic heart failure. *Am J Physiol Heart Circ Physiol* 298: H1438-1444, 2010.
26. **Huang JS, Ramamurthy SK, Lin X, and Le Breton GC.** Cell signalling through thromboxane A2 receptors. *Cell Signal* 16: 521-533, 2004.
27. **Jang Y, Kim M, and Hwang SW.** Molecular mechanisms underlying the actions of arachidonic acid-derived prostaglandins on peripheral nociception. *J Neuroinflammation* 17: 30, 2020.
28. **Narumiya S, Sugimoto Y, and Ushikubi F.** Prostanoid receptors: structures, properties, and functions. *Physiol Rev* 79: 1193-1226, 1999.
29. **Borbiro I, and Rohacs T.** Regulation of Piezo Channels by Cellular Signaling Pathways. *Curr Top Membr* 79: 245-261, 2017.
30. **Eijkelkamp N, Linley JE, Torres JM, Bee L, Dickenson AH, Gringhuis M, Minett MS, Hong GS, Lee E, Oh U, Ishikawa Y, Zwartkuis FJ, Cox JJ, and Wood JN.** A role for Piezo2 in EPAC1-dependent mechanical allodynia. *Nat Commun* 4: 1682, 2013.
31. **Rollins KS, Butenas ALE, Williams AC, and Copp SW.** Sensory neuron inositol-1,4,5-trisphosphate (IP3) receptors contribute to chronic mechanoreflex sensitization in rats with simulated peripheral artery disease. *Am J Physiol Regul Integr Comp Physiol* 321: R768-R780, 2021.
32. **Dubin AE, Schmidt M, Mathur J, Petrus MJ, Xiao B, Coste B, and Patapoutian A.** Inflammatory signals enhance piezo2-mediated mechanosensitive currents. *Cell reports* 2: 511-517, 2012.

33. **Hucho TB, Dina OA, and Levine JD.** Epac mediates a cAMP-to-PKC signaling in inflammatory pain: an isolectin B4(+) neuron-specific mechanism. *J Neurosci* 25: 6119-6126, 2005.
34. **National Research Council (U.S.). Committee for the Update of the Guide for the Care and Use of Laboratory Animals., Institute for Laboratory Animal Research (U.S.), and National Academies Press (U.S.).** Guide for the care and use of laboratory animals. Washington, D.C.: National Academies Press., 2011, p. xxv, 220 p.
35. **Musch TI, and Terrell JA.** Skeletal muscle blood flow abnormalities in rats with a chronic myocardial infarction: rest and exercise. *AmJPhysiol* 262: H411-H419, 1992.
36. **Kolettis TM, Agelaki MG, Baltogiannis GG, Vlahos AP, Mourouzis I, Fotopoulos A, and Pantos C.** Comparative effects of acute vs. chronic oral amiodarone treatment during acute myocardial infarction in rats. *Europace* 9: 1099-1104, 2007.
37. **Butenas ALE, Colburn TD, Baumfalk DR, Ade CJ, Hageman KS, Copp SW, Poole DC, and Musch TI.** Angiotensin converting enzyme inhibition improves cerebrovascular control during exercise in male rats with heart failure. *Respir Physiol Neurobiol* 103613, 2021.
38. **Smith SA, Mitchell JH, and Garry MG.** Electrically induced static exercise elicits a pressor response in the decerebrate rat. *JPhysiol* 537: 961-970, 2001.
39. **Kempf EA, Rollins KS, Hopkins TD, Butenas AL, Santin JM, Smith JR, and Copp SW.** Chronic femoral artery ligation exaggerates the pressor and sympathetic nerve responses during dynamic skeletal muscle stretch in decerebrate rats. *Am J Physiol Heart Circ Physiol* 314: H246-H254, 2018.
40. **Craig JC, Colburn TD, Hirai DM, Musch TI, and Poole DC.** Sexual dimorphism in the control of skeletal muscle interstitial Po<sub>2</sub> of heart failure rats: effects of dietary nitrate supplementation. *J Appl Physiol (1985)* 126: 1184-1192, 2019.
41. **Copp SW, Kim JS, Ruiz-Velasco V, and Kaufman MP.** The mechano-gated channel inhibitor GsMTx4 reduces the exercise pressor reflex in rats with ligated femoral arteries. *Am J Physiol Heart Circ Physiol* 310: H1233-1241, 2016.
42. **Stebbins CL, Brown B, Levin D, and Longhurst JC.** Reflex effect of skeletal muscle mechanoreceptor stimulation on the cardiovascular system. *JApplPhysiol* 65: 1539-1547, 1988.
43. **Daniels JW, Stebbins CL, and Longhurst JC.** Hemodynamic responses to static and dynamic muscle contractions at equivalent workloads. *AmJPhysiol* 279 (5): R1849-R1855, 2000.

44. **Gafni J, Munsch JA, Lam TH, Catlin MC, Costa LG, Molinski TF, and Pessah IN.** Xestospongins: potent membrane permeable blockers of the inositol 1,4,5-trisphosphate receptor. *Neuron* 19: 723-733, 1997.
45. **Azab W, Gramatica A, Herrmann A, and Osterrieder N.** Binding of alphaherpesvirus glycoprotein H to surface alpha4beta1-integrins activates calcium-signaling pathways and induces phosphatidylserine exposure on the plasma membrane. *mBio* 6: e01552-01515, 2015.
46. **Nakagawa M, Endo M, Tanaka N, and Gen-Pei L.** Structures of xestospongins A, B, C and D, novel vasodilative compounds from marine sponge, *xestospongia exigua*. *Tetrahedron letters* 25: 3227-3230, 1984.
47. **Ruiz A, Matute C, and Alberdi E.** Endoplasmic reticulum Ca(2+) release through ryanodine and IP(3) receptors contributes to neuronal excitotoxicity. *Cell Calcium* 46: 273-281, 2009.
48. **Sylantsev S, Jensen TP, Ross RA, and Rusakov DA.** Cannabinoid- and lysophosphatidylinositol-sensitive receptor GPR55 boosts neurotransmitter release at central synapses. *Proc Natl Acad Sci U S A* 110: 5193-5198, 2013.
49. **Hayes SG, Kindig AE, and Kaufman MP.** Cyclooxygenase blockade attenuates responses of group III and IV muscle afferents to dynamic exercise in cats. *Am J Physiol Heart Circ Physiol* 290: H2239-H2246, 2006.
50. **McCord JL, Hayes SG, and Kaufman MP.** PPADS does not block contraction-induced prostaglandin E2 synthesis in cat skeletal muscle. *Am J Physiol Heart Circ Physiol* 295: H2043-H2045, 2008.
51. **Stebbins CL, Carretero OA, Mindroiu T, and Longhurst JC.** Bradykinin release from contracting skeletal muscle of the cat. *J Appl Physiol* 69: 1225-1230, 1990.
52. **Leal AK, McCord JL, Tsuchimochi H, and Kaufman MP.** Blockade of the TP receptor attenuates the exercise pressor reflex in decerebrated rats with chronic femoral artery occlusion. *Am J Physiol Heart Circ Physiol* 301: H2140-H2146, 2011.
53. **Smith JR, Hart CR, Ramos PA, Akinsanya JG, Lanza IR, Joyner MJ, Curry TB, and Olson TP.** Metabo- and mechanoreceptor expression in human heart failure: Relationships with the locomotor muscle afferent influence on exercise responses. *Exp Physiol* 105: 809-818, 2020.

54. **Butenas ALE, Rollins KS, Matney JE, Williams AC, Kleweno TE, Parr SK, Hammond ST, Ade CJ, Hageman KS, Musch TI, and Copp SW.** No effect of endoperoxide 4 or thromboxane A2 receptor blockade on static mechanoreflex activation in rats with heart failure. *Exp Physiol* 105: 1840-1854, 2020.
55. **Zhou Y, Li GD, and Zhao ZQ.** State-dependent phosphorylation of epsilon-isozyme of protein kinase C in adult rat dorsal root ganglia after inflammation and nerve injury. *J Neurochem* 85: 571-580, 2003.
56. **Gallagher KM, Fadel PJ, Smith SA, Norton KH, Querry RG, Olivencia-Yurvati A, and Raven PB.** Increases in intramuscular pressure raise arterial blood pressure during dynamic exercise. *J Appl Physiol (1985)* 91: 2351-2358, 2001.
57. **Stone AJ, Copp SW, McCord JL, and Kaufman MP.** Femoral artery ligation increases the responses of thin-fiber muscle afferents to contraction. *J Neurophysiol* 113: 3961-3966, 2015.
58. **Amann M, Venturelli M, Ives SJ, Morgan DE, Gmelch B, Witman MA, Jonathan Groot H, Walter Wray D, Stehlik J, and Richardson RS.** Group III/IV muscle afferents impair limb blood in patients with chronic heart failure. *Int J Cardiol* 174: 368-375, 2014.

**Table 4.1**

Table 4.1. Body and tissue weights and heart morphometrics in SHAM and HF-rEF rats

|                           | SHAM (n=19) | HF-rEF (n=40) | P-value |
|---------------------------|-------------|---------------|---------|
| Body mass (g)             | 460±26      | 444±20        | 0.650   |
| Lung/body mass (mg/g)     | 3.22±0.11   | 3.55±0.10     | 0.049*  |
| RV/body mass (mg/g)       | 0.51±0.02   | 0.57±0.01     | 0.032*  |
| LV/body mass (mg/g)       | 1.99±0.04   | 2.15±0.04     | 0.015*  |
| Atria/body mass (mg/g)    | 0.15±0.01   | 0.21±0.01     | 0.004*  |
| LV EDV (mL)               | 0.96±0.06   | 1.94±0.13     | <0.001* |
| LV ESV (mL)               | 0.19±0.02   | 1.20±0.14     | <0.001* |
| Stroke volume (mL)        | 0.78±0.06   | 0.80±0.05     | 0.807   |
| Fractional shortening (%) | 43±2        | 20±2          | <0.001* |
| Ejection fraction (%)     | 80±2        | 45±3          | <0.001* |
| LV infarct size (%)       | -           | 29±1          | -       |

Values are means ± SEM. LV, left ventricle; RV, right ventricle; EDV, end diastolic volume; ESV, end systolic volume. Data were compared using student's test. Asterisks indicate a statistically significant difference between groups (P<0.05).

**Table 4.2**Table 4.2. Baseline MAP, baseline HR, and Peak  $\Delta$ HR in SHAM and HF-rEF rats.

|  | Pharmacological agent          | <i>n</i> | Control      | Postcondition | <i>P</i> value |
|--|--------------------------------|----------|--------------|---------------|----------------|
| Baseline MAP, mmHg                                 |                                |          |              |               |                |
| SHAM stretch                                       | 5 $\mu$ g Xestospongine C i.a. | 5M/3F    | 88 $\pm$ 7   | 79 $\pm$ 6    | 0.116          |
| HF-rEF stretch                                     | 5 $\mu$ g Xestospongine C i.a. | 3M/2F    | 85 $\pm$ 3   | 91 $\pm$ 7    | 0.272          |
| SHAM stretch                                       | 45 $\mu$ g PKC $\epsilon$ i.a. | 3M/3F    | 96 $\pm$ 12  | 97 $\pm$ 11   | 0.858          |
| HF-rEF stretch                                     | 45 $\mu$ g PKC $\epsilon$ i.a. | 4M/3F    | 87 $\pm$ 4   | 82 $\pm$ 10   | 0.464          |
| HF-rEF stretch                                     | 45 $\mu$ g PKC $\epsilon$ i.v. | 3M/1F    | 84 $\pm$ 5   | 87 $\pm$ 6    | 0.596          |
| HF-rEF stretch                                     | 2.25% DMSO i.a.                | 1M/3F    | 79 $\pm$ 1   | 87 $\pm$ 4    | 0.307          |
| HF-rEF lactic acid injection                       | 45 $\mu$ g PKC $\epsilon$ i.a. | 1M/4F    | 81 $\pm$ 10  | 81 $\pm$ 15   | 0.966          |
| HF-rEF $\alpha$ , $\beta$ -methylene ATP injection | 45 $\mu$ g PKC $\epsilon$ i.a. | 2M/2F    | 96 $\pm$ 13  | 95 $\pm$ 13   | 0.903          |
| HF-rEF bradykinin injection                        | 45 $\mu$ g PKC $\epsilon$ i.a. | 2M/2F    | 94 $\pm$ 2   | 95 $\pm$ 2    | 0.586          |
| SHAM contraction                                   | 45 $\mu$ g PKC $\epsilon$ i.a. | 3M/2F    | 93 $\pm$ 6   | 94 $\pm$ 9    | 0.851          |
| HF-rEF contraction                                 | 45 $\mu$ g PKC $\epsilon$ i.a. | 5M/1F    | 87 $\pm$ 6   | 88 $\pm$ 5    | 0.793          |
| Baseline HR, bpm                                   |                                |          |              |               |                |
| SHAM stretch                                       | 5 $\mu$ g Xestospongine C i.a. | 5M/3F    | 459 $\pm$ 11 | 474 $\pm$ 8   | 0.261          |
| HF-rEF stretch                                     | 5 $\mu$ g Xestospongine C i.a. | 3M/2F    | 445 $\pm$ 16 | 468 $\pm$ 17  | 0.325          |
| SHAM stretch                                       | 45 $\mu$ g PKC $\epsilon$ i.a. | 3M/3F    | 481 $\pm$ 17 | 488 $\pm$ 14  | 0.542          |
| HF-rEF stretch                                     | 45 $\mu$ g PKC $\epsilon$ i.a. | 4M/3F    | 463 $\pm$ 13 | 459 $\pm$ 18  | 0.730          |
| HF-rEF stretch                                     | 45 $\mu$ g PKC $\epsilon$ i.v. | 3M/1F    | 467 $\pm$ 11 | 476 $\pm$ 11  | 0.013*         |
| HF-rEF stretch                                     | 2.25% DMSO i.a.                | 1M/3F    | 469 $\pm$ 8  | 469 $\pm$ 10  | 0.847          |
| HF-rEF lactic acid injection                       | 45 $\mu$ g PKC $\epsilon$ i.a. | 1M/4F    | 485 $\pm$ 29 | 482 $\pm$ 28  | 0.898          |
| HF-rEF $\alpha$ , $\beta$ -methylene ATP injection | 45 $\mu$ g PKC $\epsilon$ i.a. | 2M/2F    | 507 $\pm$ 7  | 512 $\pm$ 9   | 0.166          |
| HF-rEF bradykinin injection                        | 45 $\mu$ g PKC $\epsilon$ i.a. | 2M/2F    | 455 $\pm$ 25 | 449 $\pm$ 26  | 0.414          |
| SHAM contraction                                   | 45 $\mu$ g PKC $\epsilon$ i.a. | 3M/2F    | 409 $\pm$ 22 | 408 $\pm$ 18  | 0.967          |
| HF-rEF contraction                                 | 45 $\mu$ g PKC $\epsilon$ i.a. | 5M/1F    | 446 $\pm$ 10 | 442 $\pm$ 9   | 0.425          |
| Peak $\Delta$ HR, bpm                              |                                |          |              |               |                |
| SHAM stretch                                       | 5 $\mu$ g Xestospongine C i.a. | 5M/3F    | 8 $\pm$ 2    | 9 $\pm$ 4     | 0.924          |
| HF-rEF stretch                                     | 5 $\mu$ g Xestospongine C i.a. | 3M/2F    | 10 $\pm$ 2   | 12 $\pm$ 5    | 0.728          |
| SHAM stretch                                       | 45 $\mu$ g PKC $\epsilon$ i.a. | 3M/3F    | 8 $\pm$ 2    | 10 $\pm$ 5    | 0.556          |
| HF-rEF stretch                                     | 45 $\mu$ g PKC $\epsilon$ i.a. | 4M/3F    | 24 $\pm$ 9   | 9 $\pm$ 4     | 0.221          |
| HF-rEF stretch                                     | 45 $\mu$ g PKC $\epsilon$ i.v. | 3M/1F    | 14 $\pm$ 5   | 9 $\pm$ 5     | 0.085          |
| HF-rEF stretch                                     | 2.25% DMSO i.a.                | 1M/3F    | 14 $\pm$ 4   | 14 $\pm$ 6    | 0.812          |
| HF-rEF lactic acid injection                       | 45 $\mu$ g PKC $\epsilon$ i.a. | 1M/4F    | 3 $\pm$ 1    | 2 $\pm$ 1     | 0.895          |
| HF-rEF $\alpha$ , $\beta$ -methylene ATP injection | 45 $\mu$ g PKC $\epsilon$ i.a. | 2M/2F    | 1 $\pm$ 1    | 2 $\pm$ 1     | 0.391          |
| HF-rEF bradykinin injection                        | 45 $\mu$ g PKC $\epsilon$ i.a. | 2M/2F    | 6 $\pm$ 3    | 10 $\pm$ 5    | 0.414          |
| SHAM contraction                                   | 45 $\mu$ g PKC $\epsilon$ i.a. | 3M/2F    | 22 $\pm$ 5   | 36 $\pm$ 11   | 0.158          |
| HF-rEF contraction                                 | 45 $\mu$ g PKC $\epsilon$ i.a. | 5M/1F    | 11 $\pm$ 4   | 11 $\pm$ 3    | 0.956          |

Values are mean $\pm$ SEM. MAP, mean arterial pressure; HR, heart rate. Data were compared with Student's *t*-tests. Asterisks indicate statistically significant differences between conditions ( $P < 0.05$ ).

**Table 4.3**

Table 4.3. Tension-time index in SHAM and HF-rEF rats.

|                    | Pharmacological agent          | <i>n</i> | Control    | Postcondition | <i>P</i> value |
|--------------------|--------------------------------|----------|------------|---------------|----------------|
| $\Delta$ TTI, kg·s |                                |          |            |               |                |
| SHAM stretch       | 5 $\mu$ g Xestospongine C i.a. | 5M/3F    | 17 $\pm$ 2 | 16 $\pm$ 1    | 0.563          |
| HF-rEF stretch     | 5 $\mu$ g Xestospongine C i.a. | 3M/2F    | 17 $\pm$ 2 | 17 $\pm$ 2    | 0.631          |
| SHAM stretch       | 45 $\mu$ g PKC $\epsilon$ i.a. | 3M/3F    | 17 $\pm$ 1 | 16 $\pm$ 1    | 0.203          |
| HF-rEF stretch     | 45 $\mu$ g PKC $\epsilon$ i.a. | 4M/3F    | 18 $\pm$ 1 | 19 $\pm$ 1    | 0.520          |
| HF-rEF stretch     | 45 $\mu$ g PKC $\epsilon$ i.v. | 3M/1F    | 15 $\pm$ 1 | 16 $\pm$ 1    | 0.189          |
| HF-rEF stretch     | 2.25% DMSO i.a.                | 1M/3F    | 14 $\pm$ 1 | 14 $\pm$ 1    | 0.167          |
| SHAM contraction   | 45 $\mu$ g PKC $\epsilon$ i.a. | 3M/2F    | 12 $\pm$ 2 | 12 $\pm$ 2    | 0.986          |
| HF-rEF contraction | 45 $\mu$ g PKC $\epsilon$ i.a. | 5M/1F    | 17 $\pm$ 2 | 16 $\pm$ 2    | 0.206          |

Values are mean $\pm$ SEM.  $\Delta$ TTI, tension-time index. Data were compared with Student's *t*-tests.

Figure 4.1 :

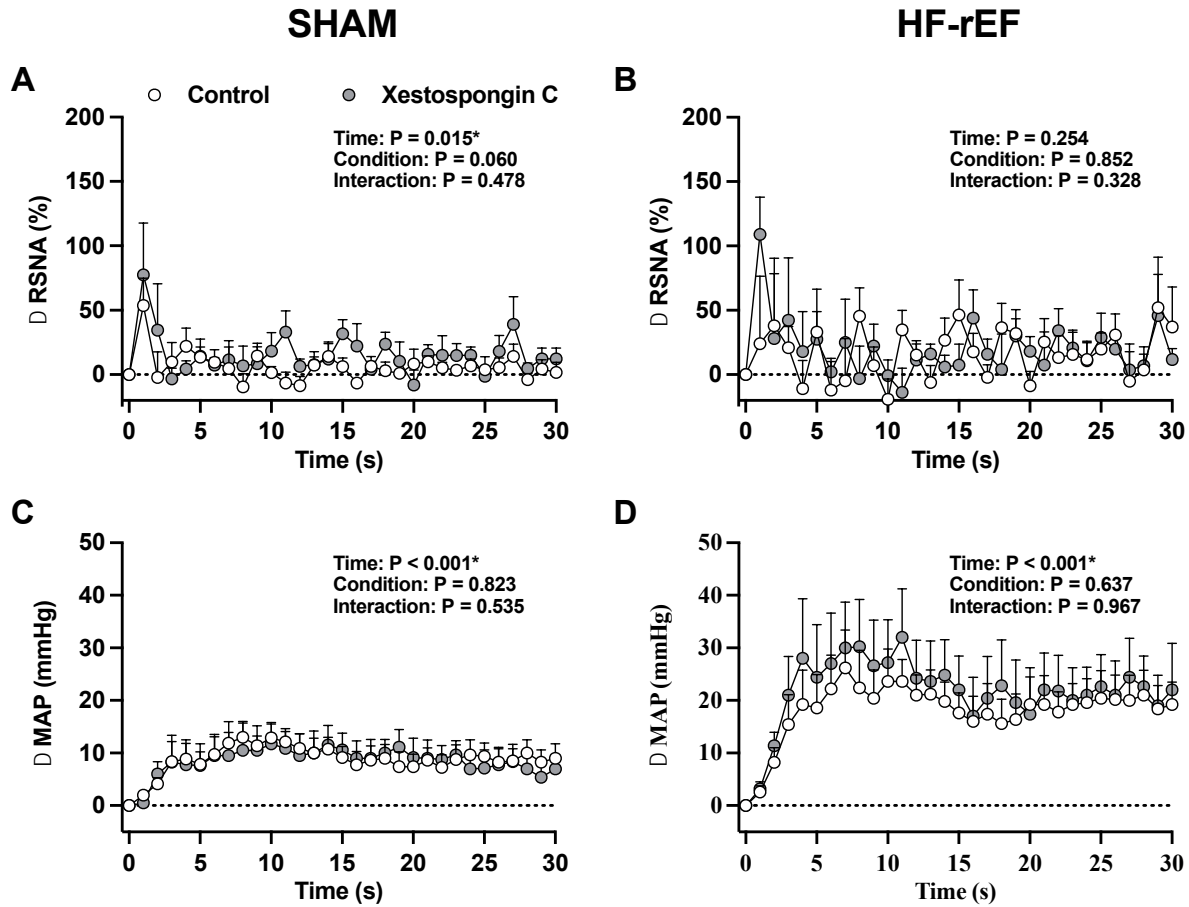


Figure 1: Effect of inositol 1,4,5-trisphosphate ( $IP_3$ ) receptor blockade with Xestospongine C on the time course of isolated mechanoreflex activation. The  $\Delta$  renal sympathetic nerve activity ( $\Delta$  RSNA, A and B) and  $\Delta$  mean arterial pressure ( $\Delta$  MAP, C and D) response to 30 s of 1 Hz dynamic hindlimb skeletal muscle stretch before and after injection of the  $IP_3$  receptor antagonist Xestospongine C ( $5 \mu\text{g}$ ) into the arterial supply of the hindlimb of SHAM (left,  $n=5\text{M}/3\text{F}$ ) and HF-rEF (right,  $n=3\text{M}/2\text{F}$ ) rats. Data were analyzed with two-way repeated-measures ANOVA and Šidák multiple comparisons tests. Asterisks indicate statistically significant differences between conditions ( $P < 0.05$ ).



Figure 4.2 :

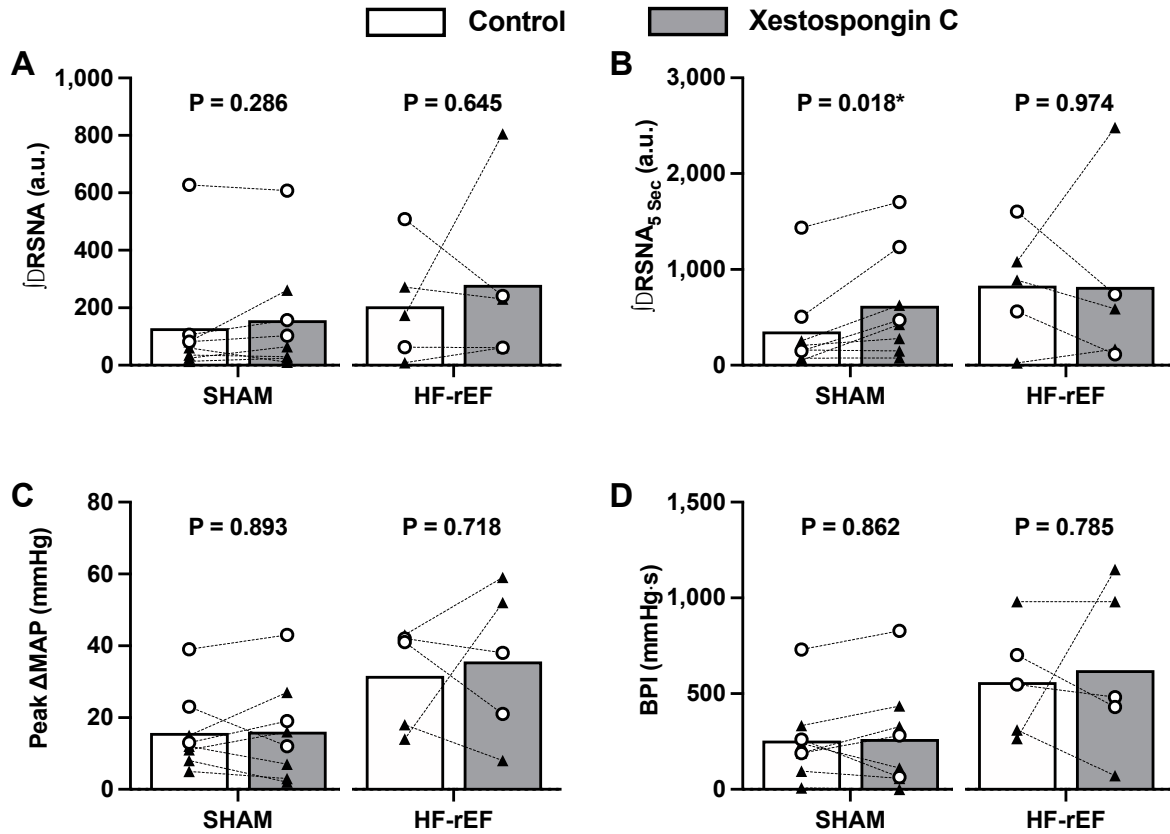


Figure 2: Effect of inositol 1,4,5-trisphosphate (IP<sub>3</sub>) receptor blockade with Xestospongine C on isolated mechanoreflex activation. The integrated  $\Delta$  in RSNA during the 1 Hz dynamic hindlimb skeletal muscle stretch maneuver for the full 30 s ( $\int \Delta \text{RSNA}$ , A) and first 5 seconds ( $\int \Delta \text{RSNA}_{5 \text{ Sec}}$ , B), as well as the peak change in mean arterial pressure (Peak  $\Delta \text{MAP}$ , C) and blood pressure index (BPI, D) response to the stretch maneuver before and after injection of the IP<sub>3</sub> receptor antagonist Xestospongine C (5  $\mu\text{g}$ ) into the arterial supply of the hindlimb of SHAM (n=5M/3F) and HF-rEF (n=3M/2F) rats. Data were analyzed with multiple *t*-tests and are expressed as mean values overlaid with individual responses (males in closed triangles, females in open circles). Asterisks indicate statistically significant differences between conditions ( $P < 0.05$ ).

Figure 4.3

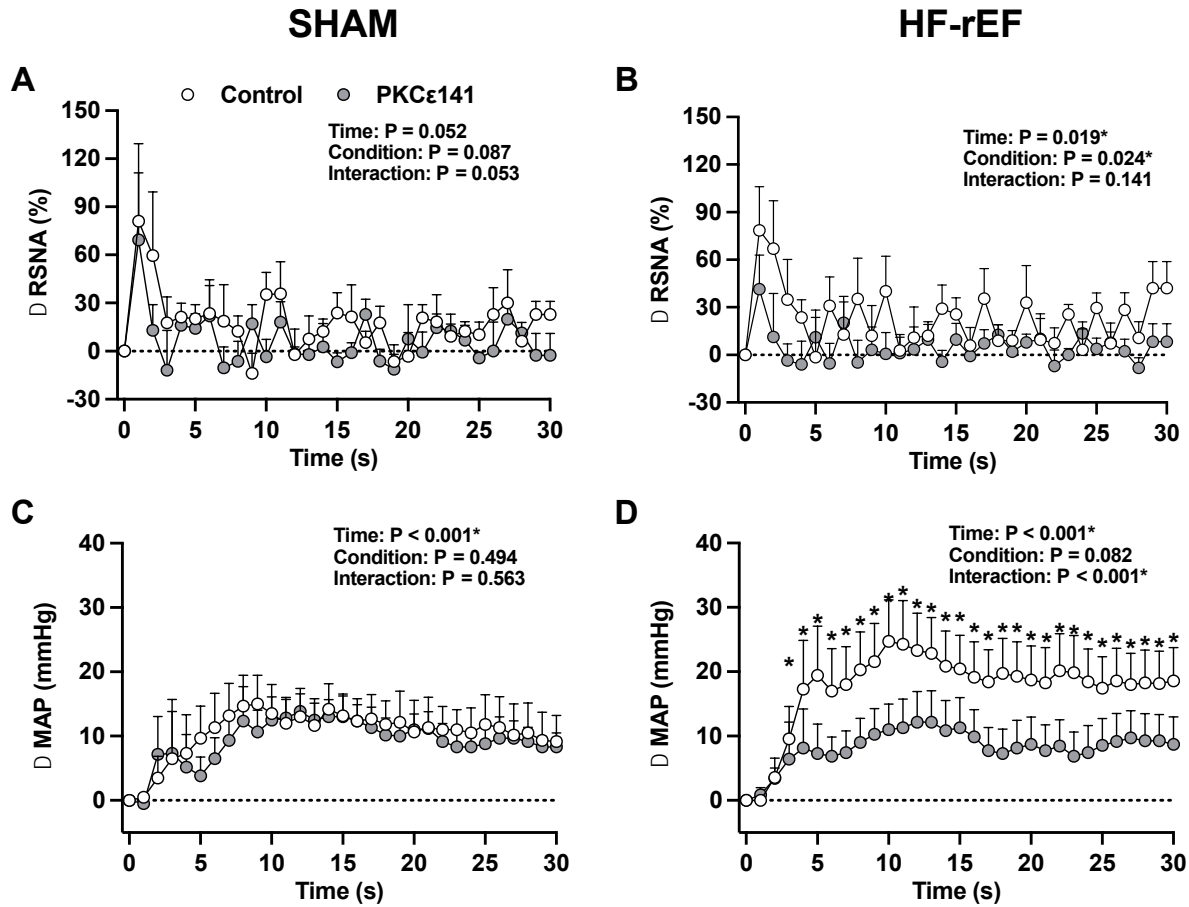


Figure 3: Effect of protein kinase C epsilon (PKC $\epsilon$ ) receptor blockade with PKC $\epsilon$ 141 on the time course of isolated mechanoreflex activation. The  $\Delta$  renal sympathetic nerve activity ( $\Delta$  RSNA, A and B) and  $\Delta$  mean arterial pressure ( $\Delta$  MAP, C and D) response to 30 s of 1 Hz dynamic hindlimb skeletal muscle stretch before and after injection of the PKC $\epsilon$  inhibitor PKC $\epsilon$ 141 (45  $\mu$ g) into the arterial supply of the hindlimb of SHAM (left, n=3M/3F) and HF-rEF (right, n=4M/3F) rats. Data were analyzed with two-way repeated-measures ANOVA and Šidák multiple comparisons tests. Asterisks indicate statistically significant differences between conditions ( $P < 0.05$ ).

Figure 4.4

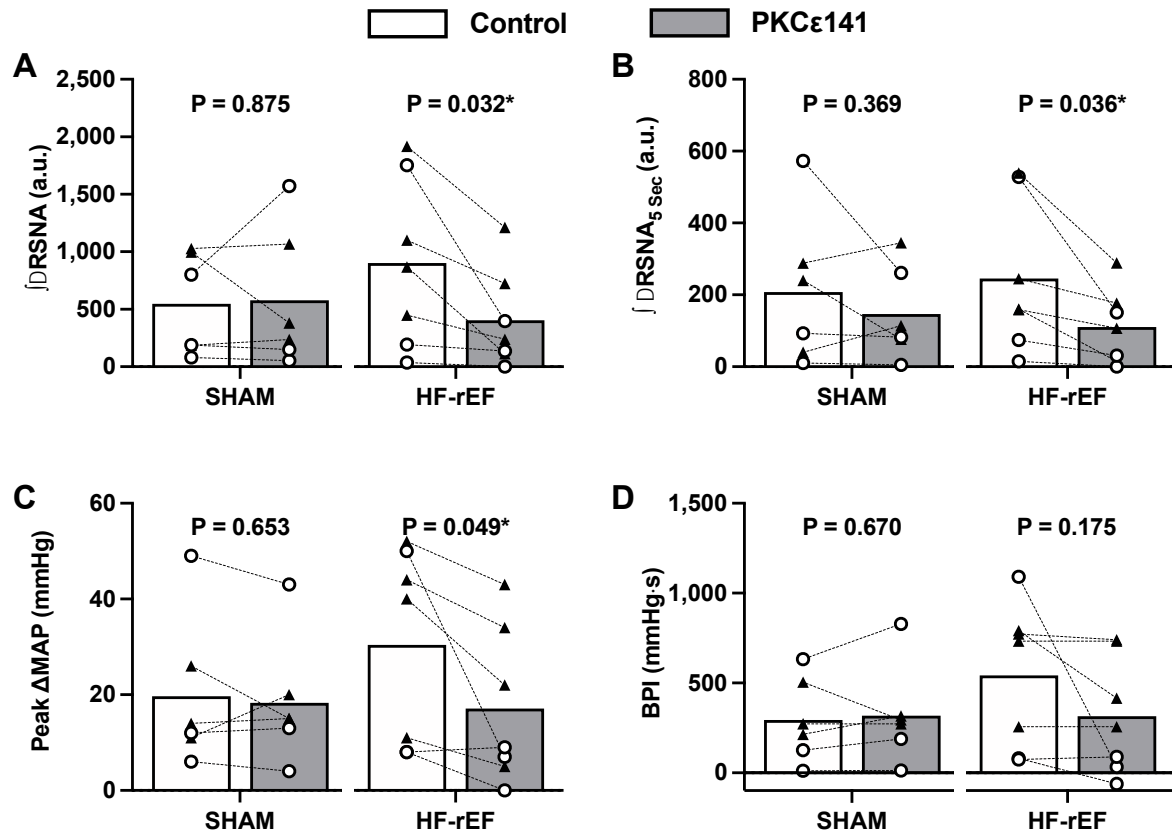
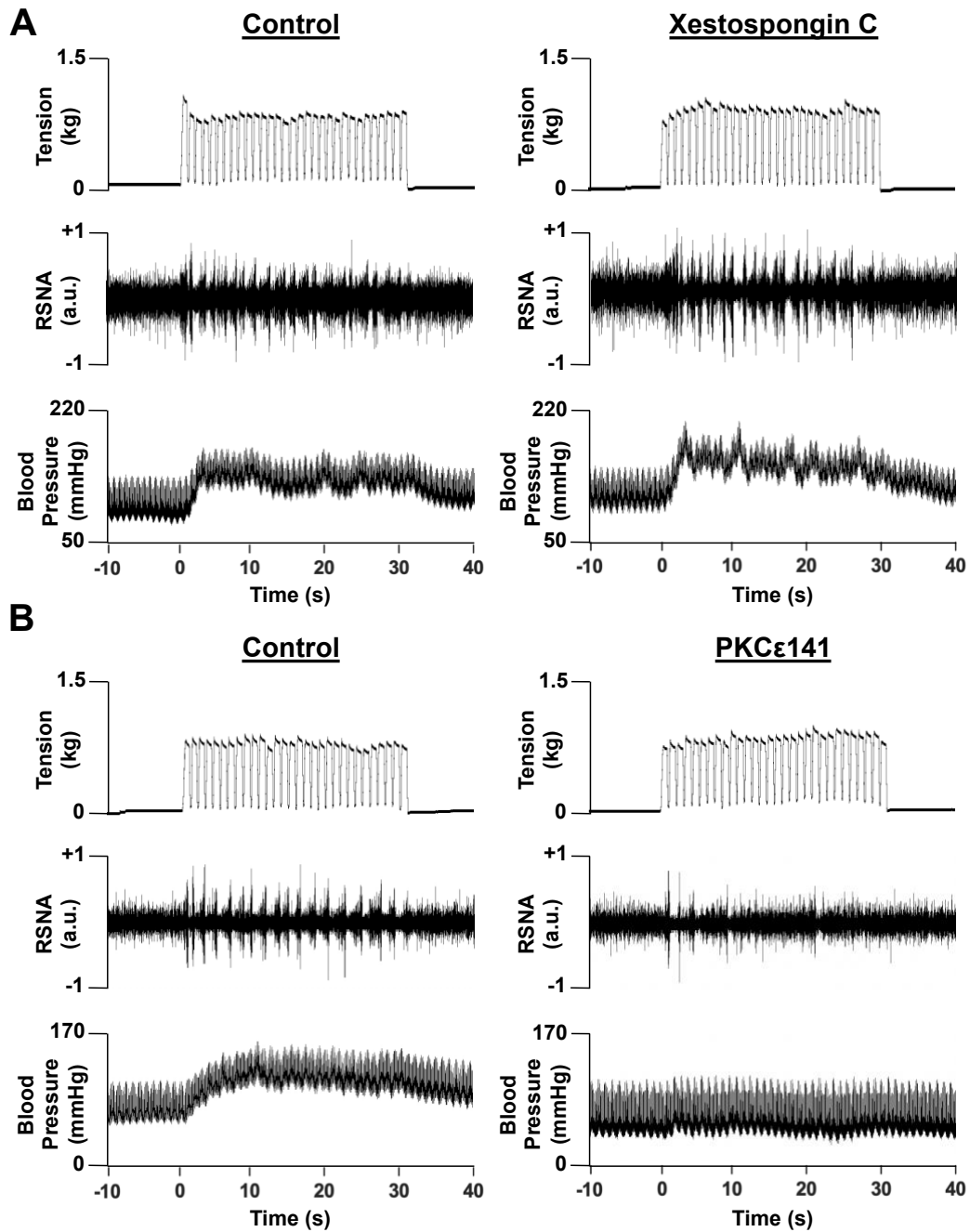


Figure 4: Effect of protein kinase C epsilon (PKC $\epsilon$ ) inhibition with PKC $\epsilon$ 141 on isolated mechanoreflex activation. The integrated  $\Delta$  in RSNA during the 1 Hz dynamic hindlimb skeletal muscle stretch maneuver for the full 30 s ( $\int \Delta \text{RSNA}$ , A) and first 5 seconds ( $\int \Delta \text{RSNA}_{5 \text{ sec}}$ , B), as well as the peak change in mean arterial pressure (Peak  $\Delta \text{MAP}$ , C) and blood pressure index (BPI, D) response to the stretch maneuver before and after injection of the PKC $\epsilon$  inhibitor PKC $\epsilon$ 141 (45  $\mu\text{g}$ ) into the arterial supply of the hindlimb of SHAM (n=3M/3F) and HF-rEF (n=4M/3F) rats. Data were analyzed with multiple *t*-tests and are expressed as mean values overlaid with individual responses (males in closed triangles, females in open circles). Asterisks indicate statistically significant differences between conditions (P < 0.05).

**Figure 4.5**



*Figure 5:* Original tracings from two HF-rEF rats showing the renal sympathetic and blood pressure response to 30 s of 1 Hz dynamic hindlimb skeletal muscle stretch before (left) and after (right) injecting either the inositol 1,4,5-trisphosphate (IP<sub>3</sub>) receptor inhibitor Xestospongine C (5µg; Panel A) or the PKCε inhibitor PKCε141 (45 µg; Panel B) into the arterial supply of the hindlimb.

Figure 4.6

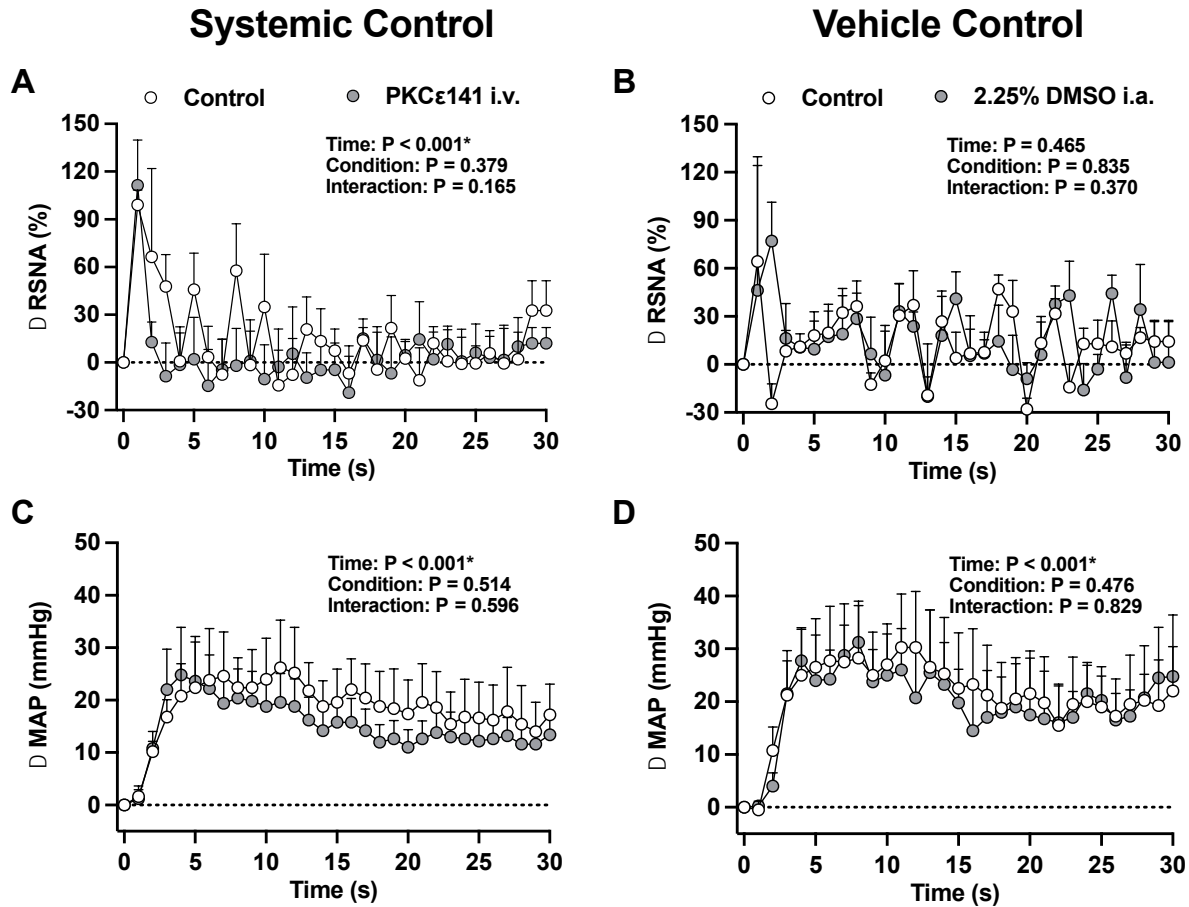


Figure 6: Systemic and vehicle controls for the protein kinase C epsilon (PKC $\epsilon$ ) inhibitor PKC $\epsilon$ 141 on isolated mechanoreflex activation. The  $\Delta$  renal sympathetic nerve activity ( $\Delta$  RSNA, A and B) and  $\Delta$  mean arterial pressure ( $\Delta$  MAP, C and D) response to 30 s of 1 Hz dynamic hindlimb skeletal muscle stretch in HF-rEF rats before and after intravenous injection (jugular vein) of the PKC $\epsilon$  receptor antagonist PKC $\epsilon$ 141 (45  $\mu$ g; n=3M/2F) as well as before and after injection of the vehicle for the PKC $\epsilon$  inhibitor PKC $\epsilon$ 141 into the arterial supply of the hindlimb (*i.e.*, 0.2mL saline containing 2.25% DMSO; n=1M/3F). Data were analyzed with two-way repeated-measures ANOVA and Šidák multiple comparisons tests. Asterisks indicate statistically significant differences between conditions ( $P < 0.05$ ).

Figure 4.7 :

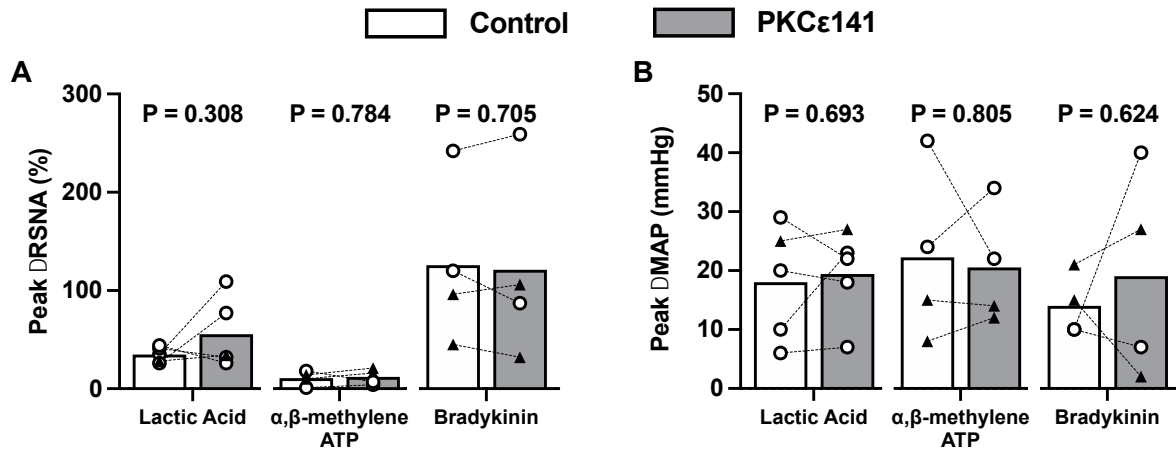


Figure 7: Effect of protein kinase C epsilon (PKC $\epsilon$ ) inhibition with PKC $\epsilon$ 141 on isolated metaboreflex activation in HF-rEF rats. The peak  $\Delta$  in mean arterial pressure (Peak  $\Delta$ MAP, A) and peak  $\Delta$  in renal sympathetic nerve activity (Peak  $\Delta$ RSNA, B) response to hindlimb arterial injection of lactic acid (24mMol; n=1M/4F),  $\alpha,\beta$ -methylene ATP (20  $\mu$ g; n=2M/2F), and bradykinin (5  $\mu$ g; n=2M/2F) before and after injection of the PKC $\epsilon$  inhibitor PKC $\epsilon$ 141 (45  $\mu$ g) into the arterial supply of the hindlimb. Data were analyzed with multiple *t*-tests and are expressed as mean values overlaid with individual responses (males in closed triangles, females in open circles). Asterisks indicate statistically significant differences between conditions (P < 0.05).

Figure 4.8

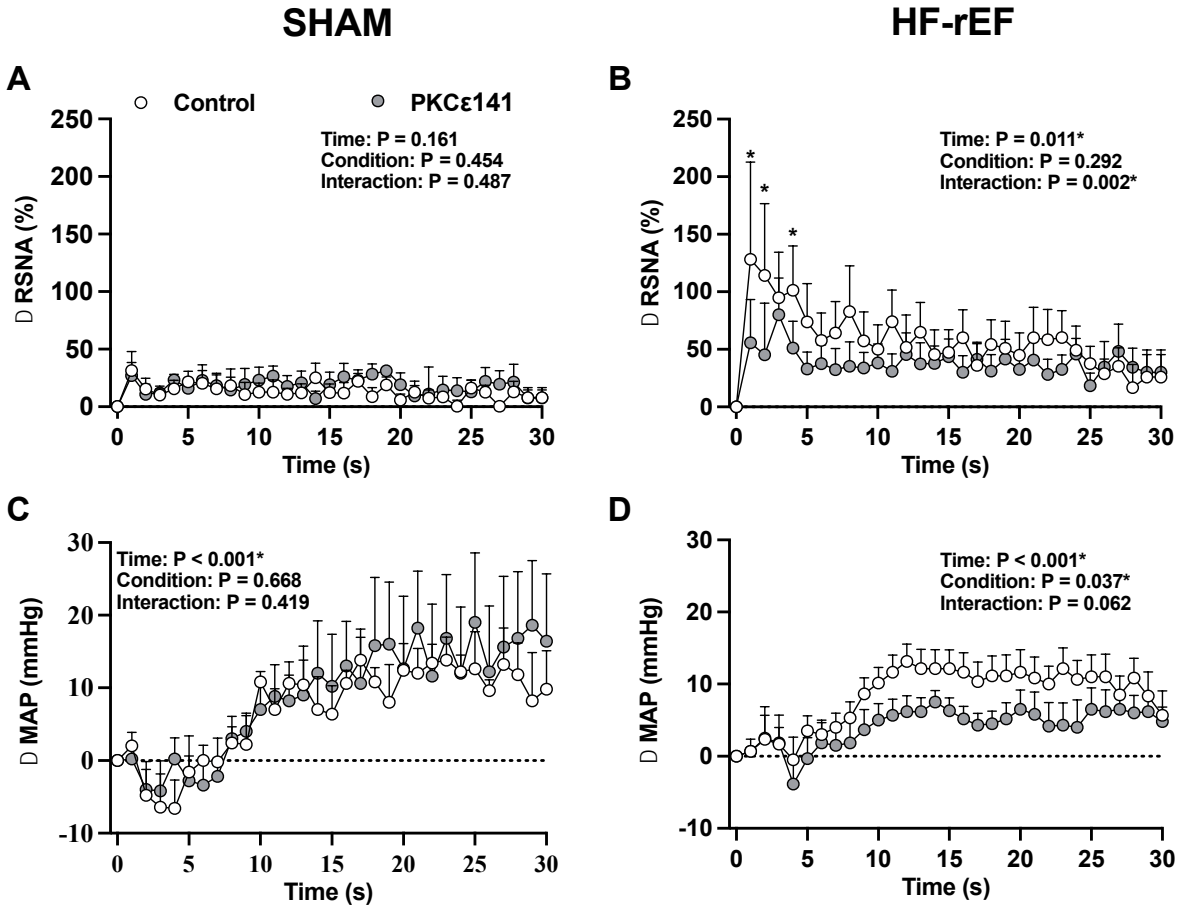


Figure 8: Effect of protein kinase C epsilon (PKC $\epsilon$ ) receptor blockade with PKC $\epsilon$ 141 on the time course of exercise pressor reflex activation. The  $\Delta$  renal sympathetic nerve activity ( $\Delta$  RSNA, A and B) and  $\Delta$  mean arterial pressure ( $\Delta$  MAP, C and D) response to 30 s of 1 Hz dynamic hindlimb skeletal muscle contraction before and after injection of the PKC $\epsilon$  inhibitor PKC $\epsilon$ 141 (45  $\mu$ g) into the arterial supply of the hindlimb of SHAM (left, n=3M/2F) and HF-rEF (right, n=5M/1F) rats. Data were analyzed with two-way repeated-measures ANOVA and Šidák multiple comparisons tests. Asterisks indicate statistically significant differences between conditions (P < 0.05).

Figure 4.9 :

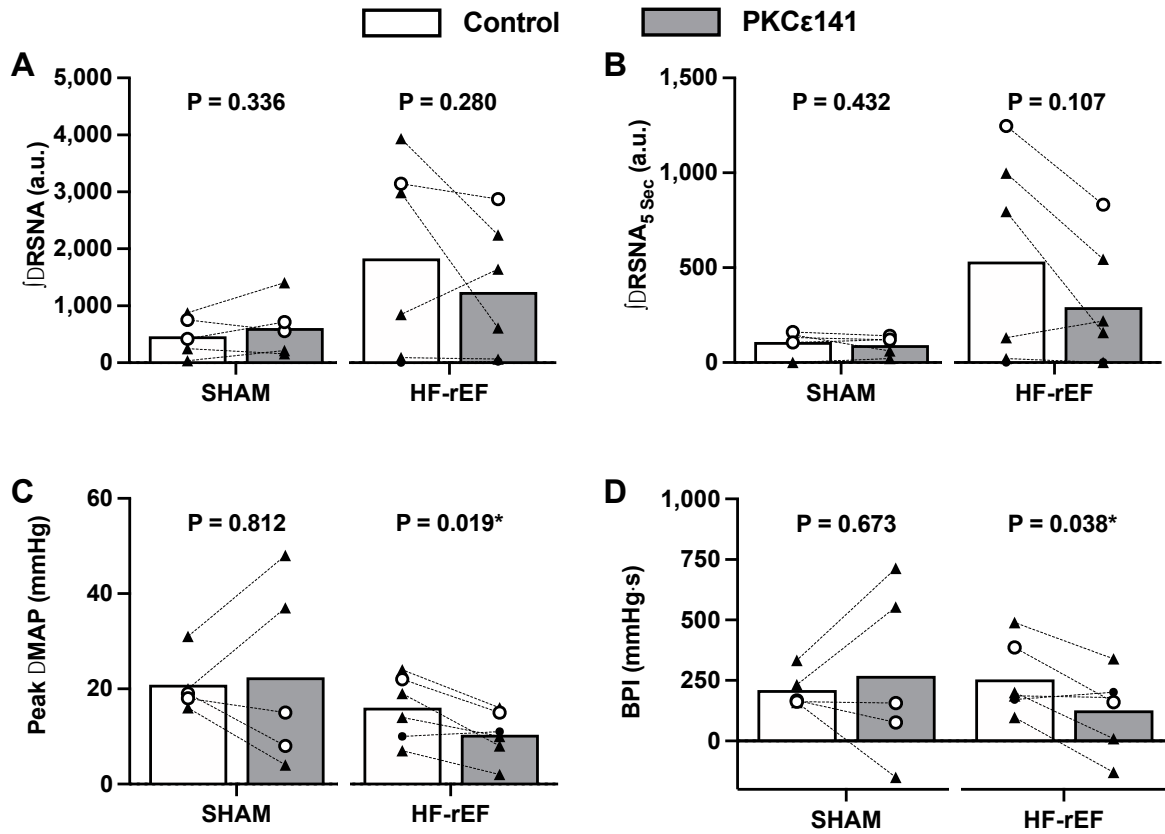


Figure 9: Effect of protein kinase C epsilon (PKC $\epsilon$ ) inhibition with PKC $\epsilon$ 141 on exercise pressor reflex activation. The integrated  $\Delta$  in RSNNA during the 1 Hz dynamic hindlimb skeletal muscle stretch maneuver for the full 30 s ( $\int\Delta$ RSNA, A) and first 5 seconds ( $\int\Delta$ RSNA<sub>5 Sec</sub>, B), as well as the peak change in mean arterial pressure (Peak  $\Delta$ MAP, C) and blood pressure index (BPI, D) response to the contraction maneuver before and after injection of the PKC $\epsilon$  inhibitor PKC $\epsilon$ 141 (45  $\mu$ g) into the arterial supply of the hindlimb of SHAM (n=3M/2F) and HF-rEF (n=5M/1F) rats. Data were analyzed with multiple *t*-tests and are expressed as mean values overlaid with individual responses (males in closed triangles, females in open circles). Asterisks indicate statistically significant differences between conditions (P < 0.05).



Figure 4.10

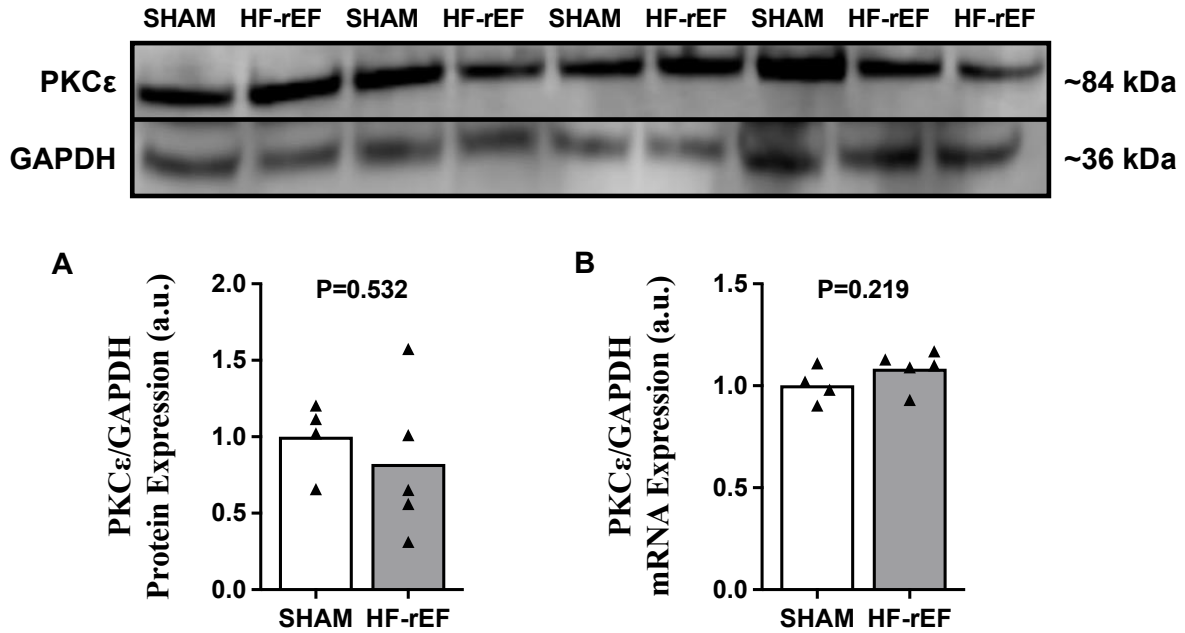


Figure 10: Effect of HF-rEF on PKCε expression in DRG tissue. PKCε protein (A) and mRNA (B) expression within L<sub>4</sub>/L<sub>5</sub> DRG tissue from SHAM (n=4M) and HF-rEF (n=5M) rats. GAPDH was used as protein loading control and as a reference gene sample. Top: cropped images from a Western blot showing the results after staining of anti- PKCε and anti-GAPDH on L<sub>4</sub>/L<sub>5</sub> DRG tissue from SHAM and HF-rEF rats. Data were analyzed with Student's t-tests and are expressed as mean overlaid with individual responses.

# **Chapter 5 - Novel mechanosensory role for acid sensing ion channel subtype 1a in evoking the exercise pressor reflex in rats with heart failure**

## **5.1 Abstract**

Mechanical and metabolic signals associated with skeletal muscle contraction stimulate the sensory endings of thin fibre muscle afferents which, in turn, generates reflex increases in sympathetic nerve activity (SNA) and blood pressure (the exercise pressor reflex; EPR). EPR activation in patients and animals with heart failure with reduced ejection fraction (HF-rEF) results in exaggerated increases in SNA and promotes exercise intolerance. In the healthy decerebrate rat, a subtype of acid sensing ion channel (ASIC) on the sensory endings of thin fibre muscle afferents, namely ASIC1a, has been shown to contribute to the metabolically sensitive portion of the EPR (i.e., metaboreflex), but not the mechanically sensitive portion of the EPR (i.e., the mechanoreflex). However, the role played by ASIC1a in evoking the EPR in HF-rEF is unknown. We hypothesized that, in decerebrate, unanesthetized HF-rEF rats, injection of the ASIC1a antagonist psalmotoxin-1 (PcTx-1; 100ng) into the hindlimb arterial supply would reduce the reflex increase in renal SNA (RSNA) evoked via 30s of electrically-induced static hindlimb muscle contraction, but not static hindlimb muscle stretch (model of mechanoreflex activation isolated from contraction-induced metabolite-production). We found that PcTx-1 reduced the reflex increase in RSNA evoked in response to muscle contraction (n=8;  $\int \Delta$ RSNA pre: 1,343 (588); post: 816 (573)a.u.; P=0.026) and muscle stretch (n=6;  $\int \Delta$ RSNA pre: 688 (583); post: 304 (370)a.u.; P=0.025). Our data suggest that, in HF-rEF rats, ASIC1a contributes to activation of the exercise pressor reflex and that contribution includes a novel role for ASIC1a in mechanosensation that is not present in healthy rats.

## **5.2 Introduction**

During exercise, a withdrawal of parasympathetic nervous system activity and an increase in sympathetic nervous system activity (SNA) facilitates numerous cardiovascular adjustments which include increases in heart rate (HR), cardiac contractility and blood pressure (BP; 1). The exercise pressor reflex is a feedback autonomic control mechanism that contributes importantly to those exercise-induced changes in autonomic activity (1-6). The reflex is activated when the

sensory endings of thinly myelinated group III and unmyelinated group IV skeletal muscle afferents (collectively termed thin fibre muscle afferents) are stimulated by mechanical and/or metabolic signals associated with muscle contraction (4, 5, 7-11).

A family of acid sensing ion channels (ASICs) distributed throughout the central and peripheral nervous systems plays an important role in detecting acidic stimuli and regulating the cardiovascular system (12). On the sensory endings of thin fibre muscle afferents, ASICs principally form heterotrimeric channels composed of ASIC1a, ASIC2, and ASIC3 subunits (13). During exercise, ASICs are stimulated by acidic products of skeletal muscle contraction, which contributes importantly to the activation of the metabolic portion of the exercise pressor reflex (14, 15) (i.e., the metaboreflex). In support of this notion, local infusion/injection of the non-selective ASIC inhibitor amiloride attenuated the pressor and MSNA response to static handgrip exercise in healthy humans (16) as well as the pressor and thin fibre muscle afferent response to static hindlimb muscle contraction in healthy cats (15, 17, 18). Ducrocq et al. (19), Ducrocq et al. (20) recently extended those findings by demonstrating that local selective ASIC1a blockade attenuated the pressor response to electrically-induced static hindlimb muscle contraction in healthy rats. The remaining two subclasses of ASICs present on the sensory endings of thin fibre muscle afferents are either activated via noxious pH levels not likely present during skeletal muscle contraction (i.e., ASIC2 with a pK<sub>a</sub> of 4.5; 21) or, in the case of ASIC3, have been shown to play little (22) or no (23-25) independent role in evoking the exercise pressor reflex in healthy rats. Thus, it appears that ASIC1a, but not ASIC2 or ASIC3, plays a key role in evoking the exercise pressor reflex, at least in the healthy rat.

In comparison to healthy subjects, activation of the exercise pressor reflex in patients/animals with heart failure with reduced ejection fraction (HF-rEF) results in an exaggerated increase in SNA (26-29) and altered cardiovascular responses (30-34) which include augmented peripheral (30, 35) and coronary (34) vasoconstriction. Thus, whereas activation of the exercise pressor reflex in healthy subjects supports exercise performance (36, 37), activation of the reflex in HF-rEF patients likely contributes to exacerbated fatigue, exercise intolerance and elevated cardiovascular risk.

In HF-rEF, the accumulation of acidic products of skeletal muscle contraction is greater than that found during skeletal muscle contraction in healthy subjects (38). For example, in HF-rEF patients muscle pH decreases and lactate ions increase to a greater extent during exercise

compared to the changes found in healthy control subjects (39); an effect which may produce greater ASIC stimulation during exercise in HF-rEF patients. A role for ASIC3 in the exaggerated exercise pressor reflex in HF-rEF is unlikely given the findings of Xing et al. (40) that, compared to healthy control rats, HF-rEF rats had lower ASIC3 protein expression in L4/L5 dorsal root ganglia (DRG) tissue and a lower percentage of DRG neurons expressing ASIC3-like currents. ASIC1a, however, is an appealing candidate as a possible contributor to the exaggerated exercise pressor reflex in HF-rEF. For example, HF-rEF is a proinflammatory condition (41) and experimentally-induced inflammation has been shown to increase ASIC1a expression (42) and potentiate ASIC1a responsiveness (43) in rat sensory neurons. Unfortunately, however, the role played by ASIC1a in evoking the exercise pressor reflex in HF-rEF has not been investigated.

Based on the information above, the purpose of this investigation was to determine the role played by ASIC1a on the sensory endings of group III/IV muscle afferents in evoking the exercise pressor reflex in a myocardial infarction (MI)-induced rat model of HF-rEF. Specifically, we tested the hypothesis that, in decerebrate, unanesthetized rats, hindlimb arterial injection of the ASIC1a antagonist Psalmotoxin-1 (PcTx-1) would reduce the reflex increase in renal SNA (RSNA), BP, and HR evoked in response to 30 seconds of electrically-induced static hindlimb skeletal muscle contraction to a greater extent in HF-rEF rats when compared to sham-operated healthy control rats (SHAM rats). We also tested the hypothesis that ASIC1 mRNA and ASIC1a protein expression in L4/L5 DRG tissue would be greater in HF-rEF rats compared to SHAM rats.

### **5.3 Methods**

#### *Ethical Approval*

All experimental procedures were approved by the Institutional Animal Care and Use Committee of Kansas State University (Protocol #4552) and conducted in accordance with the National Institutes of Health Guide for the Care and Use of Laboratory Animals (44). Experiments were performed on ~14-19-week-old male Sprague-Dawley rats (n=102; Charles River Laboratories). Rats were housed two per cage in temperature (maintained at ~22°C) and light (12-12-hour light-dark cycle running from 7 AM to 7 PM)-controlled accredited facilities with standard rat chow and water provided ad libitum.

#### *Surgical Procedure*

Myocardial infarction (MI) was induced in 59 of the 102 rats by surgically ligating the left main coronary artery (45). Briefly, rats were anesthetized initially with a 5% isoflurane-O<sub>2</sub> mixture

(Butler Animal Health Supply, Elk Grove Village, IL, and Linweld, Dallas, TX) and maintained subsequently on 2.5% isoflurane-O<sub>2</sub> and then intubated and mechanically ventilated with a rodent respirator (Harvard model 680, Harvard Instruments, Holliston, MA) for the duration of the surgical procedure. After a single injection of the antiarrhythmic drug amiodarone (100 mg/kg ip), which was administered to improve survival rate following the ensuing coronary artery ligation surgery (46), a left thoracotomy was performed to expose the heart through the fifth intercostal space, and the left main coronary artery was ligated 1–2 mm distal to the edge of the left atrium with a 6-0 braided polyester suture. The thorax was then closed with 2-0 gut, and the skin was closed with 2-0 silk. Prior to termination of anesthesia, bupivacaine (1.5 mg/kg sc) and buprenorphine (~0.03 mg/kg im) were administered to reduce pain associated with the surgery, along with ampicillin (50 mg/kg im) to reduce the risk of infection. After rats were removed from mechanical ventilation and anesthesia, they were monitored closely for ~6 h post-surgery. In the remaining 43 of 102 rats, a sham ligation of the coronary artery was performed in which 6-0 braided polyester suture was passed under the left main coronary artery, but not tied. These rats are referred to as “SHAM” rats from this point forward. Following completion of either MI or SHAM procedures, rats were housed one per cage for ten days to minimize risk of infection of the surgical site. During these ten days, the antibiotic Baytril (100 mg/mL) was administered in the drinking water. Following completion of the Baytril treatment, rats were housed two per cage as described above. All animals were monitored daily for 14 days following the MI or SHAM procedure for changes in behavior, gait/posture, breathing, appetite and body weight.

#### *Echocardiograph Measurements*

Transthoracic echocardiograph measurements were performed with a commercially available system (LOGIQ e; GE Health Care, Milwaukee, WI) no more than one week before the final experimental protocol. Briefly, the rats were anaesthetized as described above. Once the rat was fully anesthetized, the isoflurane mixture was reduced to 2.5% isoflurane-O<sub>2</sub>. Following 5 min at 2.5% isoflurane, echocardiograph measurements began. The transducer was positioned on the left anterior chest, and left ventricular dimensions were measured. The left ventricular fractional shortening (FS), ejection fraction (EF), end diastolic (LVEDV), end systolic volume (LVESV), and stroke volume (SV) were determined by echocardiographic measurements as previously described (47). Rats with HF-rEF were required to meet an inclusion criterion of either an FS ≤ 30% and/or a left ventricular infarct size of ≥ 15% (see below for method of infarct size

determination), which is consistent with criterion previously established by our laboratory (48-50). We have previously shown that, compared with SHAM operated healthy control rats, HF-rEF rats that meet similar criterion have a reduced maximal oxygen uptake and time to exhaustion to treadmill running (48).

#### *Surgical Procedures for Experimental Protocols.*

In vivo experiments were performed on 69 rats (30 SHAM, 39 HF-rEF) between six and eight weeks following the MI or SHAM procedure. Importantly, this time frame post MI procedure ensures the development of HF-rEF as well as reduced maximal oxygen uptake and time to exhaustion during treadmill running (48). On the day of the experiment, rats were anesthetized as described above. Adequate depth of anesthesia was confirmed by the absence of toe-pinch and blink reflexes. The trachea was cannulated, and the lungs were mechanically ventilated (Harvard Apparatus, Holliston, MA) with a 2% isoflurane-balance O<sub>2</sub> gaseous mixture until the decerebration was completed (see below). The right jugular vein and both carotid arteries were cannulated with PE-50 catheters which were used for the injection of fluids, measurement of arterial blood pressure (physiological pressure transducer, AD Instruments), and sampling of arterial blood gasses (Radiometer). HR was calculated from the R-R interval measured by electrocardiogram (AD Instruments). The left superficial epigastric artery was cannulated with a PE-8 catheter whose tip was placed near the junction of the superficial epigastric and femoral arteries. A reversible snare was placed around the left iliac artery and vein (i.e., proximal to the location of the catheter placed in the superficial epigastric artery). The left calcaneal bone was severed and linked by string to a force transducer (Grass FT03), which, in turn, was attached to a rack and pinion. A ~1-2 cm section of the left sciatic nerve was exposed by reflecting the overlying skeletal muscles.

Upon completion of the initial surgical procedures, rats were placed in a Kopf stereotaxic frame. After administering dexamethasone (0.2 mg i.v.) to minimize swelling of the brainstem, a pre-collicular decerebration was performed in which all brain tissue rostral to the superior colliculi was removed (51). The cranial cavity was filled with cotton balls and covered with glue (Kwik-Sil, World Precision Instruments). Following decerebration, anesthesia was reduced to 0.5%. A retroperitoneal approach was used to expose bundles of the left renal sympathetic nerve, which were then glued with Kwik-Sil onto a pair of thin stainless-steel recording electrodes connected to a high impedance probe (Grass Model HZP) and amplifier (Grass P511). Multiunit signals from

the renal sympathetic nerve fibres were filtered at high and low frequencies (1 KHz and 100 Hz, respectively) for the measurement of RSNA.

Upon completion of all surgical procedures, anesthesia was terminated, and the rats' lungs were ventilated with room air. Experimental protocols commenced at least one hour after termination of isoflurane. Experiments were performed on decerebrate, unanesthetized rats because anesthesia has been shown to markedly blunt the exercise pressor reflex in the rat (51). Body core temperature was measured via a rectal probe and maintained at ~37–38°C by an automated heating system (Harvard Apparatus) and heat lamp. Arterial pH and blood gases were analyzed periodically throughout the experiment from arterial blood samples (~75 µL) and maintained within physiological ranges (pH: 7.35–7.45, PCO<sub>2</sub>: ~38–40 mmHg, PO<sub>2</sub>: ~100 mmHg) by administration of sodium bicarbonate and/or adjusting ventilation as necessary. At the end of all experiments in which an experimental solution was injected into the arterial supply of the left hindlimb through the superficial epigastric artery catheter, Evans blue dye was injected in the same manner as the experimental solution to confirm that the injectate had access to the triceps surae muscle circulation. The triceps surae muscles were observed to stain blue in all experiments. Then, postganglionic sympathetic nerve activity was abolished with administration of hexamethonium bromide (10mg; 0.5mL saline i.v.) to allow for the quantification of background noise as described previously (52). Rats were then anaesthetized with 5% isoflurane and humanely euthanized with an injection of potassium chloride (>3 mg/kg ia). A pneumothorax was then performed, and the heart was excised. The atria and right ventricle (RV) were separated from the left ventricle (LV) and septum, and the RV, LV, and atria were weighed. In rats with HF-rEF, the LV infarction surface area was measured using planimetry and expressed as percent of LV endocardial surface area as described previously (53).

#### *Lactic acid injection protocol.*

In 23 rats (12 SHAM, 11 HF-rEF), we attempted to confirm the efficacy of PcTx-1 in blocking ASIC1a on the sensory endings of thin fibre muscle afferents by reproducing the previous finding from Ducrocq, Kim, Estrada and Kaufman (20) that hindlimb arterial injection of PcTx-1 (100ng; 0.1mL saline) reduced the pressor and cardioaccelerator response to hindlimb arterial injection of lactic acid (24mMol; 0.2mL saline). Briefly, the lactic acid solution was injected as a bolus into the arterial supply of the left hindlimb through the superficial epigastric artery catheter. Following a ~5 min recovery, the snare around the left iliac artery and vein was tightened and

PcTx-1 was injected into the arterial supply of the hindlimb through the superficial epigastric artery catheter. The snare was released 5 min after injecting PcTx-1 and, following a 5 min recovery period a second lactic acid injection was performed. Evans blue dye was injected in the same manner as the lactic acid and PcTx-1 and the triceps surae muscles were observed to stain blue in all experiments.

*Effect of ASIC1a blockade on the exercise pressor reflex.*

In 15 rats (7 SHAM, 8 HF-rEF), we compared the renal sympathetic, pressor, and cardioaccelerator responses evoked in response to 30 seconds of static hindlimb muscle contraction before and after the injection of PcTx-1 into the arterial supply of the left hindlimb. Following recovery of isoflurane anesthesia, baseline muscle tension was set to ~100 g and baseline RSNA, blood pressure, and HR were measured for ~30 seconds. The sciatic nerve was then electrically stimulated using stainless steel electrodes for 30 seconds at a voltage of ~1.5x motor threshold (0.01 ms pulse duration, 40 Hz frequency) which produced static contractions of the triceps surae muscles. Approximately 10 min following the control contraction maneuver, the snare on the left iliac artery and vein was tightened and PcTx-1 was injected into the femoral artery using the superficial epigastric artery catheter as described above. PcTx-1 remained snared in the hindlimb circulation for 5 min, at which time the iliac snare was released. The hindlimb was reperfused for 5 min and the contraction maneuver was then repeated exactly as described above. At the end of all experiments, we injected the paralytic pancuronium bromide (0.5mg; 0.5 mL saline i.v.) and the sciatic nerve was stimulated for 30 seconds with the same parameters as those used to elicit contraction to ensure that the increase in RSNA, blood pressure, and HR during contraction was not due to the electrical activation of the axons of the thin fibre muscle afferents in the sciatic nerve. No increase in RSNA, blood pressure or HR, were observed during the stimulation period following the administration of pancuronium bromide.

*Control for possible effect of vehicle for PcTx-1 on the exercise pressor reflex*

In 7 rats (3 SHAM, 4 HF-rEF), we compared the renal sympathetic, pressor, and cardioaccelerator responses evoked in response to 30 seconds of contraction before and after the injection of the vehicle for PcTx-1 (i.e., 0.1mL saline) into the catheter placed in the superficial epigastric artery. Successful RSNA recordings were accomplished in all but three of these rats (two SHAM, one HF-rEF). These three rats were used in the vehicle control protocols to maximize the statistical power of the RSNA comparisons in the main experimental protocols.



*Control for possible blockade of ASIC1a within the central nervous system*

PcTx-1 is a large molecule (4,689 Da) and therefore unlikely able to cross the blood brain barrier (pore size of ~600 Da) and exert an effect in the central nervous system (54). Nevertheless, we investigated the possibility that systemic circulation of PcTx-1 and consequent inhibition of ASIC1a within the central nervous system (e.g., spinal cord, brain stem) may have accounted for the attenuating effects in the main experimental group in which PcTx-1 was injected into the hindlimb arterial circulation rather than a local effect within the hindlimb. In nine rats (5 SHAM, 4 HF-rEF), we compared the renal sympathetic, pressor, and cardioaccelerator responses evoked in response to 30 seconds of contraction before and after the injection of PcTx-1 into the catheter placed in the jugular vein. Successful RSNA recordings were accomplished in all but three of these rats (two SHAM, one HF-rEF). These three rats were used in the systemic control protocols to maximize the statistical power of the RSNA comparisons in the main experimental protocols.

*Effect of ASIC1a blockade on isolated mechanoreflex activation.*

In separate groups of SHAM (n=6) and HF-rEF rats (n=7), we investigated the possibility that the effect of ASIC1a blockade with PcTx-1 on the RSNA, pressor, and cardioaccelerator response was attributed to an effect on the mechanoreflex. Specifically, we compared the RSNA, pressor, and cardioaccelerator response to static hindlimb muscle stretch, a model of static mechanoreflex activation isolated from contraction-induced metabolite production (55) before and after the injection of PcTx-1 into the arterial supply of the left hindlimb. Following recovery of isoflurane anesthesia, baseline muscle tension was set to ~100 g and baseline RSNA, blood pressure, and HR were measured for ~30 seconds. An experienced investigator then initiated the stretch protocol by rapidly turning the rack and pinion to a position which was held constant for 30 s. The investigator aimed to produce a peak tension generation of 1.0 kg during each static stretch to match the average tension developed in the contraction experiments in the present investigation. Approximately 5 min following the control stretch maneuver, the snare on the left iliac artery and vein was tightened and PcTx-1 was injected into the femoral artery using the superficial epigastric artery catheter as described above. PcTx-1 remained snared in the hindlimb circulation for 5 min, at which time the iliac snare was released. The hindlimb was reperfused for 5 min and the static stretch maneuver was then repeated exactly as described above. The tension generated during the post drug maneuvers was matched as closely as possible to that produced during the control stretch.

*Control for the possible effect of PcTx-1 activating an endogenous enkephalin pathway.*

In 5 HF-rEF rats we compared the renal sympathetic, pressor, cardioaccelerator responses to 30 seconds of static hindlimb muscle stretch before and after  $\mu$ - and  $\delta$ -opioid receptor and then after ASIC1a blockade. These experiments served as a control for the possibility that the effect of ASIC1a blockade with PcTx-1 on the integrated renal sympathetic response to static hindlimb muscle stretch (Fig. 5B & 6B) was attributed to a release of Met-enkephalin, a  $\mu$ - and  $\delta$ -opioid receptor agonist (56). During these experiments, a control stretch maneuver was performed exactly as described above. Next, following a ~5 min recovery period, naloxone (100  $\mu$ g; 0.1mL saline), a  $\mu$ - and  $\delta$ -opioid receptor antagonist, was infused at a constant rate of 10  $\mu$ L/min for 10 min into the hindlimb circulation via the catheter placed in the superficial epigastric artery as described previously (57). Approximately 5 min following injection of naloxone, a second stretch maneuver was performed. Next, after a second ~5 min recovery period, the snare on the left iliac artery and vein was tightened and PcTx-1 was injected into the femoral artery using the superficial epigastric artery catheter as described above. PcTx-1 remained snared in the hindlimb circulation for 5 min, at which time the iliac snare was released. The hindlimb was reperfused for 5 min and the static stretch maneuver was then repeated exactly as described above.

*Western blot and quantitative reverse transcriptase polymerase chain reaction experiments for ASIC1a/ASIC1 expression.*

In 36 rats (16 SHAM, 20 HF-rEF) the left and right L4 and L5 DRG were harvested. Samples were isolated into 2 mL bead mill tubes containing ~0.5g of 1.4 mm ceramic beads and 300  $\mu$ L of ML lysis buffer (Macherey-Nagel) and homogenized for 1 min at 5 m/s using Bead Mill 4 (Fisherbrand™). Total protein and mRNA from tissues were prepared with the Nucleospin miRNA/Protein Kit (Macherey-Nagel, Düren, Germany; Ref. no. 740971.50) according to the manufacturer's instructions. Total Protein and RNA concentrations were determined using the Qubit 2.0 Fluorometer (Life Technologies, Grand Island, NY, USA). Protein samples (40  $\mu$ g) were separated on 4-12% Bis-Tris Protein Gels (Invitrogen™) by gel electrophoresis in MES running buffer (Invitrogen™) employing 220 V for 22 min. Gels were then transferred to mini-PVDF membranes using the iBlot 2 Dry Transfer Device (Invitrogen™). The membrane was incubated for ~3 hours with the iBind device with iBind solution (Invitrogen™) with the primary antibodies: anti ASIC1a diluted 1:100 (Santa Cruz Biotechnology, Dallas, TX, USA; cat. no. SC-515033; RRID: AB\_2847878) and loading control antibody anti-GAPDH diluted 1:1,000

(ThermoFisher Scientific; Rockford, IL, USA; cat. no. MA5-15738; RRID: AB\_10977387) as well as the secondary antibody conjugated with Horse Radish Peroxidase diluted 1:1,500 (ThermoFisher Scientific; Rockford, IL, USA; cat. no. 31430; RRID: AB\_228307). Membranes were then incubated for 5 min with SuperSignal™ West Pico PLUS Chemiluminescent Substrate (ThermoFisher) and imaged with C-DiGit® Blot Scanner (Li-Cor). The protein bands were quantified and analyzed using the Image Studio software (Li-Cor). Complementary DNA (cDNA) was synthesized from RNA isolates (see above) using the High Capacity RNA-cDNA™ kit (ThermoFisher) according to the manufacturer's instructions as described previously (58). Quantitative reverse transcriptase polymerase chain reaction experiments were then performed on the cDNA samples using TaqMan gene expression assays specific for: ASIC1a (Sequence proprietary; Assay ID: Rn01638093\_g1), and GAPDH with forward primer: 5'-ACCGCCTGTTGCGTGTTA-3' and reverse primer: 5'-CAATCGCCAACGCCTCAA-3'. All samples were run in duplicate for the gene of interest, and the endogenous control (GAPDH). The results were analyzed with the comparative threshold ( $\Delta\Delta C_t$ ) method. A technical difficulty prevented us from determining GAPDH mRNA expression in one HF-rEF rat which resulted in 19 HF-rEF rats for the ASIC1/GAPDH mRNA expression analysis.

#### *Data analysis.*

Muscle tension, blood pressure, HR and RSNA were measured and recorded in real time with a PowerLab and LabChart data acquisition system (AD Instruments). The original RSNA data were rectified and corrected for the background noise determined after the administration of hexamethonium bromide. Baselines for mean arterial pressure (MAP), RSNA and HR were determined from the 30 second baseline periods that preceded each maneuver. The peak increase in MAP (peak  $\Delta$ MAP), RSNA (peak  $\Delta$ RSNA), and HR (peak  $\Delta$ HR) were calculated as the difference between the peak values wherever they occurred during the maneuvers and their corresponding baseline value. The integrated RSNA ( $\int\Delta$ RSNA) was calculated by integrating the  $\Delta$ RSNA ( $>0$ ) during the maneuver. The change in tension-time index ( $\Delta$ TTI) and blood pressure index (BPI) were calculated by integrating the area under curve during the maneuver and subtracting the integrated area under the curve during the baseline period. Time courses of the increase in RSNA, MAP, HR and tension were plotted as their change from baseline (mean $\pm$ SEM is shown to enhance clarity of the time course data) and were analyzed with Two-Way ANOVAs with Šidák multiple comparisons tests. Multiple t-tests were performed for within animal

comparisons of baseline MAP, baseline HR, Peak  $\Delta$ MAP, Peak  $\Delta$ HR, Peak  $\Delta$ RSNA, BPI,  $\int\Delta$ RSNA, and  $\Delta$ TTI. One-way ANOVAs with Šidák multiple comparison tests were used to determine the effect of sequential blockades of  $\mu$ - and  $\delta$ -opioid receptor as well as ASIC1a on baseline MAP, baseline HR, Peak  $\Delta$ MAP, Peak  $\Delta$ HR, Peak  $\Delta$ RSNA, BPI,  $\int\Delta$ RSNA, and  $\Delta$ TTI in HF-rEF rats pretreated with Naloxone. Data for echocardiograph measurements, body mass, heart morphometrics, and protein and mRNA expression were analyzed with unpaired Student's t-tests or Mann-Whitney U tests as appropriate. Pearson correlation coefficients and linear regression analyses were used to examine the relationship between ASIC1a protein expression and ejection fraction, fractional shortening, and left ventricular infarct size. Statistical significance was defined as  $P < 0.05$ . N values indicate total number of rats. Data are presented as mean (SD).

## 5.4 Results

### *Body mass, heart morphometrics*

Body mass as well as the ratio of LV to body mass were not different between SHAM and HF-rEF rats (Table 1). The ratios of the RV and atria mass to body mass were greater in HF-rEF rats compared to SHAM rats. Additionally, LVEDV and LVESV were significantly greater, and ejection fraction and fractional shortening were significantly lower, in HF-rEF rats compared to SHAM rats. There was no difference in SV between groups.

### *Effect of ASIC1a blockade on reflex responses to lactic acid injections*

Injection of PcTx-1 into the arterial supply of the hindlimb reduced the renal sympathetic and pressor response to injection of lactic acid into the arterial supply of the hindlimb in both SHAM (n=12) and HF-rEF rats (n=11; Fig. 1). Baseline MAP and HR before and after ASIC1a blockade for SHAM and HF-rEF rats are shown in Table 2 and 3. These data provide evidence that injection of 100ng of PcTx-1 into the arterial supply of the hindlimb effectively blocked ASIC1a on the sensory endings of thin fibre muscle afferents (referred to as ASIC1a blockade from this point forward for simplicity). Additionally, the peak  $\Delta$ RSNA (SHAM: 71(68); HF-rEF: 100(50)%;  $P=0.259$ ) and peak  $\Delta$ MAP (SHAM: 19(12); HF-rEF: 26(21)mmHg;  $P=0.347$ ) response to lactic acid in the control conditions from these rats were not different between SHAM and HF-rEF rats.

### *Effect of ASIC1a blockade on the exercise pressor reflex*

In SHAM rats (n=7), ASIC1a blockade reduced the pressor and cardioaccelerator response to static hindlimb muscle contraction (Fig. 2, 3, 4 and Table 3). However, ASIC1a blockade had

no effect on the renal sympathetic response to contraction in SHAM rats. In HF-rEF rats (n=8), ASIC1a blockade significantly reduced the RSNA, pressor, and cardioaccelerator response to contraction (Fig. 2, 3, 4 and Table 3). There was no difference between SHAM and HF-rEF rats in the magnitude of the effect of ASIC1a blockade on the BPI response (SHAM: -179 (156); HF-rEF: -166 (126)mmHg·s; P=0.858) or peak  $\Delta$ MAP response (SHAM: -9 (7); HF-rEF: -6 (6)mmHg; P=0.475) to contraction. The tension developed during the contraction maneuver was not different between control and ASIC1a blockade conditions in either group of rats (Fig. 2 G and H). Baseline MAP and HR before and after ASIC1a blockade for SHAM and HF-rEF rats are shown in Table 2 and 3, respectively. In vehicle control experiments, injection of 0.1mL saline into the hindlimb arterial supply had no effect (P-value range: 0.124-0.775) on the RSNA, pressor, or cardioaccelerator response to hindlimb muscle contraction in SHAM (n=3) or HF-rEF (n=4) rats (data not shown).

In separate groups of SHAM (n=5) and HF-rEF rats (n=5), we investigated the possibility that systemic circulation of PcTx-1 accounted for the effect of the drug when it was injected into the arterial supply of the hindlimb. In SHAM rats, injection of PcTx1 into the jugular vein had no effect on the peak pressor (control: 22 (4); PcTx-1: 18 (7)mmHg; P=0.362), BPI (control: 405 (47); PcTx-1: 313 (123)mmHg·s; P=0.205) or peak cardioaccelerator response (Table 4) to hindlimb muscle contraction. Additionally, injection of PcTx1 into the jugular vein had no effect on the peak renal sympathetic (control: 138 (113); PcTx-1: 162 (134)%; P=0.208) or integrated renal sympathetic nerve response (control: 958 (690); PcTx-1: 845 (289)a.u.; P=0.824) to contraction in SHAM rats. Likewise, injection of PcTx1 via the jugular vein of HF-rEF rats had no effect on the peak pressor (control: 20 (8); PcTx-1: 20 (13)mmHg; P>0.999), BPI (control: 358 (199); PcTx-1: 334 (240)mmHg·s; P=0.717), or peak cardioaccelerator response (Table 3) to hindlimb muscle contraction. Additionally, injection of PcTx1 into the jugular vein had no effect on the peak renal sympathetic (control: 81 (84); PcTx-1: 53 (33)%; P=0.560) or integrated renal sympathetic (control: 884 (760); PcTx-1: 553 (325)a.u.; P=0.435) response to hindlimb muscle contraction in HF-rEF rats. The TTI of the contraction maneuver was not different between the control and i.v. PcTx-1 conditions for either SHAM (control: 25 (8); PcTx-1: 25 (9)kg·s; P>0.999) or HF-rEF rats (control: 15 (6); PcTx-1: 16 (3)kg·s; P=0.721). Baseline MAP and HR before and after injection of ASIC1a into the jugular vein for SHAM and HF-rEF rats are shown in Table 2 and 3, respectively. The results of these experiments are consistent with similar control experiments

performed by Ducrocq, Kim, Estrada and Kaufman (20) and suggest that the effect of PcTx-1 when it was injected into the hindlimb arterial supply of SHAM and HF-rEF rats was not attributable to circulating/systemic effects.

#### *Effect of ASIC1a blockade on the mechanoreflex*

In SHAM rats (n=6), ASIC1a blockade had no effect on the RSNA, pressor, or cardioaccelerator response to static hindlimb muscle stretch (Fig. 5, 6 and Table 3). In HF-rEF rats (n=7), ASIC1a blockade had no effect on the pressor or cardioaccelerator responses to stretch, but significantly reduced the RSNA response (Fig. 6D) especially within the first ~10 seconds of the stretch maneuver (Fig. 5B). The tension developed during the stretch maneuver was not different between control or ASIC1a blockade conditions at any point in either group of rats (Fig. 5 G and H). Baseline MAP and HR before and after ASIC1a blockade for SHAM and HF-rEF rats are shown in Table 2 and 3, respectively.

In a separate group of HF-rEF rats (n=5), we investigated the possibility that the effect of ASIC1a blockade with PcTx-1 on the integrated renal sympathetic response to static hindlimb muscle stretch was attributed to a release of Met-enkephalin, a  $\mu$ - and  $\delta$ -opioid receptor agonist (56). We found that pretreating HF-rEF rats with Naloxone (50 $\mu$ g; 0.1mL saline), a  $\mu$ - and  $\delta$ -opioid receptor antagonist, did not prevent the effect of ASIC1a blockade on the integrated renal sympathetic response to stretch (Fig. 7). Additionally, the pressor and cardioaccelerator response to stretch was not affected by naloxone or ASIC1a blockade in these HF-rEF rats (Table 4).

#### *DRG ASIC1a protein and ASIC1 mRNA expression.*

There was no difference between SHAM (n=16) and HF-rEF (n=20) rats in ASIC1a protein or mRNA expression within L4 and L5 DRG tissue (Fig. 8). Interestingly, HF-rEF rats displayed a greater variance in ASIC1a protein expression ( $F = 9.01$ ;  $P < 0.001$ ), but not mRNA expression ( $F = 1.70$ ;  $P = 0.306$ ) within L4 and L5 DRG tissue. Moreover, in HF-rEF rats there was no significant linear relationship between ASIC1a protein expression and ejection fraction ( $P = 0.243$ ,  $r = -0.274$ ), fractional shortening ( $P = 0.340$ ,  $r = -0.225$ ), or left ventricular infarct size ( $P = 0.149$ ,  $r = 0.335$ ).

## **5.5 Discussion**

We investigated the role played by ASIC1a in evoking the exercise pressor reflex in a rat model of HF-rEF and in SHAM-operated healthy counterparts. We found that injecting the ASIC1a antagonist PcTx-1 into the arterial supply of the hindlimb attenuated the pressor and

cardioaccelerator response to static hindlimb muscle contraction in SHAM and HF-rEF rats. We also found that ASIC1a blockade reduced the RSNA response to hindlimb muscle contraction in HF-rEF rats, but not in SHAM rats. Interestingly, in experiments investigating a possible role for ASIC1a in the mechanoreflex, we found that ASIC1a blockade reduced the RSNA response to hindlimb muscle stretch in HF-rEF rats but not in SHAM rats. Lastly, we found no difference between SHAM and HF-rEF rats in group mean ASIC1a protein or ASIC1 mRNA expression within L4/L5 DRG tissue, although HF-rEF rats did have significantly greater variance in ASIC1a protein expression. Collectively, the present results suggest that ASIC1a contributes to the activation of the exercise pressor reflex in both healthy rats and rats with HF-rEF. Moreover, the results indicate that, in HF-rEF rats, ASIC1a develops a role in mediating the mechanoreflex component of the exercise pressor reflex that is not present in healthy SHAM rats.

The tarantula toxin PcTx-1 is highly selective and highly potent ASIC1a antagonist (IC<sub>50</sub> of 1nM; 59). Ducrocq, Kim, Estrada and Kaufman (20) found that injection of ~100ng of PcTx-1 into the arterial supply of a healthy rat hindlimb attenuated the reflex increase in blood pressure evoked in response to hindlimb arterial injection of lactic acid. We reproduced those findings in SHAM rats and extended them to HF-rEF rats (Fig. 1). In the control condition, we found no difference between SHAM and HF-rEF rats in the RSNA or pressor response to lactic acid injection. In contrast, Xing, Lu and Li (40) previously reported a blunted pressor response to hindlimb arterial injection of lactic acid in HF-rEF rats compared to control rats. However, Xing, Lu and Li (40) slowly infused lactic acid over 30 seconds which likely stimulated ASIC3 to a greater extent than ASIC1a because ASIC1a currents are only generated when the pH is changed within 10 seconds (60) and because ASIC3 currents are sustained while ASIC1a currents are transient (61). Conversely, we rapidly injected (less than ~two seconds) lactic acid into the arterial supply of the hindlimb which likely resulted in a significantly greater stimulus to ASIC1a than did the method of lactic acid delivery utilized by Xing, Lu and Li (40). This difference in delivery method and possible difference in degree of ASIC1a stimulation might explain why we did not find a blunted RSNA and pressor response to hindlimb arterial injection of lactic acid in HF-rEF rats compared to SHAM rats.

Our finding in SHAM rats that ASIC1a blockade reduced the pressor and cardioaccelerator response to static hindlimb muscle contraction is an important reproduction of the findings from Ducrocq, Kim, Estrada and Kaufman (19), Ducrocq, Kim, Estrada and Kaufman (20). The fact

that the MAP response to contraction appeared to be reduced by ASIC1a blockade generally throughout the 30 second maneuver but with the most clear effect occurring in the latter half of the contraction (see Fig 2C), along with the fact that ASIC1a blockade had no effect on the reflex responses to hindlimb muscle stretch in SHAM rats, is consistent with the notion suggested by Ducrocq, Kim, Estrada and Kaufman (19), Ducrocq, Kim, Estrada and Kaufman (20) that, in health, ASIC1a plays a role in the metaboreflex but not the mechanoreflex. A surprising result of the present investigation was that, despite finding ASIC1a-induced reductions in the pressor and cardioaccelerator response to contraction, we found no effect of ASIC1a blockade on the RSNA response to hindlimb muscle contraction in SHAM rats. One possibility for this apparent discrepancy is that ASIC1a stimulation contributes to reflex increases in SNA directed towards vascular beds/organs other than the kidneys. Another possibility is that ASIC1a plays only a minor/secondary role in mediating the reflex increase in RSNA and that redundant mechanisms preserved the RSNA response to muscle contraction following ASIC1a blockade in SHAM rats. Nevertheless, the present data further support the recent findings (19, 20) indicating that ASIC1a plays a role in evoking the exercise pressor reflex in healthy rats.

Our finding in HF-rEF rats that ASIC1a blockade reduced the RSNA, pressor, and cardioaccelerator response to static hindlimb muscle contraction suggests that ASIC1a contributes importantly to the exercise pressor reflex in HF-rEF rats. Interestingly, the magnitude of effect of ASIC1a blockade on the pressor response was not different between SHAM and HF-rEF rats which suggests that ASIC1a does not play a greater role evoking the exercise pressor reflex in HF-rEF rats compared to SHAM rats. However, in contrast to SHAM rats, in HF-rEF rats ASIC1a blockade reduced the RSNA response to hindlimb muscle contraction. Our finding that the RSNA response to hindlimb muscle contraction was reduced following ASIC1a blockade in HF-rEF rats, but not SHAM rats, suggests that activation of ASIC1a on the sensory endings of thin fibre muscle afferents may contribute to the exaggerated renal vasoconstriction during static handgrip exercise in HF-rEF patients compared with healthy controls (62, 63). The role for ASIC1a in the heightened RSNA response to exercise pressor reflex activation in HF-rEF rats may also have important implications for our understanding of the development of cardiorenal syndrome and consequent abnormal renal function which is frequently reported in HF-rEF patients (64). Nevertheless, the effect of ASIC1a blockade on RSNA was evident in the first second of contraction and disappeared within ~10 seconds (see Fig. 2B). It seems unlikely that an accumulation of acidic byproducts of



muscle contraction and consequent stimulation of ASIC1a could account for the ASIC1a-mediated effect at the onset of muscle contraction, especially when considering data showing that the predominately metabolically sensitive group IV muscle afferents take ~5-30 seconds to be activated by static hindlimb muscle contraction (4, 8, 65). An alternative explanation is that the ASIC1a blockade-induced reduction in the RSNA response to contraction in HF-rEF rats is attributable to a role for ASIC1a in the mechanoreflex. In support of this explanation, ASIC1a blockade reduced the RSNA response to hindlimb muscle stretch in HF-rEF rats; an effect that was consistent across two different HF-rEF groups with slight variations in the experimental protocols (see experimental considerations below for more discussion on the naloxone experiments). ASIC1a blockade in HF-rEF rats, however, had no effect on the pressor or cardioaccelerator response to hindlimb muscle stretch. We interpret these findings to suggest that the primary role for ASIC1a in evoking the exercise pressor reflex involves metaboreflex-related effects on MAP and HR. Additionally, in HF-rEF, ASIC1a develops a novel, secondary role in evoking the exercise pressor reflex that involves mechanoreflex-related effects on RSNA.

Our finding that ASIC1a contributes to the mechanoreflex in HF-rEF is consistent with a growing body of literature suggesting that ASIC1a stimulation may modulate the function of mechanically activated channels on the sensory endings of thin fibre muscle afferents under various physiological conditions (66-69). For example, ASIC1a blockade with PcTx-1 has been shown to prevent the development of mechanical hyperalgesia following activity-induced pain in the mouse (69). Additionally, ASIC1 knockout mice are resistant to the typical development of mechanical hyperalgesia following injection of the inflammation-inducing carrageenan solution into the gastrocnemius muscle (70). Passive hindlimb muscle stretch as performed in the present investigation activates a model of the mechanoreflex in the absence of any contraction-induced metabolic stimulus or change in local muscle venous effluent blood lactate concentration or pH (55). Thus, the results of the stretch experiments in the present investigation provide strong evidence that the role played by ASIC1a in mechanoreflex activation in HF-rEF is not related to its role in acid/pH sensing. Moreover, the present data suggest that the mechanosensory role for ASIC1a does not develop acutely during muscle contraction but rather is chronically, or persistently, present and then revealed when the mechanical stimulus of muscle stretch/contraction is present. The precise mechanism(s) by which ASIC1a plays a role in mechanosensation in HF-rEF is unknown (see recent review by 68). Whether a “direct” role for ASICs in mechanosensation

exists in specific physiological/pathological conditions through, for example, proteins linking ASICs to the cytoskeleton, and/or whether ASIC-mediated intracellular signaling modulates the function of other “inherently” mechanosensitive proteins such as PIEZO channels (71), requires further investigation.

To our knowledge, the present investigation is the first to examine the effect of HF-rEF on ASIC1a expression in DRG neurons. In contrast to our hypothesis, we found no difference in ASIC1 mRNA or ASIC1a group mean protein expression within L4/L5 DRG tissue between SHAM and HF-rEF rats. Interestingly, however, we found greater variance in ASIC1a protein expression in HF-rEF rats compared to SHAM rats. We did not find greater variance in ASIC1 mRNA expression in HF-rEF rats although there was a trend ( $P = 0.077$ ) towards greater group mean ASIC1 mRNA expression in HF-rEF compared to SHAM rats. These findings suggest that increased ASIC1a protein expression on thin fibre muscle afferents may contribute to the role played by ASIC1a in the exaggerated exercise pressor reflex in some, but likely not the majority of, HF-rEF rats. It is important to note, however, that any such increase in ASIC1a protein expression could not account, in and of itself, for the mechanoreflex-related role played by ASIC1a; a role that was found to be remarkably consistent in the HF-rEF rats. In support of this notion, Walder, Rasmussen, Rainier, Light, Wemmie and Sluka (70) reported that carrageenan-induced mouse gastrocnemius muscle inflammation produced ASIC1a-mediated mechanical hyperalgesia in the absence of increased ASIC1 mRNA expression in lumbar DRG tissue. Our current finding that ASIC1a adopts a role in the mechanoreflex in HF-rEF rats that is not present in healthy rats in the absence of group mean differences in ASIC1a expression is consistent with those findings of Walder, Rasmussen, Rainier, Light, Wemmie and Sluka (70)

Several experimental considerations should be noted. First, only male rats were used in the present investigation. Future studies are needed to determine the role of ASIC1a signaling in the exercise pressor reflex in female rats with and without HF-rEF. Second, ASIC1a is also located on vascular smooth muscle cells which, when activated, results in vasoconstriction (72). Thus, the possibility exists that injection of PcTx-1 into the arterial supply of the hindlimb could accentuate the increases in hindlimb arterial blood flow thereby resulting in a diminished stimulus to the metaboreflex produced by contraction-induced metabolite production. However, Ducrocq, Kim, Estrada and Kaufman (20) addressed this possibility and showed that injection of PcTx-1 into the arterial supply of the rat hindlimb had no effect on blood flow to the hindlimb during static

contraction of the triceps surae muscle (assessed by popliteal artery blood flow). Third, we recognized the possibility that ASIC1a blockade with PcTx-1 may have resulted in the release of Met-enkephalin (56), a  $\mu$ - and  $\delta$ -opioid receptor agonist, which may have accounted for our finding in HF-rEF rats that ASIC1a blockade reduced the RSNA response to static hindlimb muscle stretch. However, we found that ASIC1a blockade reduced the RSNA response to static hindlimb muscle stretch in a separate group of HF-rEF rats that were pretreated with naloxone (a  $\mu$ - and  $\delta$ -opioid receptor antagonist) suggesting that  $\mu$ - and  $\delta$ -opioid receptor activation does not account for the attenuating effects of ASIC1a blockade on the mechanoreflex in HF-rEF rats. Fourth, we investigated ASIC1 mRNA and ASIC1a protein expression in whole DRG tissue. Thus, the mRNA and protein signals we investigated did not originate solely from group III and IV muscle afferents. Future studies should seek to determine ASIC1 mRNA and ASIC1a protein expression in isolated group III and IV muscle afferents from SHAM and HF-rEF rats. Fifth, during whole body exercise, the exercise pressor reflex works in concert with various other autonomic control signals which contribute to the sympathetic and cardiovascular adjustments to exercise in health and disease. For example, central command (73), the carotid chemoreflex (74-76), and the arterial baroreflex (77, 78) have all been reported to contribute to sympathetic and cardiovascular responses during exercise. The extent to which ASIC1a contributes to the sympathetic and cardiovascular adjustments to whole body exercise when all these autonomic control mechanisms are working together remains unknown. Lastly, we do not report a statistical comparison of the reflex responses to muscle contraction or stretch between SHAM and HF-rEF rats from the control condition (i.e., before ASIC1a blockade). The present study was powered only to investigate the effect of ASIC1a blockade within the SHAM and HF-rEF groups and those across group comparisons were left underpowered. Importantly, the available literature consistently demonstrates that, compared to SHAM counterparts, the reflex responses to hindlimb muscle contraction and stretch are exaggerated in the rat myocardial infarction-induced model of HF-rEF (26, 27, 29, 49, 50, 79-84). We do report the statistical comparison of the pressor response to lactic acid injection between SHAM and HF-rEF groups because, to our knowledge, this is the first investigation to report the reflex pressor and RSNA response to a bolus injection of lactic acid into the arterial supply of the hindlimb of HF-rEF rats.

## **5.6 Conclusion**

In summary, we found that ASIC1a contributed to activation of the exercise pressor reflex in SHAM and HF-rEF rats. The present findings further suggest that ASIC1a plays a role only in evoking the metaboreflex component of the exercise pressor reflex in health whereas in HF-rEF, ASIC1a plays a role in evoking both the metaboreflex and mechanoreflex components of the exercise pressor reflex. Targeting ASIC1a in HF-rEF patients may serve as a favorable therapeutic strategy aimed at mitigating exercise intolerance and cardiovascular risk. That conclusion is supported by the findings of Smith, Joyner, Curry, Borlaug, Keller-Ross, Van Iterson and Olson (35) who demonstrated that exercise pressor reflex activation in HF-rEF patients constrains increases in stroke volume and elevates systemic vascular resistance during exercise.

## 5.7 References

1. **Kaufman MP, and Forster HV.** Reflexes controlling circulatory, ventilatory and airway responses to exercise. In: *Handbook of Physiology, Section 12: Exercise: Regulation and Integration of Multiple Systems II Control of Respiratory and Cardiovascular Systems*, edited by Rowell LB, and Shepherd JT. New York, NY: Oxford University Press, 1996, p. 381-447.
2. **Mitchell JH, Kaufman MP, and Iwamoto GA.** The exercise pressor reflex: Its cardiovascular effects, afferent mechanisms, and central pathways. *AnnRevPhysiol* 45: 229-242, 1983.
3. **Strange S, Secher NH, Pawelczyk JA, Karpakka J, Christensen NJ, Mitchell JH, and Saltin B.** Neural control of cardiovascular responses and of ventilation during dynamic exercise in man. *JPhysiol* 470: 693-704, 1993.
4. **Kaufman MP, Longhurst JC, Rybicki KJ, Wallach JH, and Mitchell JH.** Effects of static muscular contraction on impulse activity of groups III and IV afferents in cats. *JApplPhysiol* 55: 105-112, 1983.
5. **McCloskey DI, and Mitchell JH.** Reflex cardiovascular and respiratory responses originating in exercising muscle. *JPhysiol* 224: 173-186, 1972.
6. **Amann M, Runnels S, Morgan DE, Trinity JD, Fjeldstad AS, Wray DW, Reese VR, and Richardson RS.** On the contribution of group III and IV muscle afferents to the circulatory response to rhythmic exercise in humans. *JPhysiol* 589: 3855-3866, 2011.
7. **Kaufman MP, Iwamoto GA, Longhurst JC, and Mitchell JH.** Effects of capsaicin and bradykinin on afferent fibers with endings in skeletal muscle. *CircRes* 50: 133-139, 1982.
8. **Kaufman MP, Rybicki KJ, Waldrop TG, and Ordway GA.** Effect of ischemia on responses of group III and IV afferents to contraction. *JApplPhysiol* 57: 644-650, 1984.
9. **Mense S, and Meyer H.** Bradykinin-induced modulation of the response behaviour of different types of feline group III and IV muscle receptors. *JPhysiol* 398: 49-63, 1988.
10. **Mense S, and Stahnke M.** Responses in muscle afferent fibers of slow conduction velocity to contractions and ischemia in the cat. *JPhysiol* 342: 383-397, 1983.
11. **Rotto DM, and Kaufman MP.** Effects of metabolic products of muscular contraction on the discharge of group III and IV afferents. *JApplPhysiol* 64: 2306-2313, 1988.
12. **Abboud FM, and Benson CJ.** ASICs and cardiovascular homeostasis. *Neuropharmacology* 94: 87-98, 2015.

13. **Gautam M, and Benson CJ.** Acid-sensing ion channels (ASICs) in mouse skeletal muscle afferents are heteromers composed of ASIC1a, ASIC2, and ASIC3 subunits. *FASEB J* 27: 793-802, 2013.
14. **Victor RG, Bertocci LA, Pryor SL, and Nunnally RL.** Sympathetic nerve discharge is coupled to muscle cell pH during exercise in humans. *J Clin Invest* 82: 1301-1305, 1988.
15. **McCord JL, Tsuchimochi H, and Kaufman MP.** Acid-sensing ion channels contribute to the metaboreceptor component of the exercise pressor reflex. *Am J Physiol Heart Circ Physiol* 297: H443-449, 2009.
16. **Campos MO, Mansur DE, Mattos JD, Paiva ACS, Videira RLR, Macefield VG, da Nobrega ACL, and Fernandes IA.** Acid-sensing ion channels blockade attenuates pressor and sympathetic responses to skeletal muscle metaboreflex activation in humans. *J Appl Physiol (1985)* 127: 1491-1501, 2019.
17. **McCord JL, Hayes SG, and Kaufman MP.** Acid-sensing ion and epithelial sodium channels do not contribute to the mechanoreceptor component of the exercise pressor reflex. *Am J Physiol Heart Circ Physiol* 295: H1017-H1024, 2008.
18. **Hayes SG, Kindig AE, and Kaufman MP.** Blockade of acid sensing ion channels attenuates the exercise pressor reflex in cats. *J Physiol* 581: 1271-1282, 2007.
19. **Ducrocq GP, Kim JS, Estrada JA, and Kaufman MP.** ASIC1a does not play a role in evoking the metabolic component of the exercise pressor reflex in a rat model of peripheral artery disease. *Am J Physiol Heart Circ Physiol* 2020.
20. **Ducrocq GP, Kim JS, Estrada JA, and Kaufman MP.** ASIC1a plays a key role in evoking the metabolic component of the exercise pressor reflex in rats. *Am J Physiol Heart Circ Physiol* 318: H78-H89, 2020.
21. **Hesselager M, Timmermann DB, and Ahring PK.** pH Dependency and desensitization kinetics of heterologously expressed combinations of acid-sensing ion channel subunits. *J Biol Chem* 279: 11006-11015, 2004.
22. **Tsuchimochi H, Yamauchi K, McCord JL, and Kaufman MP.** Blockade of acid sensing ion channels attenuates the augmented exercise pressor reflex in rats with chronic femoral artery occlusion. *J Physiol* 589: 6173-6189, 2011.

23. **Kim JS, Harms JE, Ruiz-Velasco V, and Kaufman MP.** Effect of knockout of the ASIC3 on cardiovascular reflexes arising from hindlimb muscle in decerebrated rats. *Am J Physiol Regul Integr Comp Physiol* 317: R641-R648, 2019.
24. **Kim JS, Ducrocq GP, and Kaufman MP.** Functional knockout of ASIC3 attenuates the exercise pressor reflex in decerebrated rats with ligated femoral arteries. *Am J Physiol Heart Circ Physiol* 318: H1316-H1324, 2020.
25. **Stone AJ, Copp SW, Kim JS, and Kaufman MP.** Combined, but not individual, blockade of ASIC3, P2X, and EP4 receptors attenuates the exercise pressor reflex in rats with freely perfused hindlimb muscles. *J Appl Physiol (1985)* 119: 1330-1336, 2015.
26. **Butenas ALE, Rollins KS, Williams AC, Parr SK, Hammond ST, Ade CJ, Hageman KS, Musch TI, and Copp SW.** Thromboxane A2 receptors contribute to the exaggerated exercise pressor reflex in male rats with heart failure. *Physiological reports* 9: e15052, 2021.
27. **Koba S, Xing J, Sinoway LI, and Li J.** Sympathetic nerve responses to muscle contraction and stretch in ischemic heart failure. *Am J Physiol Heart Circ Physiol* 294: H311-321, 2008.
28. **Middlekauff HR, Chiu J, Hamilton MA, Fonarow GC, Maclellan WR, Hage A, Moriguchi J, and Patel J.** Muscle mechanoreceptor sensitivity in heart failure. *Am J Physiol Heart Circ Physiol* 287: H1937-H1943, 2004.
29. **Wang HJ, Pan YX, Wang WZ, Gao L, Zimmerman MC, Zucker IH, and Wang W.** Exercise training prevents the exaggerated exercise pressor reflex in rats with chronic heart failure. *J Appl Physiol (1985)* 108: 1365-1375, 2010.
30. **Amann M, Venturelli M, Ives SJ, Morgan DE, Gmelch B, Witman MA, Jonathan Groot H, Walter Wray D, Stehlik J, and Richardson RS.** Group III/IV muscle afferents impair limb blood in patients with chronic heart failure. *Int J Cardiol* 174: 368-375, 2014.
31. **Hammond RL, Augustyniak RA, Rossi NF, Churchill PC, Lapanowski K, and O'Leary DS.** Heart failure alters the strength and mechanisms of the muscle metaboreflex. *Am J Physiol Heart Circ Physiol* 278: H818-828, 2000.
32. **Sterns DA, Ettinger SM, Gray KS, Whisler SK, Mosher TJ, Smith MB, and Sinoway LI.** Skeletal muscle metaboreceptor exercise responses are attenuated in heart failure. *Circulation* 84: 2034-2039, 1991.

33. **Piepoli M, Clark AL, Volterrani M, Adamopoulos S, Sleight P, and Coats AJ.** Contribution of muscle afferents to the hemodynamic, autonomic, and ventilatory responses to exercise in patients with chronic heart failure: effects of physical training. *Circulation* 93: 940-952, 1996.
34. **Ansorge EJ, Augustyniak RA, Perinot ML, Hammond RL, Kim JK, Sala-Mercado JA, Rodriguez J, Rossi NF, and O'Leary DS.** Altered Muscle Metaboreflex Control of Coronary Blood Flow and Ventricular Function in Heart Failure. *AmJPhysiol Heart CircPhysiol* 288: H1381-H1388, 2004.
35. **Smith JR, Joyner MJ, Curry TB, Borlaug BA, Keller-Ross ML, Van Iterson EH, and Olson TP.** Locomotor muscle group III/IV afferents constrain stroke volume and contribute to exercise intolerance in human heart failure. *J Physiol* 598: 5379-5390, 2020.
36. **Amann M, Blain GM, Proctor LT, Sebranek JJ, Pegelow DF, and Dempsey JA.** Implications of group III and IV muscle afferents for high-intensity endurance exercise performance in humans. *J Physiol* 589: 5299-5309, 2011.
37. **O'Leary DS, Augustyniak RA, Ansorge EJ, and Collins HL.** Muscle metaboreflex improves O<sub>2</sub> delivery to ischemic active skeletal muscle. *AmJPhysiol* 276: H1399-H1403, 1999.
38. **Arnolda L, Brosnan J, Rajagopalan B, and Radda GK.** Skeletal muscle metabolism in heart failure in rats. *Am J Physiol* 261: H434-442, 1991.
39. **Massie BM, Conway M, Rajagopalan B, Yonge R, Frostick S, Ledingham J, Sleight P, and Radda G.** Skeletal muscle metabolism during exercise under ischemic conditions in congestive heart failure. Evidence for abnormalities unrelated to blood flow. *Circulation* 78: 320-326, 1988.
40. **Xing J, Lu J, and Li J.** ASIC3 contributes to the blunted muscle metaboreflex in heart failure. *Med Sci Sports Exerc* 47: 257-263, 2015.
41. **Murphy SP, Kakkar R, McCarthy CP, and Januzzi JL, Jr.** Inflammation in Heart Failure: JACC State-of-the-Art Review. *J Am Coll Cardiol* 75: 1324-1340, 2020.
42. **Voilley N, de Weille J, Mamet J, and Lazdunski M.** Nonsteroid anti-inflammatory drugs inhibit both the activity and the inflammation-induced expression of acid-sensing ion channels in nociceptors. *J Neurosci* 21: 8026-8033, 2001.
43. **Smith ES, Cadiou H, and McNaughton PA.** Arachidonic acid potentiates acid-sensing ion channels in rat sensory neurons by a direct action. *Neuroscience* 145: 686-698, 2007.



44. **National Research Council (U.S.). Committee for the Update of the Guide for the Care and Use of Laboratory Animals., Institute for Laboratory Animal Research (U.S.), and National Academies Press (U.S.).** Guide for the care and use of laboratory animals. Washington, D.C.: National Academies Press,, 2011, p. xxv, 220 p.
45. **Musch TI, and Terrell JA.** Skeletal muscle blood flow abnormalities in rats with a chronic myocardial infarction: rest and exercise. *AmJPhysiol* 262: H411-H419, 1992.
46. **Kolettis TM, Agelaki MG, Baltogiannis GG, Vlahos AP, Mourouzis I, Fotopoulos A, and Pantos C.** Comparative effects of acute vs. chronic oral amiodarone treatment during acute myocardial infarction in rats. *Europace* 9: 1099-1104, 2007.
47. **Baumfalk DR, Opoku-Acheampong AB, Caldwell JT, Butenas ALE, Horn AG, Kunkel ON, Copp SW, Ade CJ, Musch TI, and Behnke BJ.** Effects of high-intensity training on prostate cancer-induced cardiac atrophy. *Am J Transl Res* 13: 197-209, 2021.
48. **Butenas ALE, Colburn TD, Baumfalk DR, Ade CJ, Hageman KS, Copp SW, Poole DC, and Musch TI.** Angiotensin converting enzyme inhibition improves cerebrovascular control during exercise in male rats with heart failure. *Respir Physiol Neurobiol* 103613, 2021.
49. **Butenas ALE, Rollins KS, Williams AC, Parr SK, Hammond ST, Ade CJ, Hageman KS, Musch TI, and Copp SW.** Exaggerated sympathetic and cardiovascular responses to dynamic mechanoreflex activation in rats with heart failure: Role of endoperoxide 4 and thromboxane A2 receptors. *Auton Neurosci* 232: 102784, 2021.
50. **Butenas ALE, Rollins KS, Matney JE, Williams AC, Kleweno TE, Parr SK, Hammond ST, Ade CJ, Hageman KS, Musch TI, and Copp SW.** No effect of endoperoxide 4 or thromboxane A2 receptor blockade on static mechanoreflex activation in rats with heart failure. *Exp Physiol* 105: 1840-1854, 2020.
51. **Smith SA, Mitchell JH, and Garry MG.** Electrically induced static exercise elicits a pressor response in the decerebrate rat. *JPhysiol* 537: 961-970, 2001.
52. **Kempf EA, Rollins KS, Hopkins TD, Butenas AL, Santin JM, Smith JR, and Copp SW.** Chronic femoral artery ligation exaggerates the pressor and sympathetic nerve responses during dynamic skeletal muscle stretch in decerebrate rats. *Am J Physiol Heart Circ Physiol* 314: H246-H254, 2018.

53. **Craig JC, Colburn TD, Hirai DM, Musch TI, and Poole DC.** Sexual dimorphism in the control of skeletal muscle interstitial Po<sub>2</sub> of heart failure rats: effects of dietary nitrate supplementation. *J Appl Physiol (1985)* 126: 1184-1192, 2019.
54. **Dibas J, Al-Saad H, and Dibas A.** Basics on the use of acid-sensing ion channels' inhibitors as therapeutics. *Neural Regen Res* 14: 395-398, 2019.
55. **Stebbins CL, Brown B, Levin D, and Longhurst JC.** Reflex effect of skeletal muscle mechanoreceptor stimulation on the cardiovascular system. *JApplPhysiol* 65: 1539-1547, 1988.
56. **Mazzuca M, Heurteaux C, Alloui A, Diochot S, Baron A, Voilley N, Blondeau N, Escoubas P, Gelot A, Cupo A, Zimmer A, Zimmer AM, Eschalier A, and Lazdunski M.** A tarantula peptide against pain via ASIC1a channels and opioid mechanisms. *Nat Neurosci* 10: 943-945, 2007.
57. **Tsuchimochi H, McCord JL, and Kaufman MP.** Peripheral mu-opioid receptors attenuate the augmented exercise pressor reflex in rats with chronic femoral artery occlusion. *AmJPhysiol Heart CircPhysiol* 299: H557-H565, 2010.
58. **Copp SW, Kim JS, Ruiz-Velasco V, and Kaufman MP.** The mechano-gated channel inhibitor GsMTx4 reduces the exercise pressor reflex in decerebrate rats. *J Physiol* 594: 641-655, 2016.
59. **Escoubas P, De Weille JR, Lecoq A, Diochot S, Waldmann R, Champigny G, Moinier D, Menez A, and Lazdunski M.** Isolation of a tarantula toxin specific for a class of proton-gated Na<sup>+</sup> channels. *J Biol Chem* 275: 25116-25121, 2000.
60. **Alijevic O, Bignucolo O, Hichri E, Peng Z, Kucera JP, and Kellenberger S.** Slowing of the Time Course of Acidification Decreases the Acid-Sensing Ion Channel 1a Current Amplitude and Modulates Action Potential Firing in Neurons. *Front Cell Neurosci* 14: 41, 2020.
61. **Yagi J, Wenk HN, Naves LA, and McCleskey EW.** Sustained currents through ASIC3 ion channels at the modest pH changes that occur during myocardial ischemia. *CircRes* 99: 501-509, 2006.
62. **Middlekauff HR, Nitzsche EU, Hoh CK, Hamilton MA, Fonarow GC, Hage A, and Moriguchi JD.** Exaggerated renal vasoconstriction during exercise in heart failure patients. *Circulation* 101: 784-789, 2000.

63. **Momen A, Bower D, Boehmer J, Kunselman AR, Leuenberger UA, and Sinoway LI.** Renal blood flow in heart failure patients during exercise. *AmJPhysiol Heart CircPhysiol* 287: H2834-H2839, 2004.
64. **Ramchandra R, Xing DT, Matear M, Lambert G, Allen AM, and May CN.** Neurohumoral interactions contributing to renal vasoconstriction and decreased renal blood flow in heart failure. *Am J Physiol Regul Integr Comp Physiol* 317: R386-R396, 2019.
65. **Wang HJ, Li YL, Gao L, Zucker IH, and Wang W.** Alteration in skeletal muscle afferents in rats with chronic heart failure. *JPhysiol* 588: 5033-5047, 2010.
66. **Page AJ, Brierley SM, Martin CM, Martinez-Salgado C, Wemmie JA, Brennan TJ, Symonds E, Omari T, Lewin GR, Welsh MJ, and Blackshaw LA.** The ion channel ASIC1 contributes to visceral but not cutaneous mechanoreceptor function. *Gastroenterology* 127: 1739-1747, 2004.
67. **Chen CC, and Wong CW.** Neurosensory mechanotransduction through acid-sensing ion channels. *J Cell Mol Med* 17: 337-349, 2013.
68. **Ruan N, Tribble J, Peterson AM, Jiang Q, Wang JQ, and Chu XP.** Acid-Sensing Ion Channels and Mechanosensation. *Int J Mol Sci* 22: 2021.
69. **Gregory NS, Gautam M, Benson CJ, and Sluka KA.** Acid Sensing Ion Channel 1a (ASIC1a) Mediates Activity-induced Pain by Modulation of Heteromeric ASIC Channel Kinetics. *Neuroscience* 386: 166-174, 2018.
70. **Walder RY, Rasmussen LA, Rainier JD, Light AR, Wemmie JA, and Sluka KA.** ASIC1 and ASIC3 play different roles in the development of Hyperalgesia after inflammatory muscle injury. *J Pain* 11: 210-218, 2010.
71. **Coste B, Mathur J, Schmidt M, Earley TJ, Ranade S, Petrus MJ, Dubin AE, and Patapoutian A.** Piezo1 and Piezo2 are essential components of distinct mechanically activated cation channels. *Science* 330: 55-60, 2010.
72. **Drummond HA, Xiang L, Chade AR, and Hester R.** Enhanced maximal exercise capacity, vasodilation to electrical muscle contraction, and hind limb vascular density in ASIC1a null mice. *Physiological reports* 5: e13368, 2017.
73. **Koba S, Gao Z, Xing J, Sinoway LI, and Li J.** Sympathetic responses to exercise in myocardial infarction rats: a role of central command. *AmJPhysiol Heart CircPhysiol* 291: H2735-H2742, 2006.

74. **Li YL, Xia XH, Zheng H, Gao L, Li YF, Liu D, Patel KP, Wang W, and Schultz HD.** Angiotensin II enhances carotid body chemoreflex control of sympathetic outflow in chronic heart failure rabbits. *Cardiovasc Res* 71: 129-138, 2006.
75. **Machado AC, Vianna LC, Gomes EAC, Teixeira JAC, Ribeiro ML, Villacorta H, Nobrega ACL, and Silva BM.** Carotid chemoreflex and muscle metaboreflex interact to the regulation of ventilation in patients with heart failure with reduced ejection fraction. *Physiological reports* 8: e14361, 2020.
76. **Stickland MK, Miller JD, Smith CA, and Dempsey JA.** Carotid chemoreceptor modulation of regional blood flow distribution during exercise in health and chronic heart failure. *Circ Res* 100: 1371-1378, 2007.
77. **Mancia G, Seravalle G, Giannattasio C, Bossi M, Preti L, Cattaneo BM, and Grassi G.** Reflex cardiovascular control in congestive heart failure. *The American journal of cardiology* 69: 17G-22G; discussion 22G-23G, 1992.
78. **Grassi G, Seravalle G, Cattaneo BM, Lanfranchi A, Vailati S, Giannattasio C, Del Bo A, Sala C, Bolla GB, and Pozzi M.** Sympathetic activation and loss of reflex sympathetic control in mild congestive heart failure. *Circulation* 92: 3206-3211, 1995.
79. **Koba S, Gao Z, and Sinoway LI.** Oxidative stress and the muscle reflex in heart failure. *J Physiol* 587: 5227-5237, 2009.
80. **Smith SA, Mammen PP, Mitchell JH, and Garry MG.** Role of the exercise pressor reflex in rats with dilated cardiomyopathy. *Circulation* 108: 1126-1132, 2003.
81. **Smith SA, Mitchell JH, Naseem RH, and Garry MG.** Mechanoreflex mediates the exaggerated exercise pressor reflex in heart failure. *Circulation* 112: 2293-2300, 2005.
82. **Smith SA, Williams MA, Mitchell JH, Mammen PP, and Garry MG.** The capsaicin-sensitive afferent neuron in skeletal muscle is abnormal in heart failure. *Circulation* 111: 2056-2065, 2005.
83. **Koba S, Xing J, Sinoway LI, and Li J.** Bradykinin receptor blockade reduces sympathetic nerve response to muscle contraction in rats with ischemic heart failure. *Am J Physiol Heart Circ Physiol* 298: H1438-1444, 2010.
84. **Morales A, Gao W, Lu J, Xing J, and Li J.** Muscle cyclo-oxygenase-2 pathway contributes to the exaggerated muscle mechanoreflex in rats with congestive heart failure. *Exp Physiol* 97: 943-954, 2012.



**Table 5.1**

Table 5.1. Body and tissue masses and heart morphometrics in SHAM and HF-rEF rats

|                           | SHAM ( <i>n</i> =43) | HF-rEF ( <i>n</i> =59) | P-value |
|---------------------------|----------------------|------------------------|---------|
| Body mass (g)             | 529 (45)             | 525 (36)               | 0.632   |
| LV/body mass (mg/g)       | 1.97 (0.34)          | 2.03 (0.42)            | 0.228   |
| RV/body mass (mg/g)       | 0.54 (0.06)          | 0.57 (0.11)            | 0.034*  |
| Atria/body mass (mg/g)    | 0.16 (0.04)          | 0.22 (0.08)            | <0.001* |
| LV EDV (mL)               | 1.23 (0.29)          | 2.10 (0.55)            | <0.001* |
| LV ESV (mL)               | 0.25 (0.15)          | 1.14 (0.51)            | <0.001* |
| Stroke volume (mL)        | 0.99 (0.20)          | 1.01 (0.24)            | 0.363   |
| Ejection fraction (%)     | 82 (7)               | 45 (18)                | <0.001* |
| Fractional shortening (%) | 46 (8)               | 21 (10)                | <0.001* |
| Infarct size (%)          | -                    | 29 (9)                 | -       |

Values are mean (SD). LV, left ventricle; RV, right ventricle; EDV, end diastolic volume; ESV, end systolic volume. Data were compared using student's t-tests. Asterisks indicate statistical significance ( $P < 0.05$ ).

**Table 5.2**

Table 5.2. Baseline MAP in SHAM and HF-rEF rats

| Experimental Group                         | Method of PcTx-1 injection | Control (mmHg) | Post injection (mmHg) | P-Value |
|--|----------------------------|----------------|-----------------------|---------|
| SHAM lactic acid injection, <i>n</i> =12   | i.a.                       | 76 (10)        | 78 (12)               | 0.514   |
| HF-rEF lactic acid injection, <i>n</i> =11 | i.a.                       | 92 (25)        | 93 (24)               | 0.434   |
| SHAM contraction, <i>n</i> =7              | i.a.                       | 88 (8)         | 90 (14)               | 0.678   |
| HF-rEF contraction, <i>n</i> =8            | i.a.                       | 75 (12)        | 75 (9)                | 0.945   |
| SHAM contraction, <i>n</i> =5              | i.v.                       | 74 (5)         | 72 (6)                | 0.535   |
| HF-rEF contraction, <i>n</i> =5            | i.v.                       | 79 (16)        | 77 (16)               | 0.726   |
| SHAM stretch, <i>n</i> =6                  | i.a.                       | 93 (22)        | 100 (16)              | 0.300   |
| HF-rEF stretch, <i>n</i> =7                | i.a.                       | 79 (12)        | 88 (13)               | 0.048*  |

Values are mean (SD). Experimental group is identified by the primary experimental maneuver performed. Data were compared with paired Student's t-tests. i.a., intraarterial; i.v., intravenous; HF-rEF, heart failure with reduced ejection fraction; MAP, mean arterial pressure; PcTx-1, psalmotoxin-1. Asterisk indicates statistical significance ( $P < 0.05$ ).

**Table 5.3**

Table 5.3. Baseline HR and cardioaccelerator responses in SHAM and HF-rEF rats

| Experimental Group                         | Method of<br>PcTx-1<br>injection | Control<br>(bpm) | Post<br>injection<br>(bpm) | P-Value |
|--|----------------------------------|------------------|----------------------------|---------|
| Baseline HR                                |                                  |                  |                            |         |
| SHAM lactic acid injection, <i>n</i> =12   | i.a.                             | 488 (25)         | 481 (10)                   | 0.318   |
| HF-rEF lactic acid injection, <i>n</i> =11 | i.a.                             | 488 (45)         | 483 (53)                   | 0.455   |
| SHAM contraction, <i>n</i> =7              | i.a.                             | 419 (62)         | 442 (53)                   | 0.198   |
| HF-rEF contraction, <i>n</i> =8            | i.a.                             | 406 (33)         | 414 (40)                   | 0.041*  |
| SHAM contraction, <i>n</i> =5              | i.v.                             | 440 (42)         | 425 (35)                   | 0.240   |
| HF-rEF contraction, <i>n</i> =5            | i.v.                             | 416 (55)         | 407 (24)                   | 0.035*  |
| SHAM stretch, <i>n</i> =6                  | i.a.                             | 490 (34)         | 493 (24)                   | 0.682   |
| HF-rEF stretch, <i>n</i> =7                | i.a.                             | 468 (27)         | 463 (39)                   | 0.534   |
| Peak $\Delta$ HR                           |                                  |                  |                            |         |
| SHAM lactic acid injection, <i>n</i> =12   | i.a.                             | 8 (7)            | 7 (5)                      | 0.024*  |
| HF-rEF lactic acid injection, <i>n</i> =11 | i.a.                             | 10 (6)           | 7 (5)                      | 0.057   |
| SHAM contraction, <i>n</i> =7              | i.a.                             | 30 (7)           | 20 (5)                     | 0.037*  |
| HF-rEF contraction, <i>n</i> =8            | i.a.                             | 37 (12)          | 28 (10)                    | 0.024*  |
| SHAM contraction, <i>n</i> =5              | i.v.                             | 28 (7)           | 24 (6)                     | 0.535   |
| HF-rEF contraction, <i>n</i> =5            | i.v.                             | 26 (12)          | 21 (14)                    | 0.138   |
| SHAM stretch, <i>n</i> =6                  | i.a.                             | 8 (5)            | 7 (4)                      | 0.767   |
| HF-rEF stretch, <i>n</i> =7                | i.a.                             | 16 (9)           | 13 (8)                     | 0.229   |

Values are mean (SD). Experimental group is identified by the primary experimental maneuver performed. Data were compared with paired Student's t-tests. i.a., intraarterial; i.v., intravenous; HF-rEF, heart failure with reduced ejection fraction; HR, heart rate; PcTx-1, psalmotoxin-1. Asterisks indicate statistical significance ( $P < 0.05$ ).



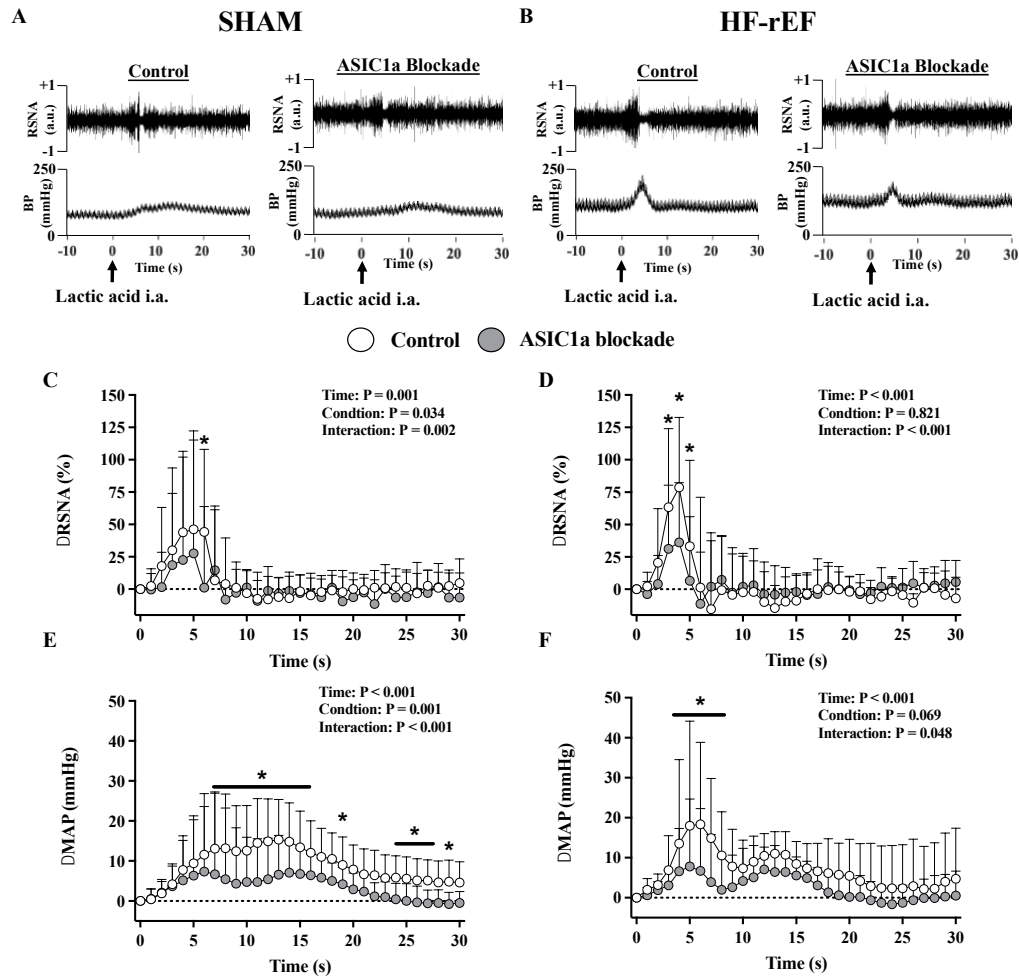
**Table 5.4**

Table 5.4. Pressor, cardioaccelerator, and peak renal sympathetic response to static hindlimb muscle stretch before (control), after  $\mu$ ,  $\delta$  opioid receptor blockade (Naloxone), and after ASIC1a blockade in HF-rEF rats ( $n=5$ )

|                         | Control   | Naloxone  | ASIC1a blockade | P-Value |
|-------------------------|-----------|-----------|-----------------|---------|
| Peak $\Delta$ MAP, mmHg | 30 (17)   | 31 (15)   | 32 (24)         | 0.975   |
| BPI, mmHg·s             | 513 (309) | 444 (412) | 503 (197)       | 0.478   |
| Baseline MAP, mmHg      | 102 (7)   | 103 (11)  | 95 (16)         | 0.361   |
| Peak $\Delta$ HR, bpm   | 13 (7)    | 10 (7)    | 12 (11)         | 0.316   |
| Baseline HR, bpm        | 471 (48)  | 470 (40)  | 469 (40)        | 0.904   |
| Peak $\Delta$ RSNA, %   | 128 (152) | 132 (81)  | 112 (89)        | 0.777   |

Values are mean (SD). Data were compared with one-way ANOVAs. HF-rEF, heart failure with reduced ejection fraction; MAP, mean arterial pressure; BPI, blood pressure index; HR, heart rate; RSNA, renal sympathetic nerve activity.

**Figure 5.1**



*Figure 1. Effect of ASIC1a blockade on renal sympathetic and pressor response to lactic acid injection. Examples of original tracings of RSNA and blood pressure (BP) in response to lactic acid injection (indicated by arrows) before and after ASIC1a blockade in a SHAM (A) and HF-rEF (B) rat.  $\Delta$  renal sympathetic nerve activity (RSNA; C & D),  $\Delta$  mean arterial pressure (MAP; E & F) in response to hindlimb arterial injection of lactic acid (24mMol) before (Control) and after ASIC1a blockade in SHAM ( $n=12$ ) and HF-rEF ( $n=11$ ) rats. Data were analyzed with two-way ANOVAs and multiple comparisons tests and are expressed as mean+SD. Asterisks and/or black lines indicate time points where comparisons were statistically significant ( $P < 0.05$ ).*

**Figure 5.2**

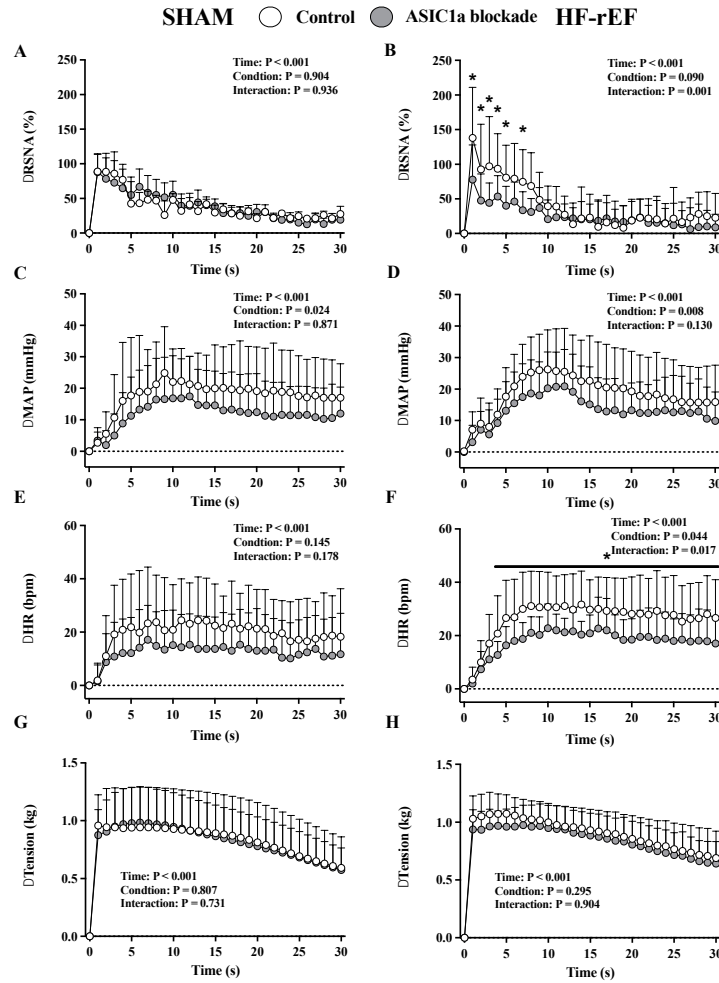


*Figure 2. Effect of ASIC1a blockade on the time course of exercise pressor reflex activation.  $\Delta$  renal sympathetic nerve activity (RSNA; A & B),  $\Delta$  mean arterial pressure (MAP; C & D),  $\Delta$  heart rate (HR; E & F), and  $\Delta$  tension (G & H) in response to 30 seconds of static hindlimb muscle contraction before (Control) and after ASIC1a blockade in SHAM ( $n=7$ ) and HF-rEF ( $n=8$ ) rats. Data were analyzed with two-way ANOVAs and Šidák multiple comparisons tests and are expressed as mean+SD. Asterisks and/or black lines indicate time points where comparisons were statistically significant ( $P < 0.05$ ).*

Figure 5.3

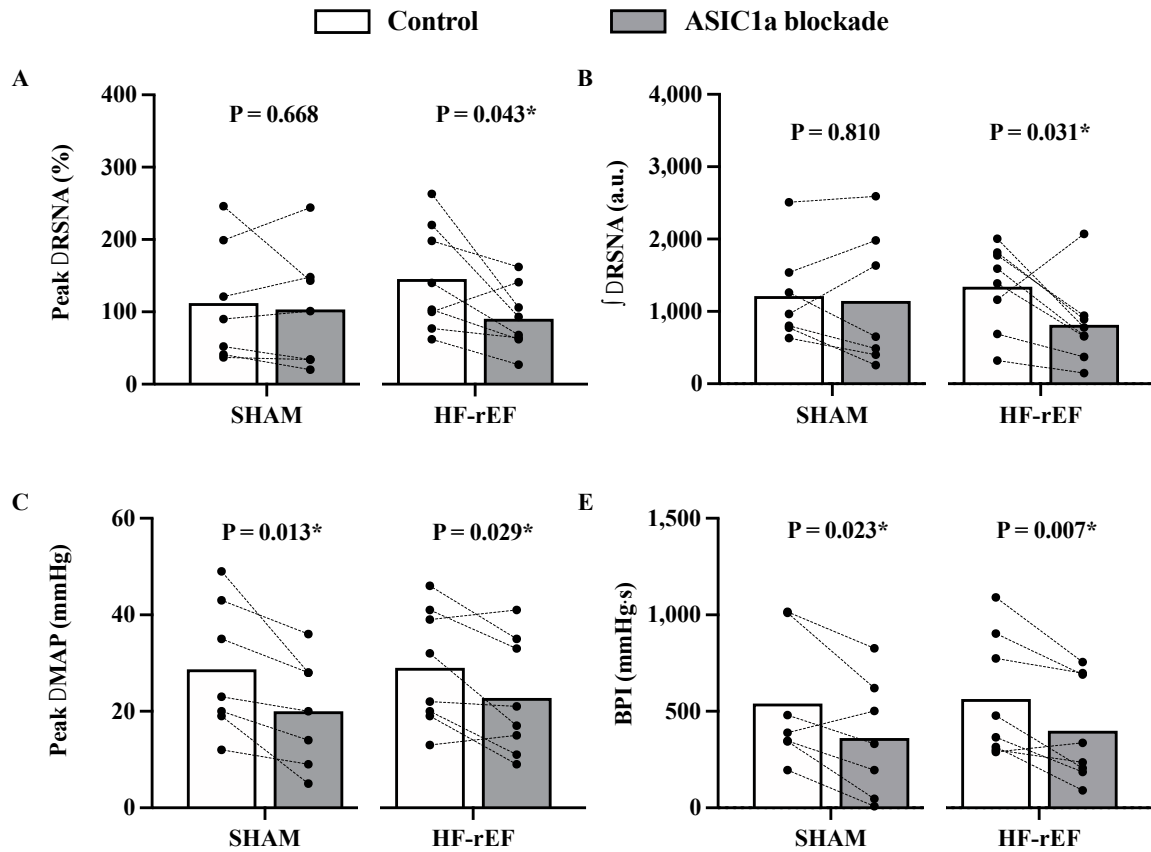
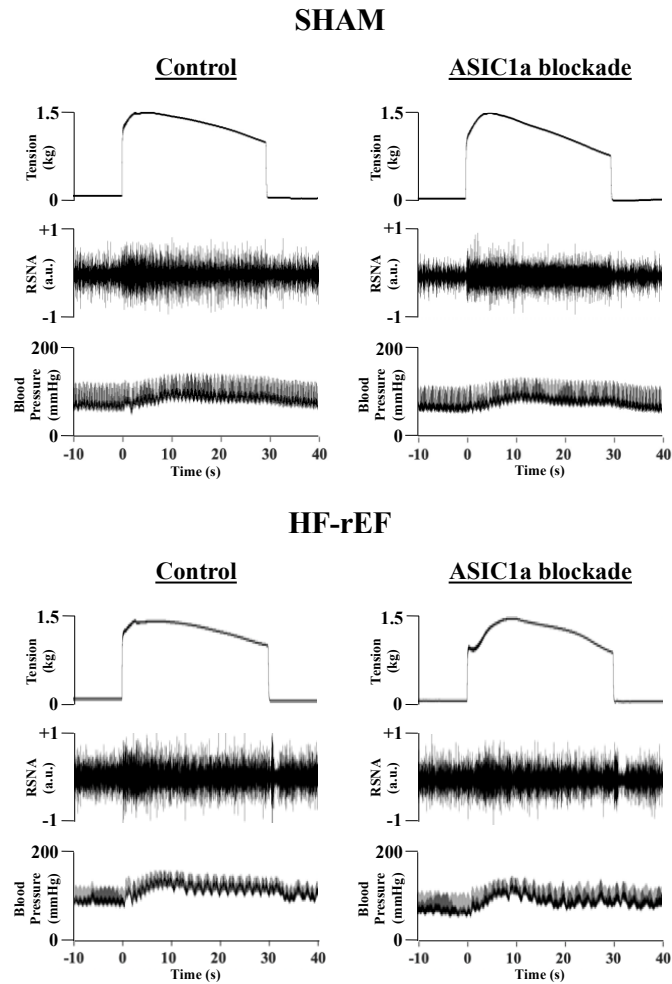


Figure 3. Effect of ASIC1a blockade on exercise pressor reflex activation. The peak  $\Delta$  renal sympathetic nerve activity (RSNA; A) and integrated change in RSNA ( $\int\Delta$ RSNA, B) as well as the peak  $\Delta$  mean arterial pressure (MAP; C) and blood pressure index (BPI, D) in response to 30 seconds of static hindlimb muscle contraction before (Control) and after ASIC1a blockade in SHAM ( $n=7$ ) and HF-rEF ( $n=8$ ) rats. Data were analyzed with multiple  $t$ -tests and are expressed as mean values overlaid with individual responses. Asterisks indicate statistically significant differences between groups ( $P < 0.05$ ).

**Figure 5.4**



*Figure 4.* Examples of original tracings of renal sympathetic nerve activity (RSNA), and blood pressure evoked during 30 seconds of static hindlimb muscle contraction before (Control) and after ASIC1a blockade in a SHAM (left) and HF-rEF (right) rat.

**Figure 5.5**

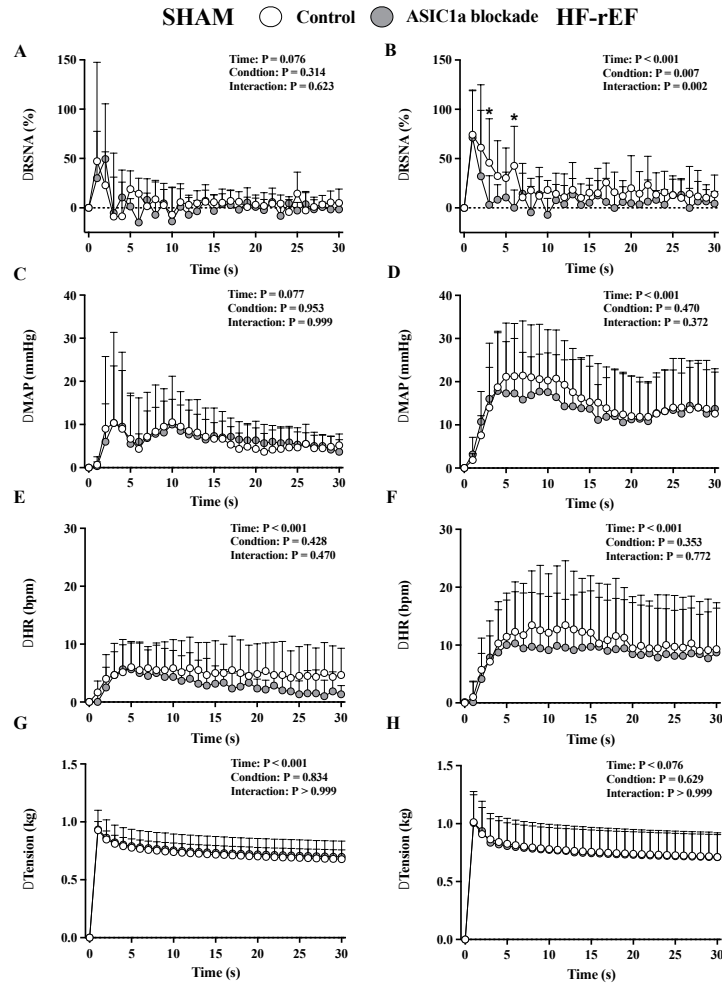


*Figure 5. Effect of ASIC1a blockade on the time course of mechanoreflex activation.  $\Delta$  renal sympathetic nerve activity (RSNA; A & B),  $\Delta$  mean arterial pressure (MAP; C & D),  $\Delta$  heart rate (HR; E & F), and  $\Delta$  tension (G & H) in response to 30 seconds of static hindlimb muscle stretch before (Control) and after ASIC1a blockade in SHAM ( $n=6$ ) and HF-rEF ( $n=7$ ) rats. Data were analyzed with two-way ANOVAs and Šidák multiple comparisons tests and are expressed as mean+SD. Asterisks indicate time points where comparisons were statistically significant ( $P < 0.05$ ).*

Figure 5.6

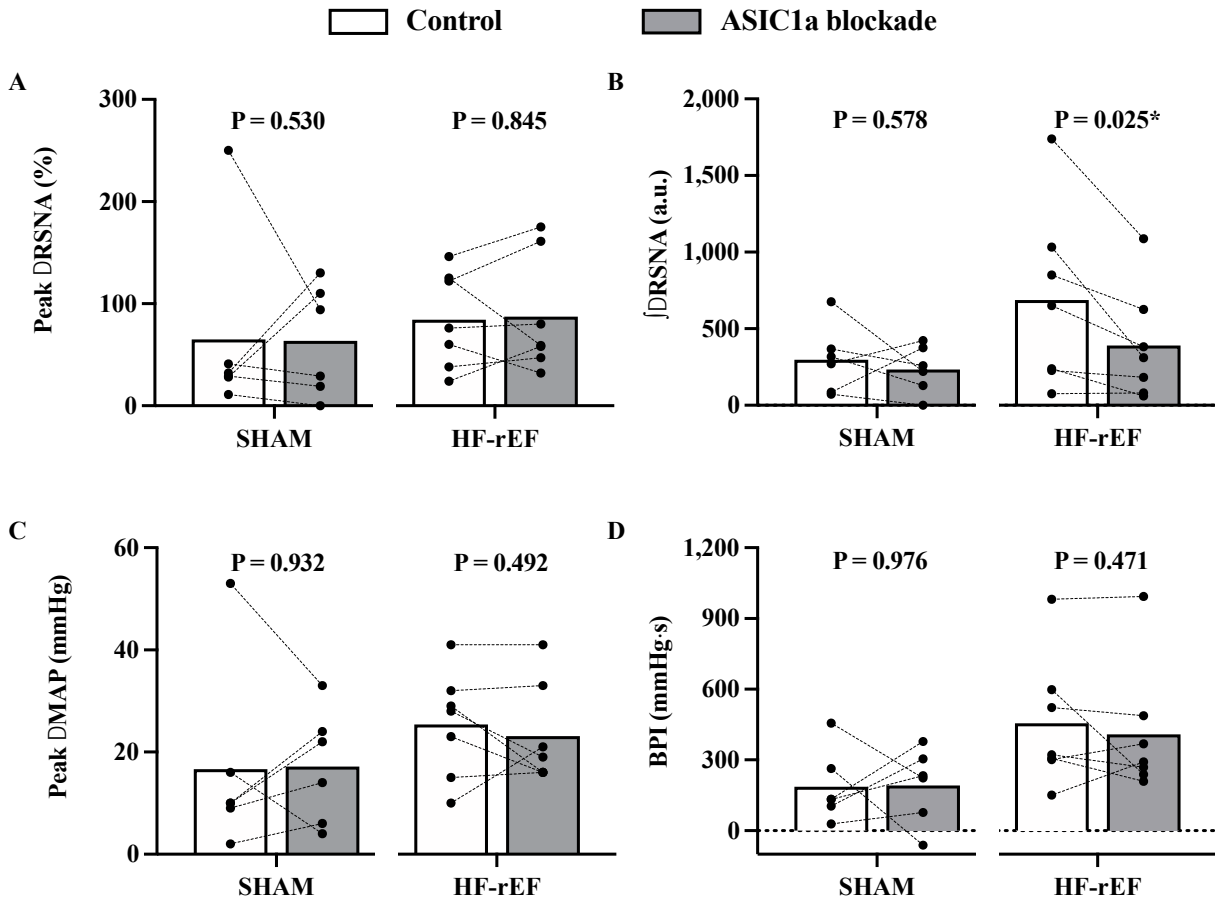
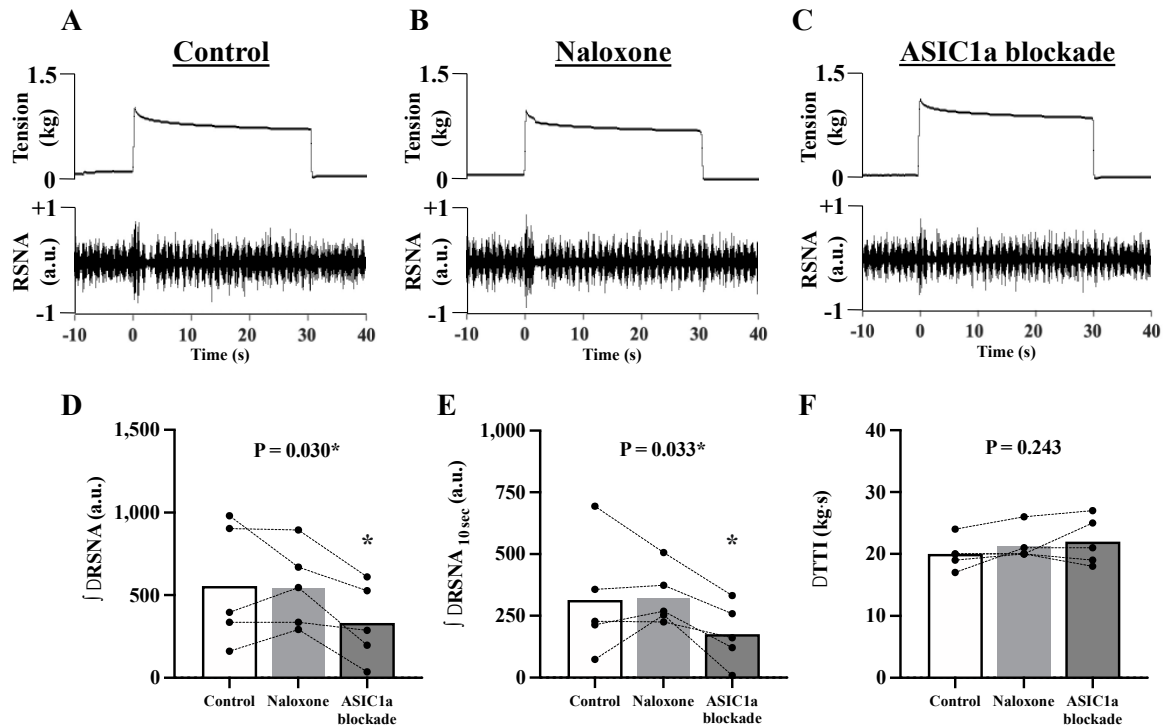


Figure 6. Effect of ASIC1a blockade on mechanoreflex activation. The peak  $\Delta$  renal sympathetic nerve activity (RSNA; A) and integrated change in RSNA ( $\int\Delta$ RSNA, B) as well as the peak  $\Delta$  mean arterial pressure (MAP; C) and blood pressure index (BPI, D) in response to 30 seconds of static hindlimb muscle stretch before (Control) and after ASIC1a blockade in SHAM ( $n=6$ ) and HF-rEF ( $n=7$ ) rats. Data were analyzed with multiple  $t$ -tests and are expressed as mean values overlaid with individual responses. Asterisks indicate statistically significant differences between conditions ( $P < 0.05$ ).

**Figure 5.7**



*Figure 7. Effect of  $\mu$ - and  $\delta$ -opioid receptor blockade and ASIC1a blockade on mechanoreflex activation in HF-rEF rats. Example of original tracings of the RSNA responses to 30 seconds of static hindlimb muscle stretch in control (A), post  $\mu$ - and  $\delta$ -opioid blockade (B), and post ASIC1a blockade conditions (C) from a HF-rEF rat. The integrated change in renal sympathetic nerve activity ( $\int \Delta RSNA$ , D) and the first 10 seconds of the integrated change in RSNA ( $\int \Delta RSNA_{10 \text{ sec}}$ , E) in response to 30 seconds of static hindlimb muscle stretch before (Control) and after  $\mu$ - and  $\delta$ -opioid receptor blockade (Naloxone) as well as after ASIC1a blockade in HF-rEF rats ( $n=5$ ). TTI (F), tension-time index. Data were analyzed with one-way ANOVAs and Šidák multiple comparisons tests and are expressed as mean values overlaid with individual responses. Asterisks indicate  $P < 0.05$  for ASIC1a blockade vs. control and  $\mu$ - and  $\delta$ -opioid blockade with Šidák multiple comparisons.*



Figure 5.8

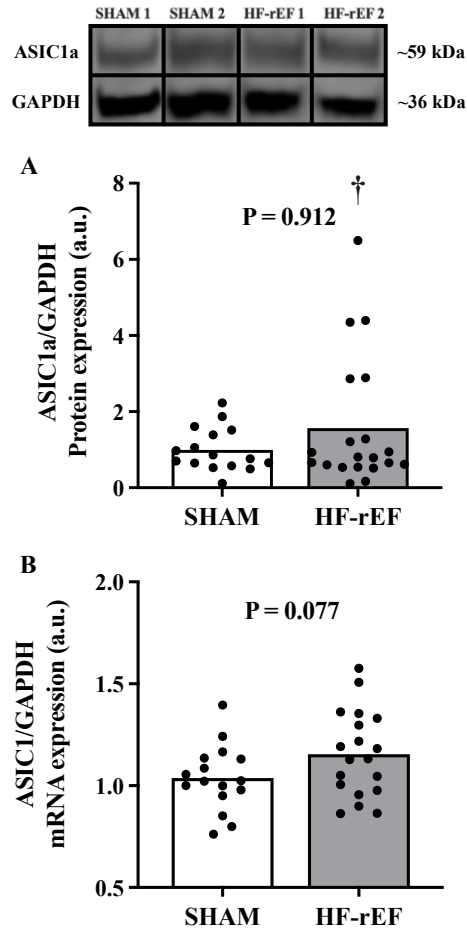


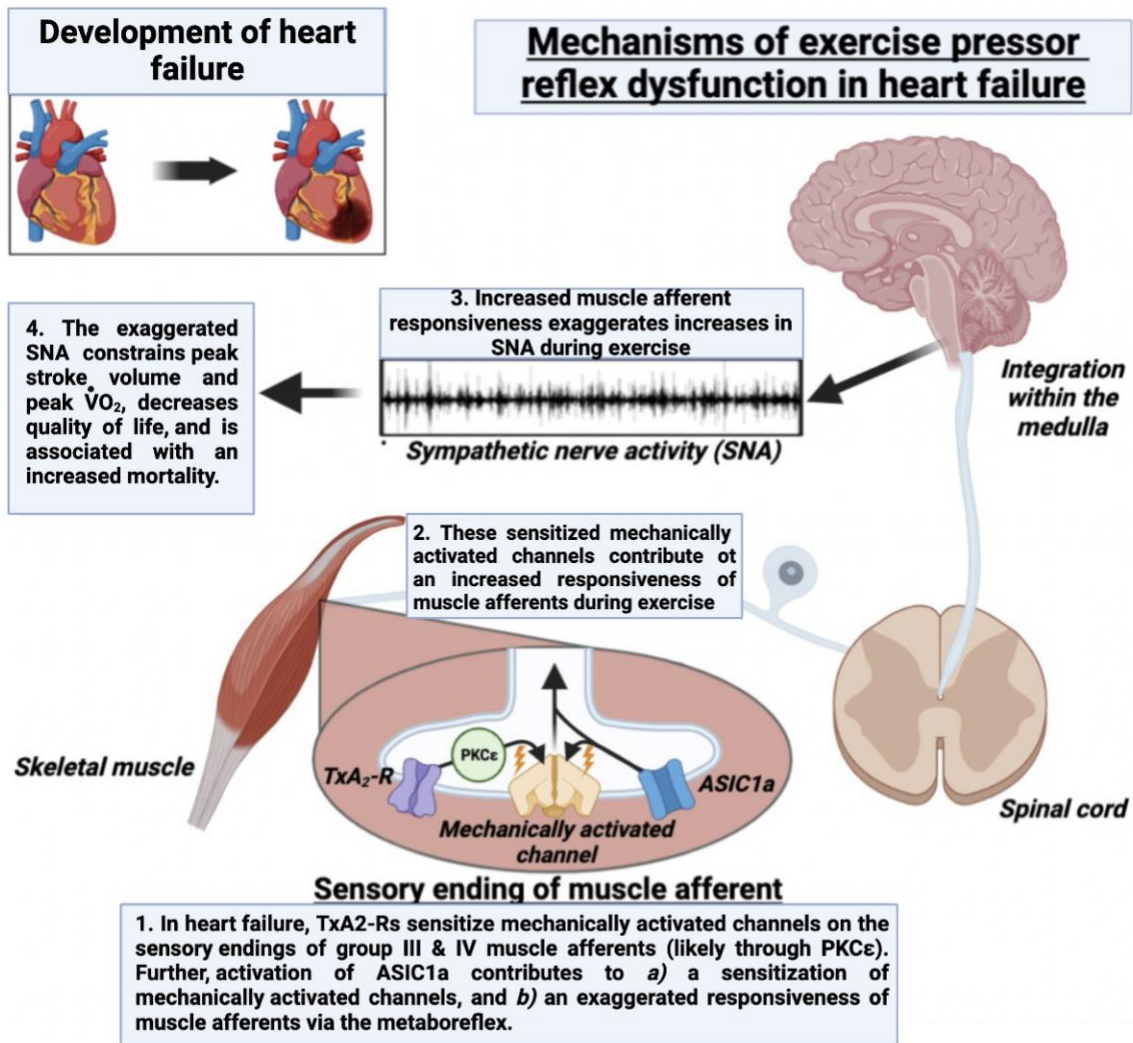
Figure 8. Effect of HF-rEF on ASIC1a expression. ASIC1a protein (A) and ASIC1 mRNA (B) in L<sub>4</sub> and L<sub>5</sub> dorsal root ganglia (DRG) tissue from SHAM (n=16) and HF-rEF (n=20) rats. GAPDH was used as a loading control (A) and reference sample (B). Examples of original western blot images from two sham and two HF-rEF rats are also shown. Data were analyzed with a Mann-Whitney test (A) or Student's *t*-test (B) and expressed as mean values overlaid with individual responses. Dagger indicates statistically significant difference in variance between groups (P < 0.05).

## Chapter 6 - Conclusion

The overall aim of the studies contained within this dissertation was to determine the mechanisms behind the exaggerated exercise pressor reflex in HF-rEF patients using a rat model of myocardial infarction-induced HF-rEF. In chapter 2, we found that TxA<sub>2</sub>-R blockade on the sensory endings of thin fiber muscle afferents reduced the sympathetic and pressor response to dynamic hindlimb muscle stretch in rats with HF-rEF, but not in SHAM rats. We also found that EP4-R blockade had no effect on the sympathetic or pressor response to stretch in either HF-rEF or SHAM rats. Those data suggested that TxA<sub>2</sub>-Rs on the sensory endings of thin fiber muscle afferents contribute to a chronic sensitization of the mechanically activated channels that underlie dynamic/rhythmic mechanoreflex activation. Although the hindlimb muscle stretch model of mechanoreflex activation may provide valuable information regarding the presence of chronic mechanoreflex sensitization in rats with HF-rEF, the model activates mechanically activated channels in a non-physiological manner. As such, in chapter 3 we sought to determine whether the exaggerated sympathetic and pressor responses to 1 Hz hindlimb muscle stretch in rats with HF-rEF translated to exaggerated responses to dynamic muscle contraction which produces physiological mechanoreflex activation consequent to muscle shortening and concurrent increases in intramuscular pressure. Consistent with our hypothesis, we found that TxA<sub>2</sub>-R blockade on the sensory endings of thin fiber muscle afferents reduced the sympathetic and pressor response to dynamic hindlimb muscle contraction in rats with HF-rEF, but not in SHAM rats. In chapter 4, we sought to determine the role played by second messenger signaling pathways associated with the TxA<sub>2</sub>-R activation, namely IP<sub>3</sub> receptors and PKC $\epsilon$ , in mediating the mechanoreflex/exercise pressor reflex sensitization. We found that IP<sub>3</sub> receptor blockade had no effect on the sympathetic or pressor response to dynamic hindlimb muscle stretch activation in HF-rEF or SHAM rats. However, we found that inhibiting PKC $\epsilon$  translocation to the cell membrane attenuated the sympathetic and pressor response to dynamic hindlimb muscle stretch and contraction in rats with HF-rEF, but not in SHAM rats. Finally, in chapter 5, we found that ASIC1a contributed to activation of the exercise pressor reflex in SHAM and HF-rEF rats. Further, we found that ASIC1a plays a role only in evoking the metaboreflex component of the exercise pressor reflex in health whereas in HF-rEF, ASIC1a plays a role in evoking both the metaboreflex and mechanoreflex components of the exercise pressor reflex. Together, these data enhance our understanding of the

mechanisms that underly the exaggerated SNA response following activation of the exercise pressor reflex in HF-rEF patients.

Figure 6.1 Summary of results



## Appendix A - Curriculum Vitae

### Alec Lloyd Edward Butenas

**Date of Birth:** March 27, 1995 (Merriam, KS, USA)

**Current Work Address:** Kansas State University  
140 Justin Hall  
Manhattan, KS 66506  
E-mail: [alec70@ksu.edu](mailto:alec70@ksu.edu)  
Office: 785-532-1096  
Cell: 913-972-3500

#### **Education**

May 2023 Ph.D. (Kinesiology)  
(*expected*) Specialization: Autonomic Neurophysiology  
Mentor: Dr. Steven W. Copp

May 2018 B.S. (Kinesiology, Kansas State University) *cum laude*.  
Minor in French.

May 2016 D.E.L.F. (French language diplomacy level B1), Université de Lyon Lumière 2—  
Lyon, France)

#### **Academic Appointments**

2022-present Instructor – *Kinesiology 335 Physiology of Exercise*

2019-present Graduate Research Assistant – *Cardio-Oncology & Autonomic Physiology Laboratory, Department of Kinesiology, Kansas State University*

2018-2020 Graduate Teaching Assistant - *Department of Kinesiology, Kansas State University*

#### **Professional Memberships**

2018-present The American Physiological Society, Environmental and Exercise Physiology Section

2019-present The American College of Sports Medicine

2020-2021 Kansas Academy of Science

2021-present American Autonomic Society

## **Awards and Honors**

Kinesiology Department's Doctoral Student of the Year Award, 2022

Neural Control & Autonomic Regulation Research Recognition Award from American Physiological Society, 2022

Environmental & Exercise Physiology Section Early Career Research Award of the American Physiological Society, 2021

Poster Presentation Award, Kansas Academy of Sciences, 2021

American Kinesiology Association National Honorable Mention, 2020

American Kinesiology Association Graduate Student Writing Award, 2020

Environmental & Exercise Physiology Section Award of the American Physiological Society, Pre-Doctoral Award, 2020

Graduate Student Council Travel Award, 2019-2022

Kinesiology Achievement Award, 2018

Office of Undergraduate Research and Creative Inquiry Research Grant Award (award provided \$1,000 to support travel to scientific conference), 2016

College of Human Ecology's Undergraduate Research and Creative Inquiry Forum, 2017

## **Grant Funding**

### ***Awarded – completed***

American College of Sports Medicine

*Title:* Mechanisms of Muscle Metaboreflex Dysfunction in Heart Failure: Role of Acid-Sensing Ion Channels

*Role:* PI, *Total costs:* \$5,000 *Status:* Completed, *Funding period:* 7/1/2021-9/30/2022

### ***Awarded - completed***

Kansas Academy of Science Doctoral Research Grant

*Title:* Skeletal Muscle Afferent Control of Ventilation in Heart Failure.

*Role:* PI, *Total costs:* \$1,500 *Status:* Completed, *Funding period:* 4/15/2020-4/14/2021

Office of Undergraduate Research and Creative Inquiry Research Grant.

*Title:* Skeletal Muscle Afferent Control of Ventilation and Blood Pressure in a Rat Model of Peripheral Artery Disease.

*Role:* PI, *Total costs:* \$1,000, *Status:* Completed, *Effective dates:* 12/5/2016-5/15/2017

### *Applied – not funded*

Ruth L. Kirschstein National Research Service Award (NRSA) Individual Predoctoral Fellowship (Parent F31)

*Title:* Determination of purinergic receptor subtype contributions to the exercise pressor reflex in peripheral artery disease

### **Published Original Research Manuscripts**

1. Kempf EA, Rollins KS, Hopkins TD, **Butenas AL**, Santin JM, Smith JR & Copp SW. (2018) Chronic femoral artery ligation exaggerates the pressor and sympathetic nerve response during dynamic skeletal muscle stretch in decerebrate rats. *Am J Physiol Heart Circ Physiol.* 314 (2) H246-H254.
2. Sanderson BC, Rollins KS, Hopkins TD, **Butenas AL**, Felice KP, Ade CJ, & Copp SW. (2019) GsMTx4 reduces the reflex pressor response during dynamic hindlimb skeletal muscle stretch in decerebrate rats. *Physiol Rep.* 7 (1) e13974.
3. Rollins KS, Hopkins TD, **Butenas AL**, Felice KP, Ade CJ, & Copp SW. (2019). Cyclooxygenase inhibition does not impact the pressor response during static or dynamic mechanoreflex activation in healthy decerebrate rats. *Am J Physiol Regul Integr Comp Physiol.* 317 (3) R369-R378.
4. **Butenas ALE**, Hopkins TD, Butenas AL, Felice KP, & Copp SW. (2019) Investigation of the mechanisms of cyclooxygenase-mediated mechanoreflex exaggeration in a rat model of simulated peripheral artery disease. *Am J Physiol Heart Circ Physiol.* 317 (5) H1050-H1061
5. Rollins KS, **Butenas ALE**, Felice KP, Matney JE, Williams AC, Kleweno TE, Copp SW. (2020) Thromboxane A2 Receptors Mediate Chronic Mechanoreflex Sensitization in a Rat Model of Simulated Peripheral Artery Disease. *Am J Physiol Heart Circ Physiol.* 319 (2) H320-H330
6. **Butenas ALE**, Smith JR, Copp SW, Hageman KS, Poole DC, Musch TI. (2020) Type II Diabetes Accentuates Diaphragm Blood Flow Increases During Submaximal Exercise in the Rat. *Respiratory Physiology Neurobiology.* 281 103518
7. **Butenas ALE**, Rollins KS, Matney JE, Williams AC, Kleweno TE, Parr SK, Hammond ST, Ade CJ, Hageman KS, Musch TI, Copp SW. (2020) No effect of endoperoxide 4 or

- thromboxane A<sub>2</sub> receptor blockade on static mechanoreflex activation in rats with heart failure. *Experimental Physiology*. 105 (11) 1840-1854
8. **Butenas ALE**, Colburn TD, Baumfalk DR, Ade CJ, Hageman KS, Copp SW, Poole DC, Musch TI. (2021) Angiotensin converting enzyme inhibition improves cerebrovascular control during exercise in male rats with heart failure. *Respiratory Physiology Neurobiology*. 286 103613
  9. Baumfalk DR, Opoku-Acheampong AB, Caldwell JT, **Butenas ALE**, Horn AG, Kunkle ON, Copp SW, Ade CJ, Musch TI, Behnke BJ. (2021) Effects of high-intensity training on prostate cancer-induced cardiac atrophy. *American Journal of Translational Research*. 113 (1) 197-209.
  10. **Butenas ALE**, Rollins KS, Williams AC, Parr SK, Hammond ST, Ade CJ, Hageman KS, Musch TI, Copp SW. (2021) Exaggerated sympathetic and cardiovascular responses to dynamic mechanoreflex activation in rats with heart failure: Role of endoperoxide 4 and thromboxane A<sub>2</sub> receptors. *Autonomic Neuroscience*. 232 102784.
  11. Rollins KS, **Butenas ALE**, Williams AC, Copp SW. (2021) Sensory neuron inositol 1, 4, 5-trisphosphate receptors contribute to chronic mechanoreflex sensitization in rats with simulated peripheral artery disease. *Am J Physiol Regul Integr Comp Physiol*. 321 (5) R768-R780.
  12. **Butenas ALE**, Rollins KS, Williams AC, Parr SK, Hammond ST, Ade CJ, Hageman KS, Musch TI, Copp SW. (2021) Thromboxane A<sub>2</sub> receptors contribute to the exaggerated exercise pressor reflex in male rats with heart failure. *Physiol Rep*. 9 (18) e15052
  13. **Butenas ALE**, Rollins KS, Parr SK, Hammond ST, Ade CJ, Hageman KS, Musch TI, Copp SW. (2022) Novel Mechanosensory Role for Acid Sensing Ion Channel Subtype 1a in Evoking the Exercise Pressor Reflex in Rats with Heart Failure. *Journal of Physiology*. 600 (9) 2105-2125
  14. **Butenas ALE**, Rollins KS, Williams AC, Copp SW. (2023) Bradykinin 2 Receptors Contribute to the Exaggerated Exercise Pressor Reflex in a Rat Model of Simulated Peripheral Artery Disease. *Am J Physiol Regul Integr Comp Physiol*. 324 (2) R183-R195.
  15. **Butenas ALE**, Copp SW, Hageman KS, Poole DC, Musch TI. (2023) Effect of co-morbid Type 2 Diabetes Mellitus and Heart Failure on rat Hindlimb and Respiratory Muscle Blood Flow during Treadmill Exercise. *J Appl Physiol*. 134 (4) 846-857.



## Presentations

American Autonomic Society Basic Science and Animal Studies Session Presenter. November 2022. “Purinergic 2X receptors subtypes 3 and 4 contribute to the exaggerated mechanoreflex in rats with simulated peripheral artery disease”

University of Missouri Graduate Seminar. October 2022. “Exercise Pressor Reflex Dysfunction in Rats with Heart Failure”

American Autonomic Society. November 2021. “Role of ASIC1a in the Exercise Pressor Reflex in Rats with Heart Failure”

Kansas Academy of Science Annual Meeting. April 2021. “*Thromboxane A<sub>2</sub> Receptors Contribute to the Exaggerated Exercise Pressor Reflex in Rats with Heart Failure*”

Kansas State University College of Arts and Sciences. December 2019. Division of Biology. “*Heart Failure with reduced ejection fraction.*”

Kansas State University College of Health and Human Sciences. December 2019. Department of Kinesiology. “*Investigation of the mechanisms of cyclooxygenase-mediated mechanoreflex sensitization in a rat model of simulated peripheral artery disease.*”

## Teaching Experience (all at Kansas State University)

### *Undergraduate level courses taught*

Biobehavioral Bases of Exercise Laboratory (2018-2020)

Physiology of Exercise Laboratory (2018-2020)

Measurement and Research Techniques Laboratory (2018-2020)

Kinesiology 335 Physiology of Exercise Lecture Course (2022-present)

## Abstracts/Conference Proceedings

1. Rollins KS, **Butenas AL**, Kempf EA, Hopkins TD, Sanderson BC, Copp SW. Blood pressure responses to hindlimb arterial bradykinin injection are mediated by bradykinin 2 receptors in decerebrate rats. *FASEB J*.
2. Sanderson BC, Rollins KS, Kempf EA, Hopkins TD, **Butenas AL**, Ade CJ, Copp SW. GsMTx4 reduces the pressor response during dynamic hindlimb muscle stretch in decerebrate rats. *FASEB J*.
3. **Butenas AL**, Hopkins TD, Rollins KS, Felice KP, Copp SW. Chronic femoral ligation increases skeletal muscle interstitial prostaglandin E<sub>2</sub> in the rat: Implications for the exercise pressor reflex. *FASEB J*.

4. Rollins KS, **Butenas AL**, Hopkins TD, Felice KP, Copp SW. Skeletal muscle stretch-induced PGE<sub>2</sub> formation does not impact the muscle mechanoreflex in decerebrate rats. *FASEB J*.
5. **Butenas ALE**, Rollins KS, Felice KP, Ade CJ, Musch TI, Copp SW. Endoperoxide 4 receptor inhibition has no effect on the pressor response evoked during isolated mechanoreflex activation in rats with heart failure. *FASEB J*. 2020.
6. Rollins KS, **Butenas AL**, Felice KP, Copp SW. Thromboxane A2 Receptors Contribute to the Exaggerated Mechanoreflex in a Rat Model of Peripheral Artery Disease. *FASEB J*. 2020.
7. Rollins KS, **Butenas ALE**, Williams AC, Copp SW. TRPV1 Channel Stimulation Reduces the Mechanoreflex in Decerebrate Rats. *FASEB J*. 2021
8. **Butenas ALE**, Rollins KS, Williams AC, Hammond ST, Ade CJ, Hageman KS, Musch TI, Copp SW. Thromboxane A2 Receptors Contribute to the Exaggerated Exercise Pressor Reflex in Rats with Heart Failure. *FASEB J*. 2021
9. **Butenas ALE**, Rollins KS, Williams AC, Parr SK, Hammond ST, Ade CJ, Hageman KS, Musch TI, Copp SW. The role played by ASIC1a in the exercise pressor reflex in rats with heart failure. American Autonomic Society. 2021
10. **Butenas ALE**, Parr SK, Hammond ST, Ade CJ, Hageman KS, Musch TI, Copp SW Protein Kinase C Epsilon Contributes to the Exaggerated Mechanoreflex in Rats with Heart Failure. *FASEB J*. 2022
11. **Butenas ALE**, Rollins KS, Williams AC, Parr SK, Hammond ST, Ade CJ, Hageman KS, Musch TI, Copp SW. The role played by ASIC1a in the exercise pressor reflex in rats with heart failure. *American Autonomic Society*. 2021
12. **Butenas ALE**, Rollins KS, Hammond ST, Parr SK, Ade CJ, Hageman KS, Musch TI, Copp SW. Mechanisms Of Mechanoreflex Activation In Rats With Heart Failure: Possible Mechanosensory Role Of ASIC1a. *American College of Sports Medicine*. 2022
13. **Butenas ALE** & Copp SW. Purinergic 2X receptors subtypes 3 and 4 contribute to the exaggerated mechanoreflex in rats with simulated peripheral artery disease. *American Autonomic Society*. 2022